Copy
RM L54L06

NACA

RESEARCH MEMORANDUM

INVESTIGATION OF AERODYNAMIC CHARACTERISTICS IN PITCH AND SIDESLIP OF A 45° SWEPTBACK-WING AIRPLANE MODEL WITH VARIOUS VERTICAL LOCATIONS OF WING AND HORIZONTAL TAIL

BASIC-DATA PRESENTATION, M = 2.01

By M. Leroy Spearman, Cornelius Driver,
and William C. Hughes

Langley Aeronautical Laboratory
Langley Field, Va.

NATIONAL ADVISORY COMMITTEE
FOR AERONAUTICS

WASHINGTON

January 20, 1955

NATIONAL ADVISORY COMMITTEE FOR AERONAUTICS

RESEARCH MEMORANDUM

INVESTIGATION OF AERODYNAMIC CHARACTERISTICS IN PITCH AND SIDESLIP OF A 45° SWEPTBACK-WING AIRPLANE MODEL WITH VARIOUS VERTICAL LOCATIONS OF WING AND HORIZONTAL TAIL

BASIC-DATA PRESENTATION, M = 2.01

By M. Leroy Spearman, Cornelius Driver, and William C. Hughes

SUMMARY

An investigation has been conducted in the Langley 4- by 4-foot supersonic pressure tunnel to determine the effects of vertical location of wing and horizontal tail on the aerodynamic characteristics in combined pitch and sideslip of a supersonic airplane configuration at a Mach number of 2.01. Both the wing and the horizontal tail were swept back 45° and had an aspect ratio of 4. The wing had a taper ratio of 0.2 with NACA 65A004 sections whereas the horizontal tail had a taper ratio of 0.4 with NACA 65A006 sections. Directional stability was provided by a slab-type vertical tail with a small ventral fin.

The configurations investigated included a high-wing, a midwing, and a low-wing arrangement, each with four horizontal-tail locations. The lowest and the highest tail positions were 0.208 semispan below and 0.556 semispan above the body center line, respectively. Tests were also made with the horizontal tail off and with both the horizontal and the vertical tails off. Results were obtained for the midwing configuration (tails off) for dihedral angles of -3°, 0°, and 3°.

For the tests, the model was mounted on a rotary-type sting support providing roll angles from 0° to 90° through an angle range of the sting from 0° to about 18°. A resolution of these angles provides the aerodynamic characteristics in combined pitch and sideslip. Six components of forces and moments were measured by an internal balance. The basic data are presented in this report without analysis.

[redacted]

INTRODUCTION

The experimentally determined effects of wing and tail position on the aerodynamic characteristics of generalized aircraft configurations can be of considerable usefulness to the designer in the estimation of the stability and performance of similar specific configurations. In addition, such generalized results may be useful in the verification of various calculative methods for the prediction of the aerodynamic characteristics of airplanes. A considerable amount of such experimental data is available at low speeds (refs. 1 to 5, for example), wherein the influence of both plan form and positions of wings and tails has been determined from wind-tunnel tests of models simulating high-speed aircraft. Similar investigations have been extended to high subsonic Mach numbers (for example, refs. 5 to 9), and some results concerning the effects of tail location on the longitudinal characteristics of some rocket-propelled models have been obtained through the transonic speed range (refs. 10 and 11). Only a limited amount of such experimental data is available at present in the supersonic speed range. One example is the investigation reported in reference 12, in which the effects of wing vertical location on the longitudinal characteristics of wing-body combinations were determined in the Mach number ranges from 0.61 to 0.91 and from 1.20 to 1.90.

In order to provide additional results of general interest to the designer for the supersonic speed range, an investigation has been conducted in the Langley 4- by 4-foot supersonic pressure tunnel at a Mach number of 2.01 to determine the effects of varying vertical locations of the wing and horizontal tail on the longitudinal and lateral aerodynamic characteristics of a complete model having both wing and tail swept back 45°. The basic results, without analysis, are presented herein.

SYMBOLS

The results are presented as standard NACA coefficients of forces and moments. The data are referred to the stability-axis system (fig. 1) with the reference center of moments located at 25 percent of the wing mean geometric chord.

The symbols are defined as follows:

C_L lift coefficient, $-Z/qS$

C_X longitudinal-force coefficient, X/qS

C_Y	lateral-force coefficient, Y/qS
C_n	yawing-moment coefficient, N/qSb
C_l	rolling-moment coefficient, L/qSb
C_m	pitching-moment coefficient, $M'/qS\bar{c}$
Z	force along Z-axis
X	force along X-axis
Y	force along Y-axis
N	moment about Z-axis
L	moment about X-axis
M'	moment about Y-axis
q	free-stream dynamic pressure
S	wing area including body intercept
A	aspect ratio
b	wing span
$\bar{c}$	wing mean geometric chord
α	angle of attack, deg
β	angle of sideslip, deg
ϕ	angle of roll, deg
λ	taper ratio
Γ	wing geometric dihedral angle, deg
Λ	angle of sweepback, deg
i_t	horizontal-tail incidence angle, deg

[redacted]

MODEL AND APPARATUS

A drawing of the model is shown in figure 2 and the geometric characteristics of the model are presented in table I.

The model fuselage was a body of revolution having a length-diameter ratio of about 11 and was composed of an ogive nose, a cylindrical midsection, and a slightly boattail rear section. The wing had 45° of sweepback at the quarter-chord line, an aspect ratio of 4, a taper ratio of 0.2, and NACA 65A004 sections in the stream direction. The horizontal tail had 45° of sweepback at the quarter-chord line, an aspect ratio of 4, a taper ratio of 0.6, and NACA 65A006 sections in the stream direction. The model was equipped with a vertical tail which had a small ventral fin and employed relatively thick slab-type sections to facilitate mounting of the horizontal tail. The position of the horizontal tail could be changed from a position below the body on the ventral fin (0.208b/2 below body center line - designated tail position 4) to three positions above the body on the vertical tail (0.208b/2, 0.382b/2, and 0.556b/2 above body center line - designated as tail positions 3, 2, and 1, respectively). The uppermost location (tail position 1) was atop the vertical tail corresponding to a T-tail arrangement. Provisions were made for varying the incidence angle of the horizontal tail. The model was so designed that the wing position could be changed from a position flush with the underside of the body to the body center line or to a position flush with the upper surface of the body. The high- and low-wing positions were achieved by merely inverting the same wing. Figure 3 shows various positions of the horizontal tail.

The midwing was composed of two separate panels. The geometric dihedral of the wing in this position could be varied from 0° to either 3° or -3°. The dihedral angle was 0° for the high and low wings and the wing incidence angle was 0° for all wings. The horizontal-tail incidence angle was zero for all configurations presented herein with the exception of the low-wing configuration with the tail below the body (tail position 4), for which the incidence angle was -3°.

Force measurements were made through the use of a six-component internal strain-gage balance. The model was mounted in the tunnel on a rotary-type sting. The range of the sting incidence angle was varied from 0° to about 18° for roll angles of 0°, 15°, 30°, 45°, 60°, 75°, and 90°.

TESTS, CORRECTIONS, AND ACCURACY

The conditions for the tests were:

Mach number	2.01
Stagnation temperature, ^{o}F	110
Stagnation pressure, lb/sq in. abs	12
Reynolds number based on $\bar{c}$	1.84×10^{6}

The stagnation dewpoint was maintained sufficiently low (-25° F or less) so that no condensation effects were encountered in the test section.

The sting angle was corrected for the deflection under load. The Mach number variation in the test section was approximately ±0.01 and the variation of the flow angle in the vertical and horizontal planes did not exceed about ±0.1°. The base pressure was measured and the longitudinal force was adjusted to a base pressure equal to the free-stream static pressure.

The estimated errors in the individual measured quantities are as follows:

C_L	±0.008
C_X	±0.002
C_m	±0.0004
C_Y	±0.001
C_n	±0.0005
C_l	±0.0004
i_t, deg	±0.2
α, deg	±0.2
β, deg	±0.2
ϕ, deg	±0.2

PRESENTATION OF RESULTS

The data figures are presented in the following manner:

[redacted]

Figure	Wing	Γ, deg	Vertical tail	Horizontal-tail position
4	Low	0	Off	Off
5	Low	0	On	Off
6	Low	0	On	1
7	Low	0	On	2
8	Low	0	On	3
9	Low	0	On	4
10	Mid	0	Off	Off
11	Mid	0	On	Off
12	Mid	0	On	1
13	Mid	0	On	2
14	Mid	0	On	3
15	Mid	0	On	4
16	High	0	Off	Off
17	High	0	On	Off
18	High	0	On	1
19	High	0	On	2
20	High	0	On	3
21	High	0	On	4
22	Mid	-3	Off	Off
23	Mid	3	Off	Off

The basic results for each configuration are presented for roll angles ϕ of 0°, 15°, 30°, 45°, 60°, 75°, and 90° through a range of sting angle from 0° to about 18°. The results at $\phi = 0^\circ$, of course, represent the usual longitudinal data, that is, the variation of the coefficients with angle of attack up to $\alpha \approx 18^\circ$ at $\beta \approx 0^\circ$; whereas the results at $\phi = 90^\circ$ represent the variation of the coefficients with angle of sideslip up to $\beta \approx 18^\circ$ at $\alpha \approx 0^\circ$. For roll angles between 0° and 90° the sting angle i and the roll angle ϕ have been resolved to angles of attack α and angles of sideslip β through the following relations (ref. 13):

$$\tan \alpha = \cos \phi \tan i$$
$$\sin \beta = \sin \phi \sin i$$

Hence, for a given roll angle, two curves are presented for each coefficient - the plain symbol (see fig. 4(b), for example) representing the coefficient variation with α and the flagged symbol representing the variation with β. By crossreading the results for each roll angle at different constant angles of attack, it is possible to obtain the variations of the coefficients with β for the constant α selected. An example of this procedure is included for the combination of low wing and body. The tabulated results for this configuration (obtained from fig. 4) are presented in table II, and the variation of the various

aerodynamic coefficients with sideslip for several angles of attack is shown in figure 24.

Numerous types of analyses, of course, are possible, but in order to expedite publication of these results, none are included in this data report.

Langley Aeronautical Laboratory,
National Advisory Committee for Aeronautics,
Langley Field, Va., November 17, 1954.

[redacted]

REFERENCES

1. Goodman, Alex: Effects of Wing Position and Horizontal-Tail Position on the Static Stability Characteristics of Models With Unswept and 45° Sweptback Surfaces With Some Reference to Mutual Interference. NACA TN 2504, 1951.

2. Brewer, Jack D., and Lichtenstein, Jacob H.: Effect of Horizontal Tail on Low-Speed Static Lateral Stability Characteristics of a Model Having 45° Sweptback Wing and Tail Surfaces. NACA TN 2010, 1950.

3. Queijo, M. J., and Wolhart, Walter D.: Experimental Investigation of the Effect of Vertical-Tail Size and Length and of Fuselage Shape and Length on the Static Lateral Stability Characteristics of a Model with 45° Sweptback Wing and Tail Surfaces. NACA Rep. 1049, 1951. (Supersedes NACA TN 2168.)

4. Goodman, Alex, and Thomas, David F., Jr.: Effects of Wing Position and Fuselage Size on the Low-Speed Static and Rolling Stability Characteristics of a Delta-Wing Model. NACA TN 3063, 1954.

5. Wiggins, James W., Kuhn, Richard E., and Fournier, Paul G.: Wind-Tunnel Investigation To Determine the Horizontal- and Vertical-Tail Contributions to the Static Lateral Stability Characteristics of a Complete-Model Swept-Wing Configuration at High Subsonic Speeds. NACA RM L53E19, 1953.

6. Morrison, William D., Jr., and Alford, William J., Jr.: Effects of Horizontal-Tail Height and a Wing Leading-Edge Modification Consisting of a Full-Span Flap and a Partial-Span Chord-Extension on the Aerodynamic Characteristics in Pitch at High Subsonic Speeds of a Model with a 45° Sweptback Wing. NACA RM L53E06, 1953.

7. Alford, William J., and Pasteur, Thomas B., Jr.: The Effects of Changes in Aspect Ratio and Tail Height on the Longitudinal Stability Characteristics at High Subsonic Speeds of a Model With a Wing Having 32.6° Sweepback. NACA RM L53L09, 1954.

8. Goodson, Kenneth W., and Becht, Robert E.: Wind-Tunnel Investigation at High Subsonic Speeds of the Stability Characteristics of a Complete Model Having Sweptback-, M-, W-, and Cranked-Wing Plan Forms and Several Horizontal-Tail Locations. NACA RM L54C29, 1954.

9. Few, Albert G., Jr., and King, Thomas J., Jr.: Some Effects of Tail Height and Wing Plan Form on the Static Longitudinal Stability Characteristics of a Small-Scale Model at High Subsonic Speeds. NACA RM L54G12, 1954.

[redacted]

10. Parks, James H., and Kehlet, Alan B.: Longitudinal Stability, Trim, and Drag Characteristics of a Rocket-Propelled Model of an Airplane Configuration Having a 45° Sweptback Wing and an Unswept Horizontal Tail. NACA RM L52F05, 1952.

11. Parks, James H., and Kehlet, Alan B.: Longitudinal Stability and Trim of Two Rocket-Propelled Airplane Models Having 45° Sweptback Wings and Tails With the Horizontal Tail Mounted in Two Positions. NACA RM L53J12a, 1953.

12. Heitmeyer, John C.: Effect of Vertical Position of the Wing on the Aerodynamic Characteristics of Three Wing-Body Combinations. NACA RM A52L15a, 1953.

13. Spearman, M. Leroy, and Driver, Cornelius: Wind-Tunnel Investigation at a Mach Number of 2.01 of the Aerodynamic Characteristics in Combined Pitch and Sideslip of Some Canard-Type Missiles Having Cruciform Wings and Canard Surfaces With 70° Delta Plan Forms. NACA RM L54F09, 1954.

TABLE I

GEOMETRIC CHARACTERISTICS OF MODEL

Wing:	
Area, sq in.	144
Span, in.	24
Root chord, in.	10
Tip chord, in.	2
Taper ratio	0.2
Aspect ratio	4
Mean geometric chord, in.	6.89
Spanwise location of mean geometric chord, percent wing semispan	38.9
Incidence, deg	0
Sweep of quarter-chord line, deg	45
Section	NACA 65A004
Horizontal tail:	
Area, sq in.	28.6
Span, in.	10.73
Root chord, in.	3.353
Tip chord, in.	2.012
Taper ratio	0.6
Aspect ratio	4
Sweep of quarter-chord line, deg	45
Section	NACA 65A006
Vertical tail (excluding ventral fin):	
Area to body center line, sq in.	43.5
Span from body center line, in.	7.48
Root chord, in.	8.17
Tip chord, in.	3.44
Taper ratio	.42
Aspect ratio	1.29
Sweep of leading edge, deg	35
Section	Wedge nose, slab side with constant thickness of 0.437 in.
Ventral fin:	
Exposed area, sq in.	8.54
Body:	
Length, in.	36.50
Diameter (maximum), in.	3.33
Diameter (base), in.	2.67
Length-diameter ratio	10.96

[redacted]

TABLE II

TABULATED RESULTS FOR COMBINATION OF LOW WING AND BODY

AT COMBINED ANGLES OF ATTACK AND SIDESLIP

ϕ, deg	α, deg	β, deg	C_L	C_m	C_X	C_l	C_n	C_Y
0	4	0	0.186	-0.035	-0.033	0	-0.0001	-0.0002
0	8	0	.333	-.056	-.064	-.0001	-.0001	0
0	12	0	.480	-.072	-.120	-.0003	0	0
0	16	0	.625	-.078	-.194	-.0005	-.0001	0
15	4	1.0	.170	-.036	-.031	.0003	-.003	-.005
15	8	2.1	.325	-.060	-.064	.0001	-.006	-.010
15	12	2.9	.470	-.079	-.120	-.0017	-.009	-.015
15	16	4.2	.625	-.080	-.192	-.0051	-.0108	-.035
30	4	2.3	.155	-.036	-.030	.0005	-.005	-.006
30	8	4.6	.305	-.063	-.062	.0009	-.011	-.020
30	12	6.8	.445	-.082	-.112	-.0020	-.0156	-.045
30	16	8.9	.560	-.072	-.179	-.0085	-.015	-.095
45	4	4.0	.175	-.038	-.030	.0015	-.008	-.017
45	8	8.0	.330	-.070	-.064	.0018	-.016	-.040
45	12	11.8	.675	-.080	-.114	-.0040	-.021	-.100
60	4	6.8	.205	-.047	-.034	.0035	-.012	-.020
60	8	13.6	.390	-.078	-.073	.0012	-.023	-.100
75	4	14.7	.220	-.060	-.034	.0085	-.026	-.115
90	0	4.0	.005	-.007	-.190	.0040	-.0065	-.0200
90	0	8.0	.006	-.021	-.190	.0080	-.0130	-.0450
90	0	12.0	.003	-.031	-.190	.0123	-.0210	-.0830
90	0	16.0	-.020	-.020	-.190	.0164	-.0290	-.1360

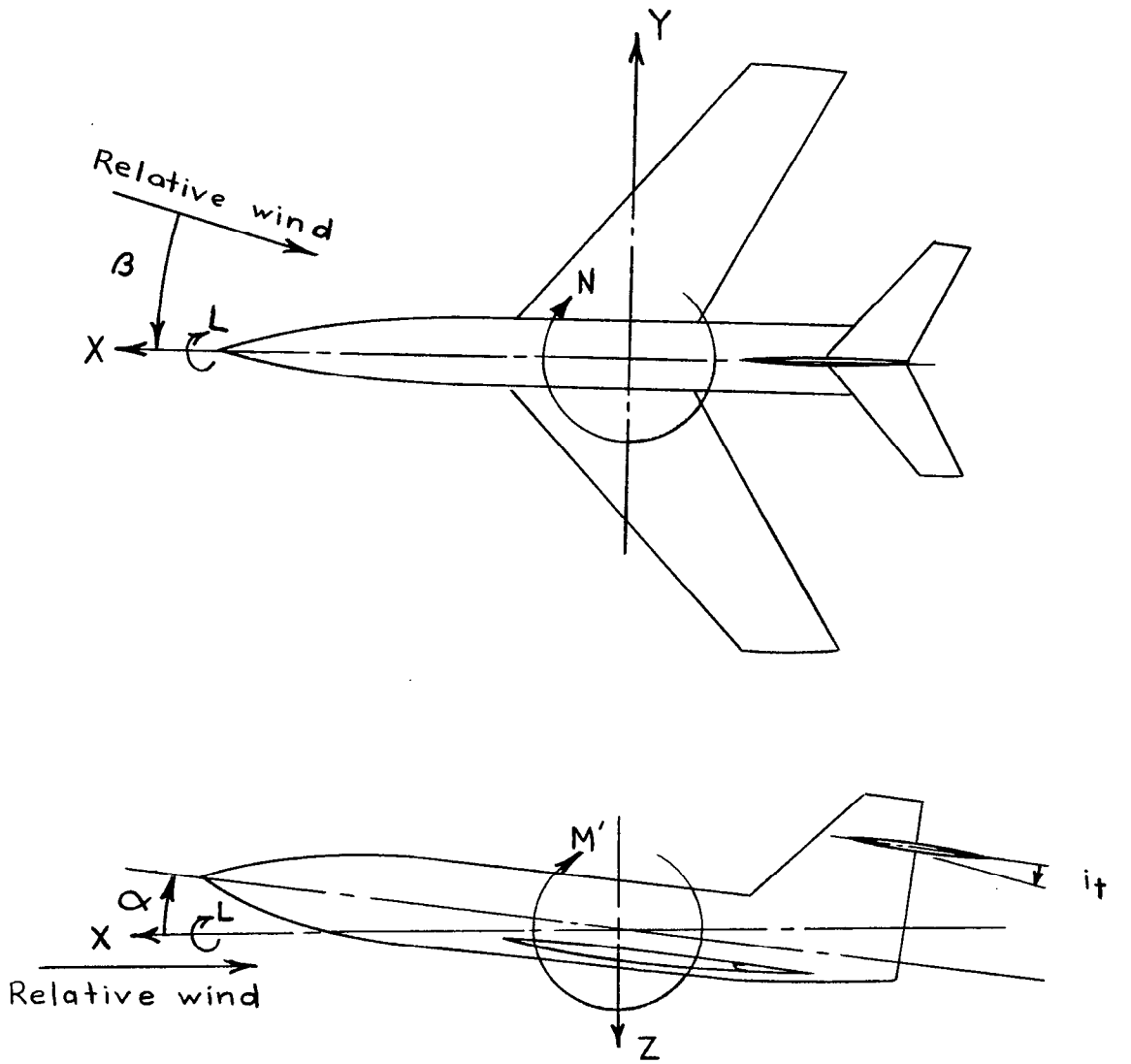

Figure 1.- System of stability axes. Arrows indicate positive directions.

[redacted]

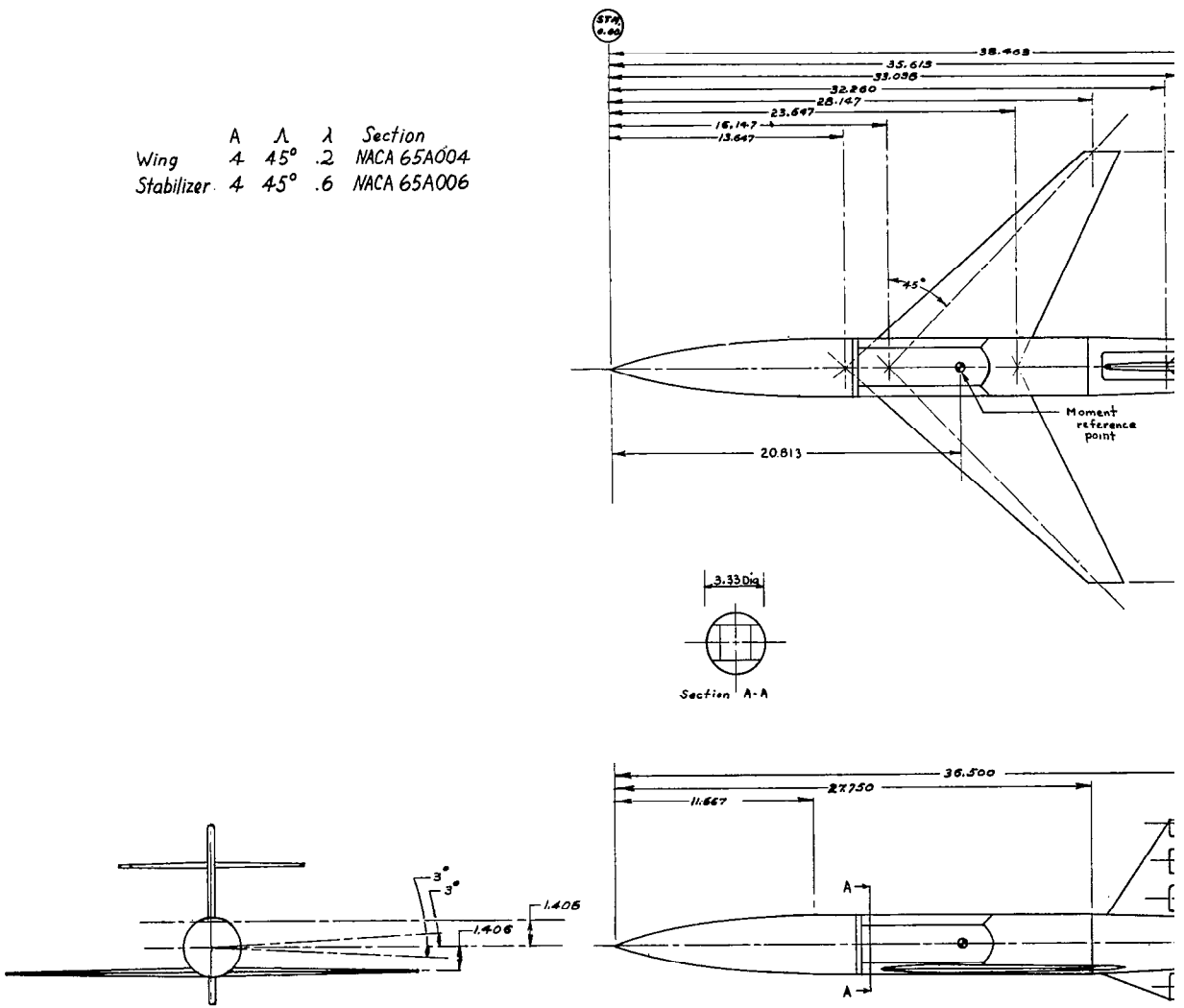

Figure 2.- Three-view drawing of model. All dimensions in inches otherwise noted.

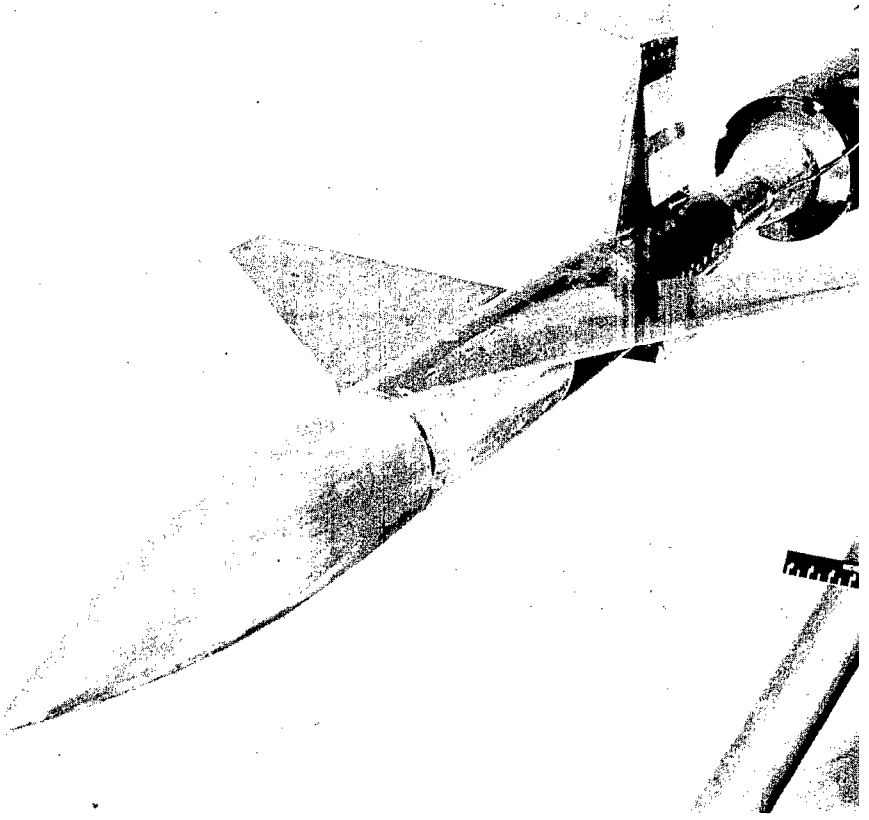

(a) High wing; horizontal-tail location 1.

Figure 3.- Photographs of model.

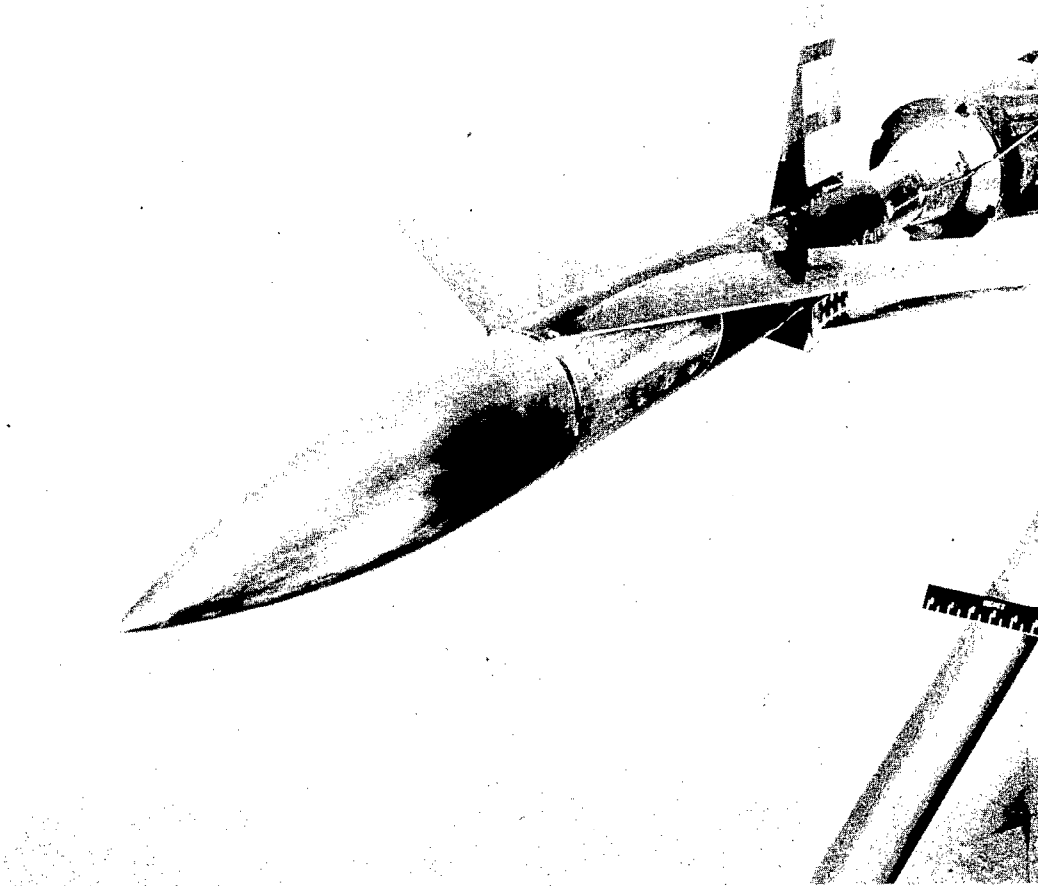

(b) High wing; horizontal-tail location 4.

Figure 3.- Continued.

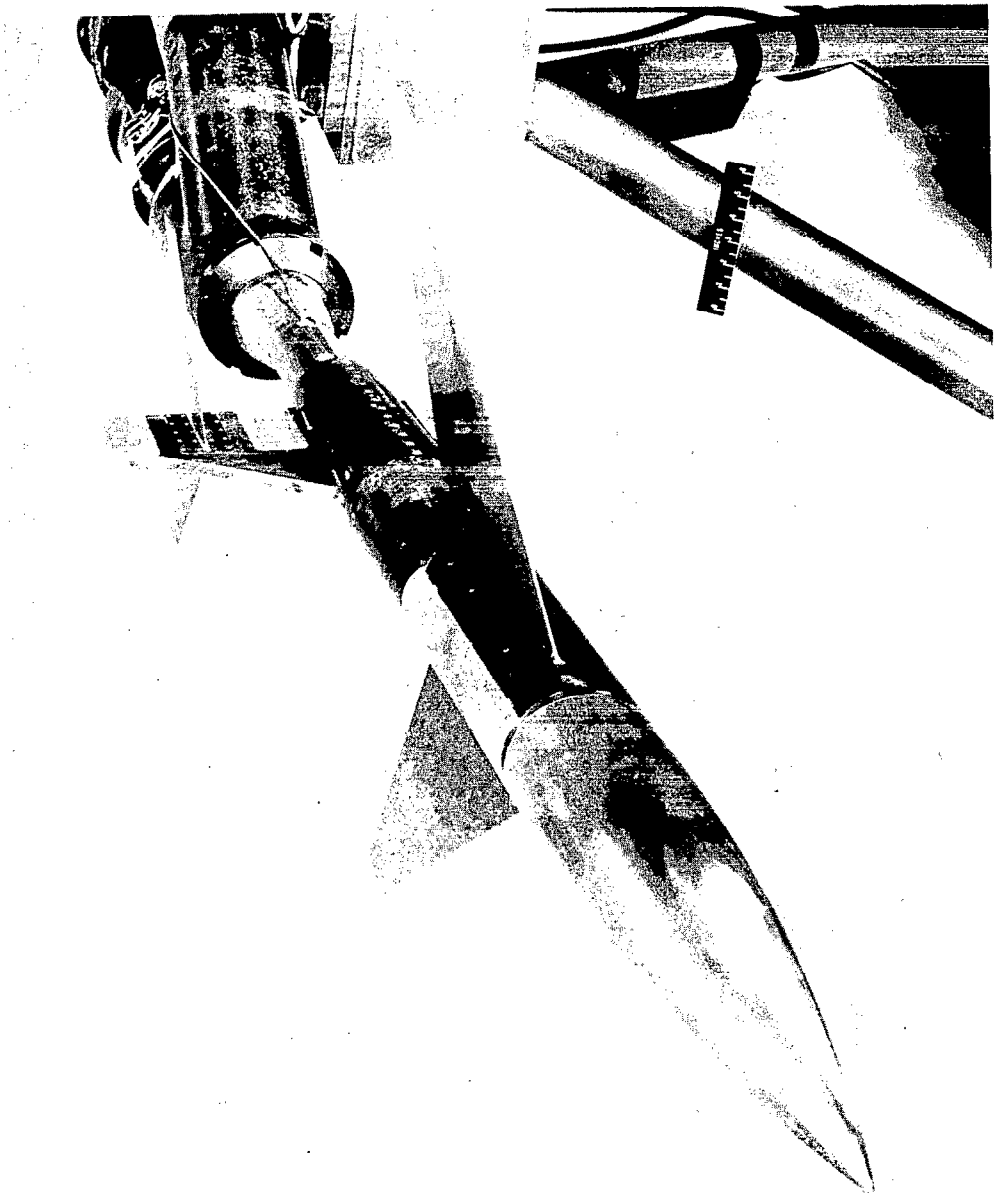

L-82755

(c) Midwing; horizontal-tail location 2.

Figure 3.- Continued.

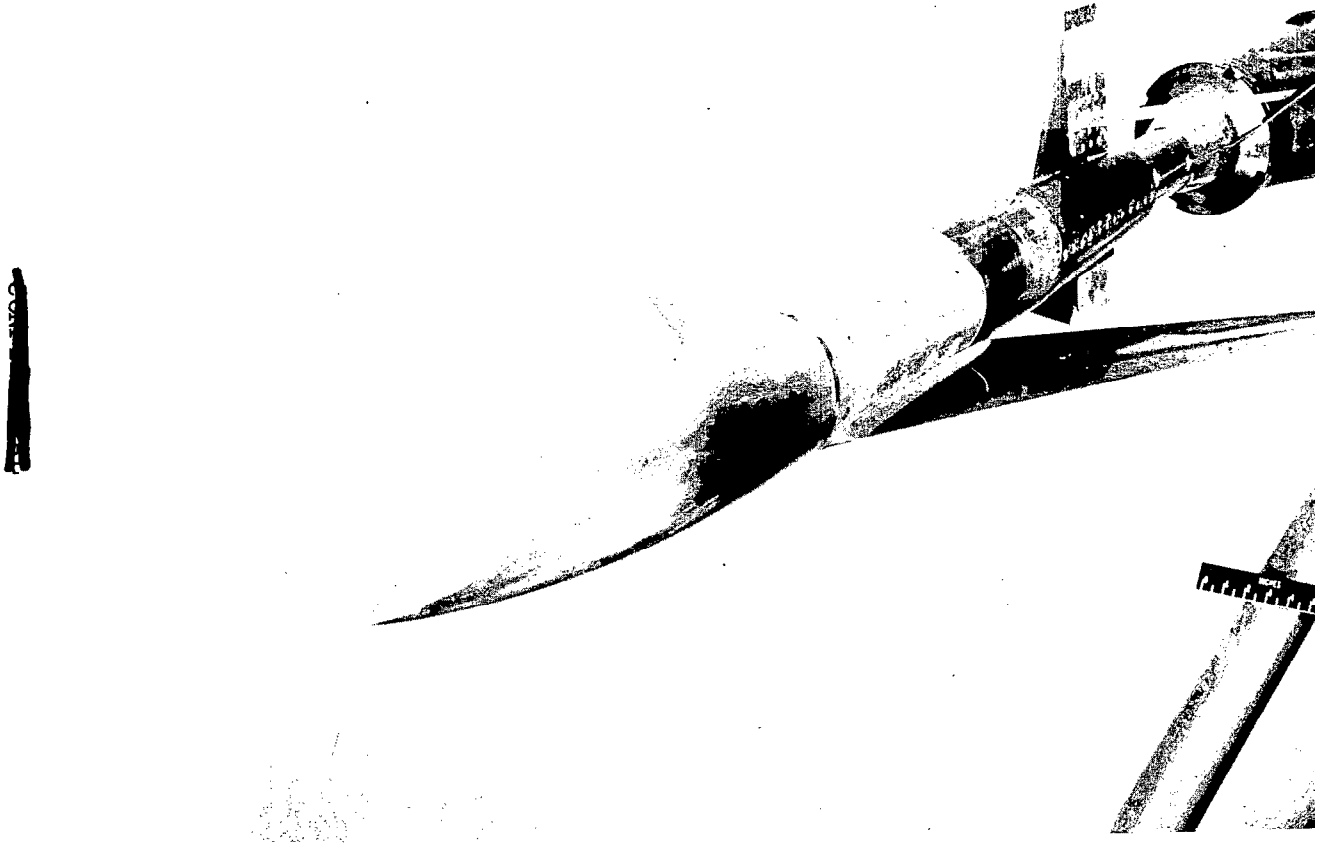

(d) Low wing; horizontal-tail location 3.

Figure 3.- Concluded.

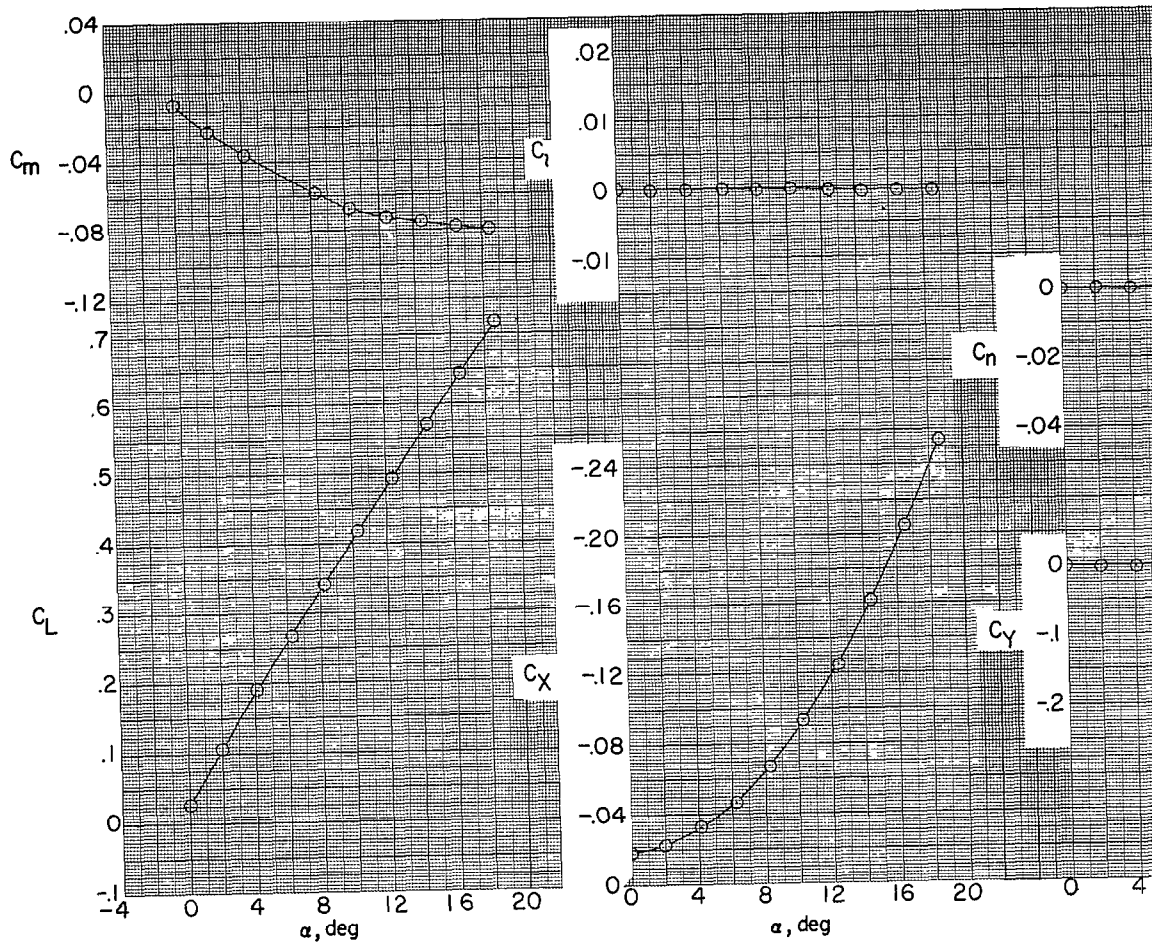

(a) $\phi = 0^{o}$.

Figure 4.- Aerodynamic characteristics at various roll angle
tails off. Flagged symbols are for variations with β; u
symbols are for variations with α.

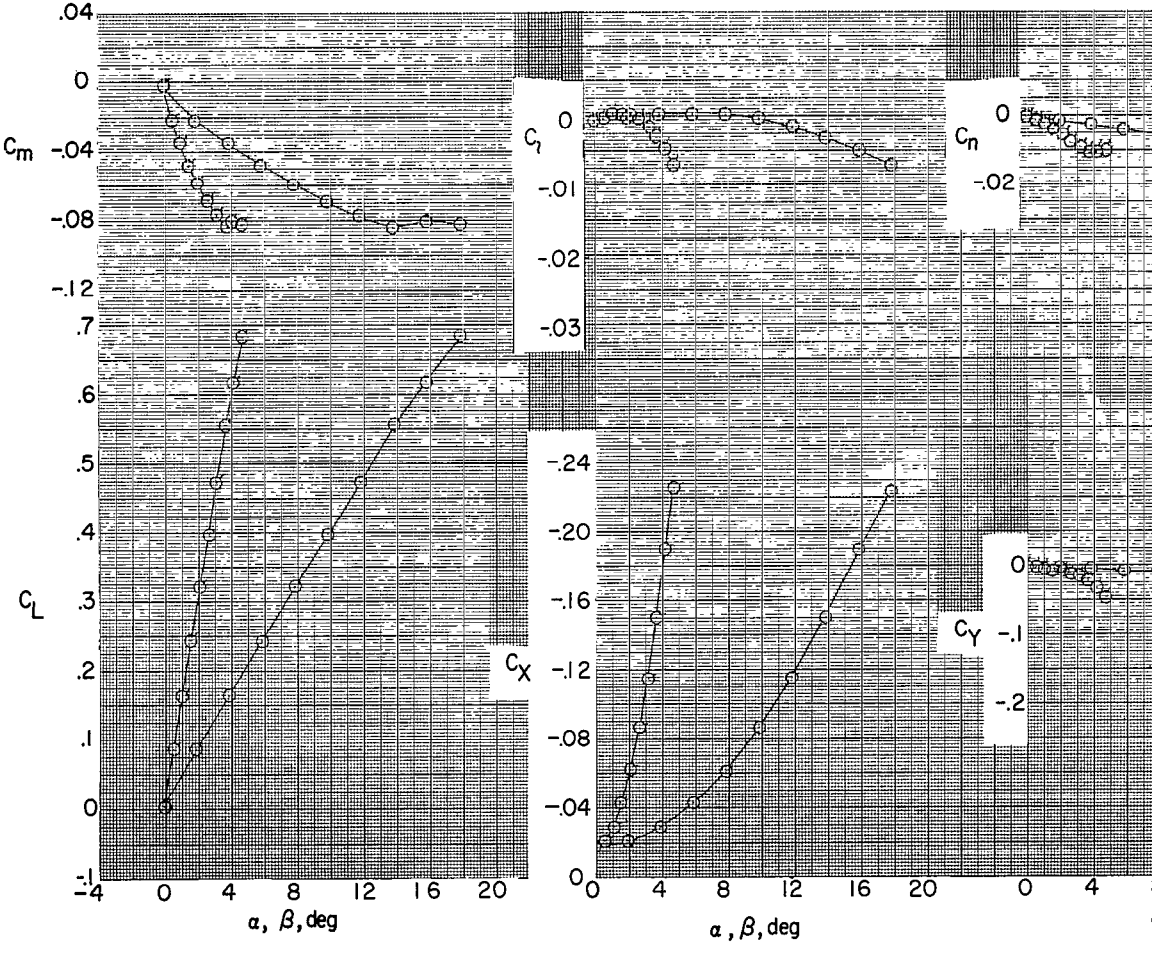

(b) $\phi = 15^{\circ}$.

Figure 4.- Continued.

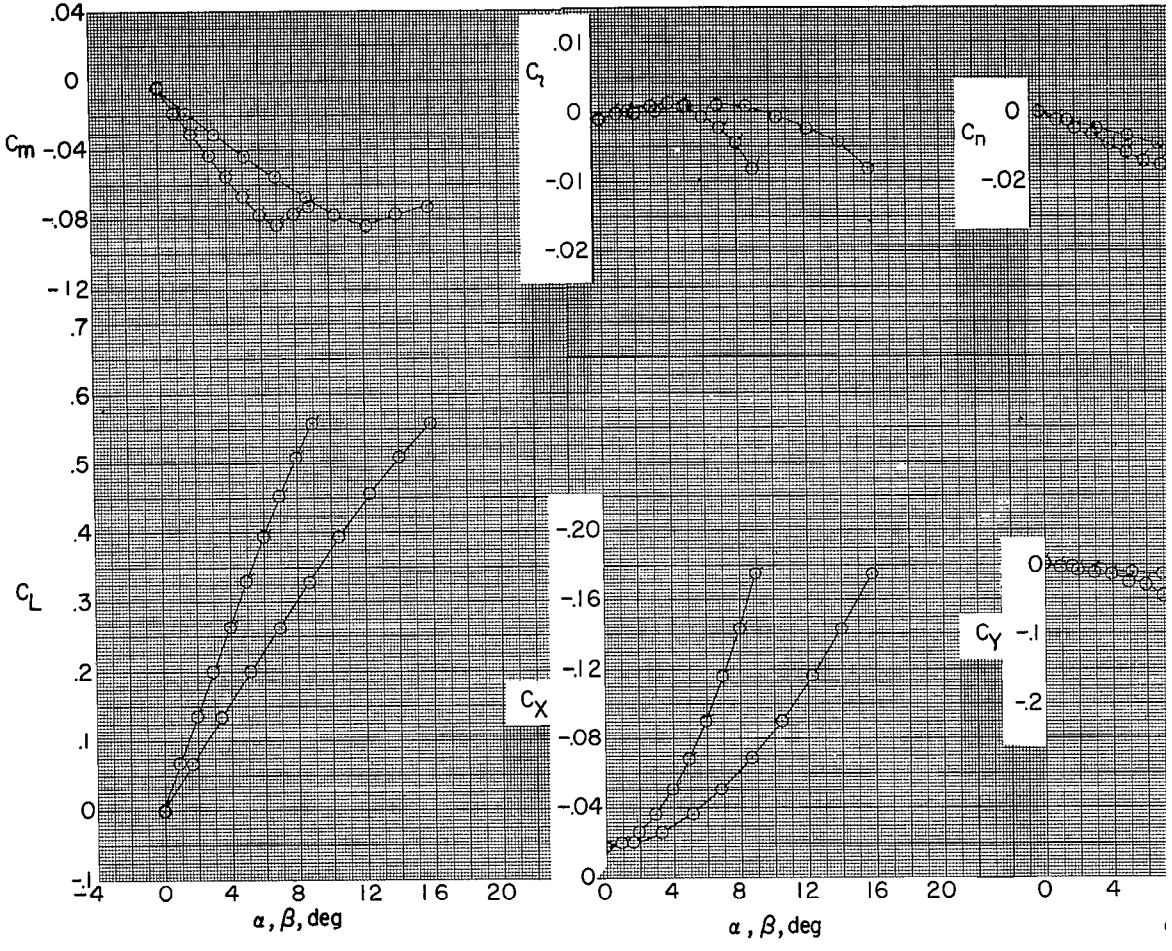

(c) $\phi = 30^{\circ}$.

Figure 4.- Continued.

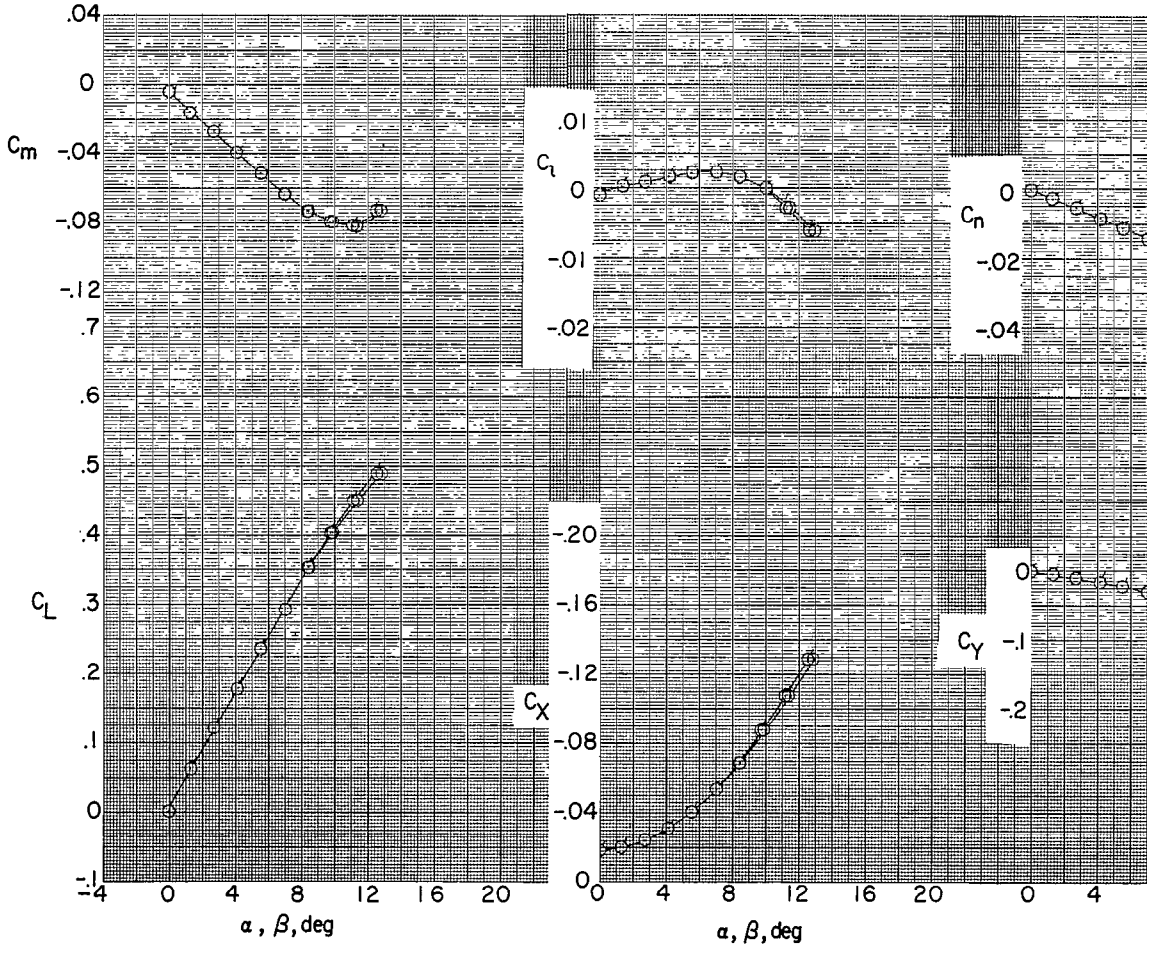

(d) $\phi = 45^{\circ}$.

Figure 4.- Continued.

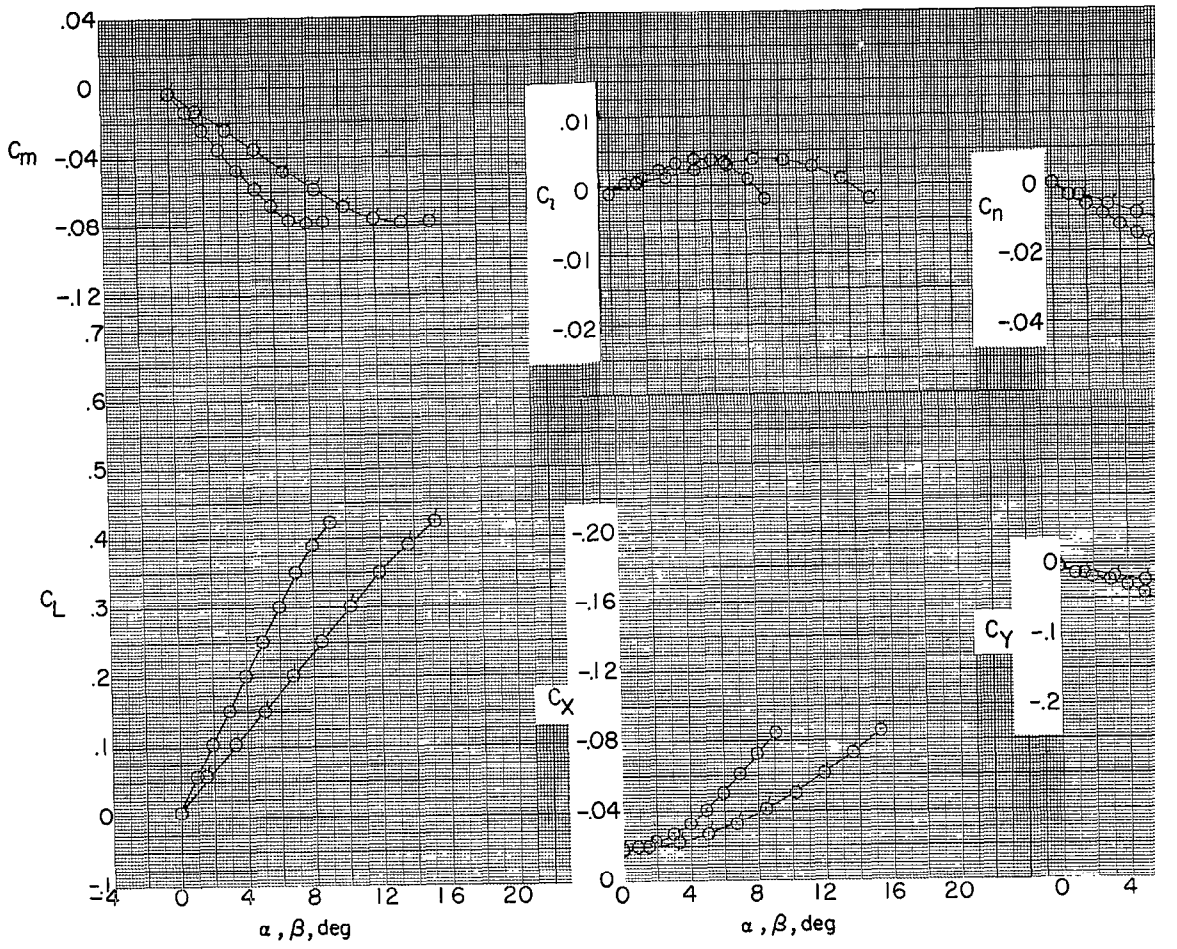

(e) $\phi = 60^{\circ}$.

Figure 4.- Continued.

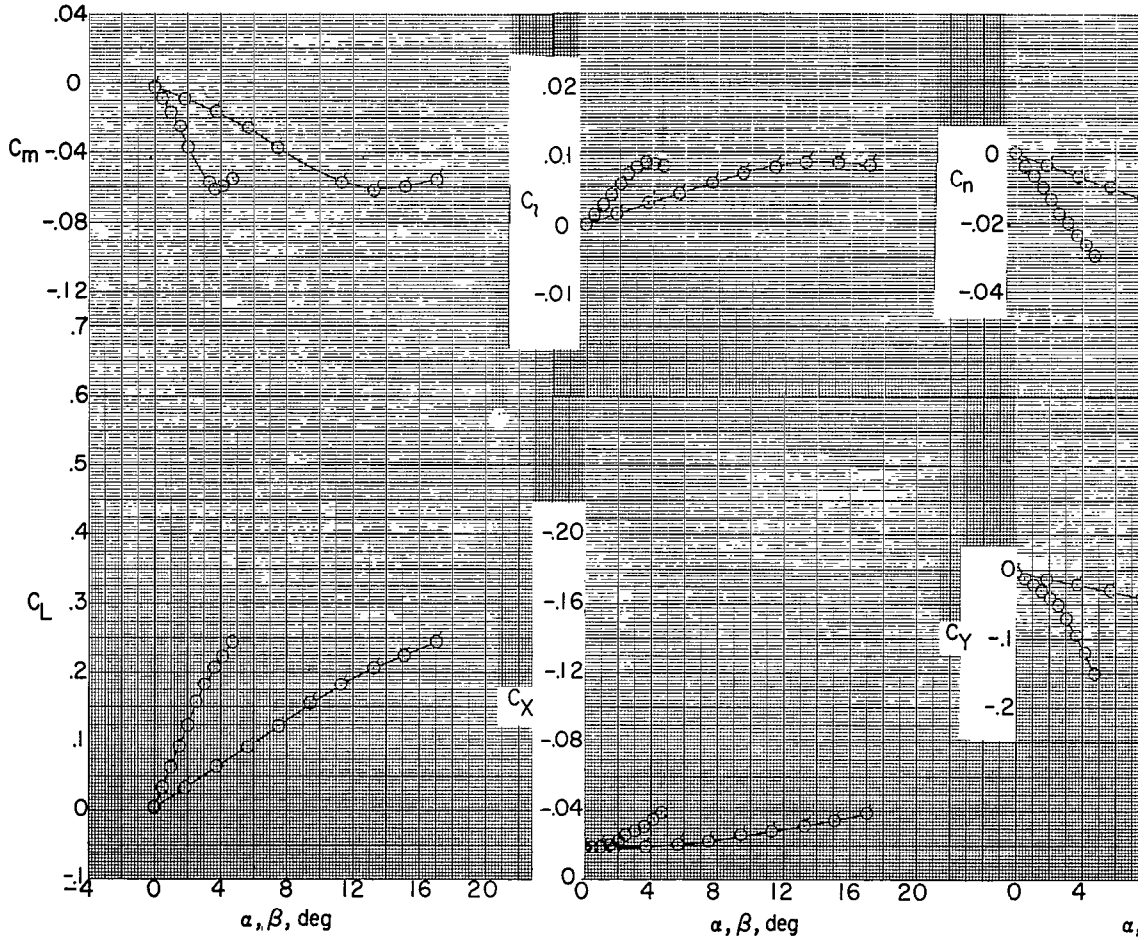

(f) $\phi = 75^{\circ}$.

Figure 4.- Continued.

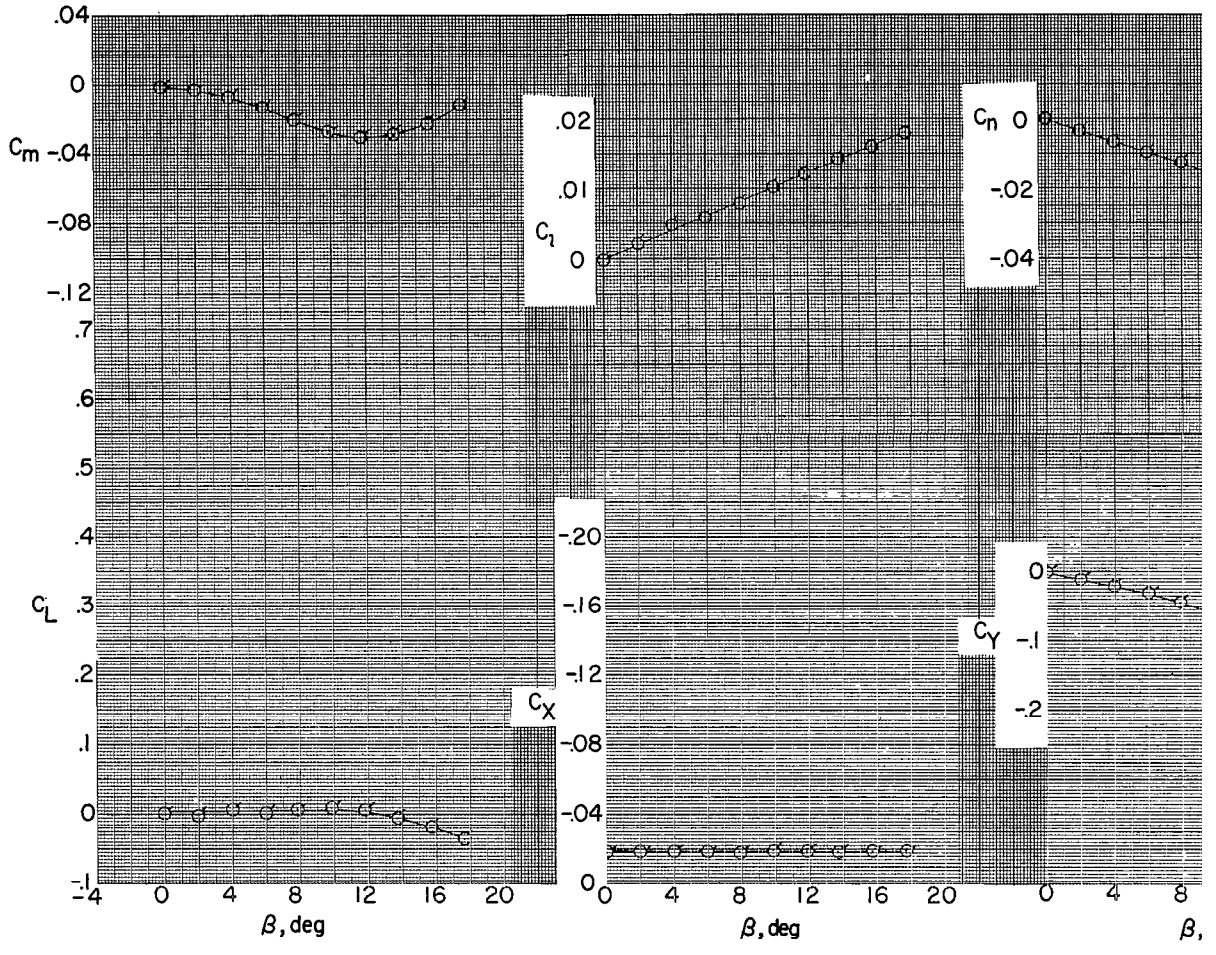

(g) $\phi = 90^{\circ}$.

Figure 4.- Concluded.

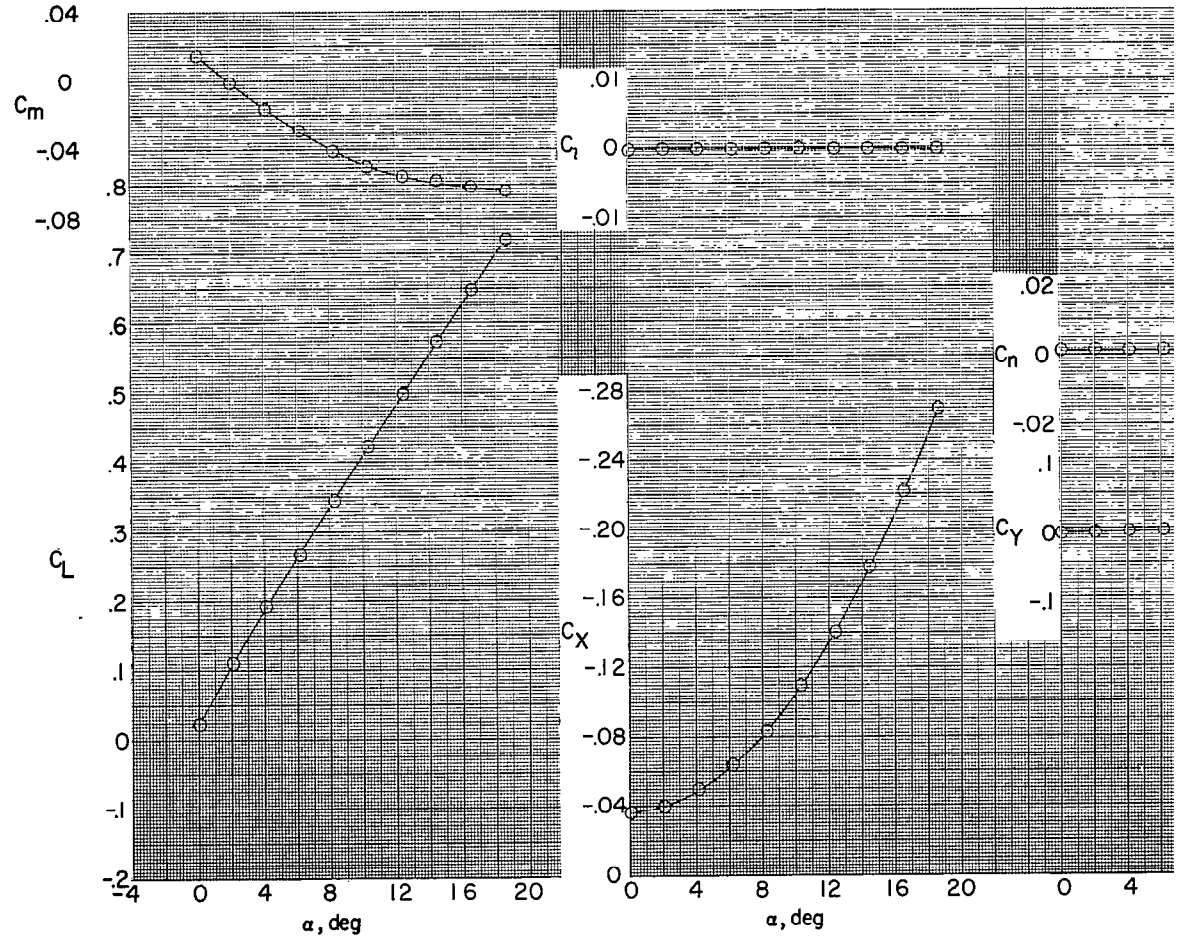

(a) $\phi = 0^{\circ}$.

Figure 5.- Aerodynamic characteristics at various roll angles. I horizontal tail off. Flagged symbols are for variations with unflagged symbols are for variations with α.

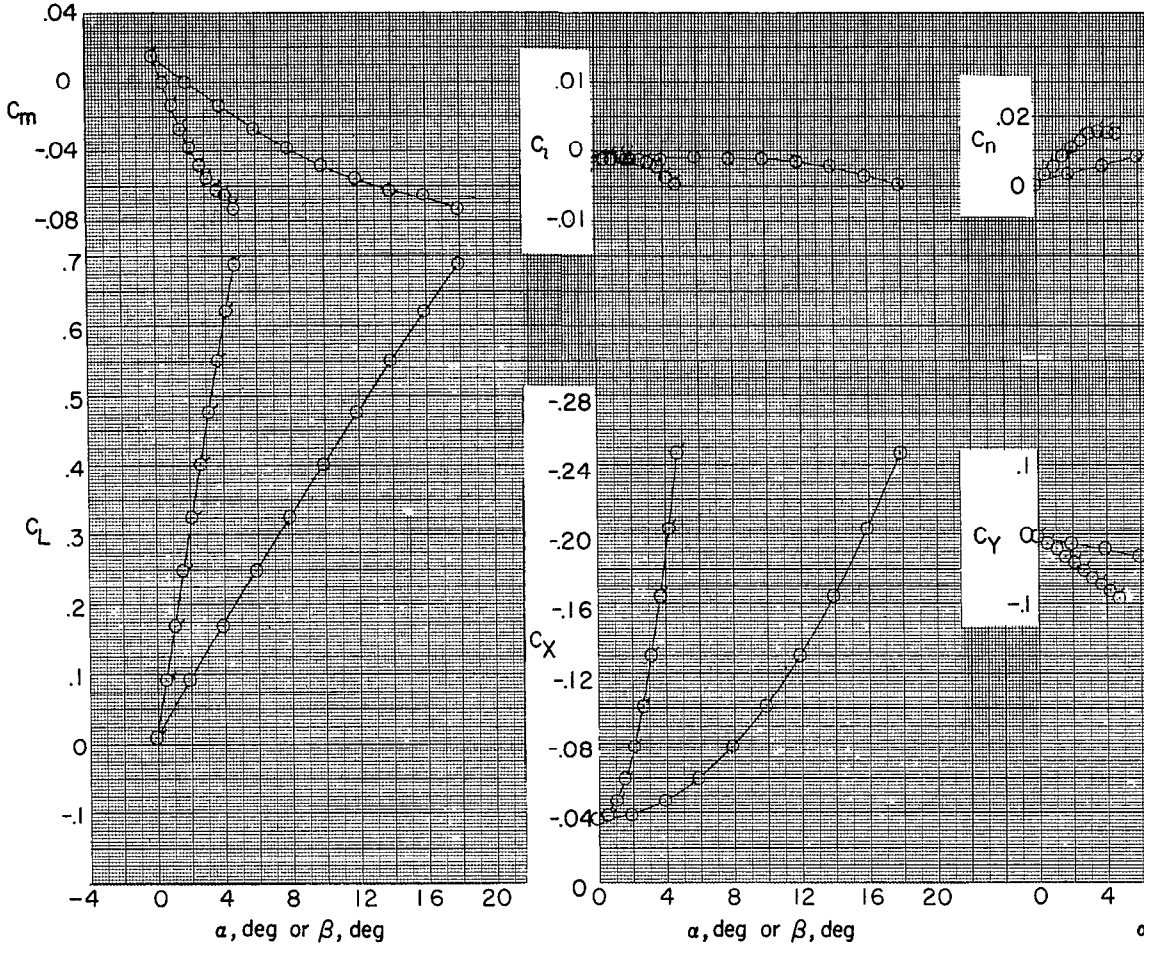

(b) $\phi = 15^{\circ}$.

Figure 5.- Continued.

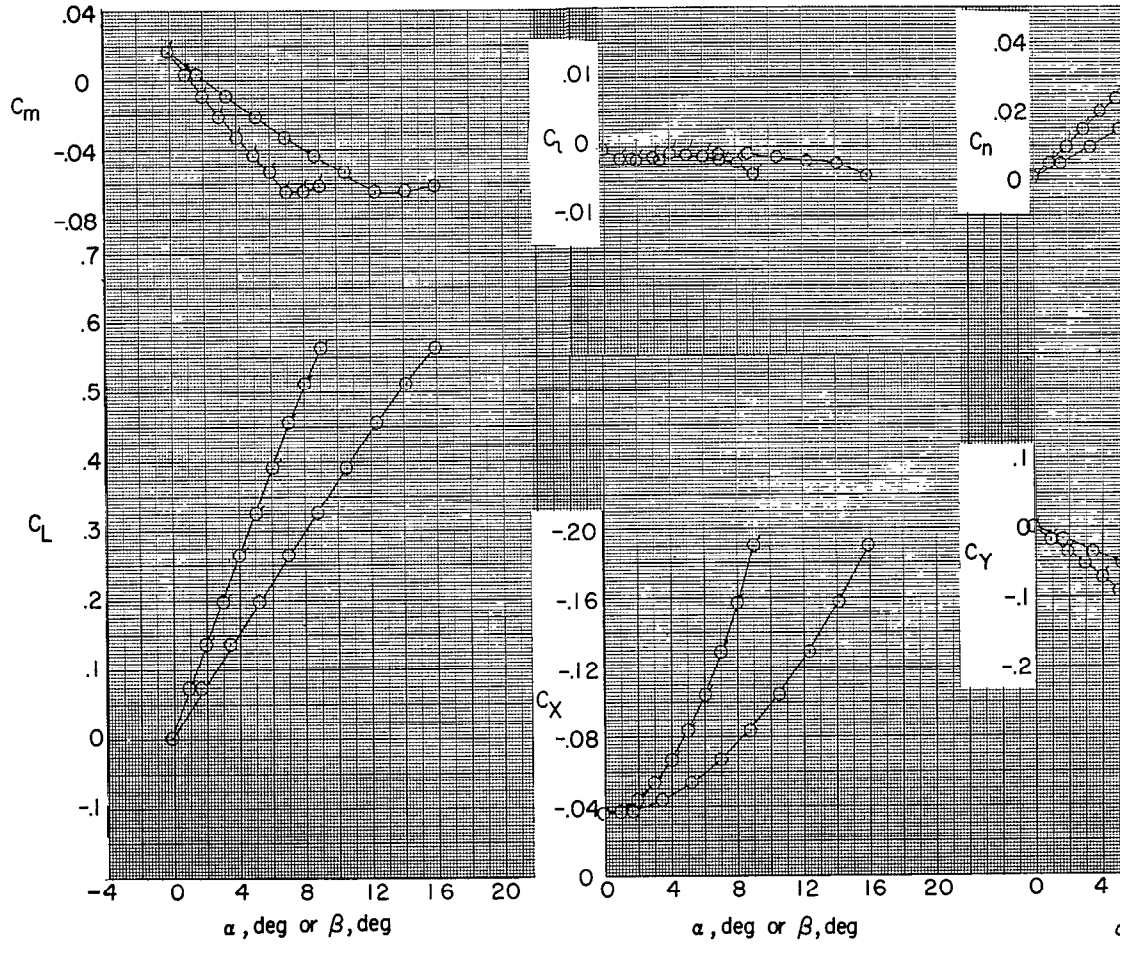

(c) $\phi = 30^{\circ}$.

Figure 5.- Continued.

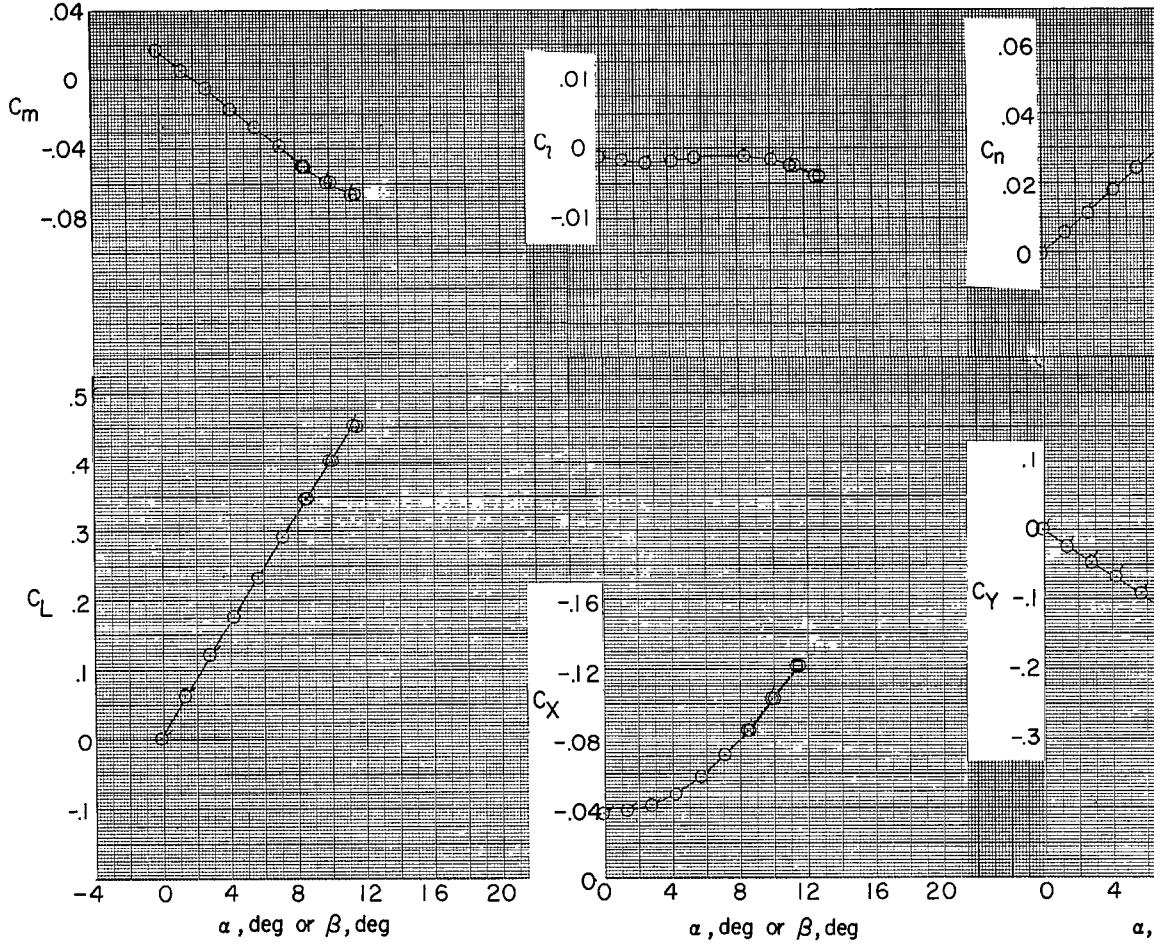

(d) $\phi = 45°$.

Figure 5.- Continued.

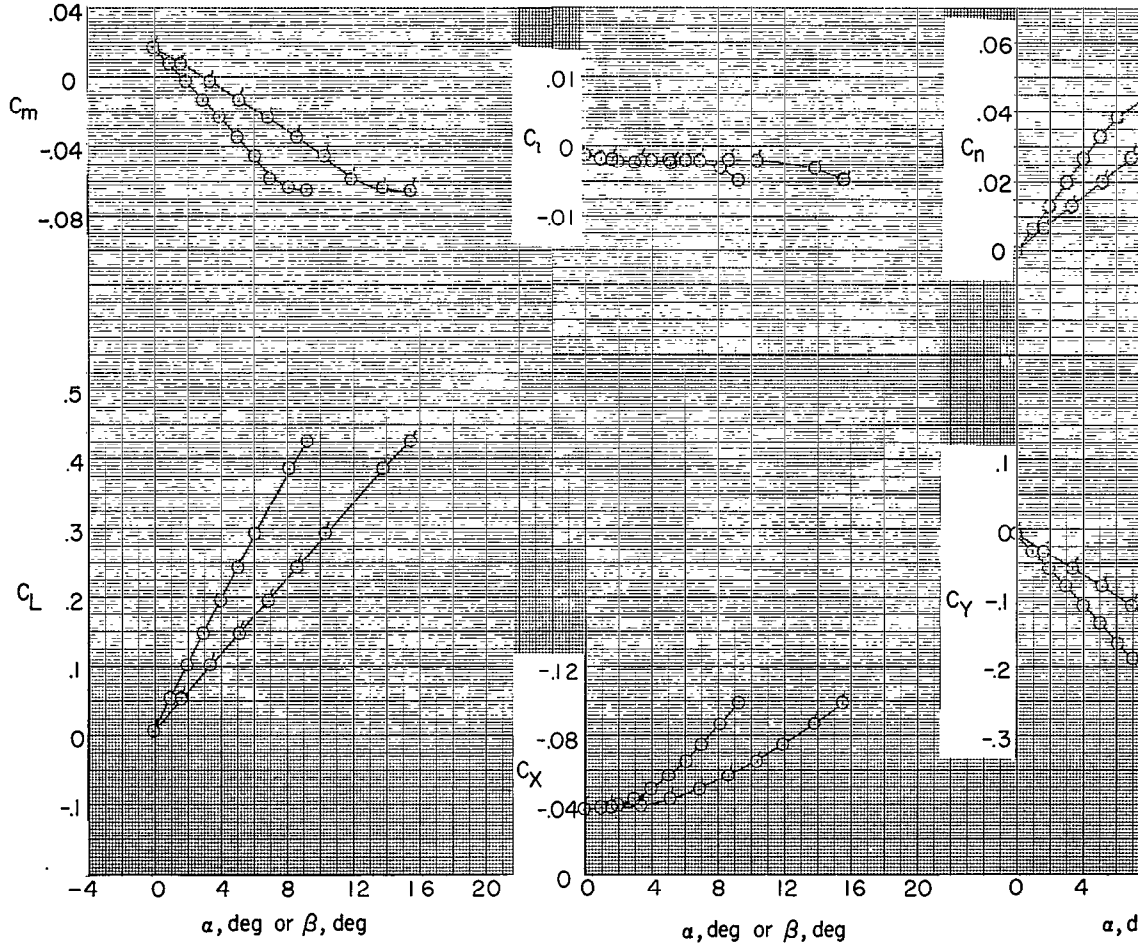

(e) $\phi = 60^{\circ}$.

Figure 5.- Continued.

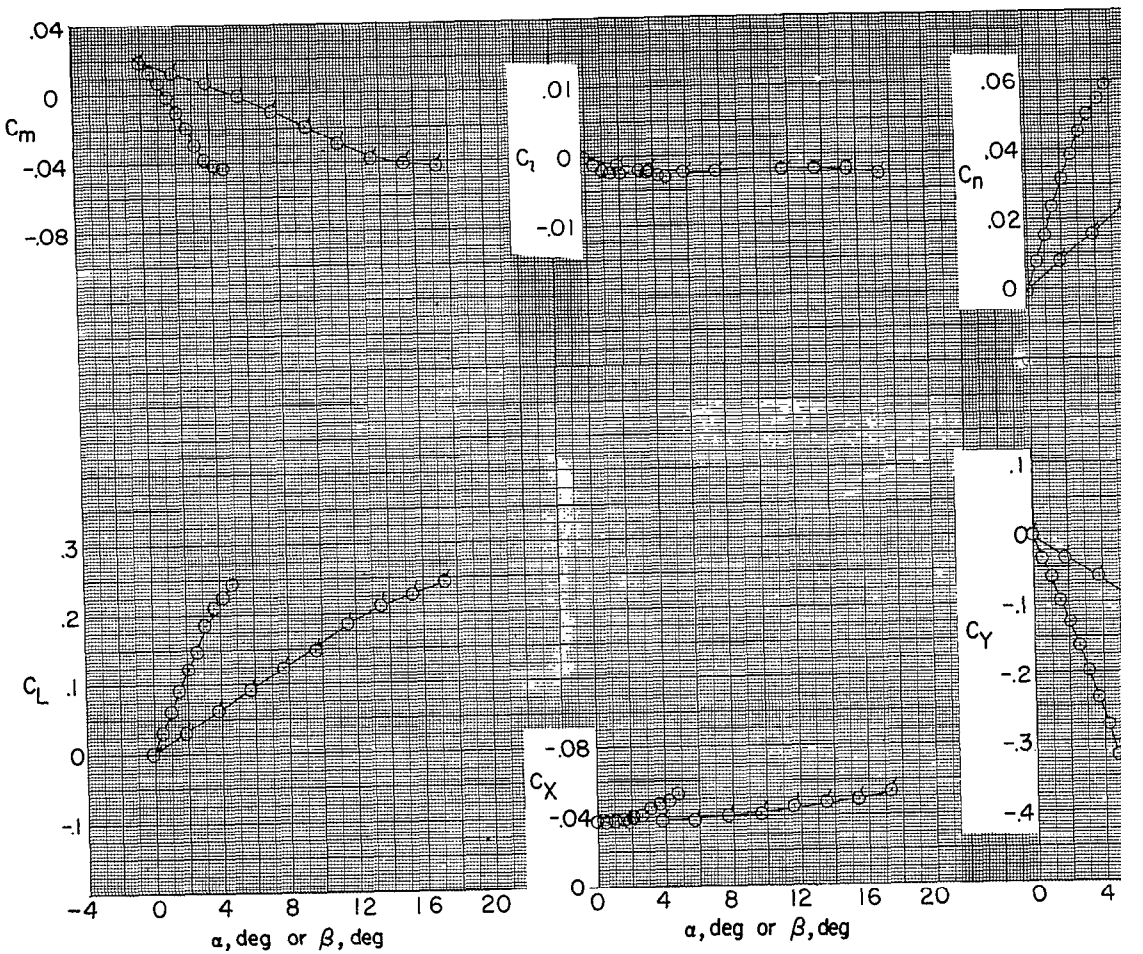

(f) $\phi = 75°$.

Figure 5.- Continued.

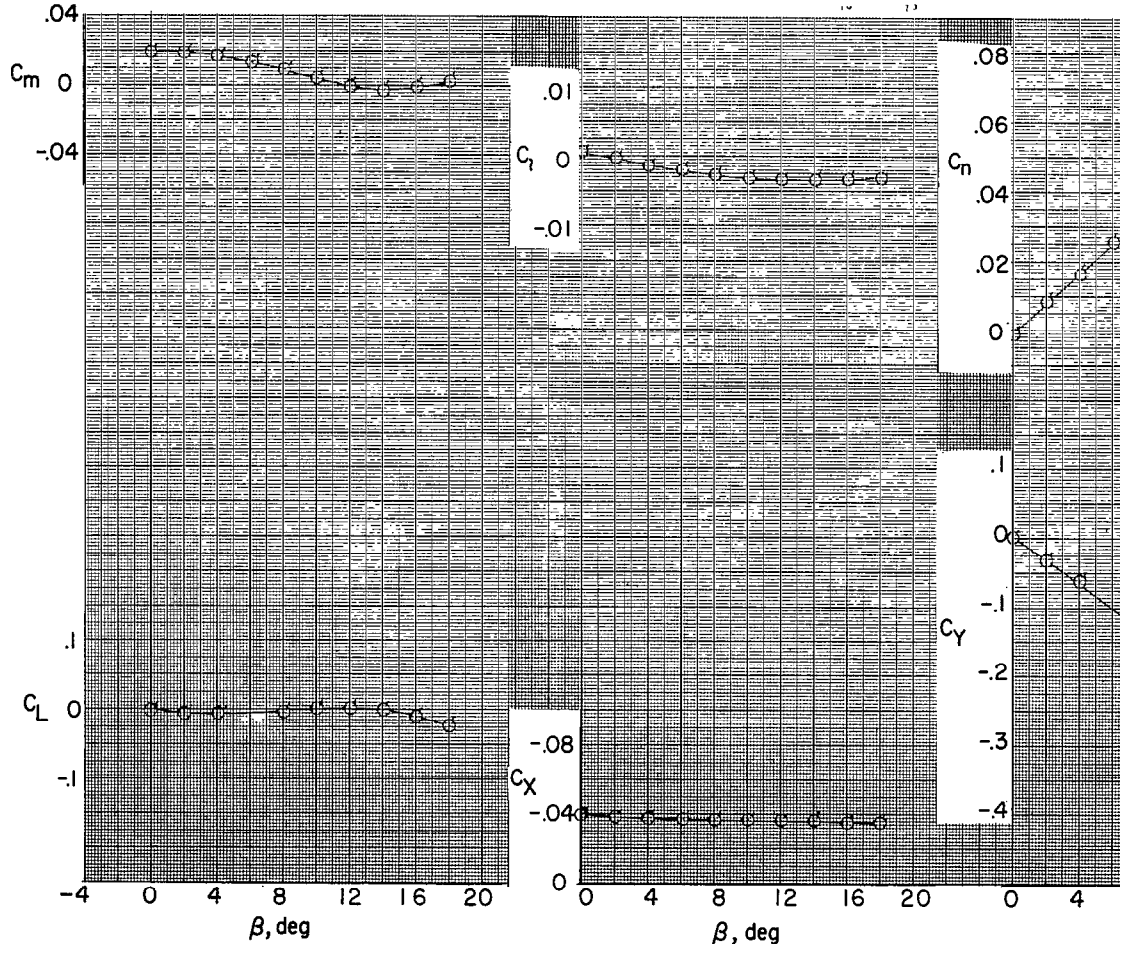

(g) $\phi = 90^{\circ}$.

Figure 5.- Concluded.

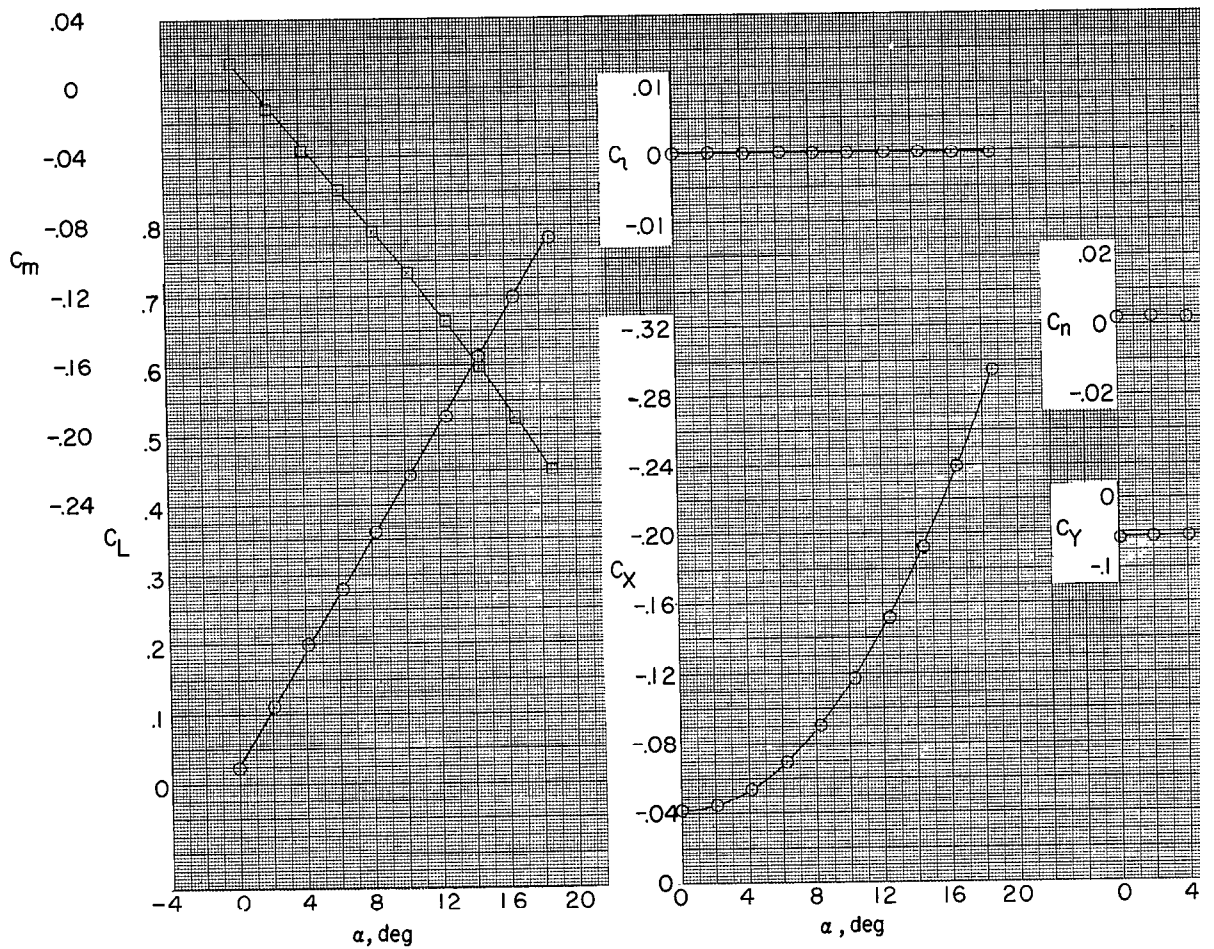

(a) $\phi = 0^{\circ}$.

Figure 6.- Aerodynamic characteristics at various roll angles. Lc
horizontal tail position 1; $i_t = 0^{\circ}$. Flagged symbols are for v
with β; unflagged symbols are for variations with α.

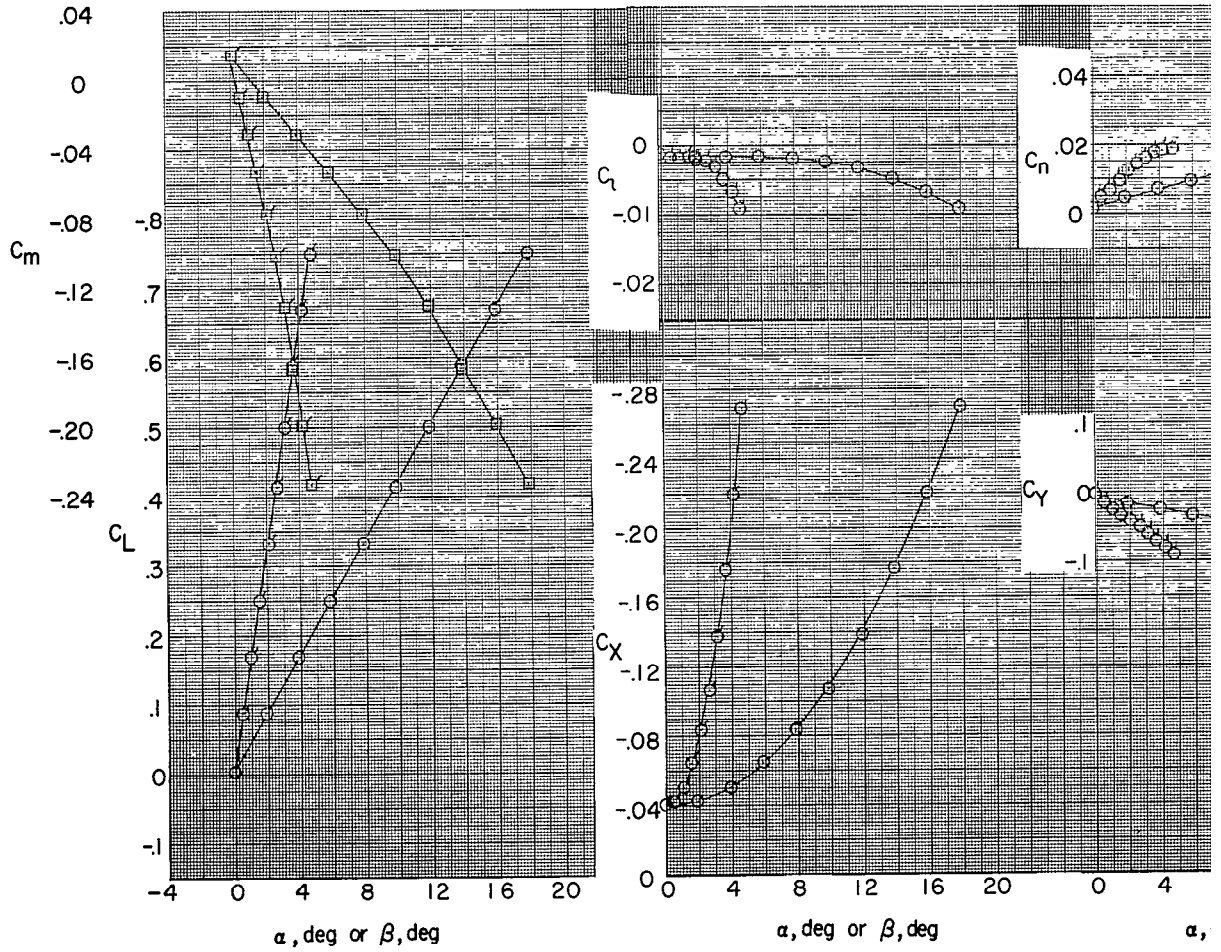

(b) $\phi = 15^\circ$.

Figure 6.- Continued.

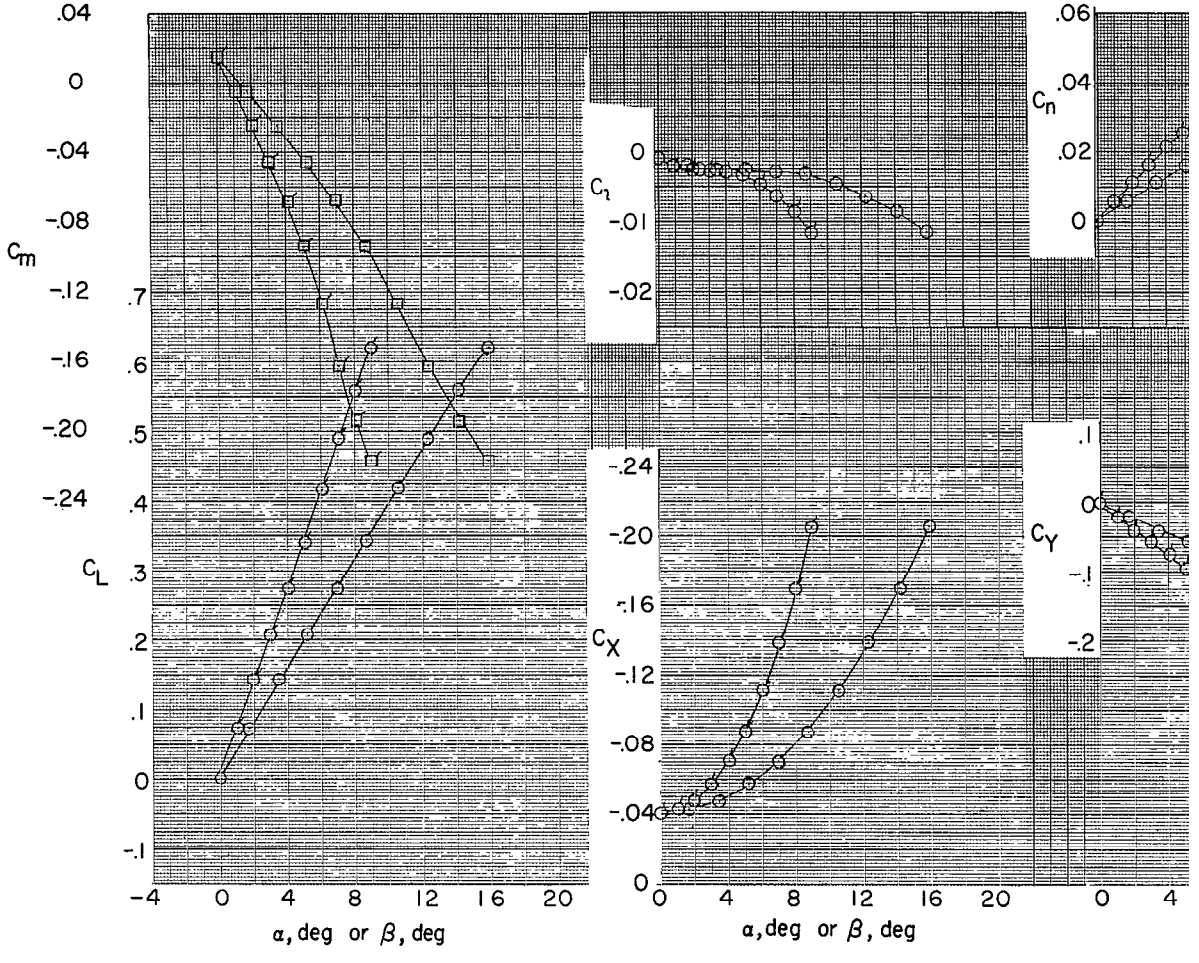

(c) $\phi = 30^{\circ}$.

Figure 6.- Continued.

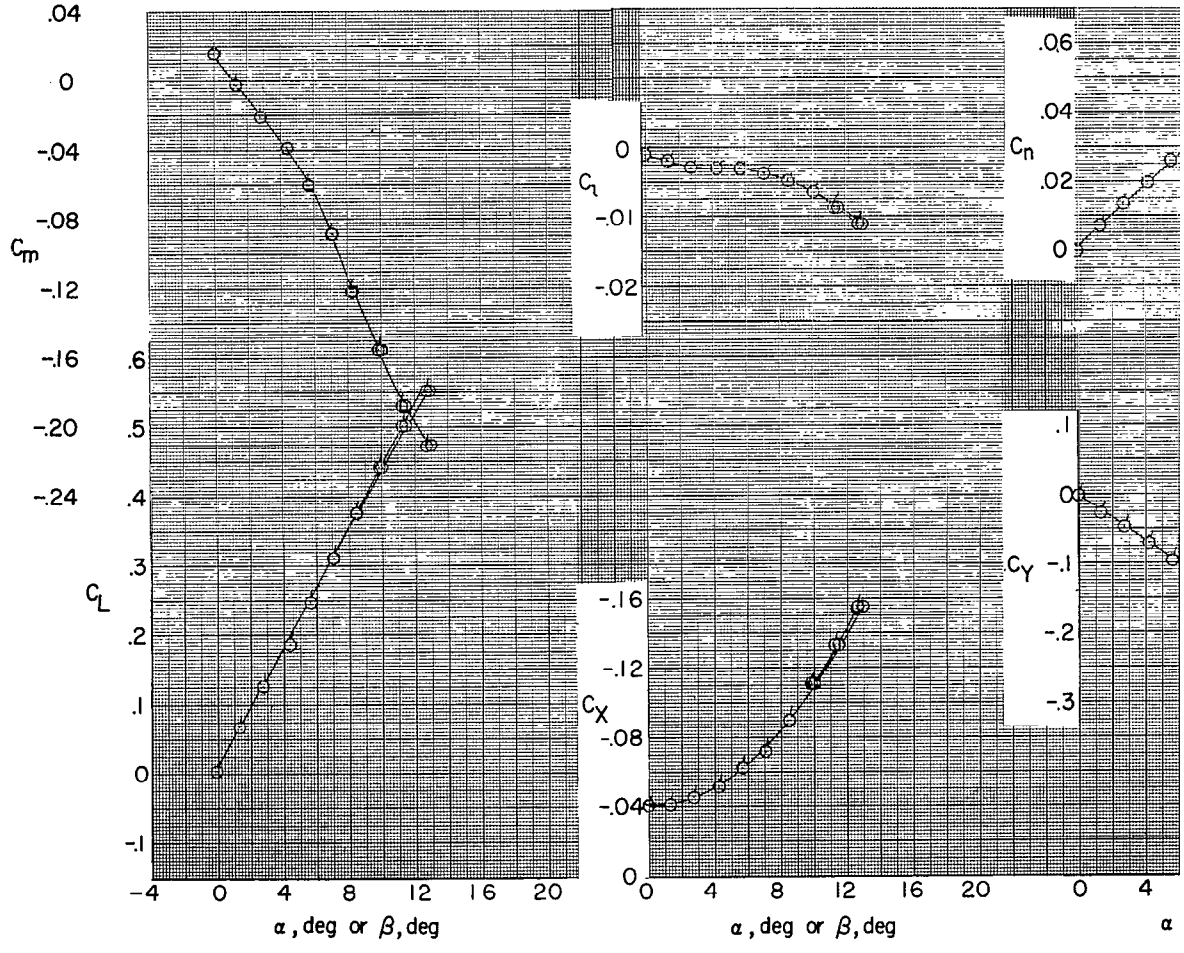

(d) $\phi = 45^\circ$.

Figure 6.- Continued.

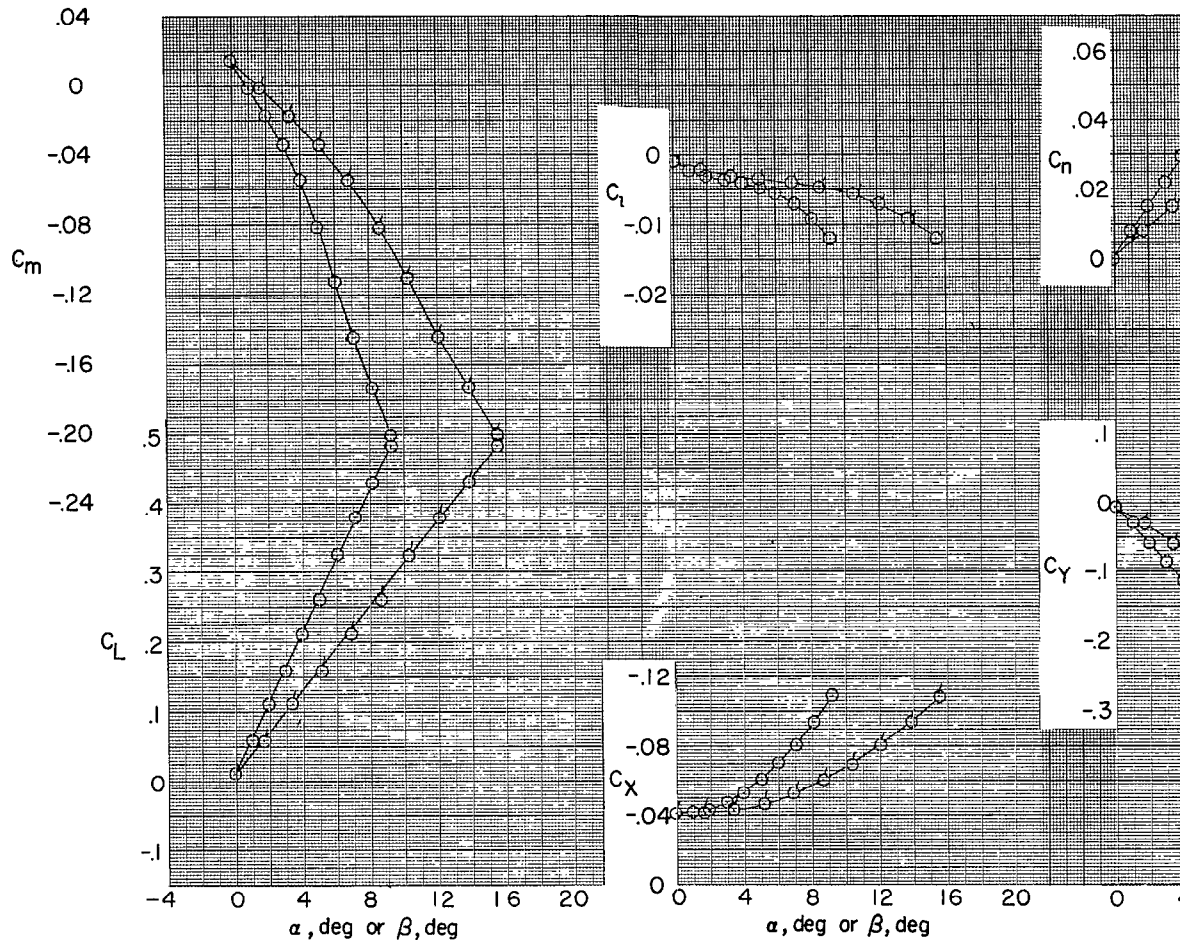

(e) $\phi = 60^{\circ}$.

Figure 6.- Continued.

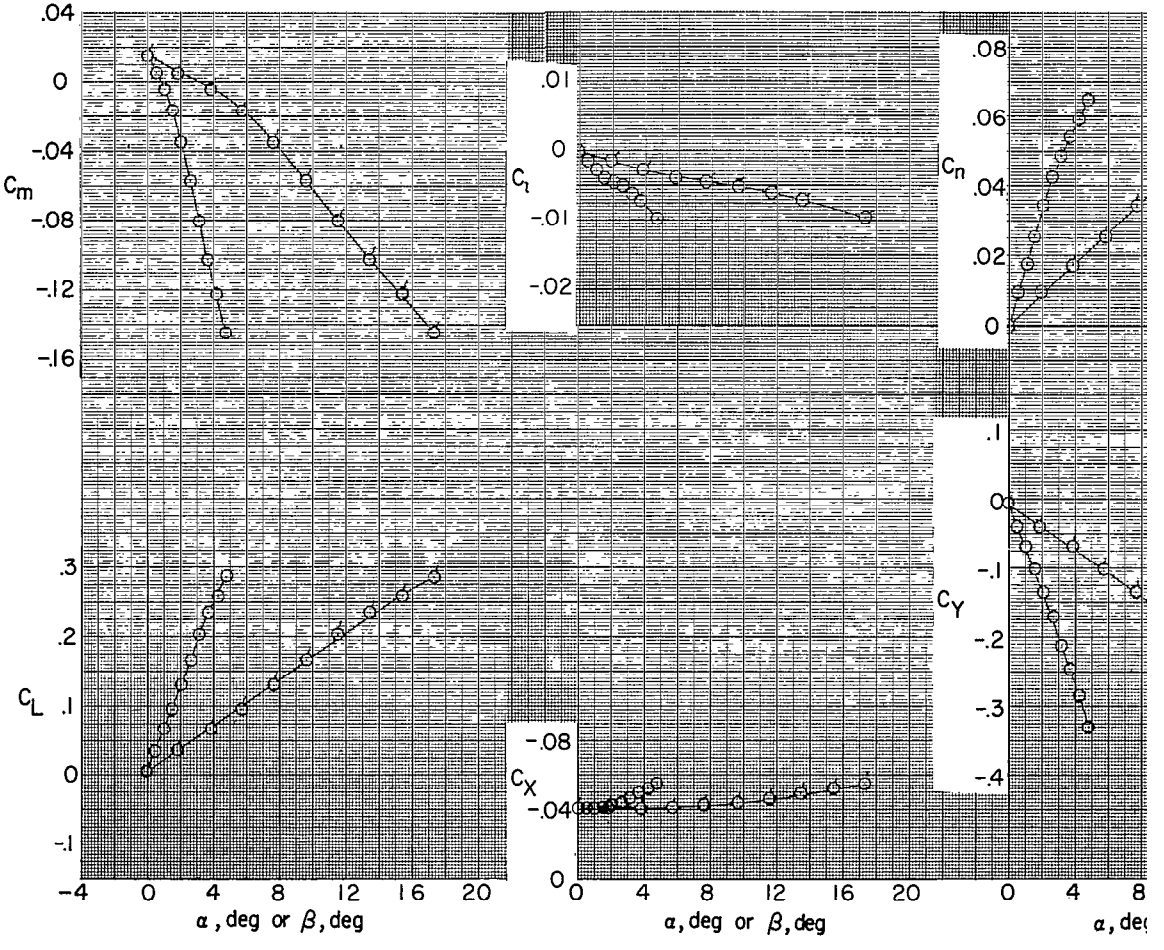

(f) $\phi = 75^{\circ}$.

Figure 6.- Continued.

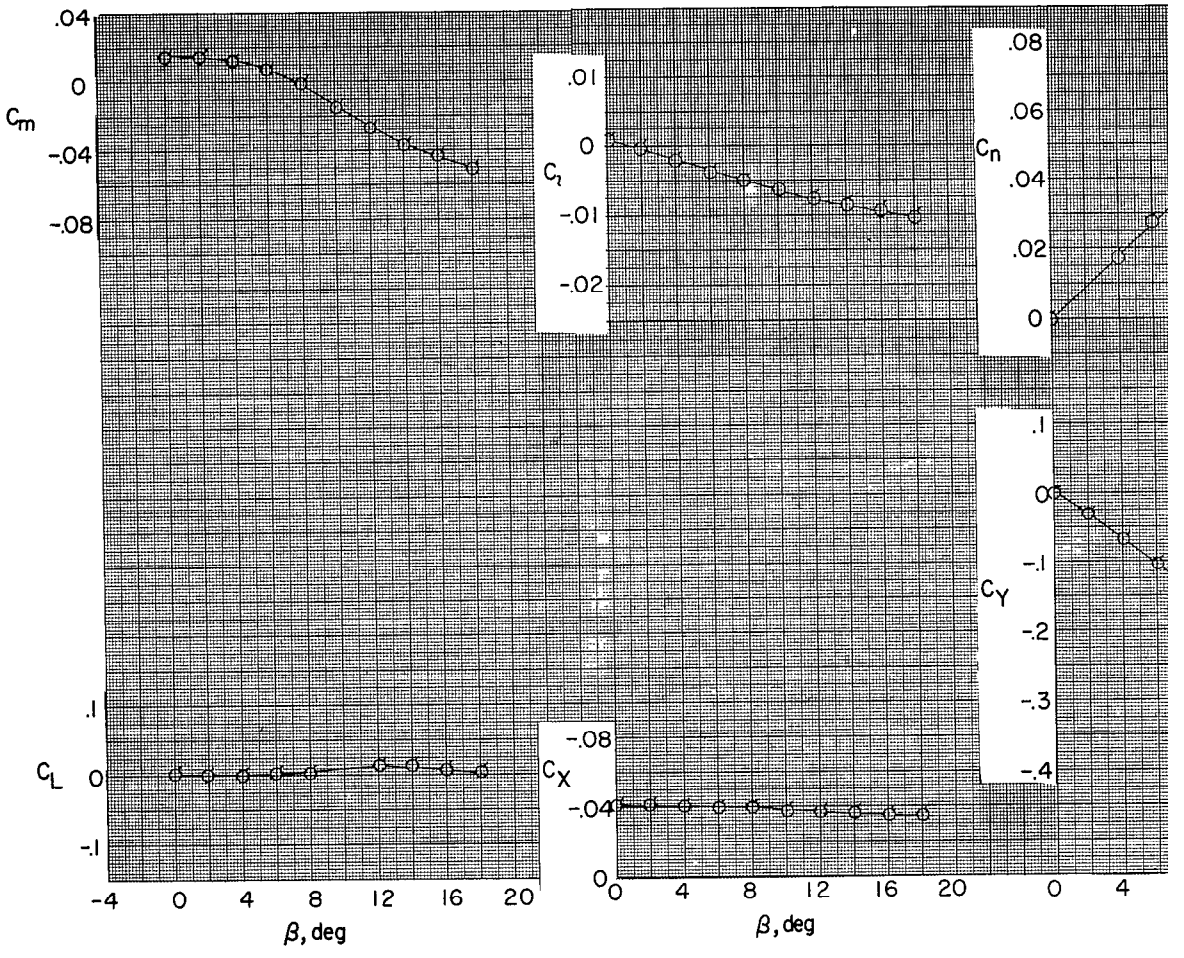

(g) $\phi = 90^{\circ}$.

Figure 6.- Concluded.

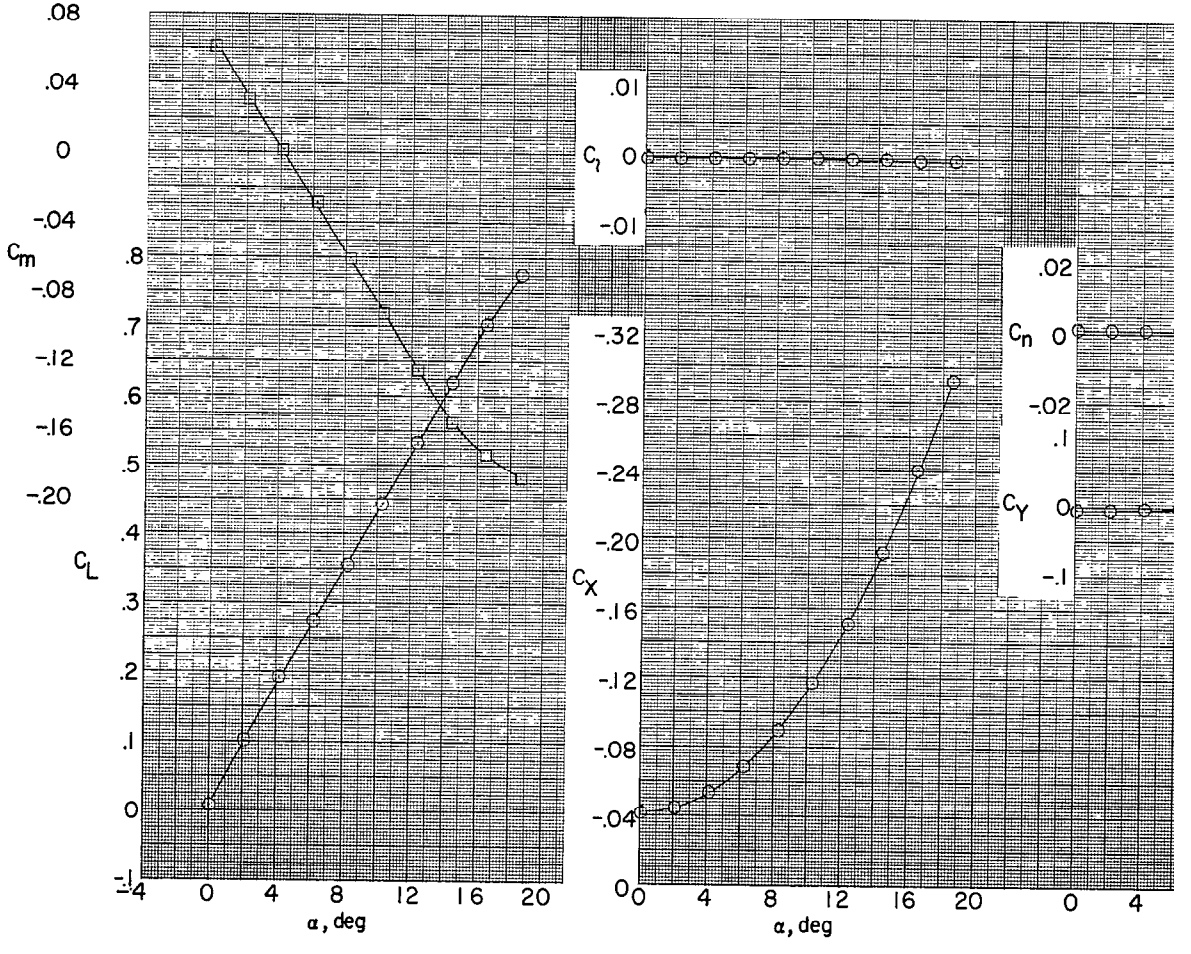

(a) $\phi = 0^{\circ}$.

Figure 7.- Aerodynamic characteristics at various roll angles. Lo horizontal tail position 2; $i_t = 0^{\circ}$. Flagged symbols are for v with β; unflagged symbols are for variations with α.

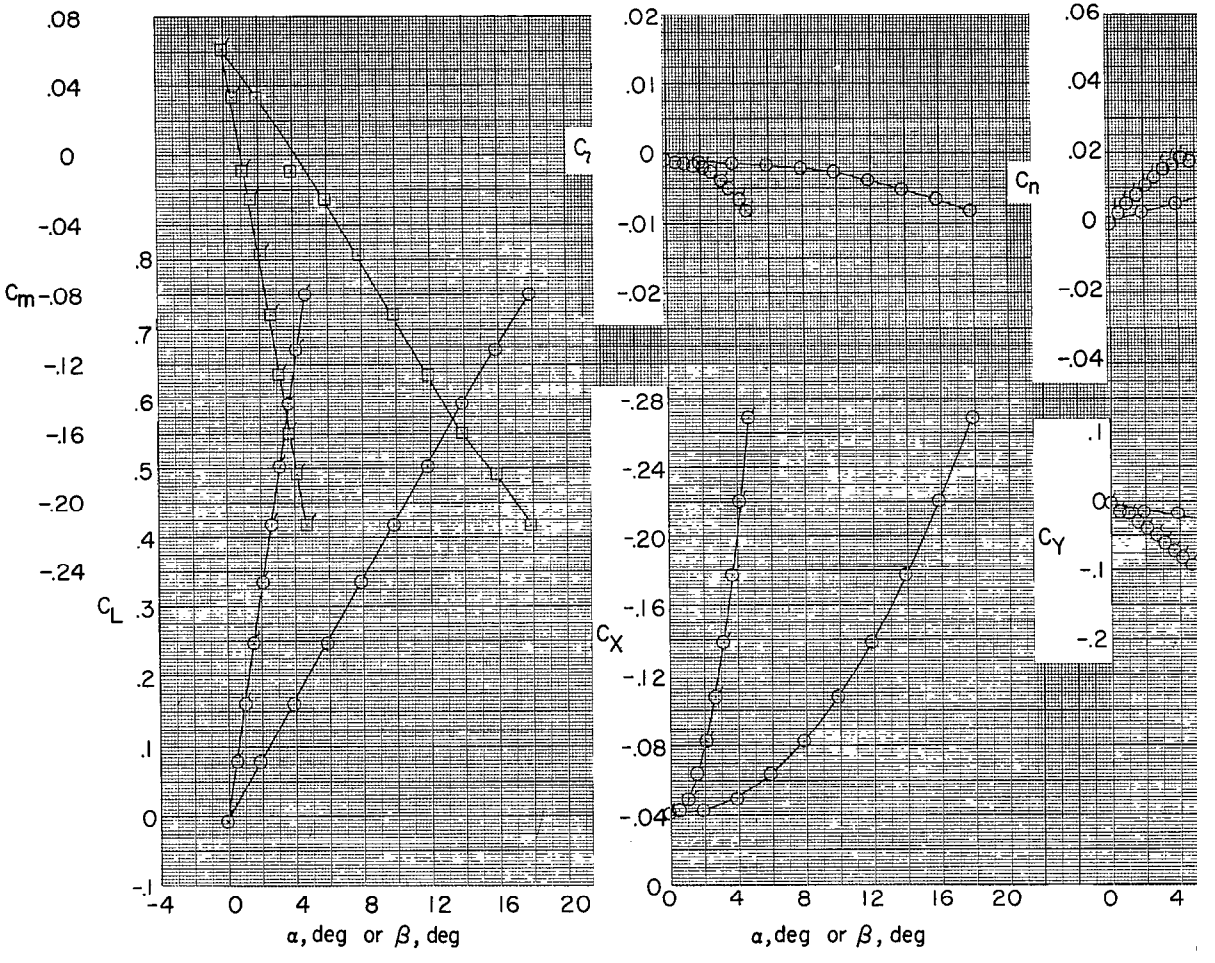

(b) $\phi = 15^\circ$.

Figure 7.- Continued.

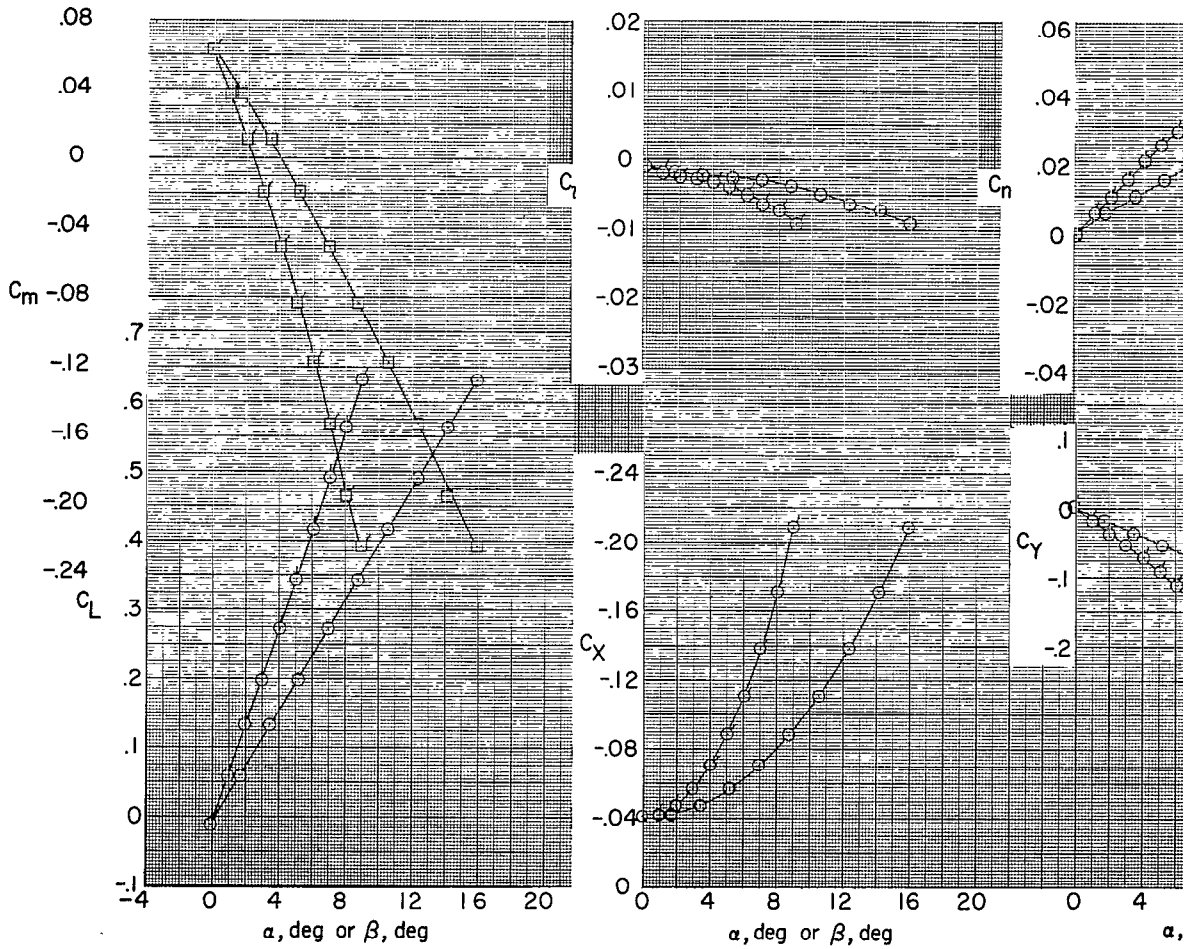

(c) $\phi = 30^{\circ}$.

Figure 7.- Continued.

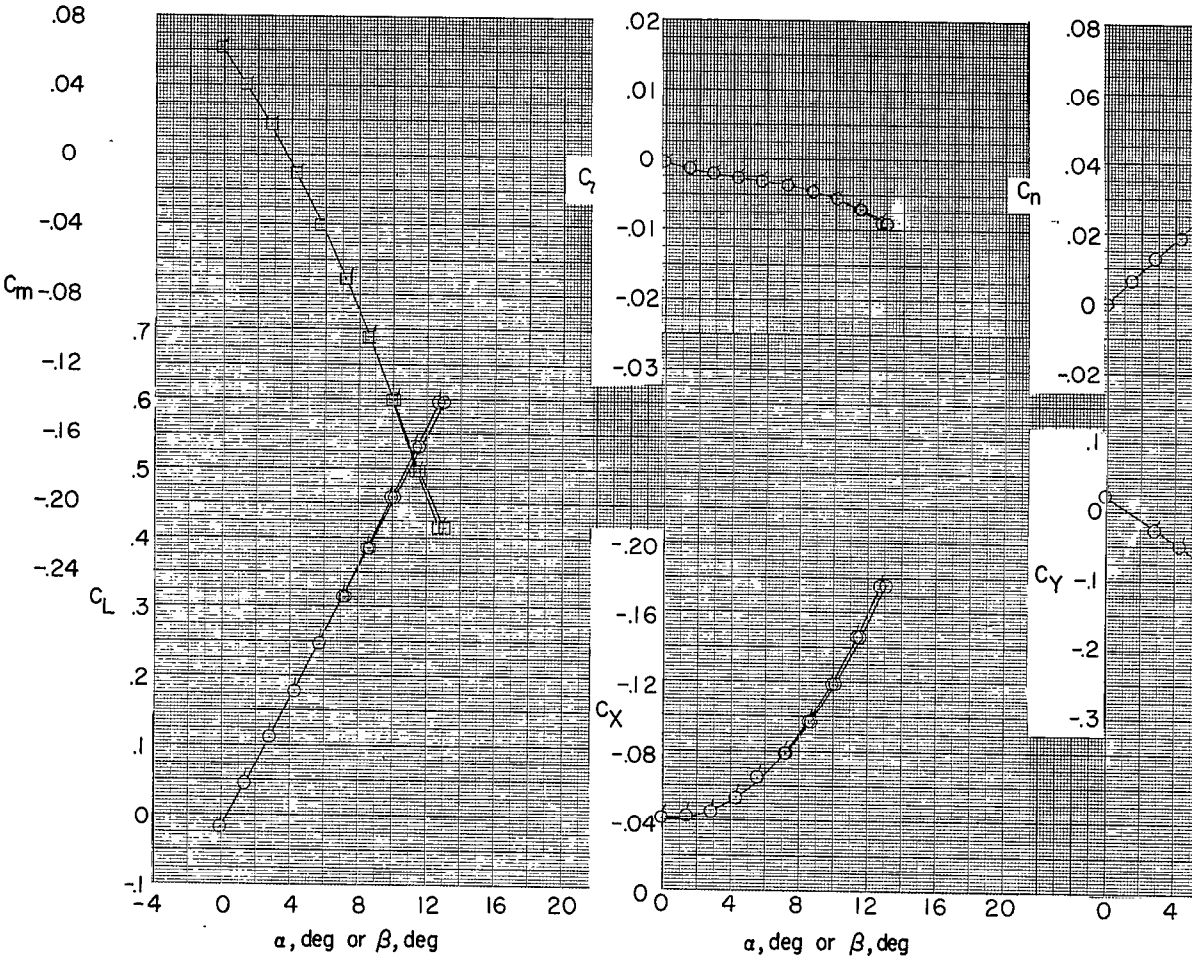

(d) $\phi = 45^{\circ}$.

Figure 7.- Continued.

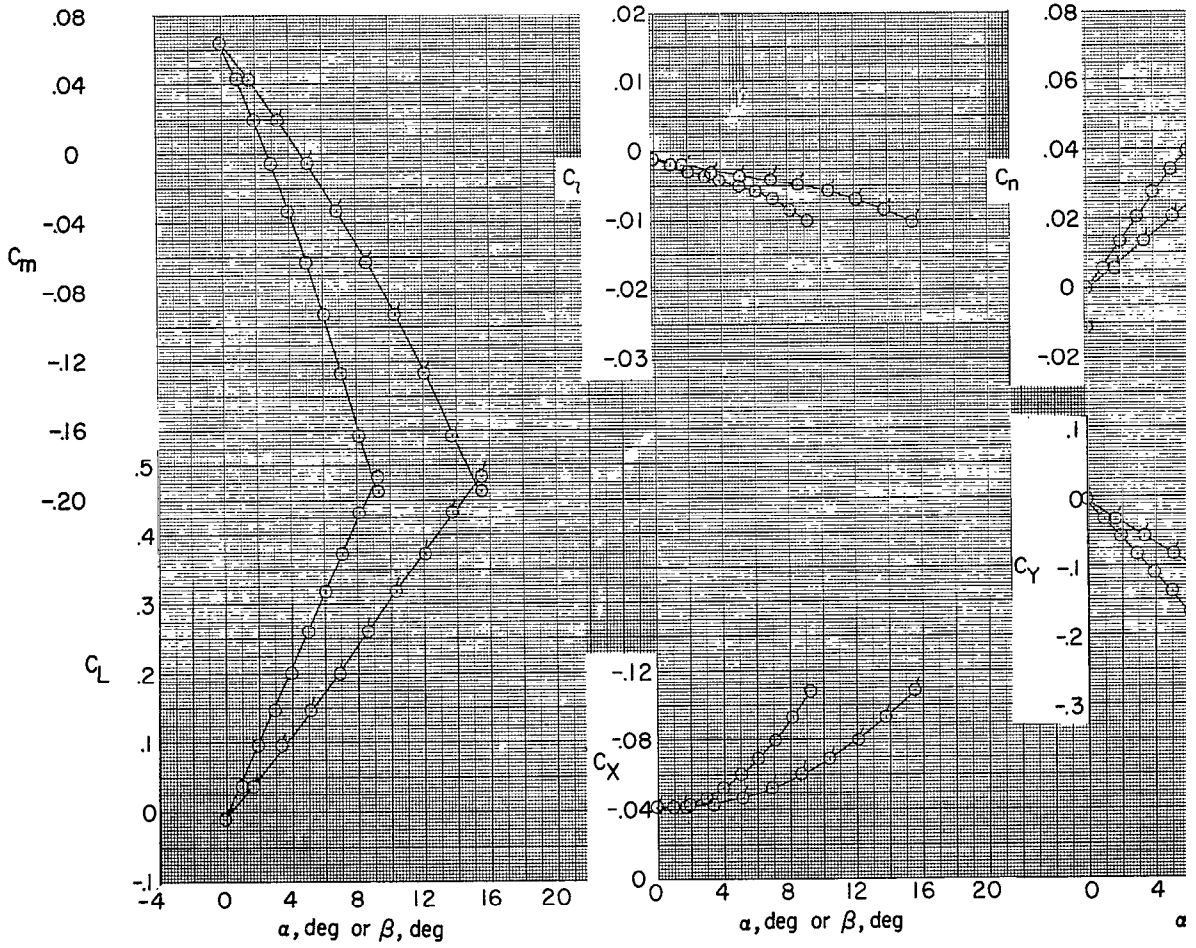

(e) $\phi = 60^{\circ}$.

Figure 7.- Continued.

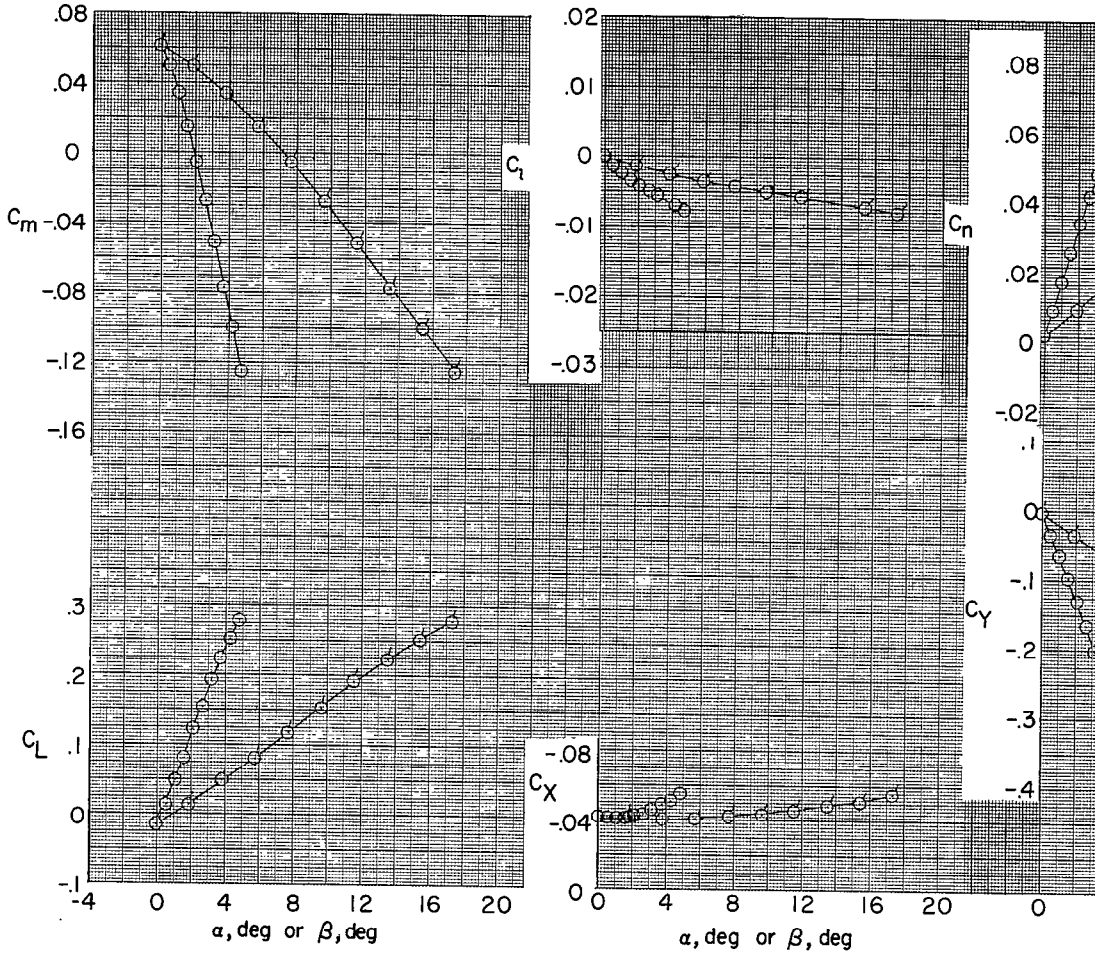

(f) $\phi = 75^{\circ}$.

Figure 7.- Continued.

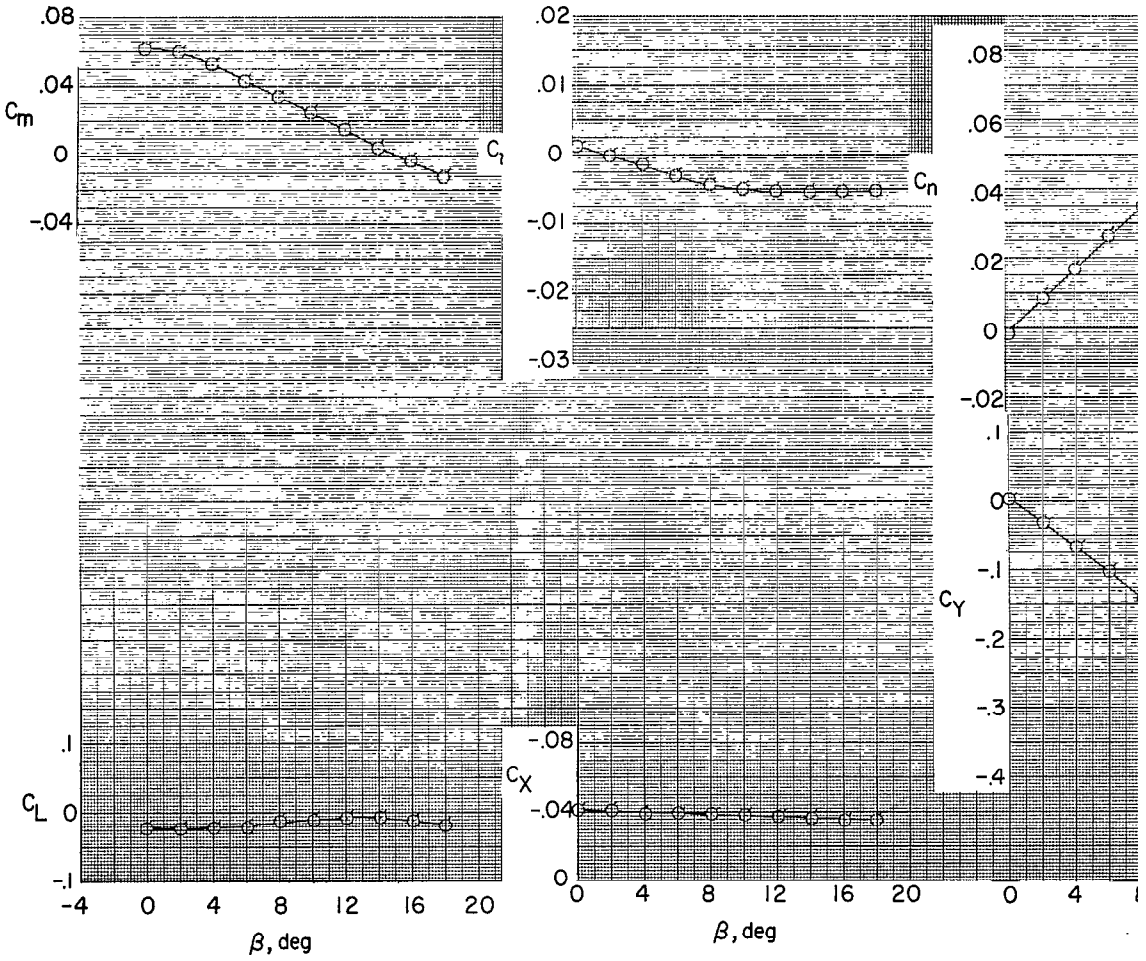

(g) $\phi = 90^{\circ}$.

Figure 7.- Concluded.

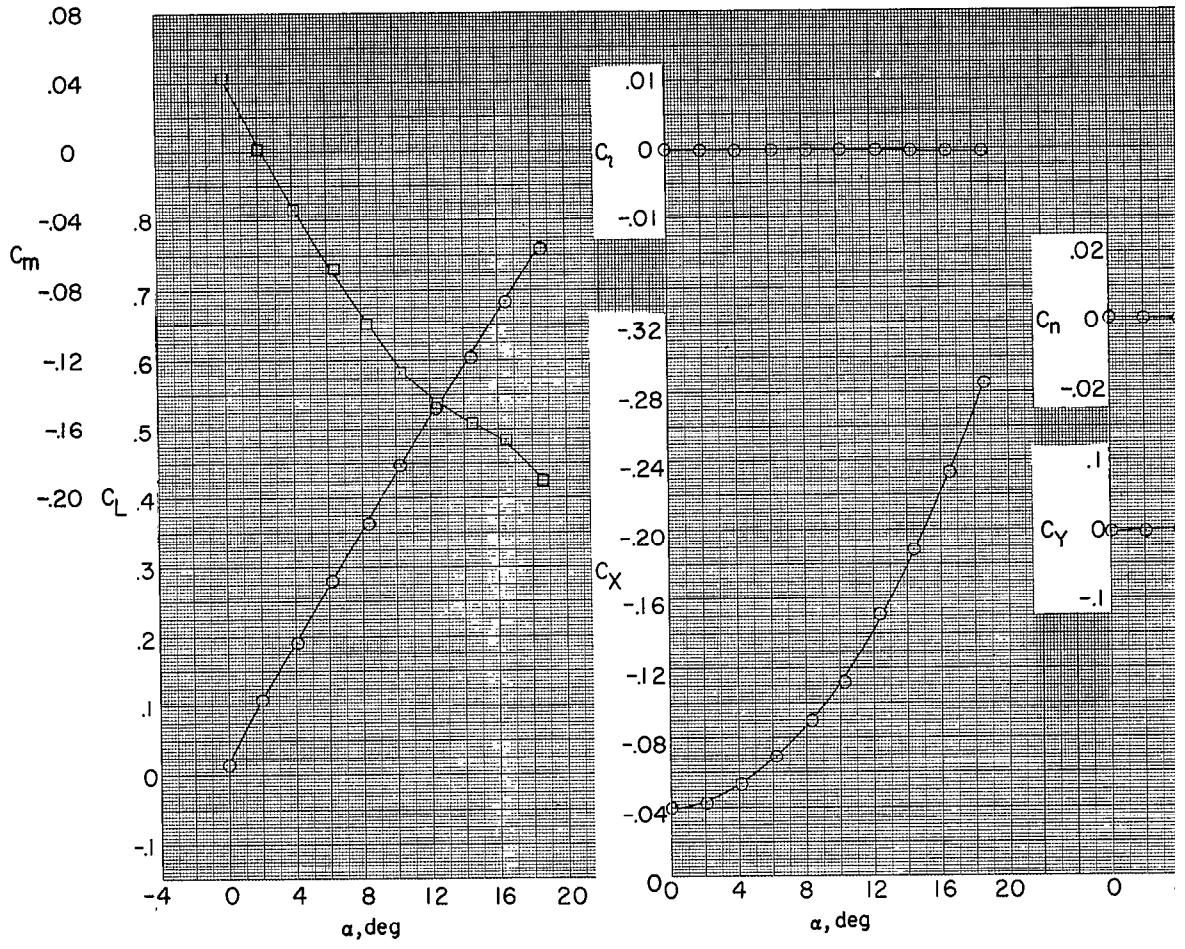

(a) $\phi = 0^{\circ}$.

Figure 8.- Aerodynamic characteristics at various roll angles. horizontal tail position 3; $i_t = 0^{\circ}$. Flagged symbols are f with β; unflagged symbols are for variations with α.

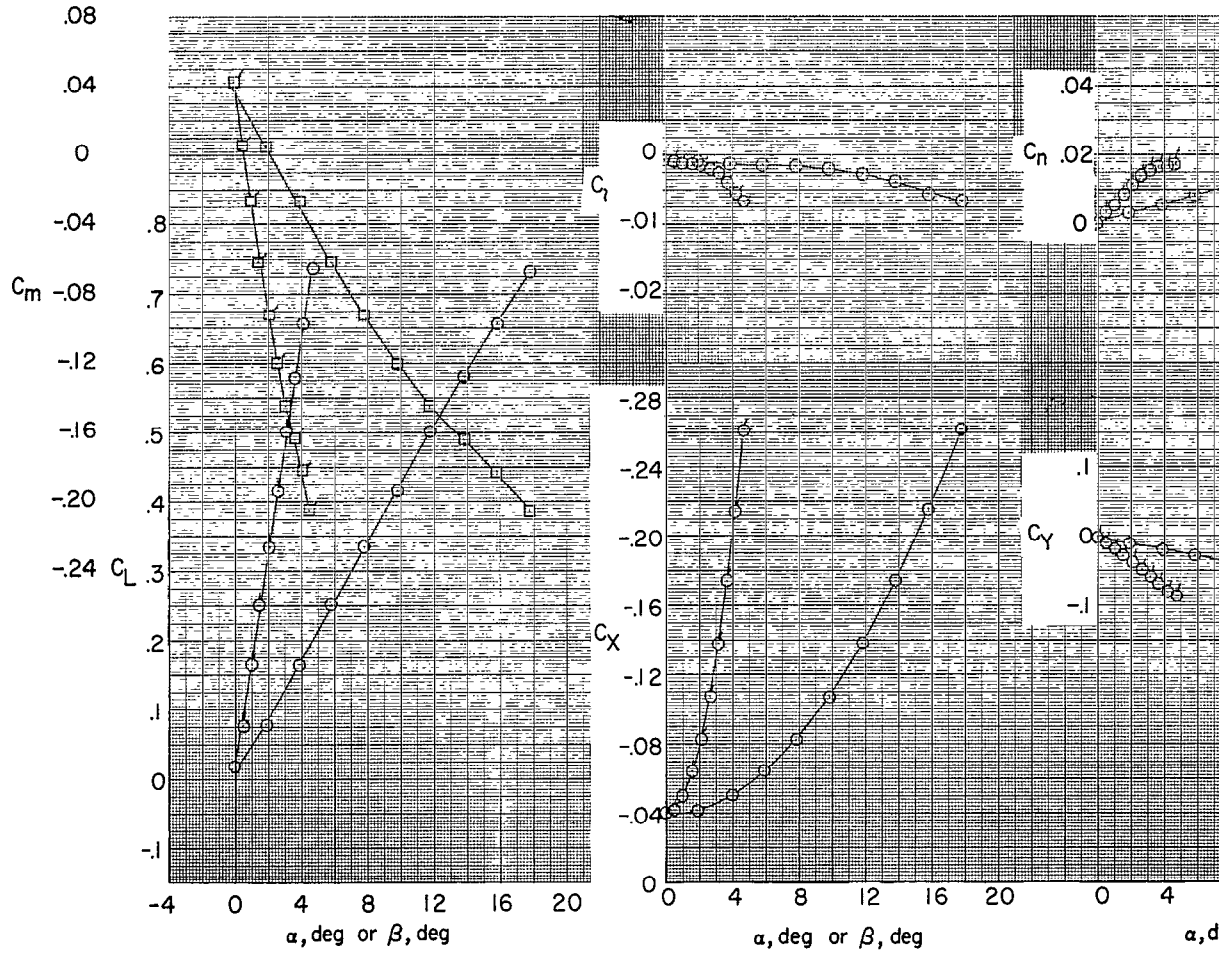

(b) $\phi = 15^{\circ}$.

Figure 8.- Continued.

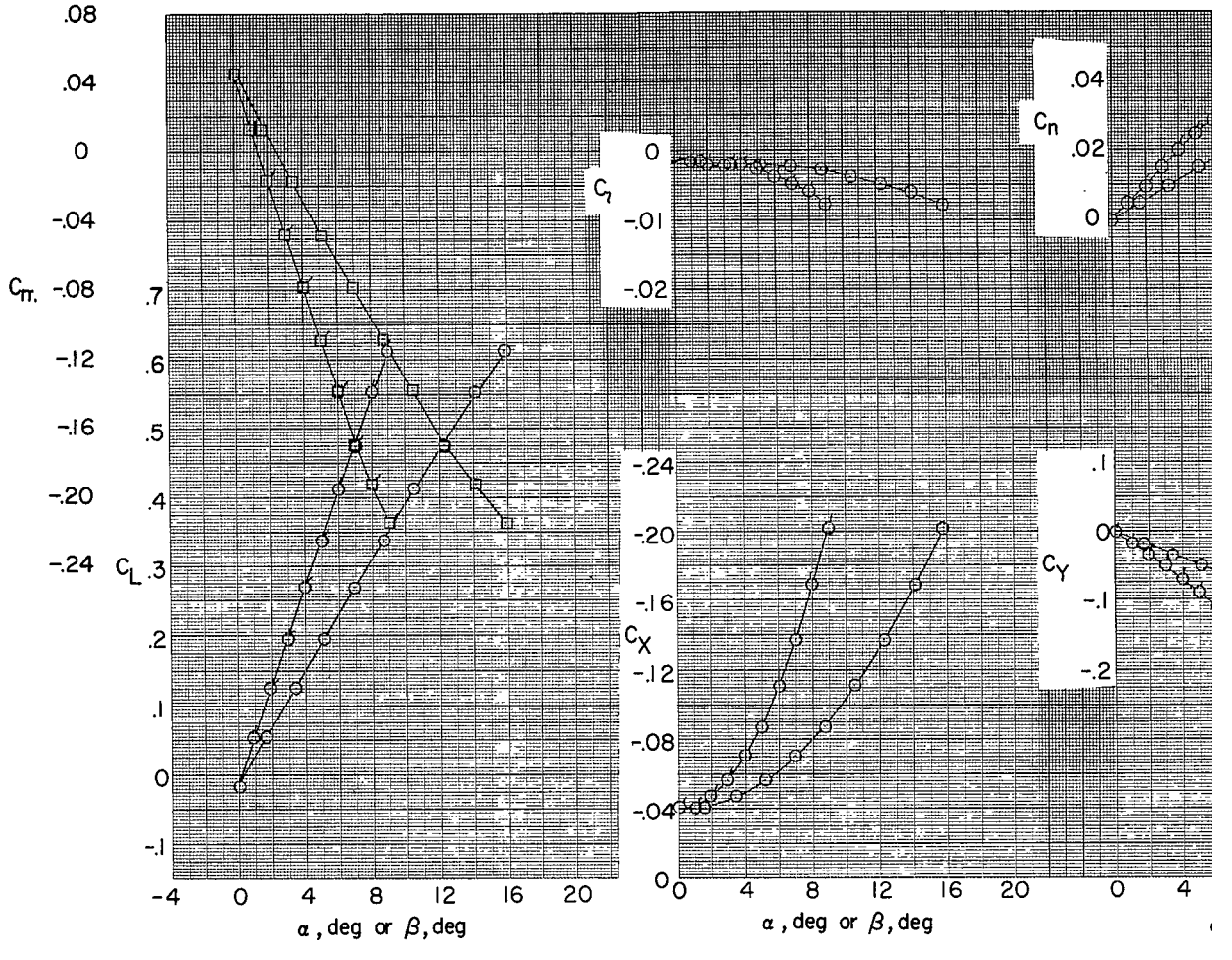

(c) $\phi = 30^{\circ}$.

Figure 8.- Continued.

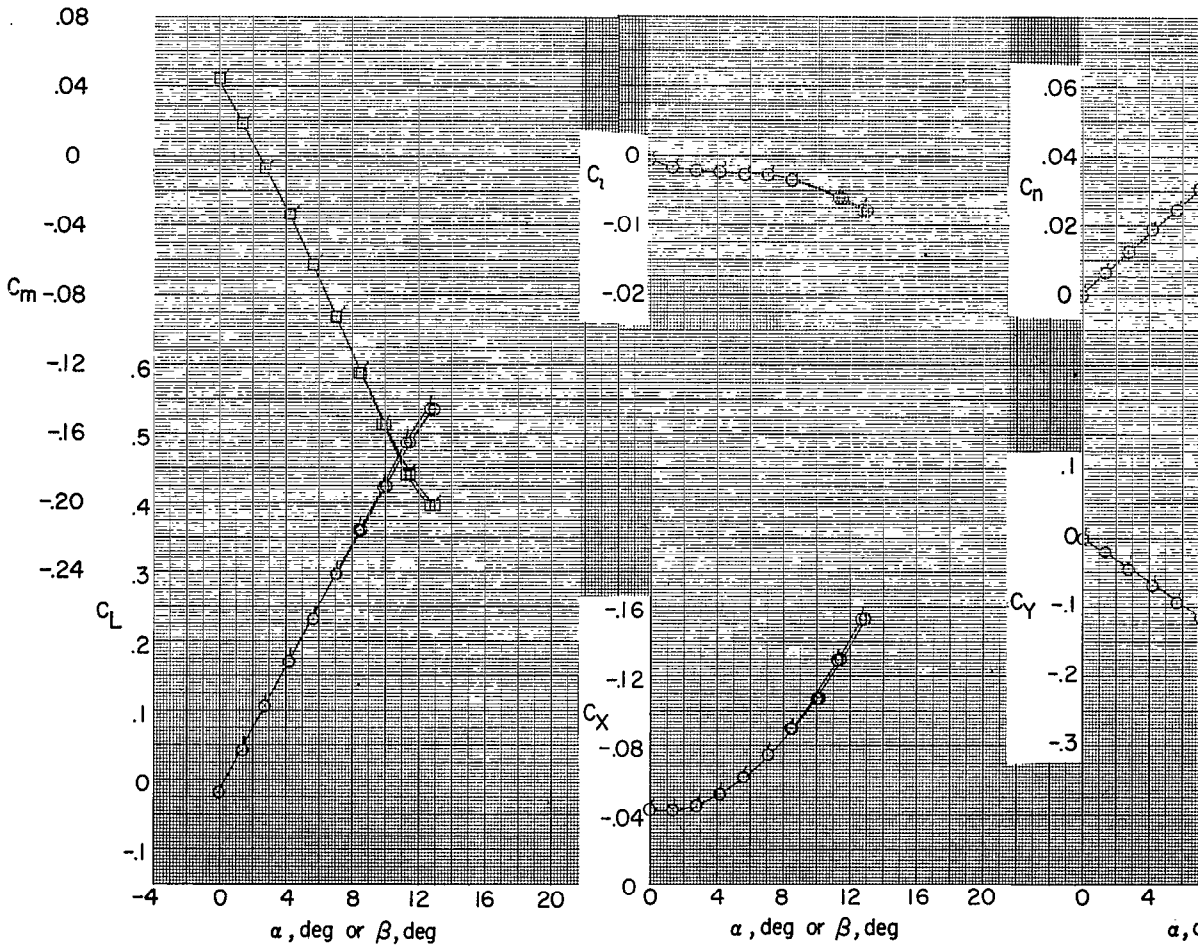

(d) $\phi = 45°$.

Figure 8.- Continued.

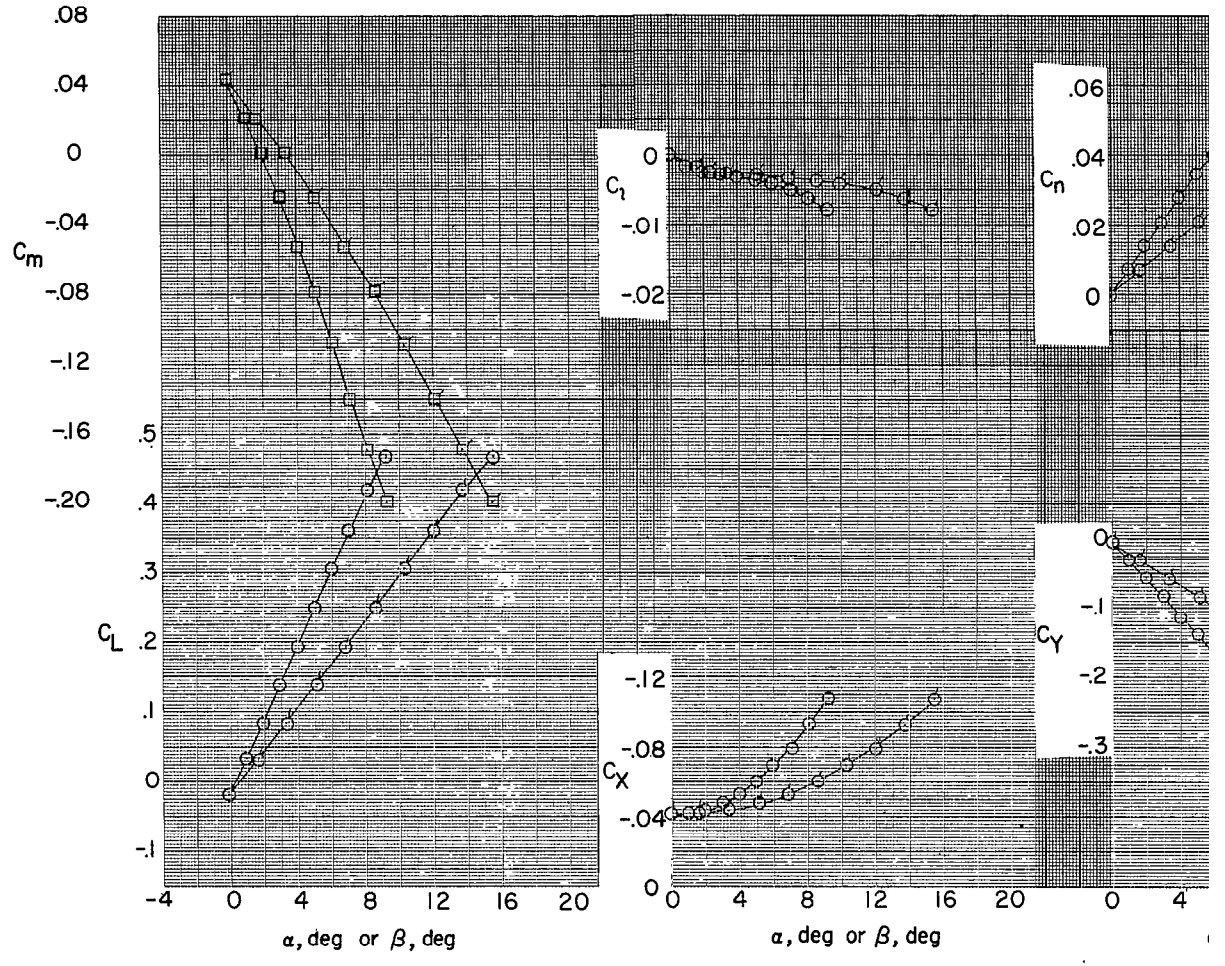

(e) $\phi = 60^{\circ}$.

Figure 8.- Continued.

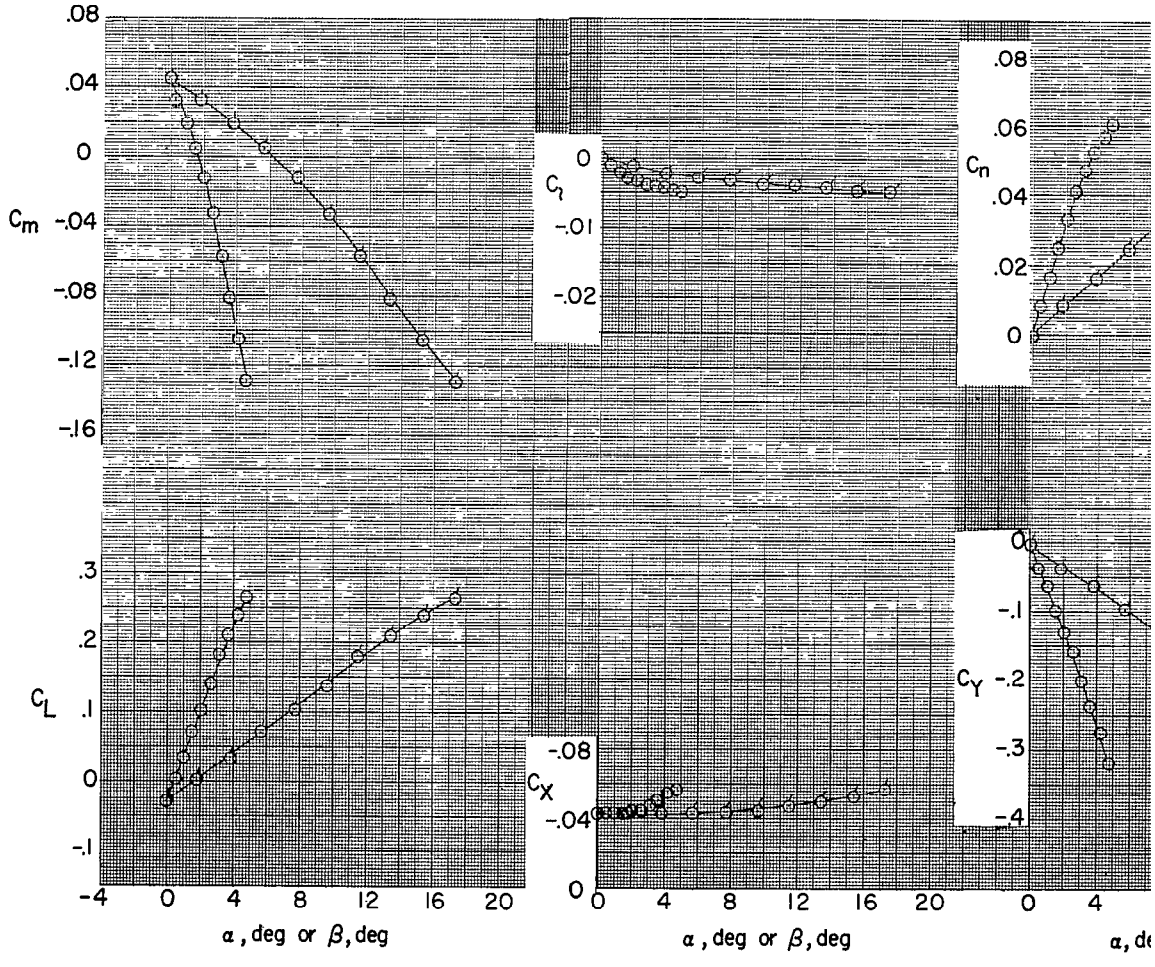

(f) $\phi = 75^{\circ}$.

Figure 8.- Continued.

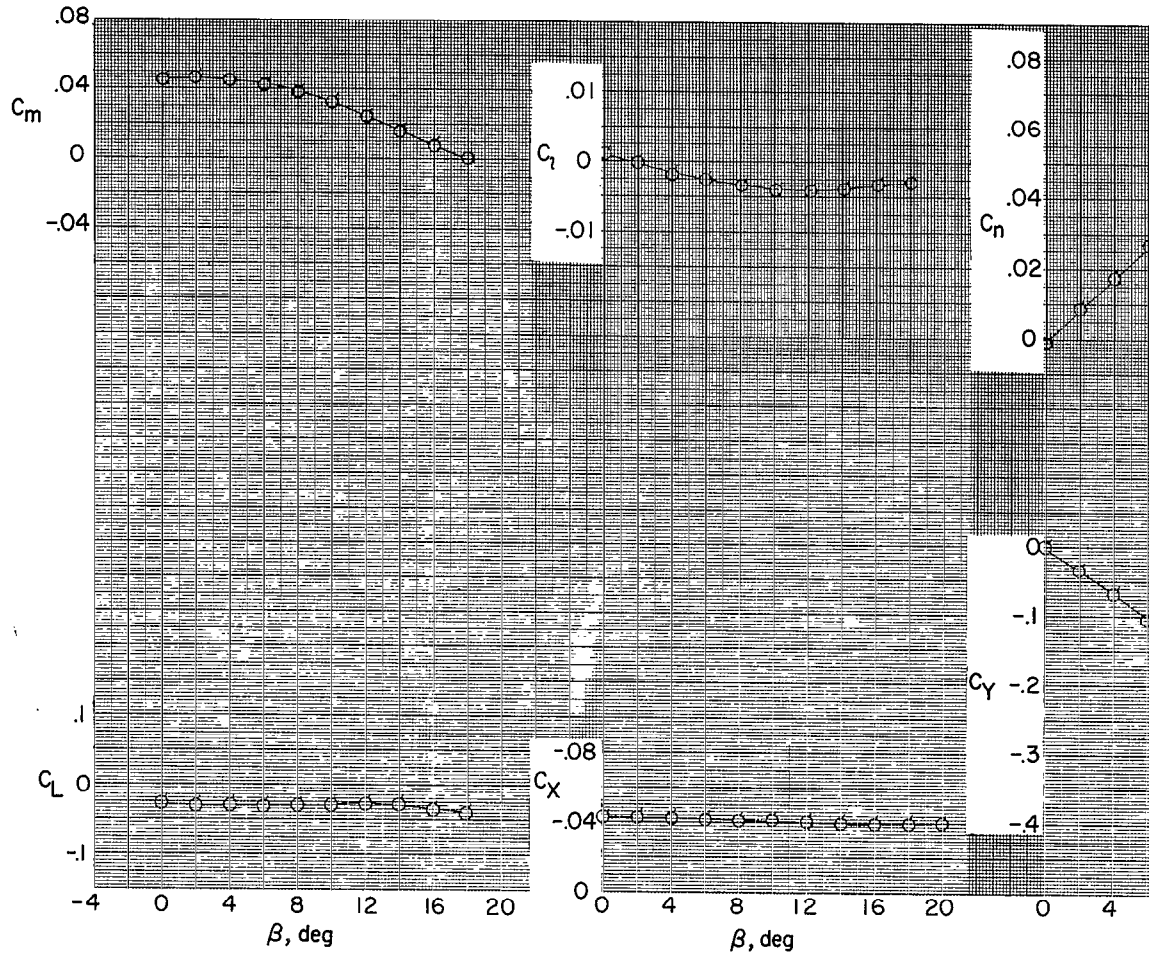

(g) $\phi = 90^\circ$.

Figure 8.- Concluded.

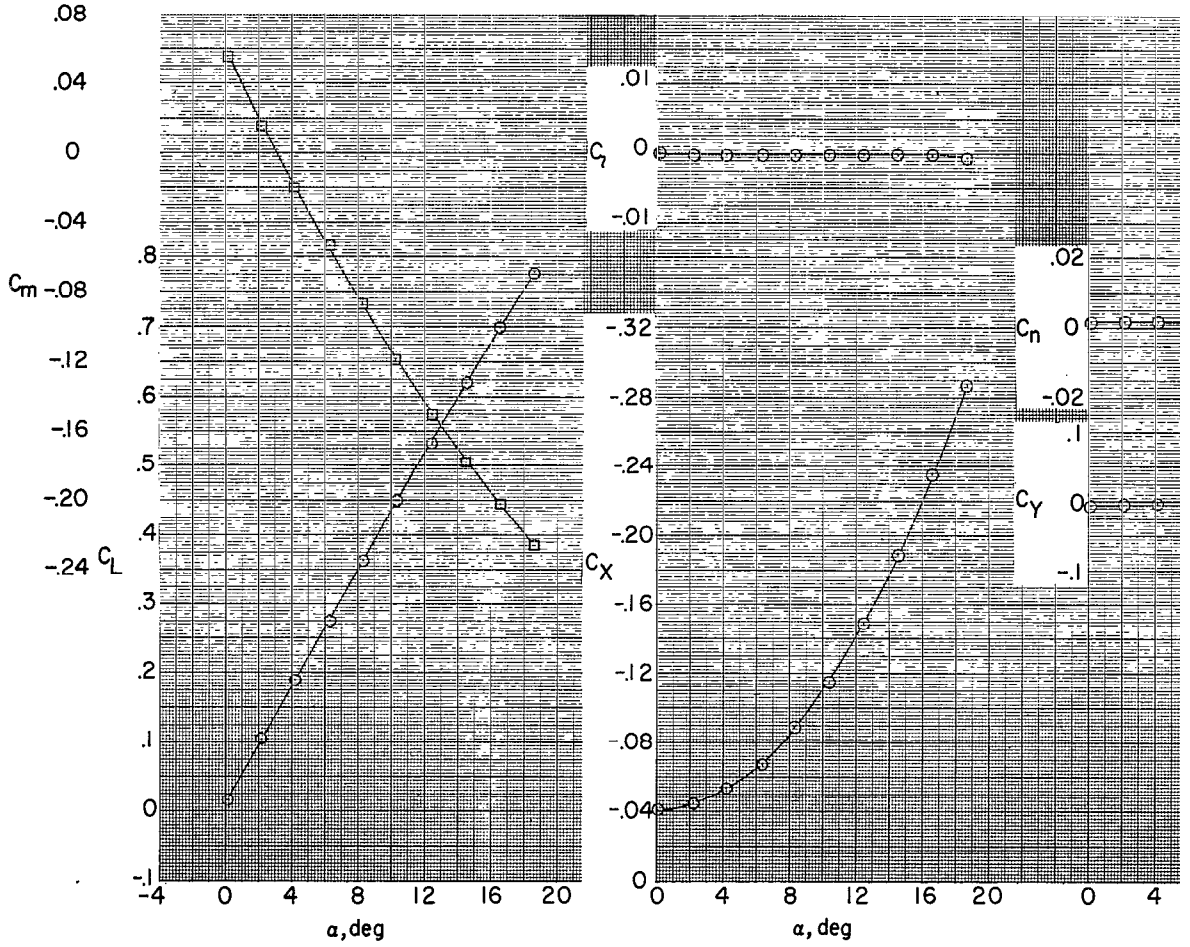

(a) $\phi = 0^{\circ}$.

Figure 9.- Aerodynamic characteristics at various roll angles. Lo
horizontal tail position 4; $i_t = -3^{\circ}$. Flagged symbols are for
with β; unflagged symbols are for variations with α.

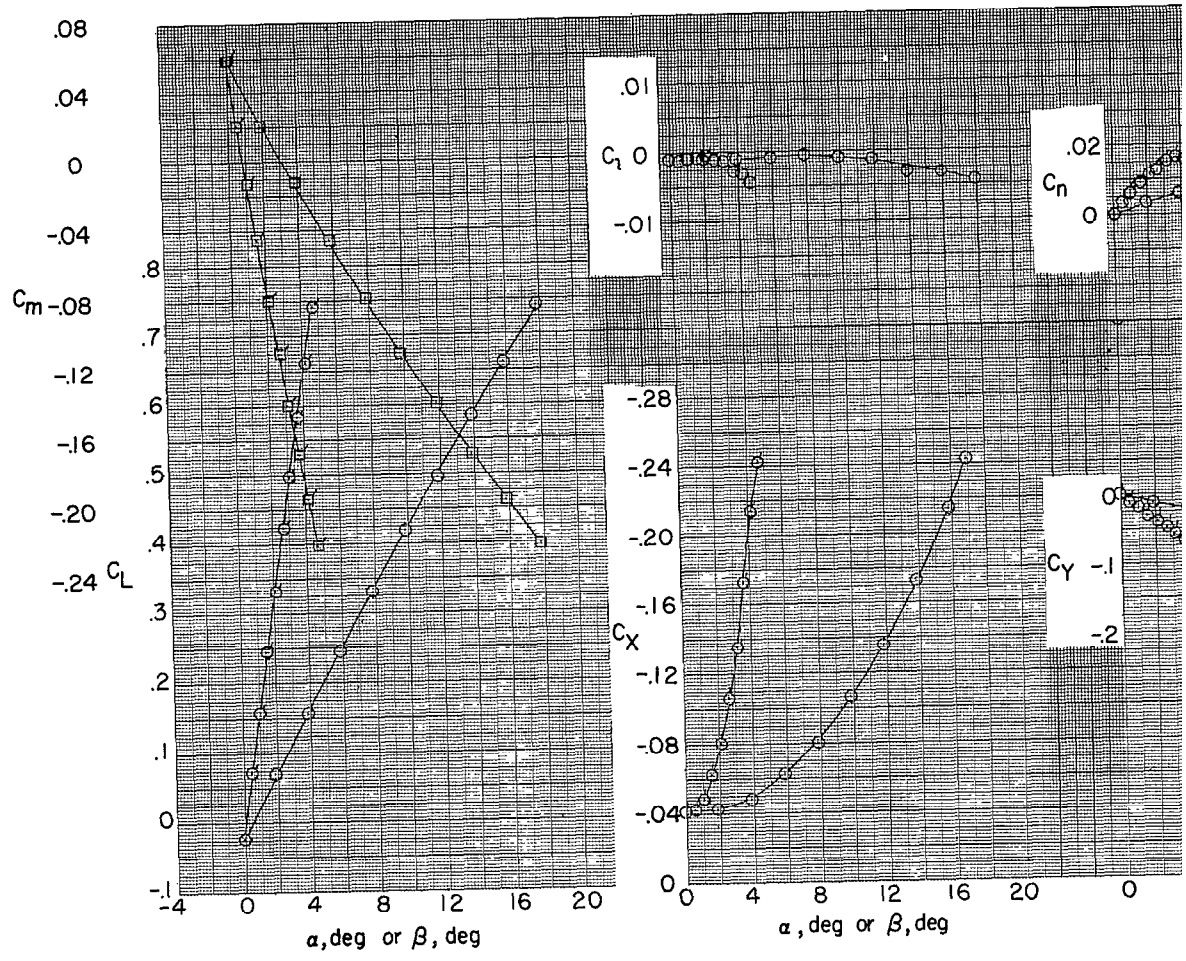

(b) $\phi = 15^{\circ}$.

Figure 9.- Continued.

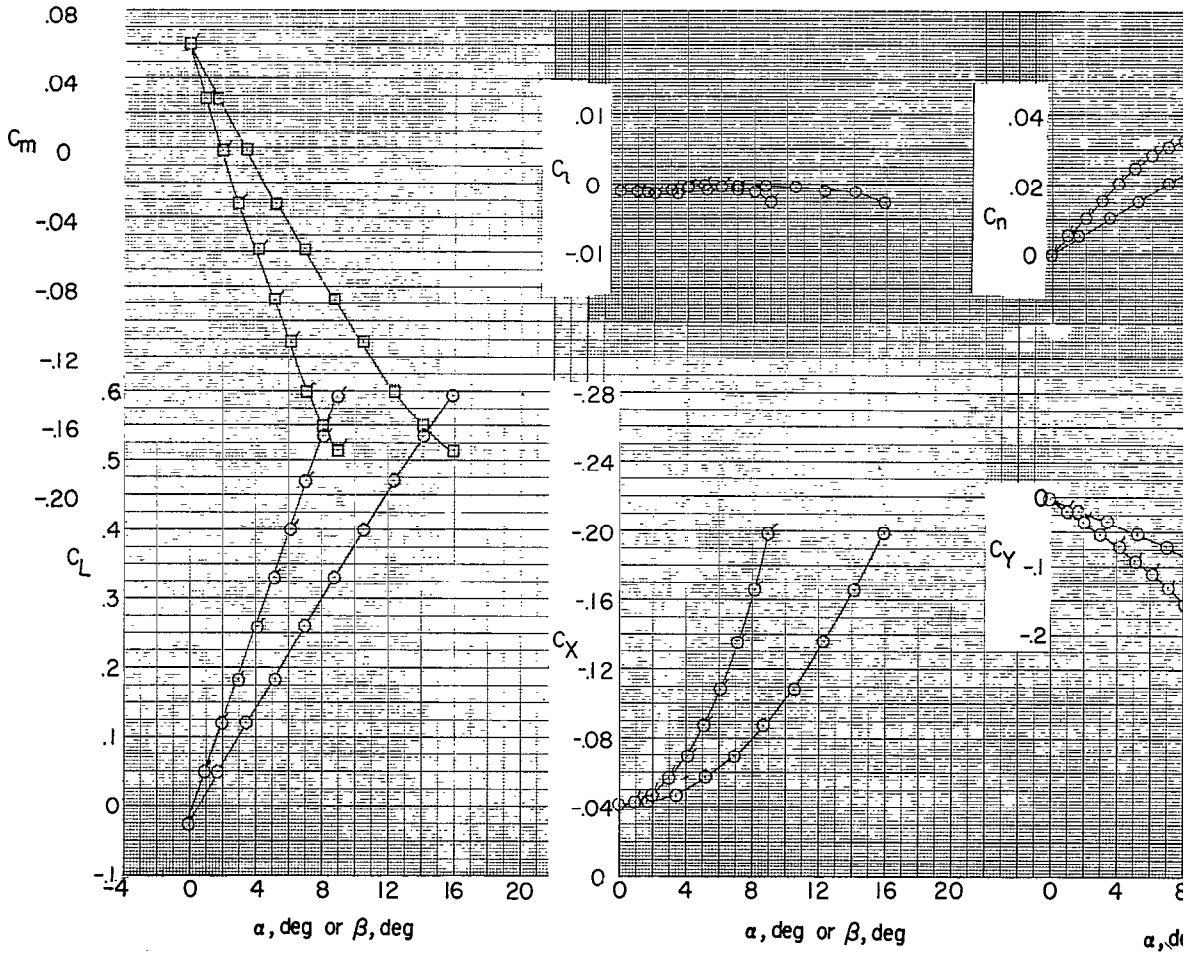

(c) $\phi = 30^{\circ}$.

Figure 9.- Continued.

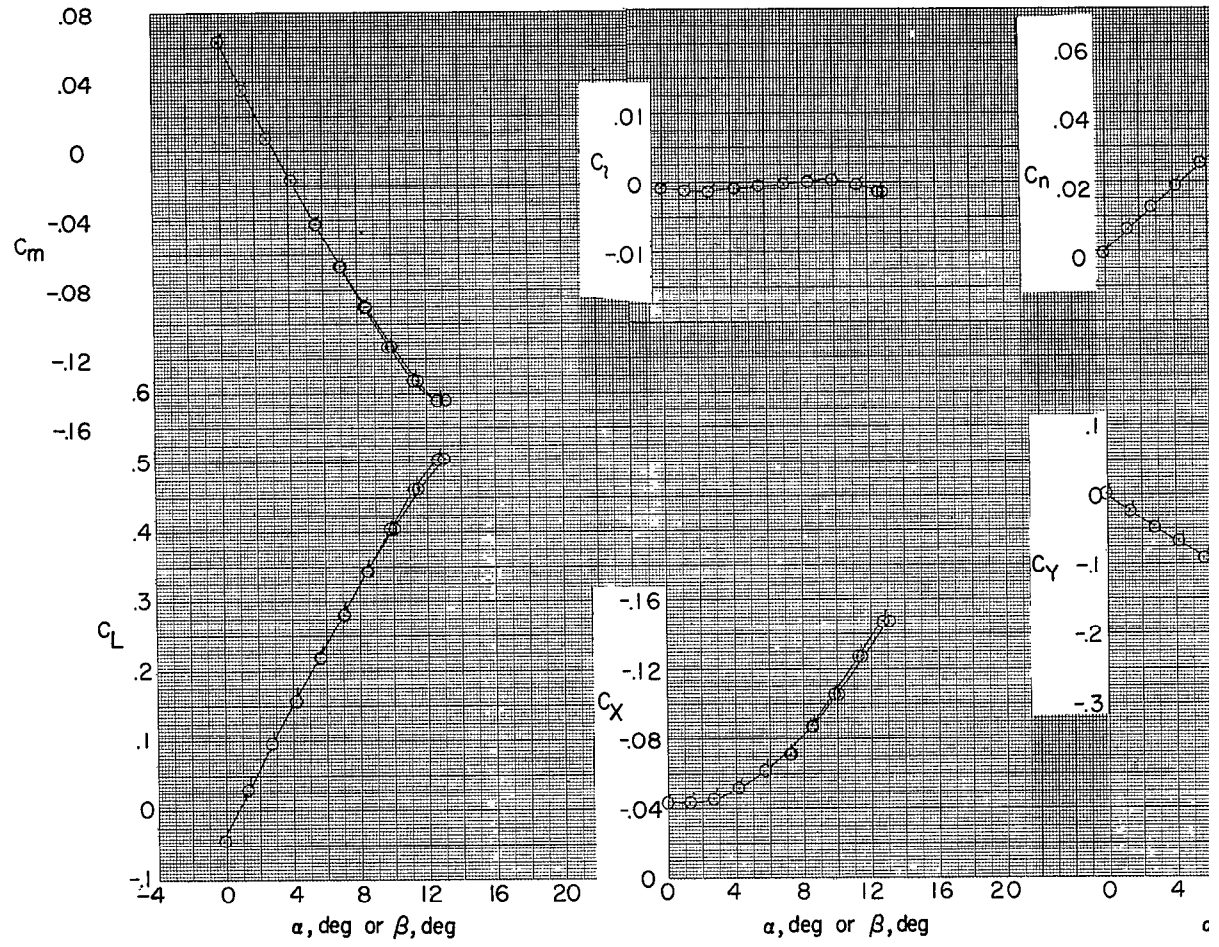

(d) $\phi = 45^{\circ}$.

Figure 9.- Continued.

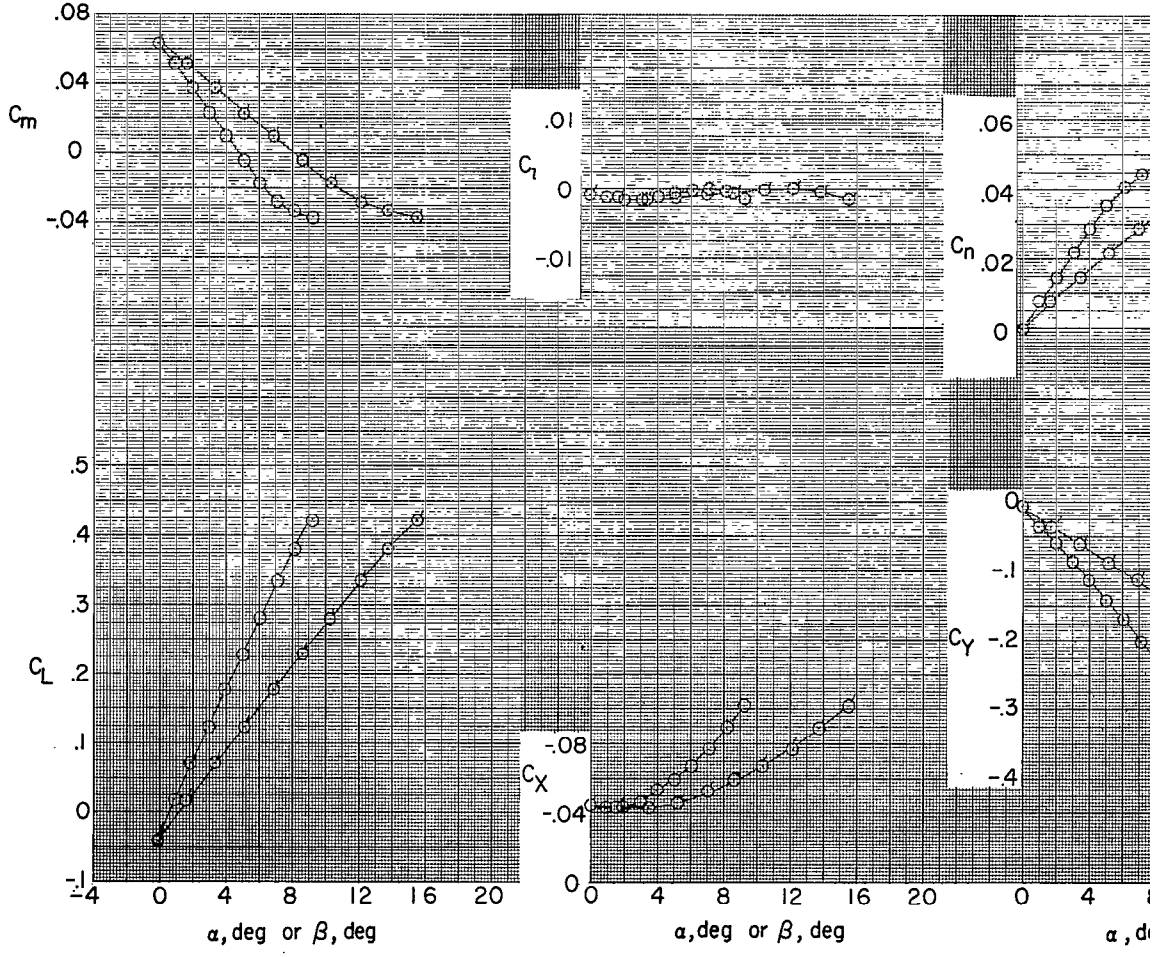

(e) $\phi = 60^{\circ}$.

Figure 9.- Continued.

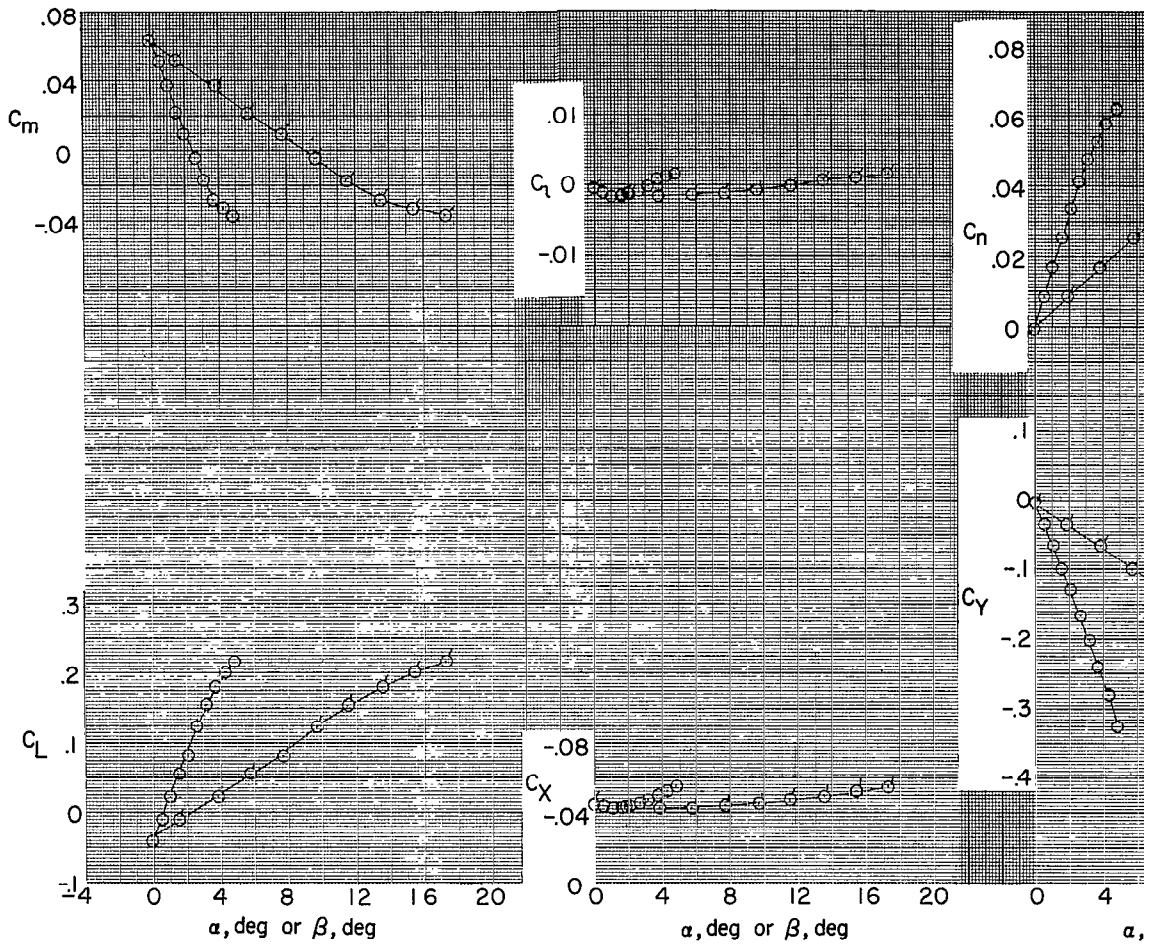

(f) $\phi = 75^{\circ}$.

Figure 9.- Continued.

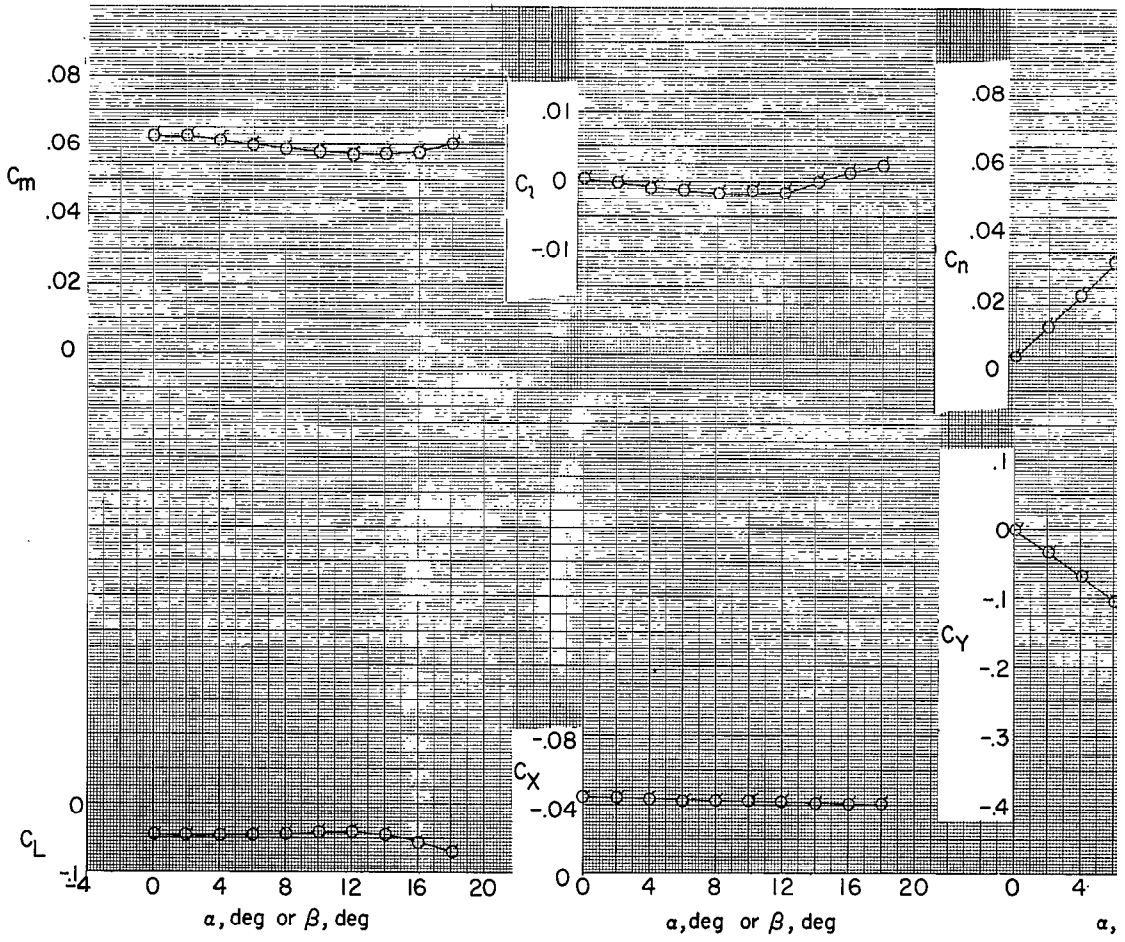

(g) $\phi = 90^{\circ}$.

Figure 9.- Concluded.

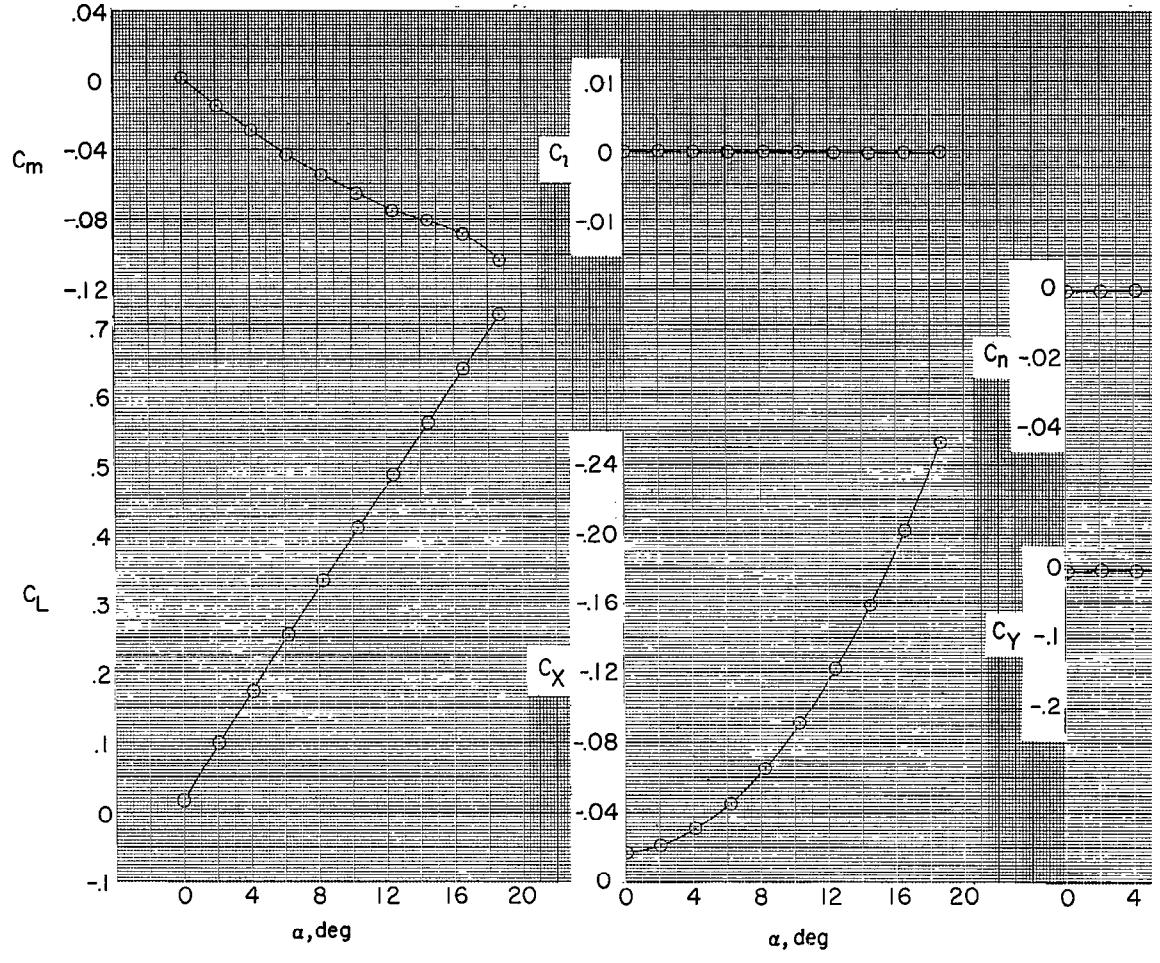

(a) $\phi = 0^{\circ}$.

Figure 10.- Aerodynamic characteristics at various roll angle
Midwing ($\Gamma = 0^{\circ}$); tails off. Flagged symbols are for vari
with β; unflagged symbols are for variations with α.

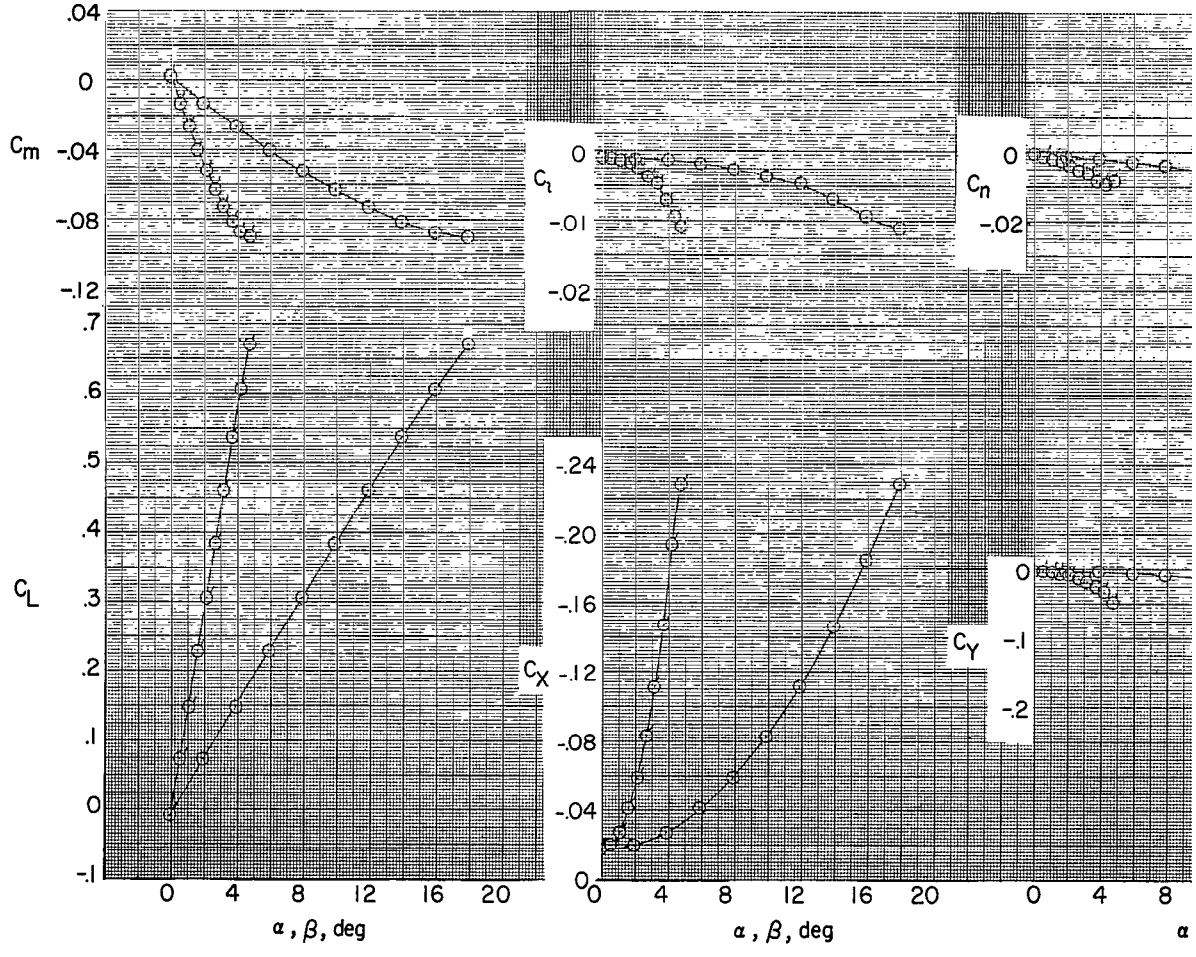

(b) $\phi = 15^{\circ}$.

Figure 10.- Continued.

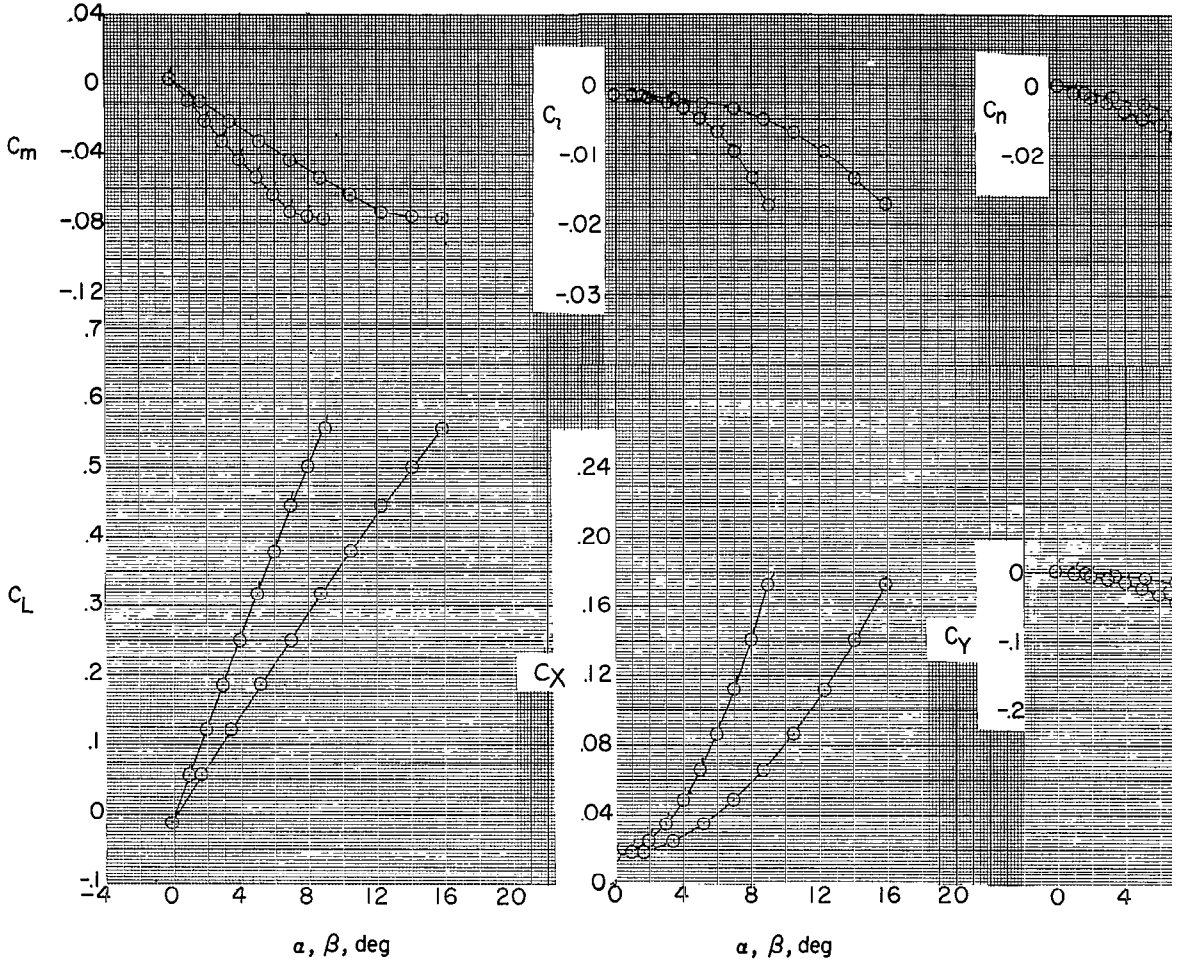

(c) $\phi = 30^{\circ}$.

Figure 10.- Continued.

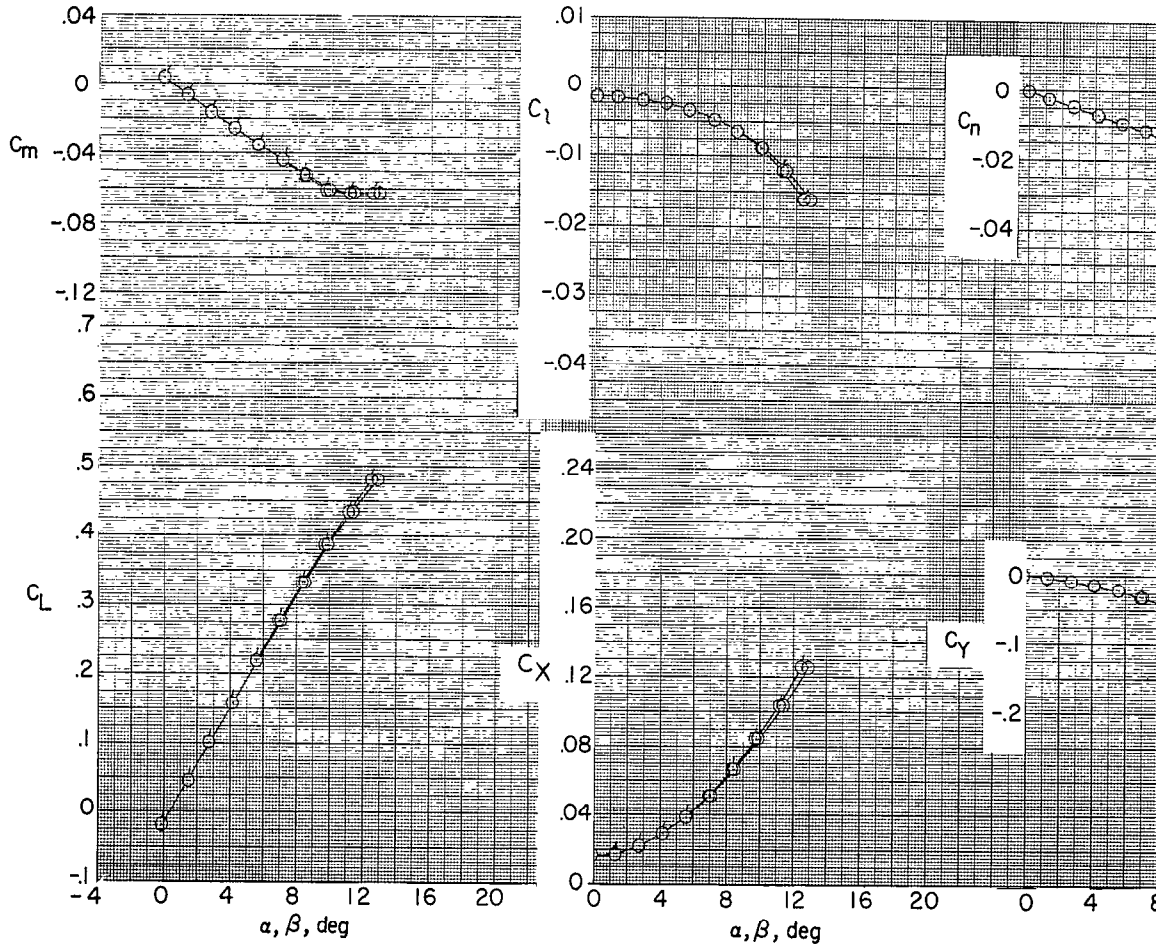

(d) $\phi = 45^{\circ}$.

Figure 10.- Continued.

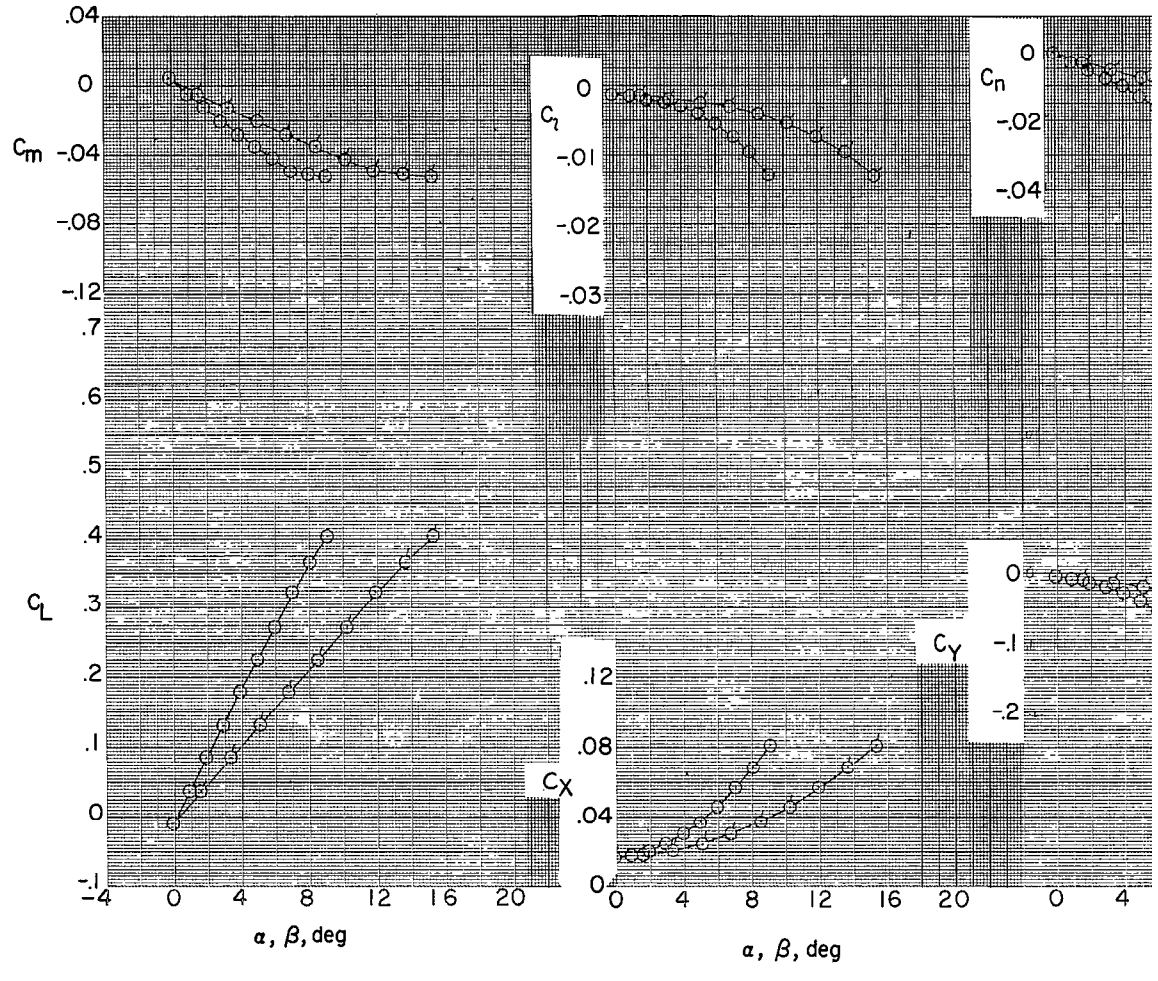

(e) $\phi = 60^{\circ}$.

Figure 10.- Continued.

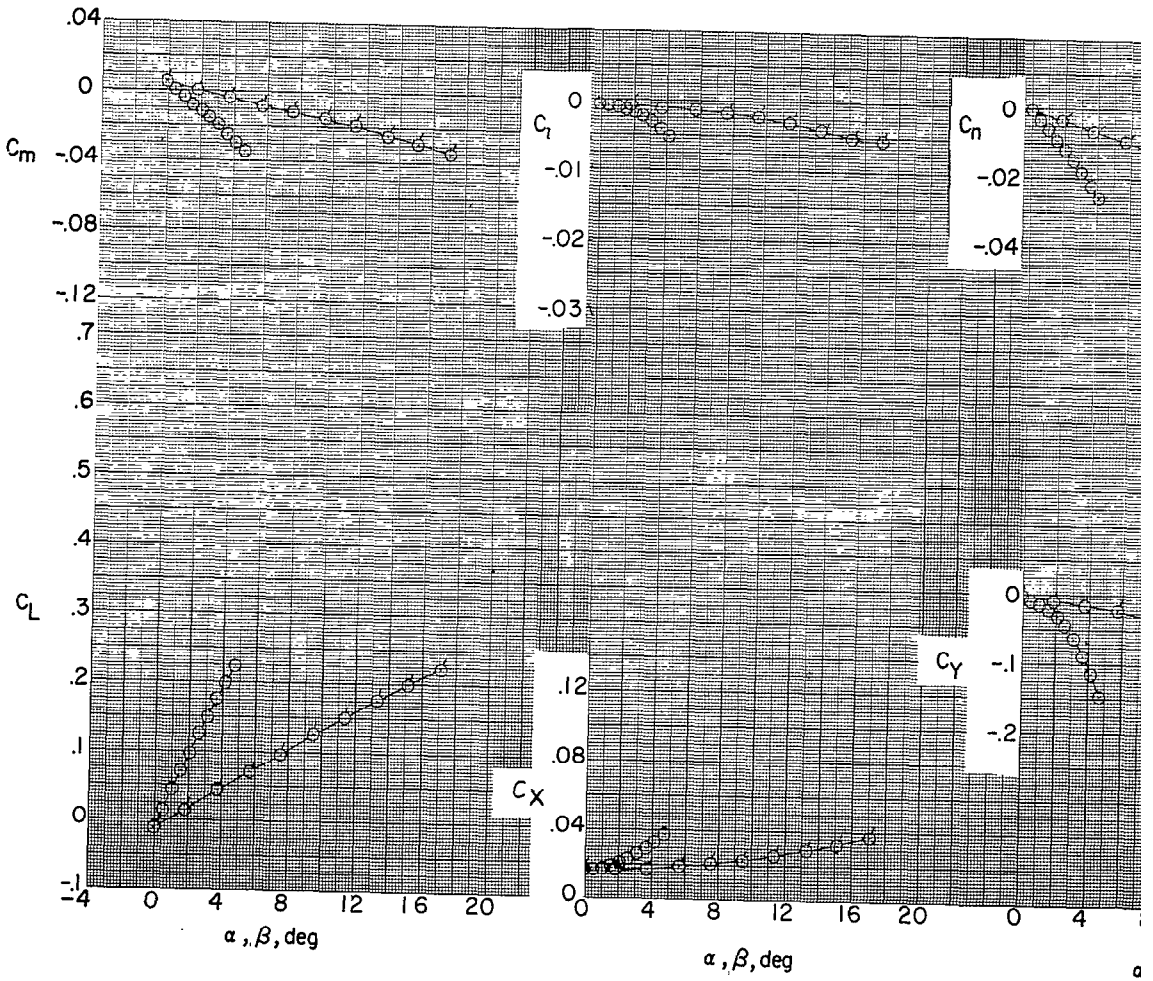

(f) $\phi = 75^{\circ}$.

Figure 10.- Continued.

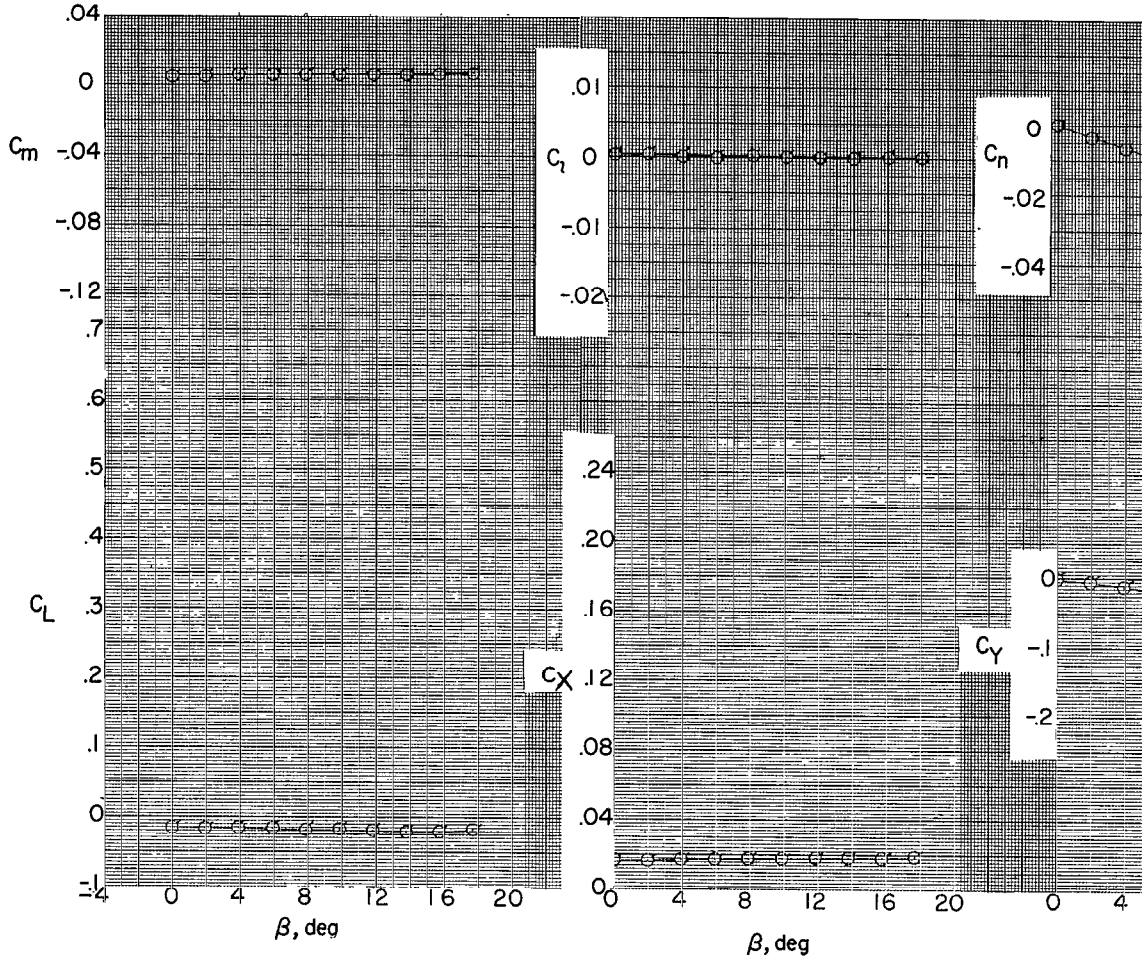

(g) $\phi = 90^{\circ}$.

Figure 10.- Concluded.

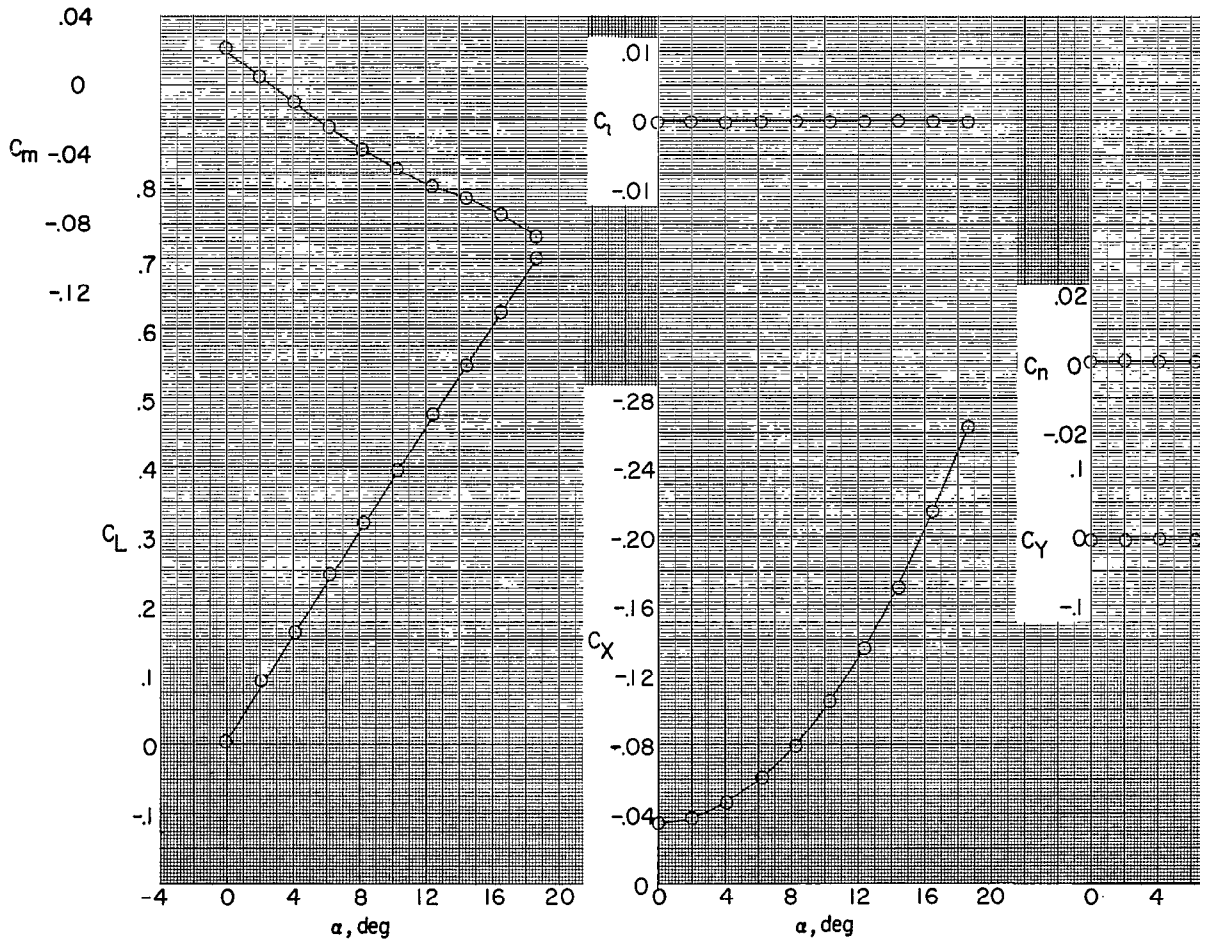

(a) $\phi = 0^{\circ}$.

Figure 11.- Aerodynamic characteristics at various roll angles. Midwing ($\Gamma = 0^{\circ}$); horizontal tail off. Flagged symbols are variations with β; unflagged symbols are for variations wi

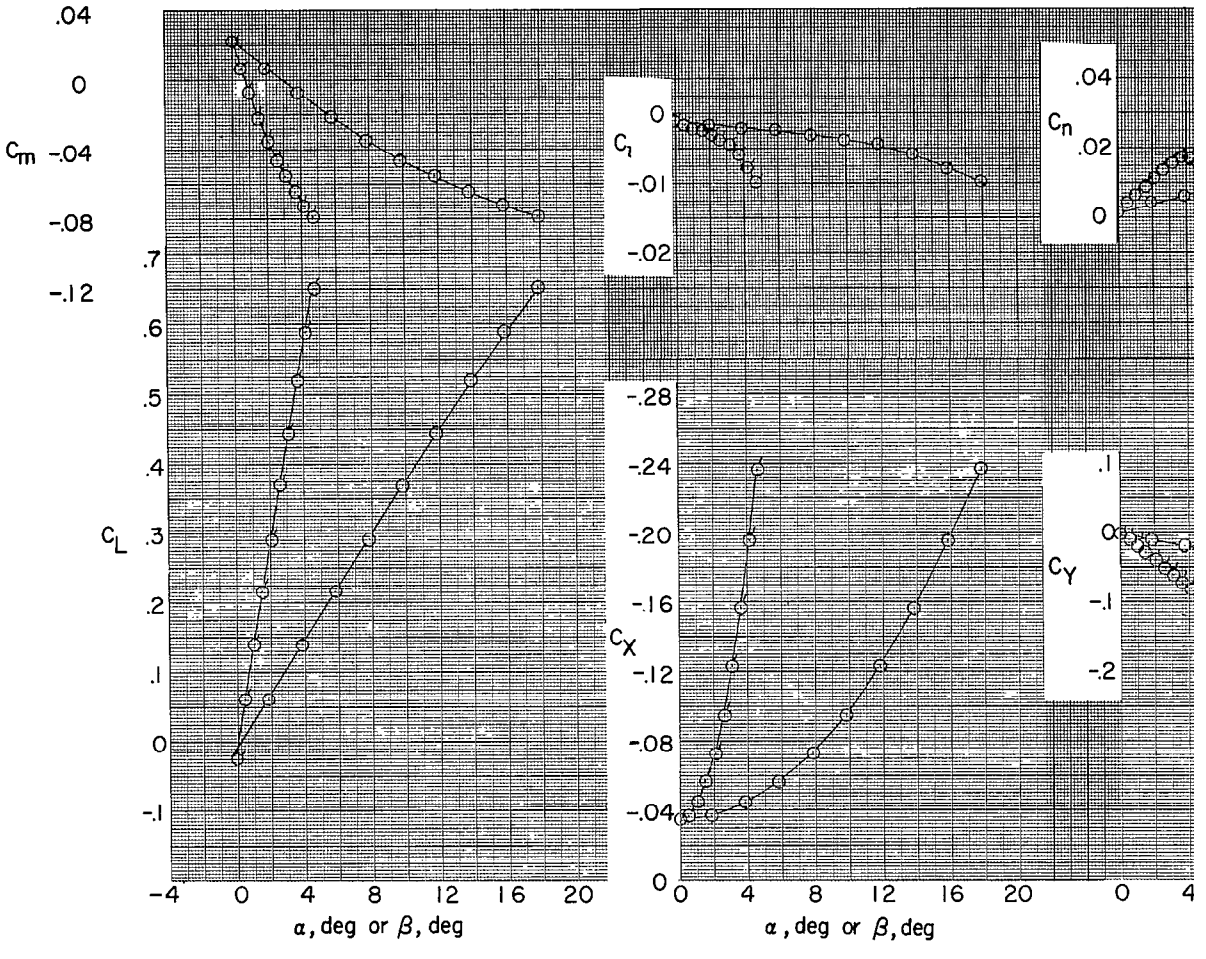

(b) $\phi = 15^{\circ}$.

Figure 11.- Continued.

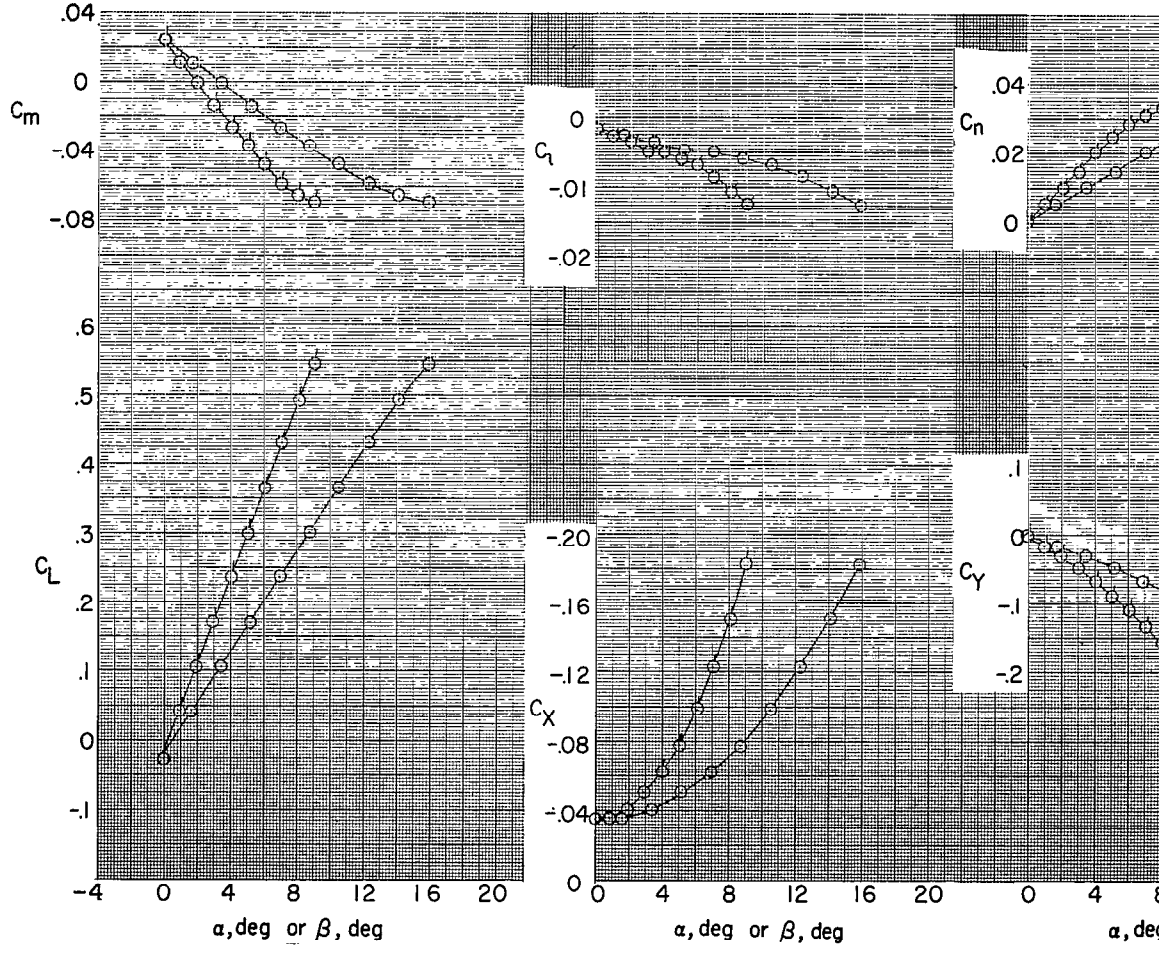

(c) $\phi = 30^{\circ}$.

Figure 11.- Continued.

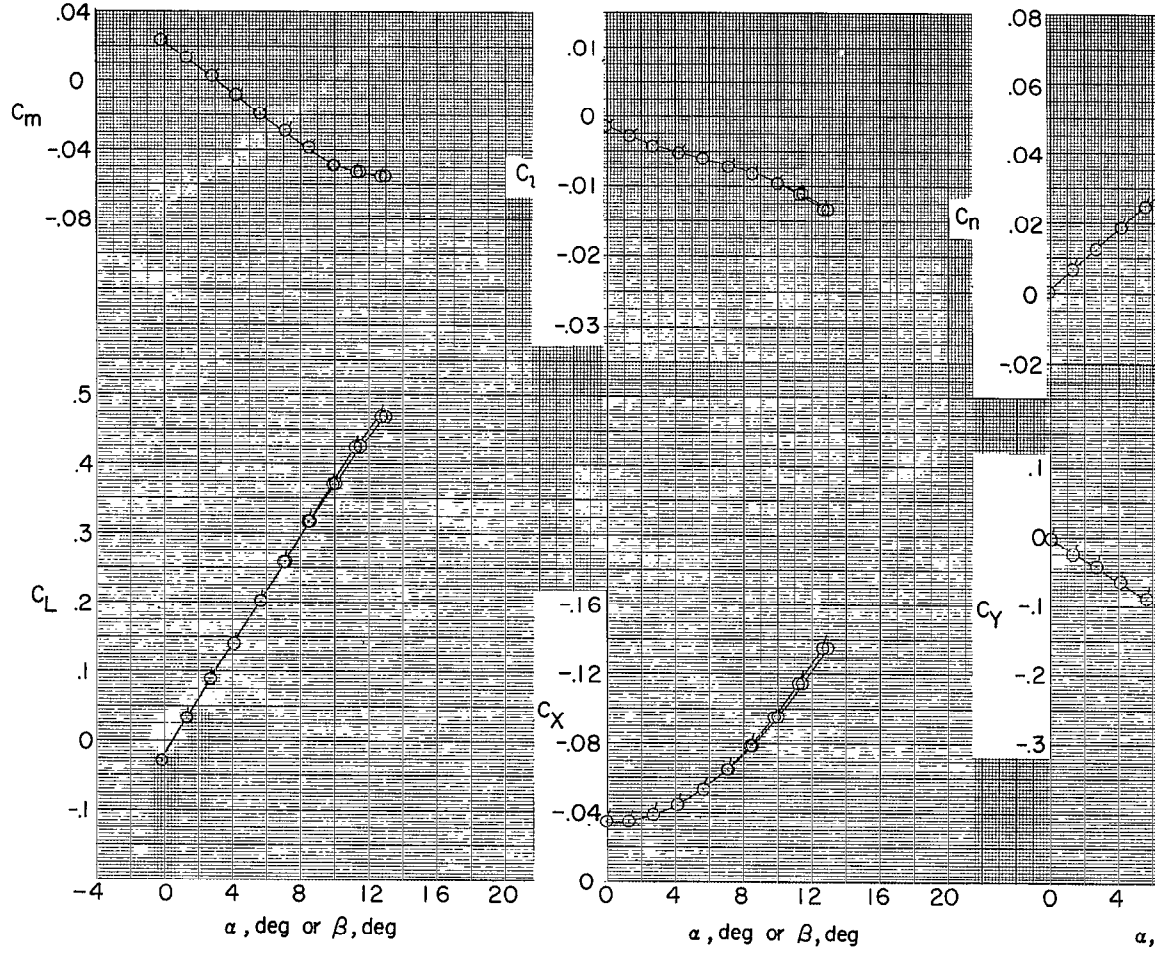

(d) $\phi = 45°$.

Figure 11.- Continued.

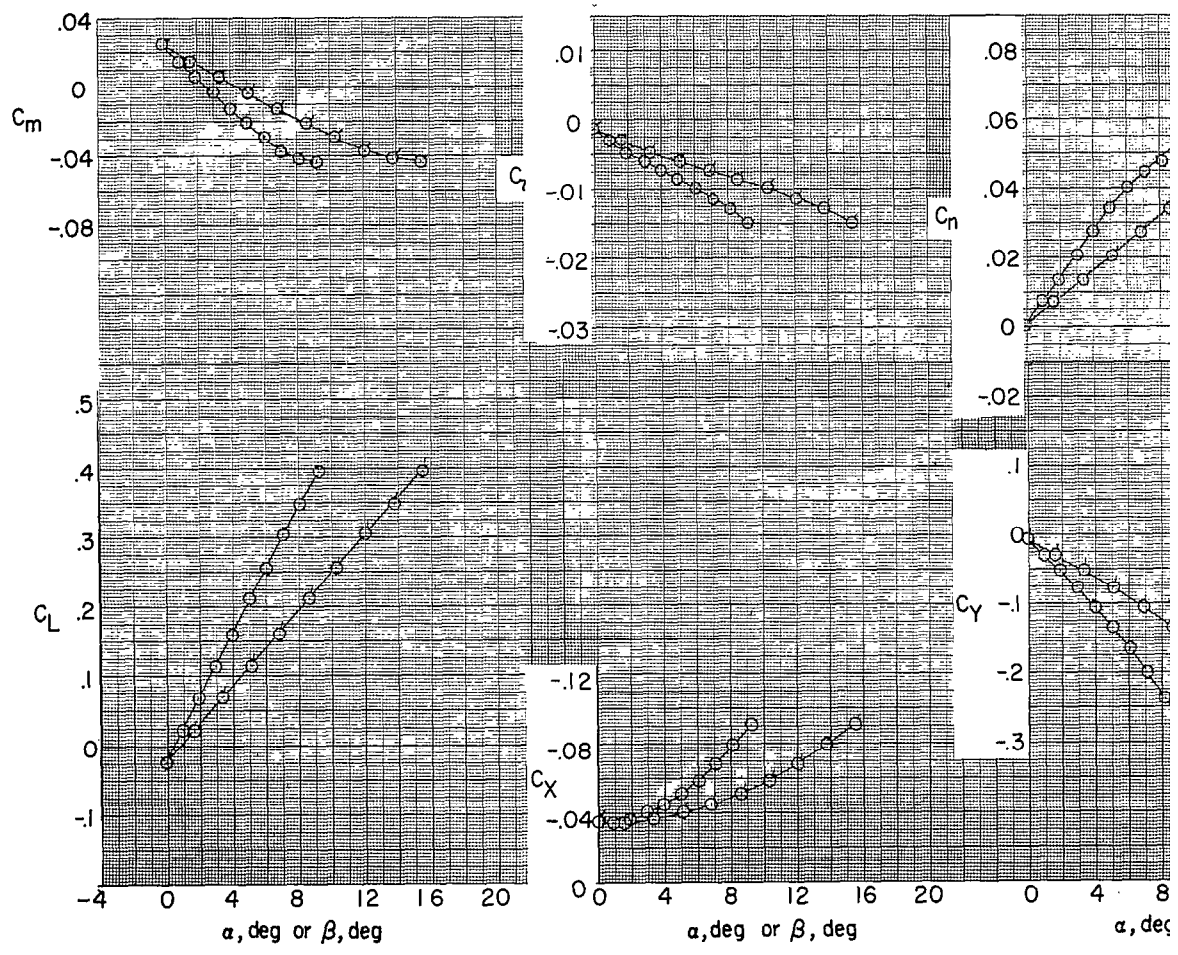

(e) $\phi = 60^{o}$.

Figure 11.- Continued.

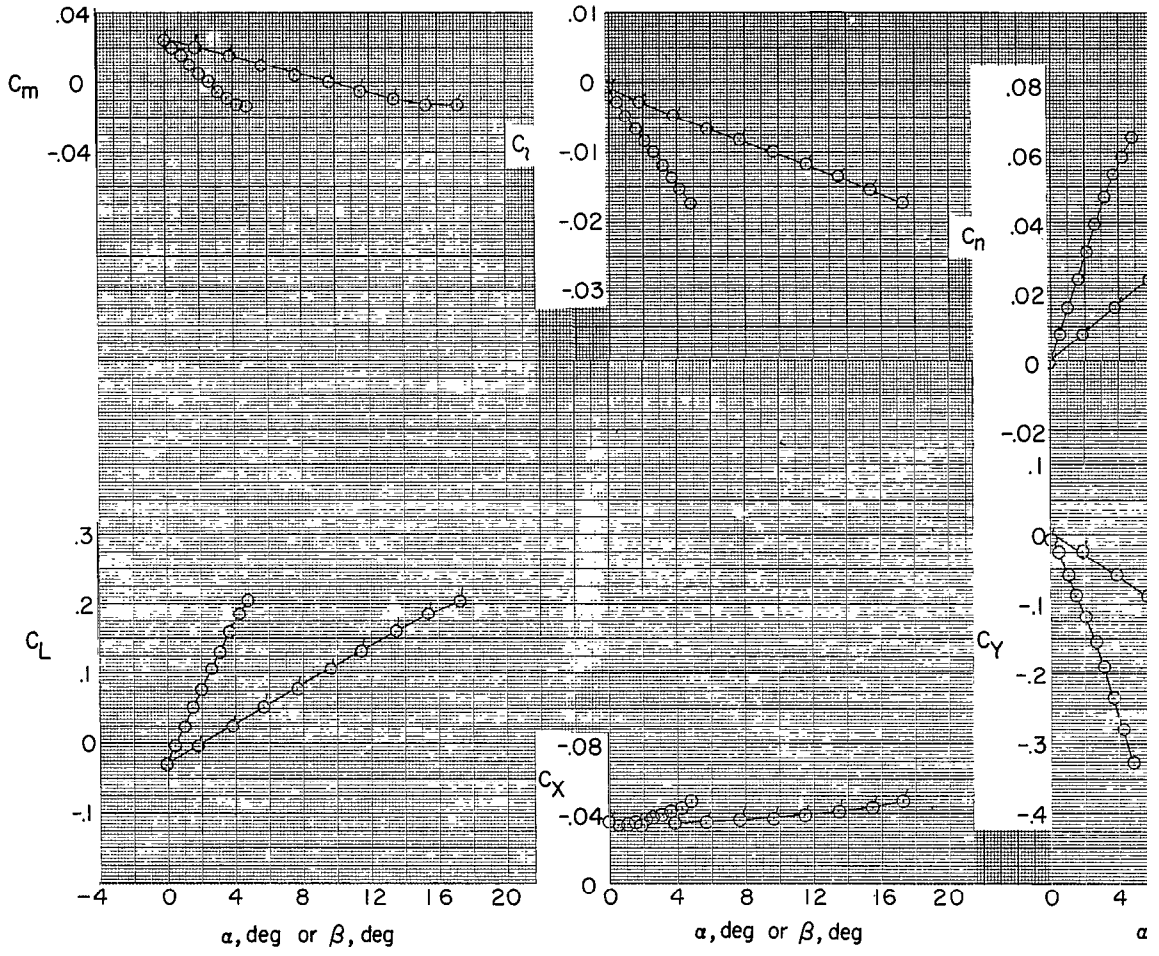

(f) $\phi = 75^{\circ}$.

Figure 11.- Continued.

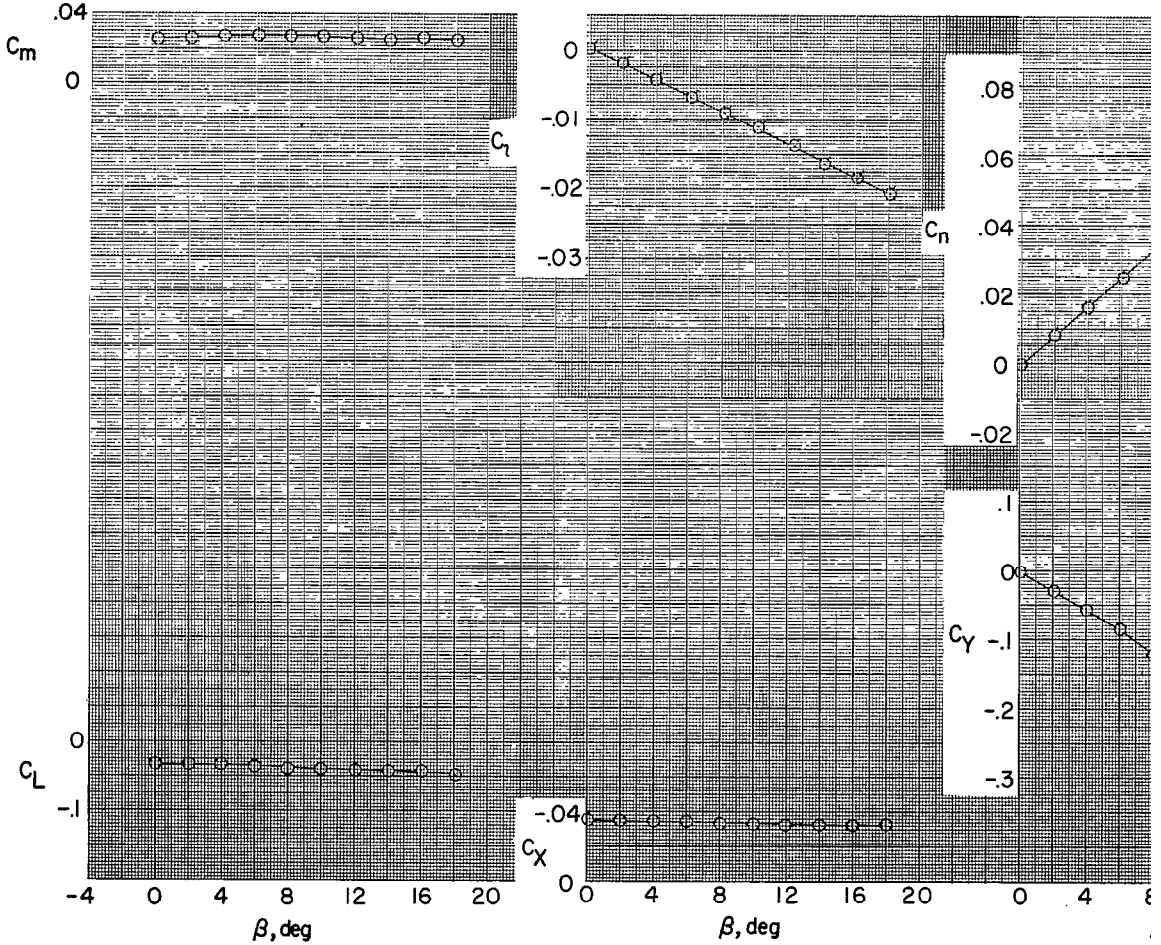

(g) $\phi = 90^{\circ}$.

Figure 11.- Concluded.

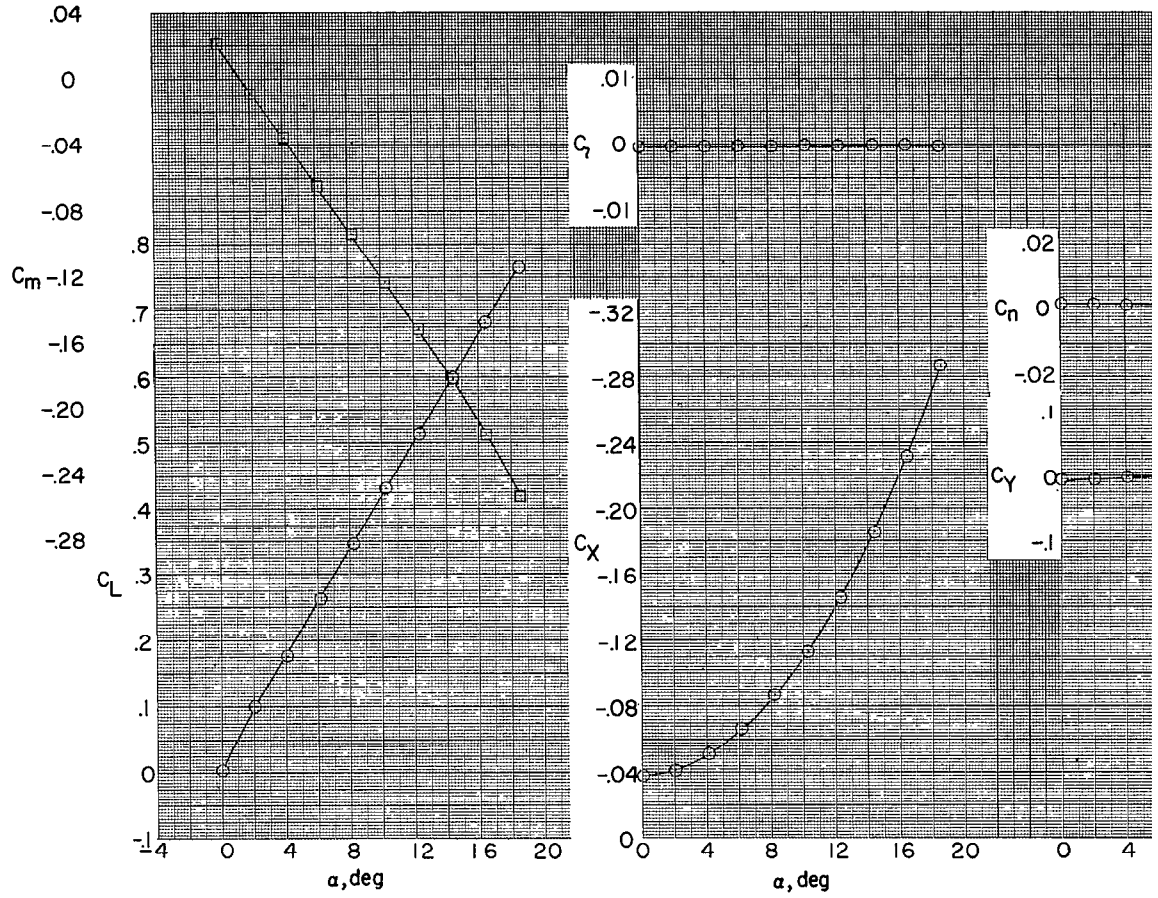

(a) $\phi = 0^{\circ}$.

Figure 12.- Aerodynamic characteristics at various roll angles Midwing ($\Gamma = 0^{\circ}$); horizontal tail position 1; $i_t = 0^{\circ}$. Fla symbols are for variations with β; unflagged symbols are f variations with α.

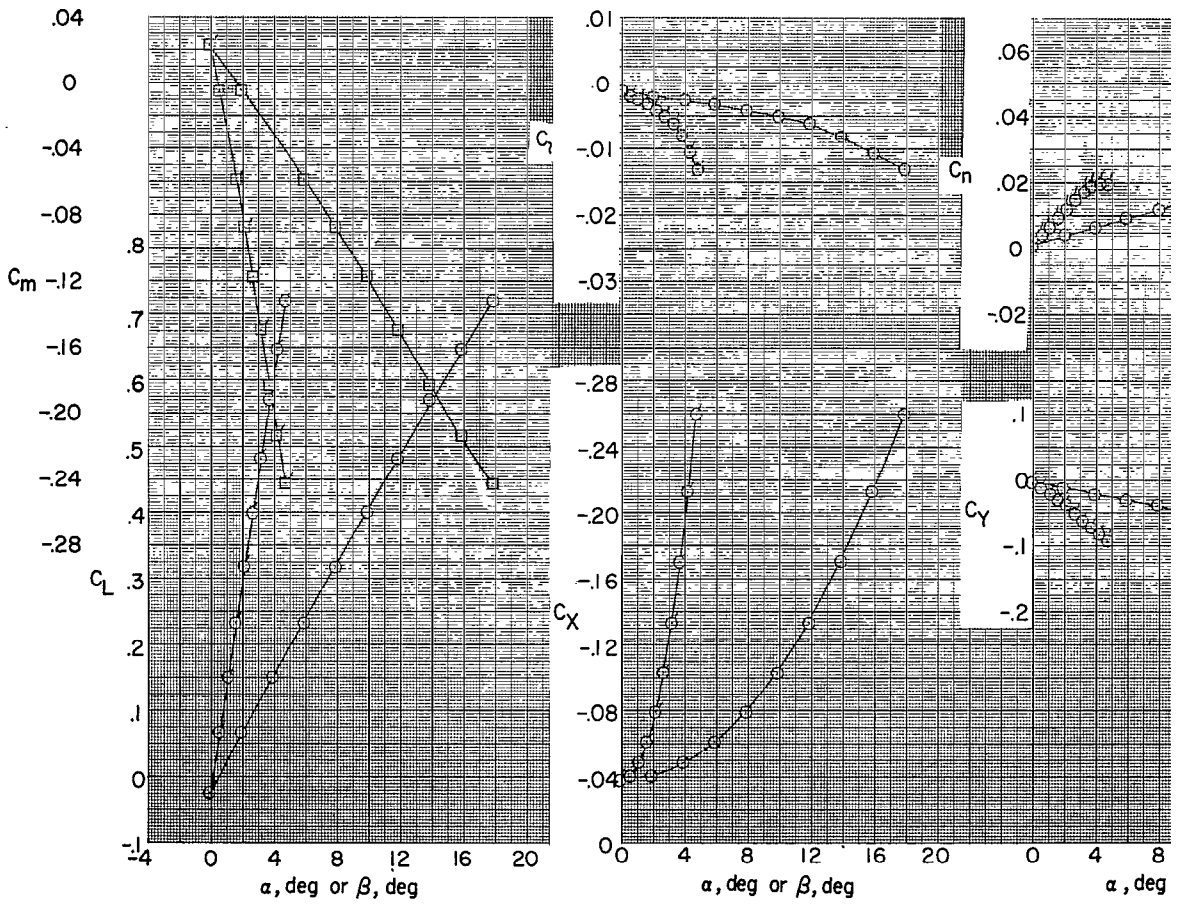

(b) $\phi = 15^{\circ}$.

Figure 12.- Continued.

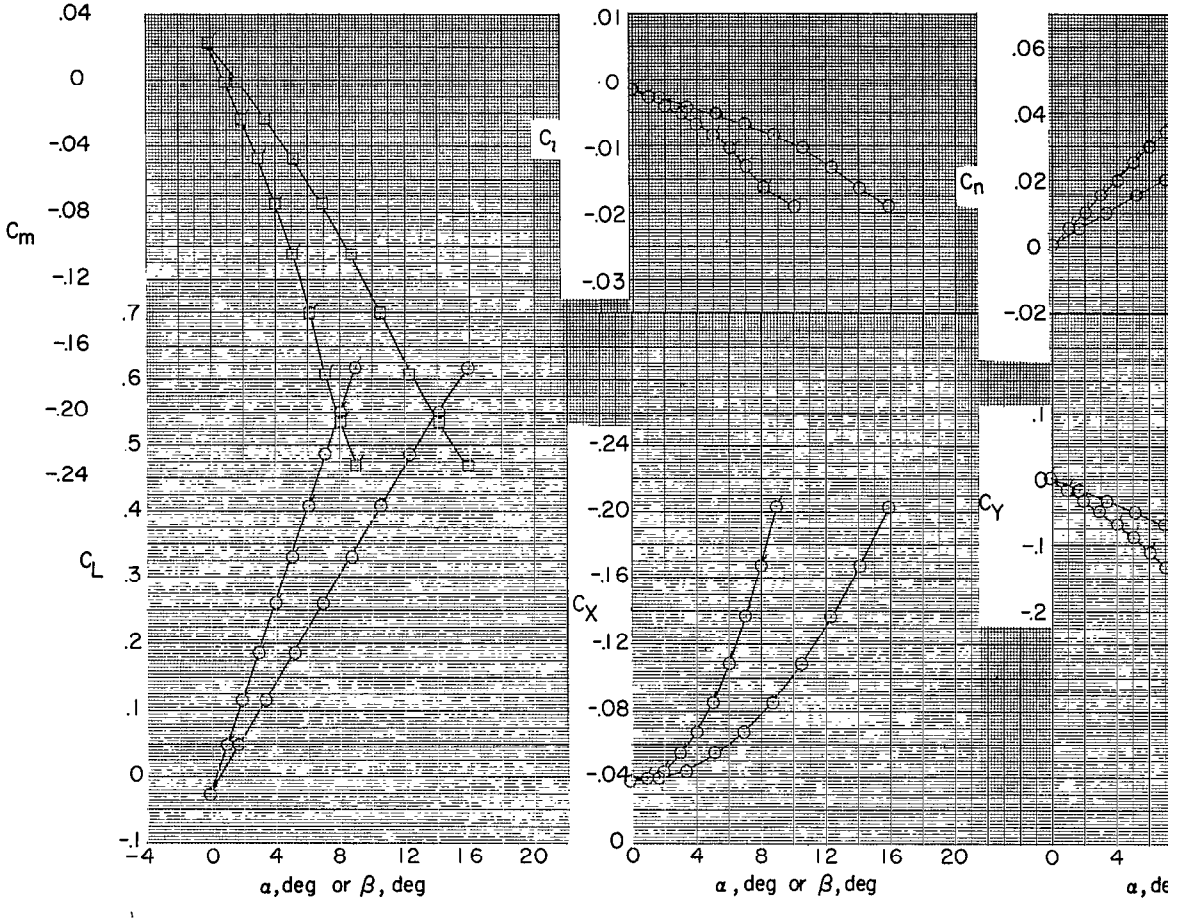

(c) $\phi = 30^{\circ}$.

Figure 12.- Continued.

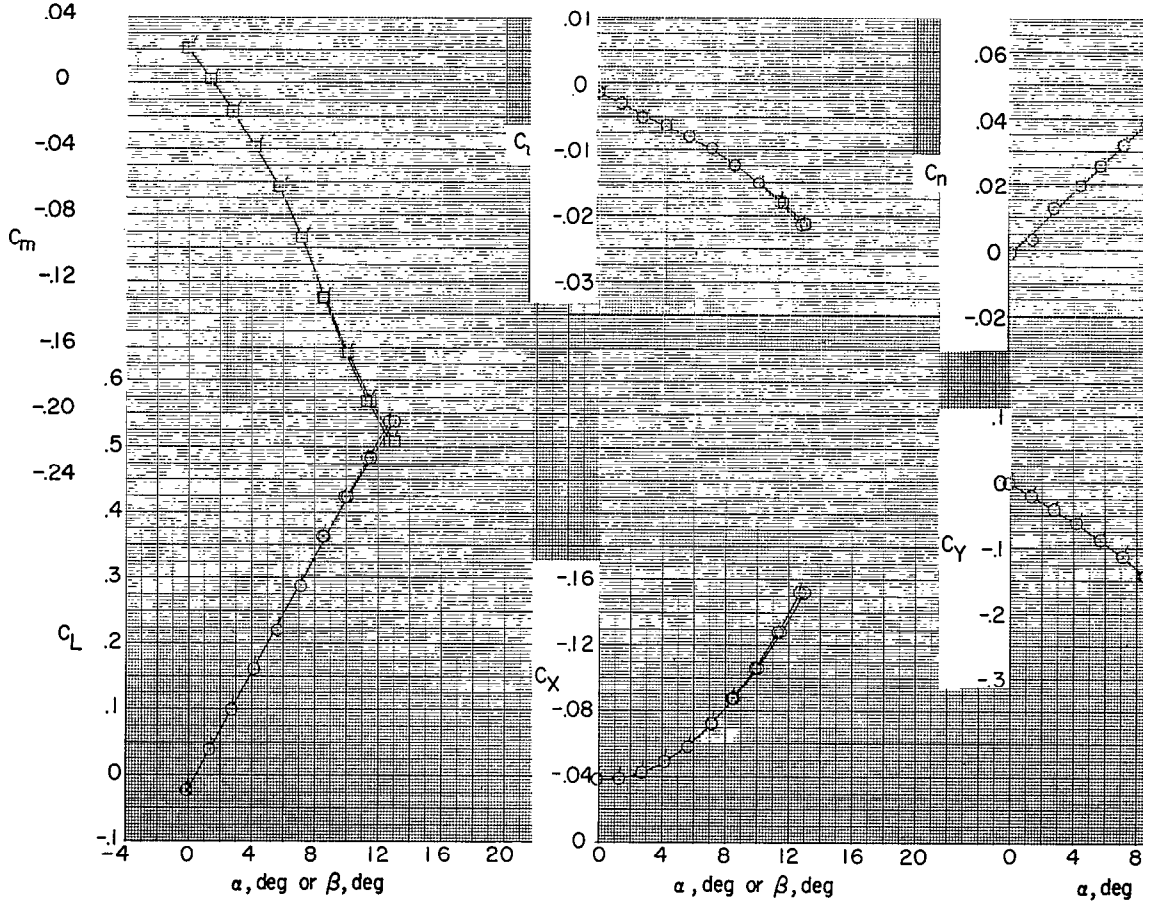

(d) $\phi = 45^\circ$.

Figure 12.- Continued.

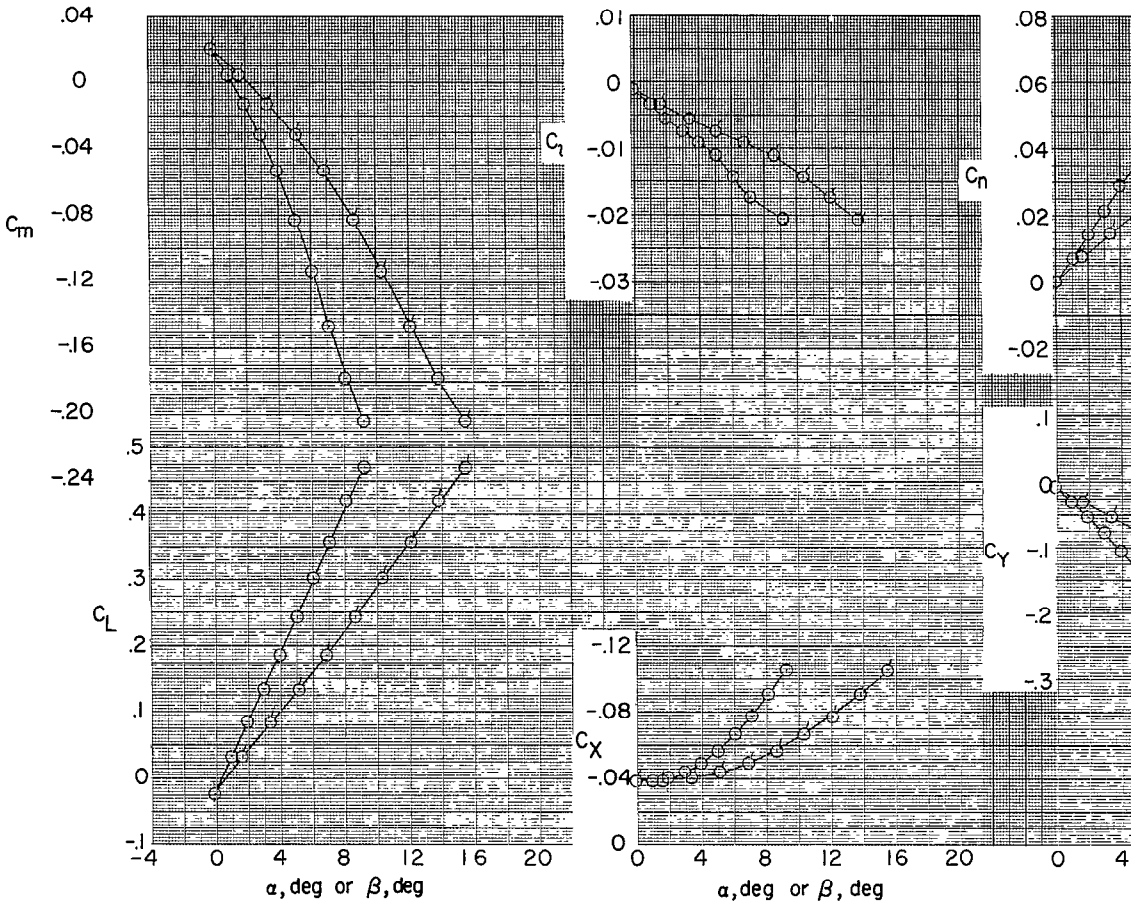

(e) $\phi = 60^{\circ}$.

Figure 12.- Continued.

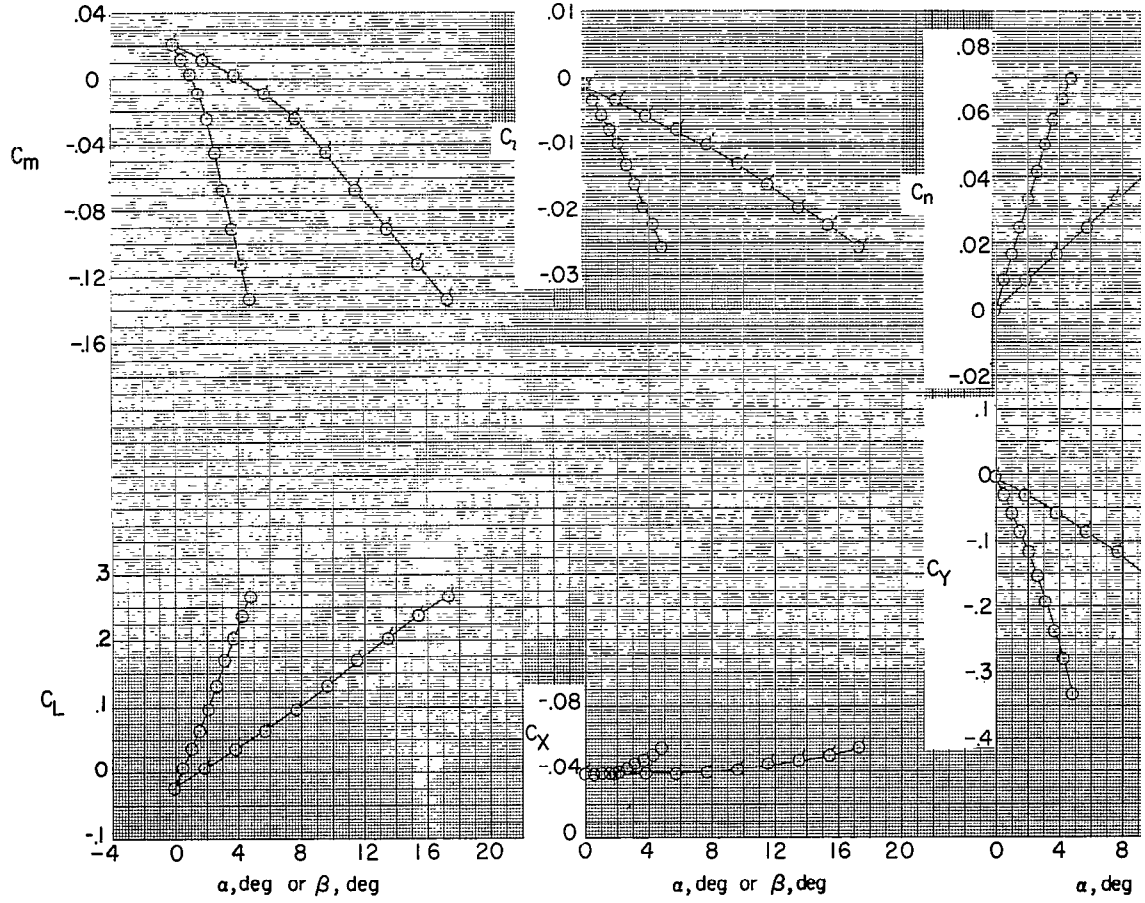

(f) $\phi = 75^{\circ}$.

Figure 12.- Continued.

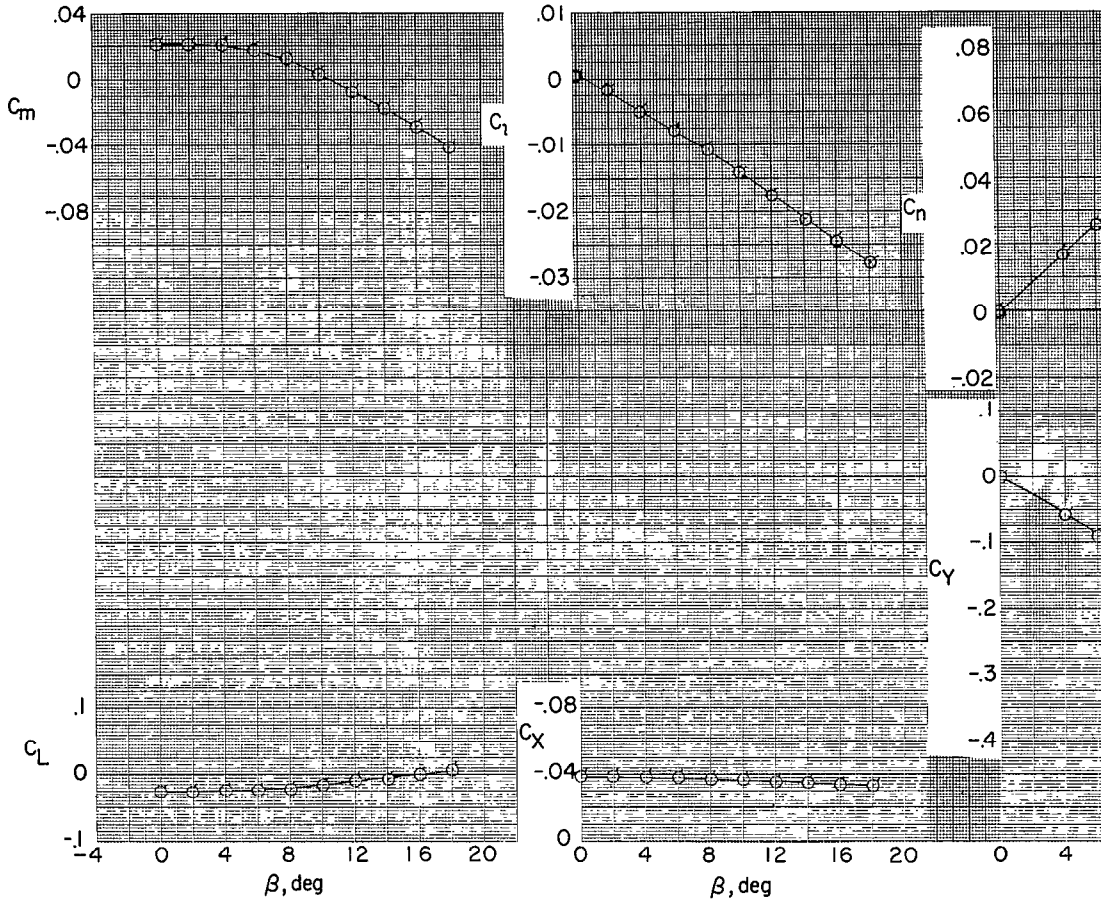

(g) $\phi = 90^{\circ}$.

Figure 12.- Concluded.

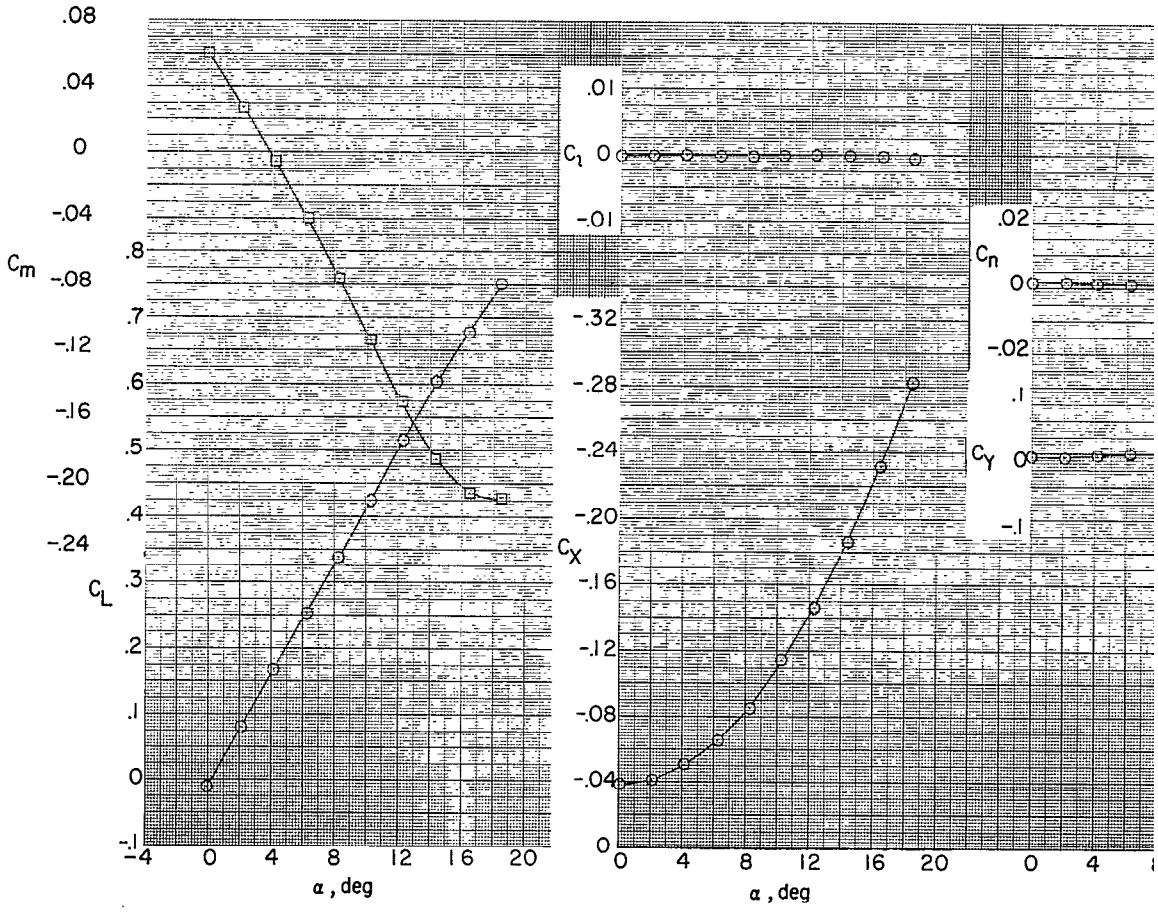

(a) $\phi = 0^\circ$.

Figure 13.- Aerodynamic characteristics at various roll angles Midwing ($\Gamma = 0^\circ$); horizontal tail position 2; $i_t = 0^\circ$. Fla symbols are for variations with β; unflagged symbols are f variations with α.

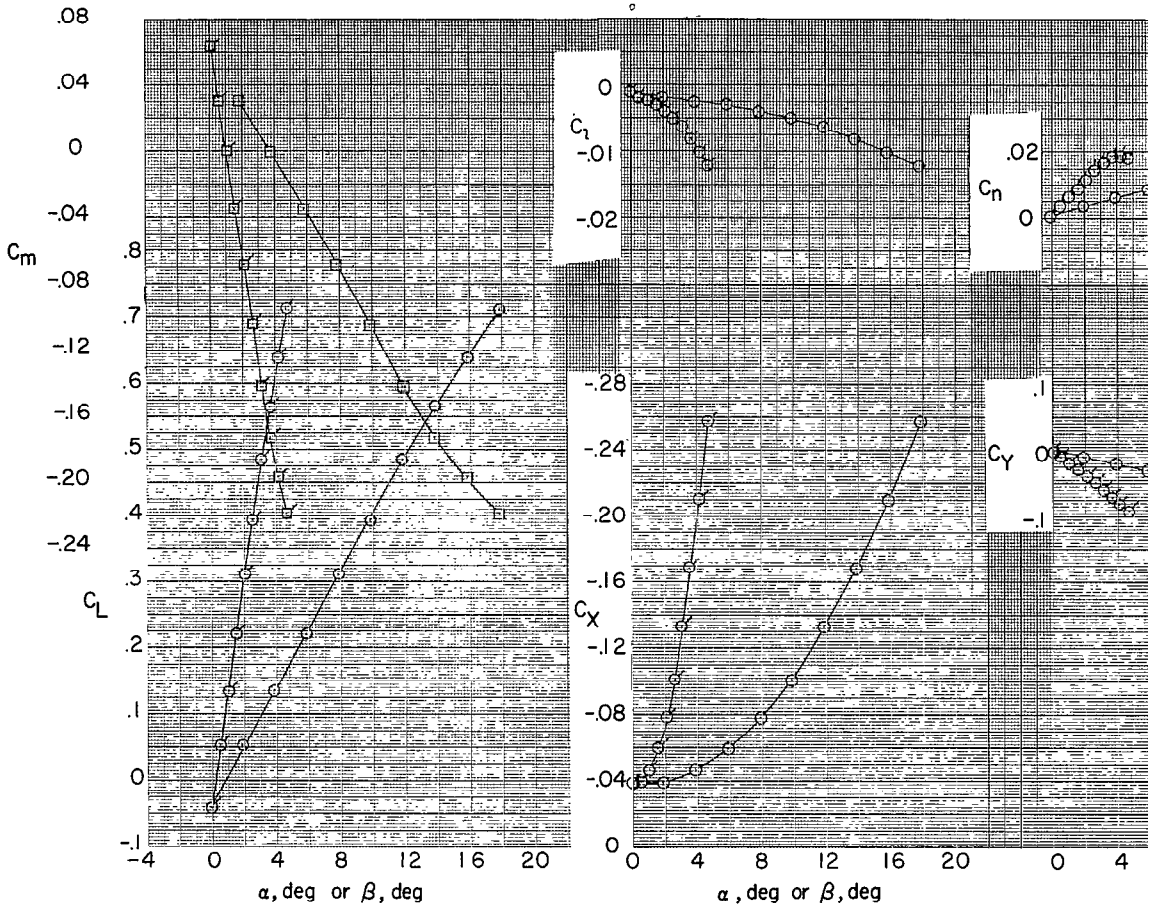

(b) $\phi = 15°$.

Figure 13.- Continued.

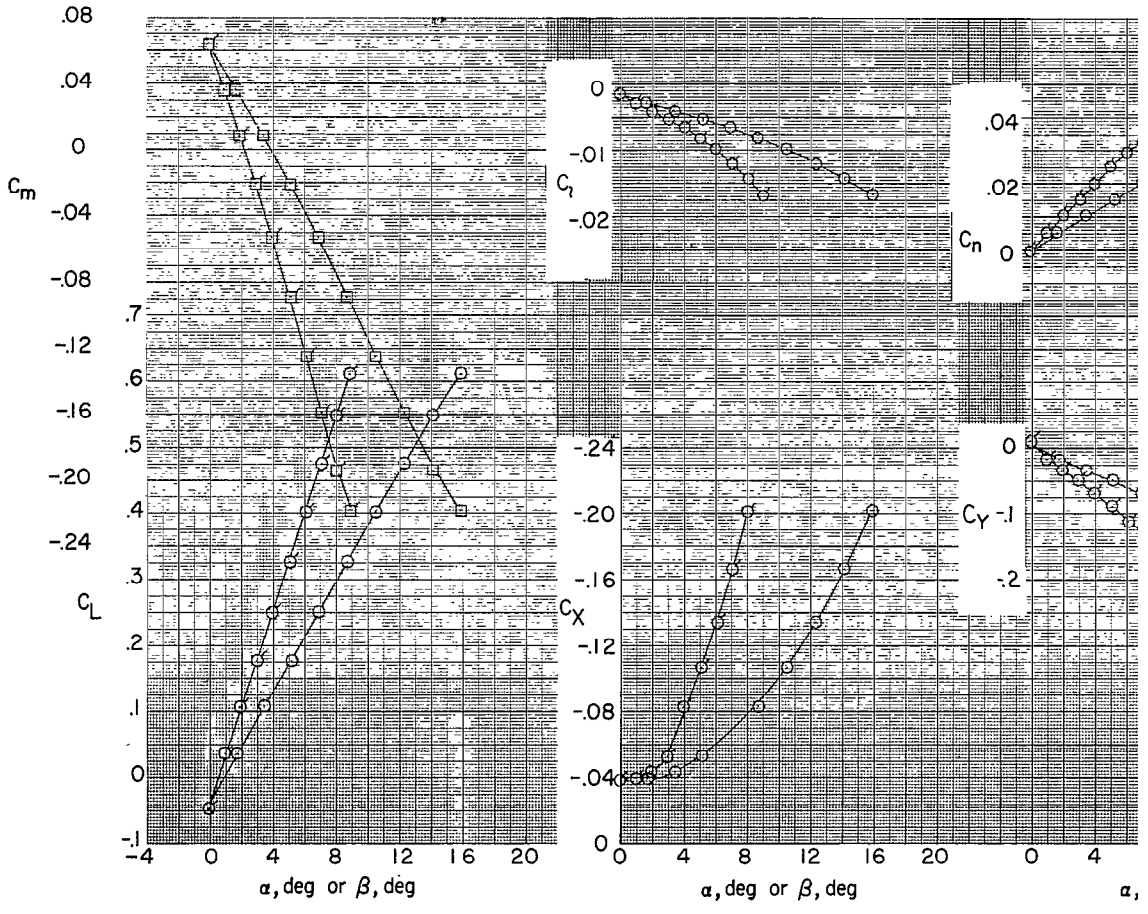

(c) $\phi = 30^{\circ}$.

Figure 13.- Continued.

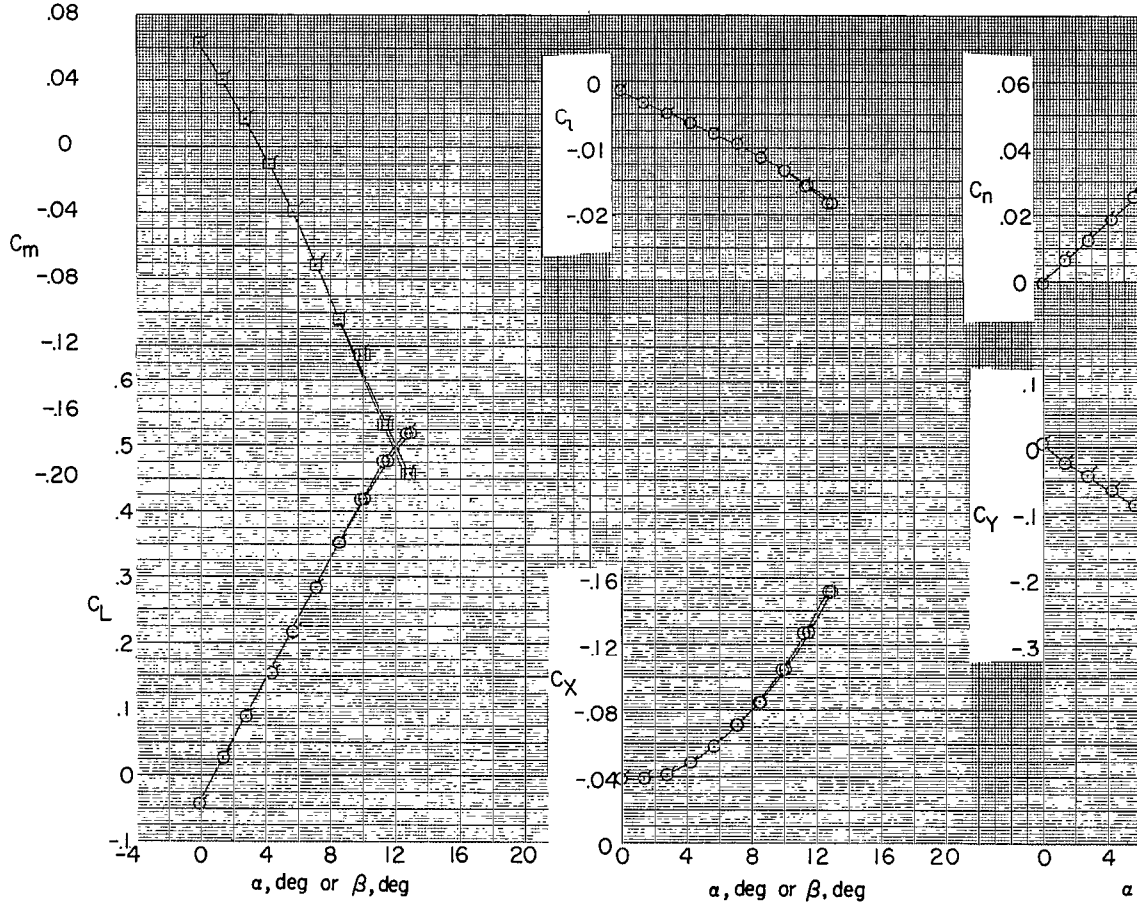

(d) $\phi = 45^{\circ}$.

Figure 13.- Continued.

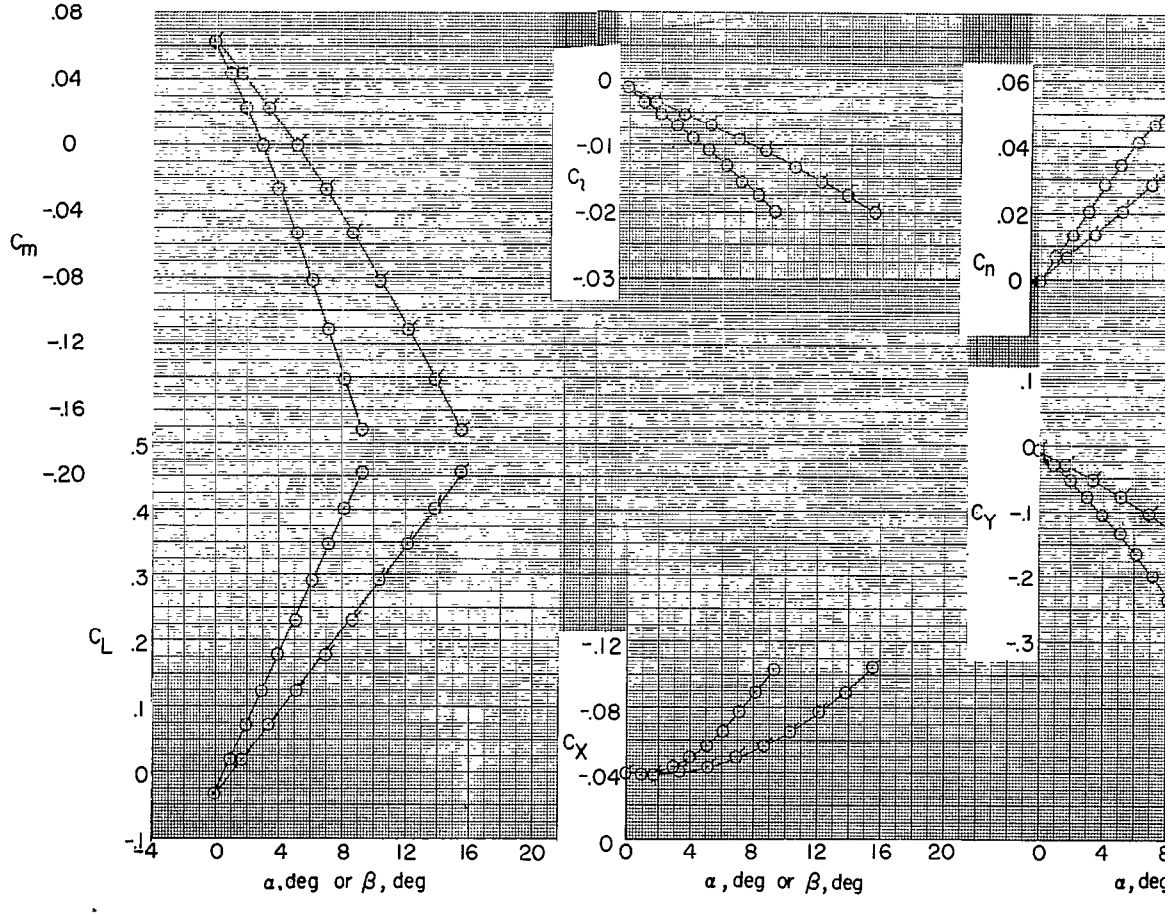

(e) $\phi = 60^{\circ}$.

Figure 13.- Continued.

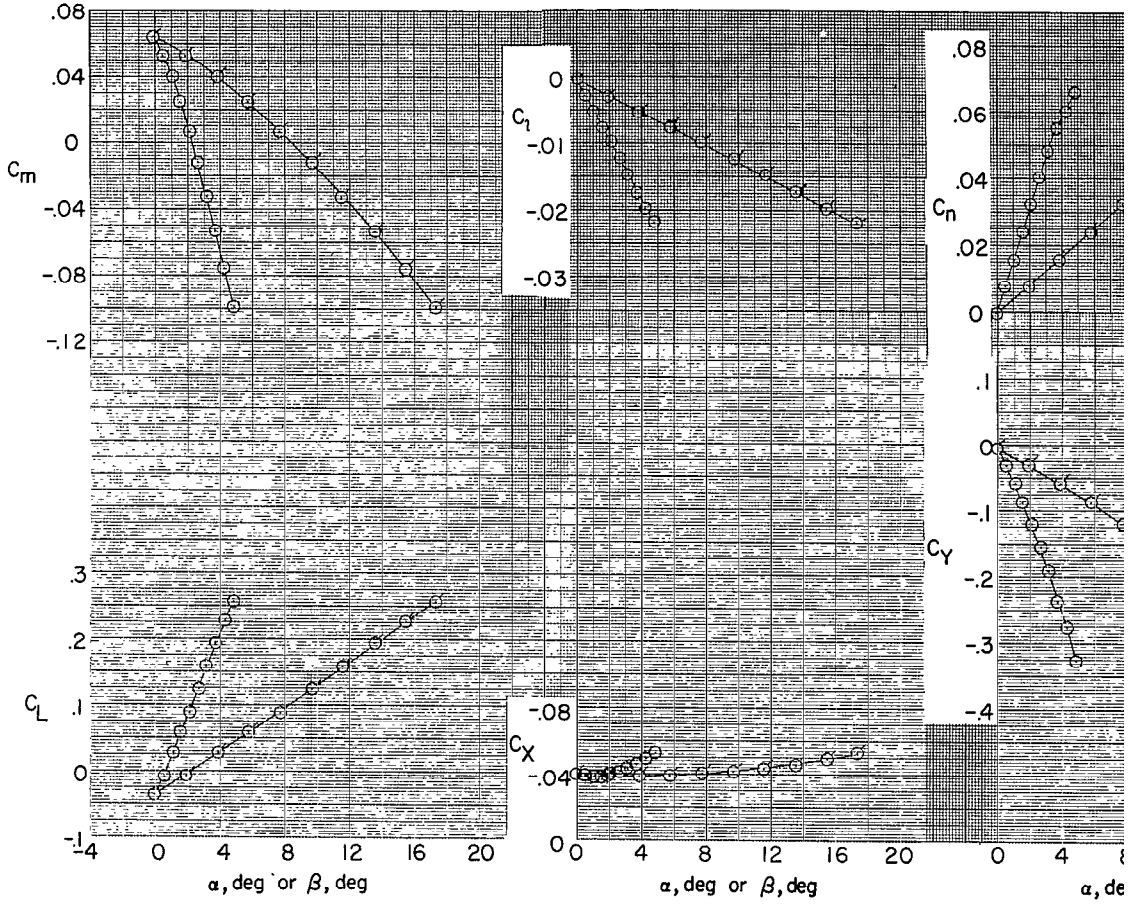

(f) $\phi = 75^{\circ}$.

Figure 13.- Continued.

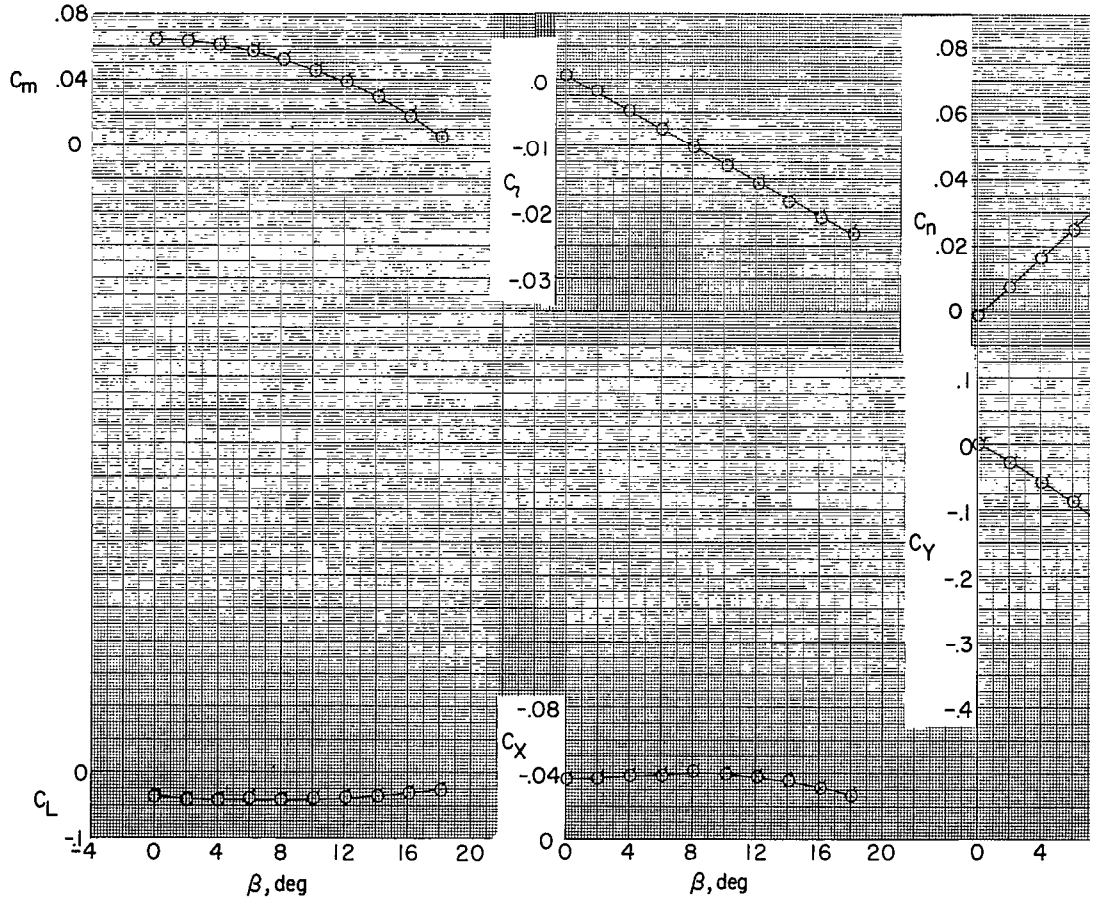

(g) $\phi = 90^{\circ}$.

Figure 13.- Concluded.

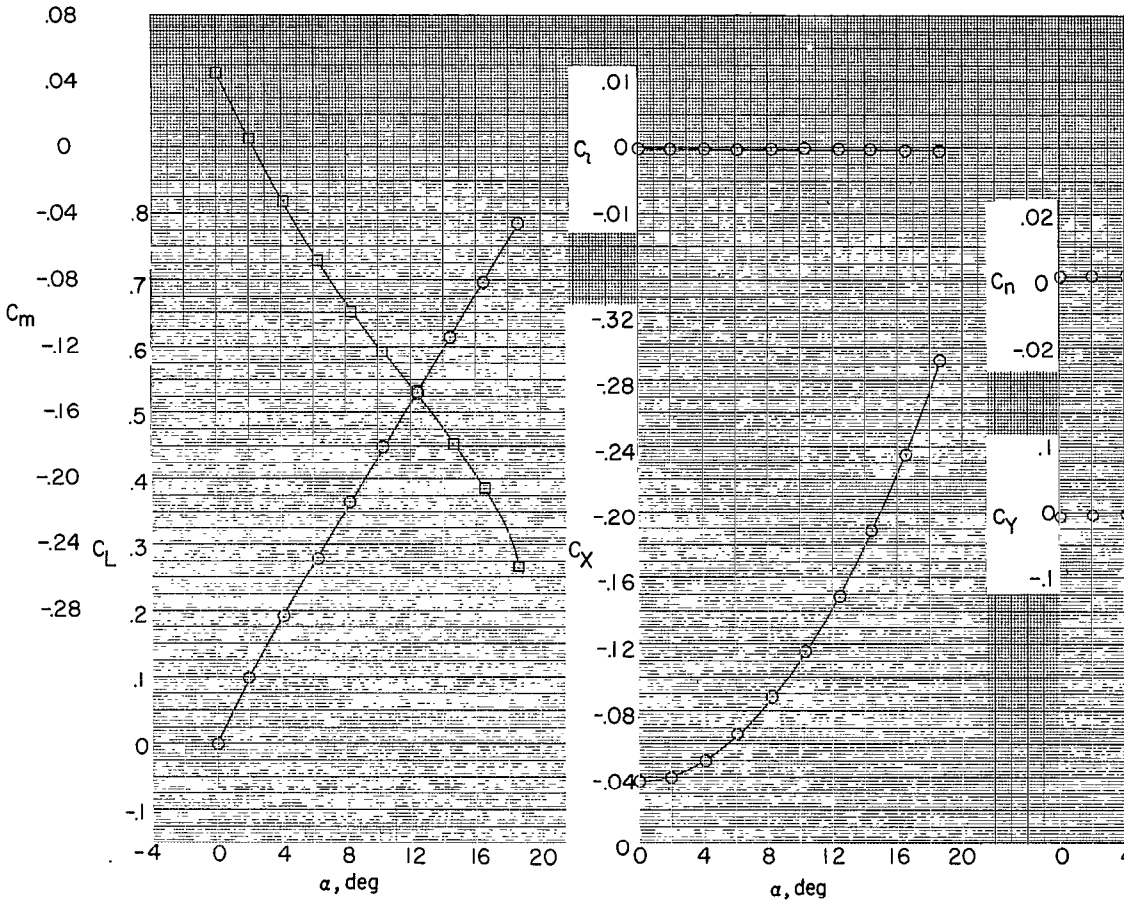

(a) $\phi = 0^{\circ}$.

Figure 14.- Aerodynamic characteristics at various roll ang
Midwing ($\Gamma = 0^{\circ}$); horizontal tail position 3; $i_t = 0^{\circ}$. I
symbols are for variations with β; unflagged symbols are
variations with α.

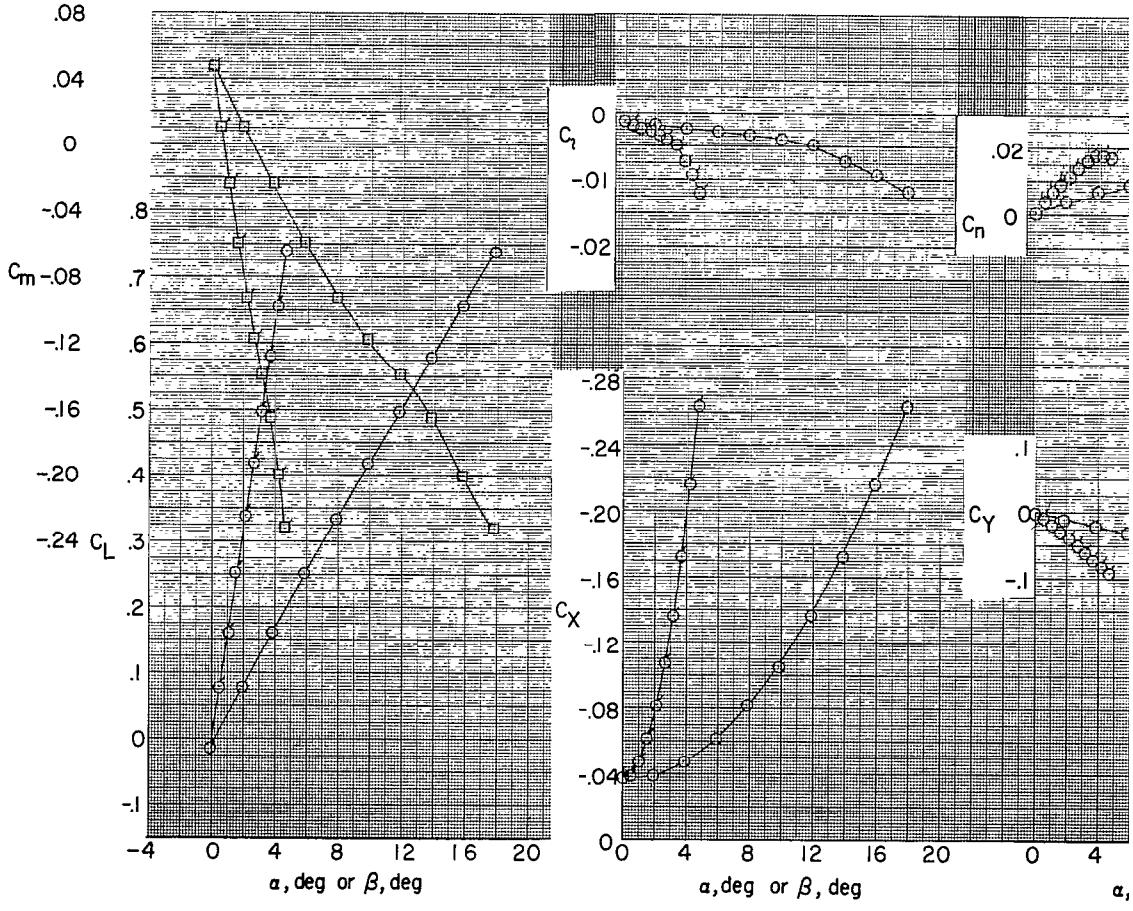

(b) $\phi = 15^{\circ}$.

Figure 14.- Continued.

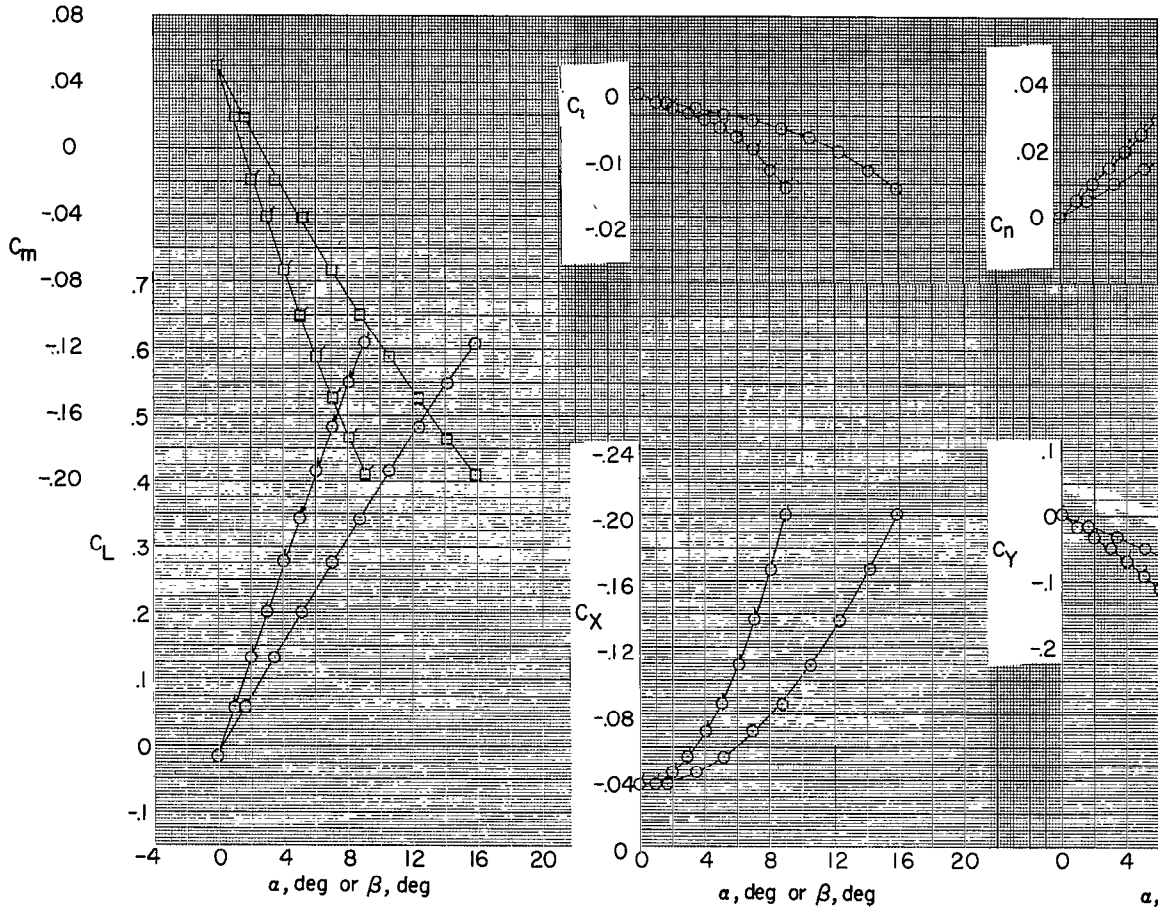

(c) $\phi = 30^{\circ}$.

Figure 14.- Continued.

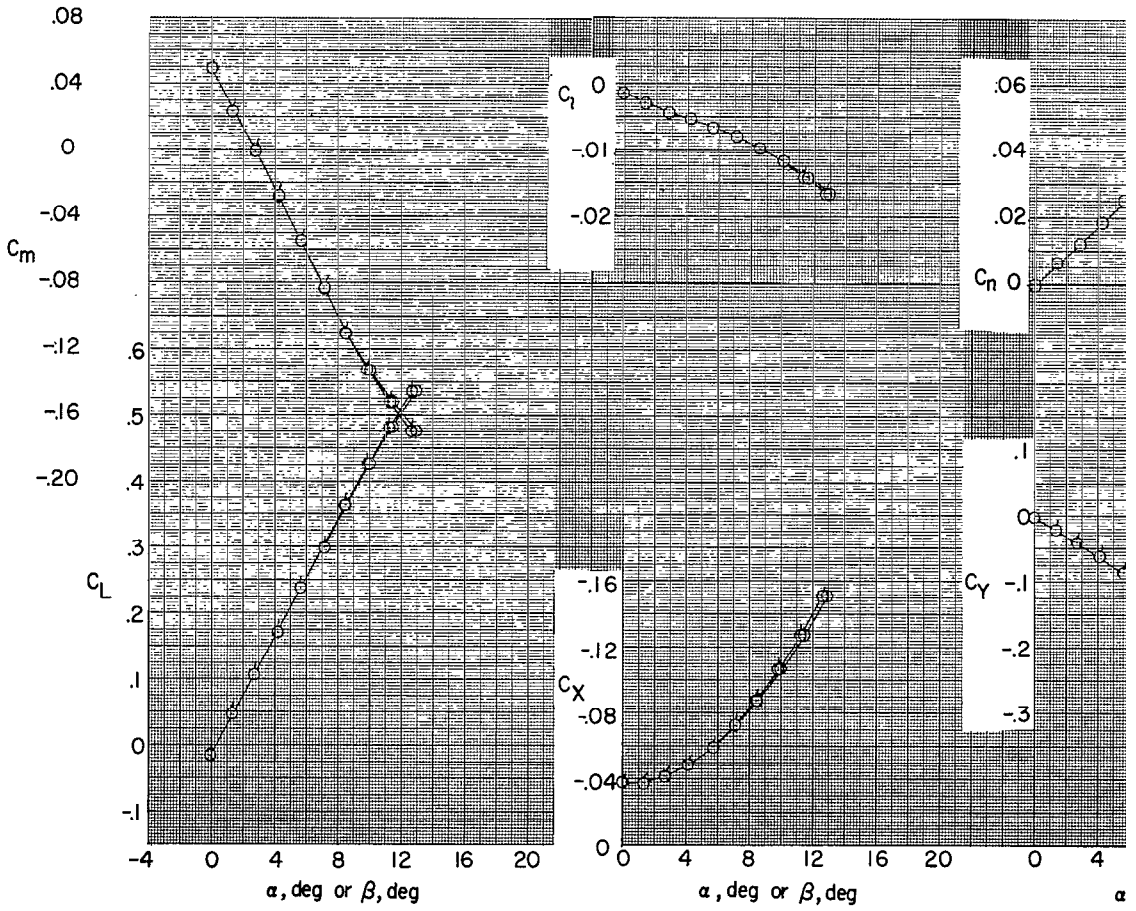

(d) $\phi = 45^{\circ}$.

Figure 14.- Continued.

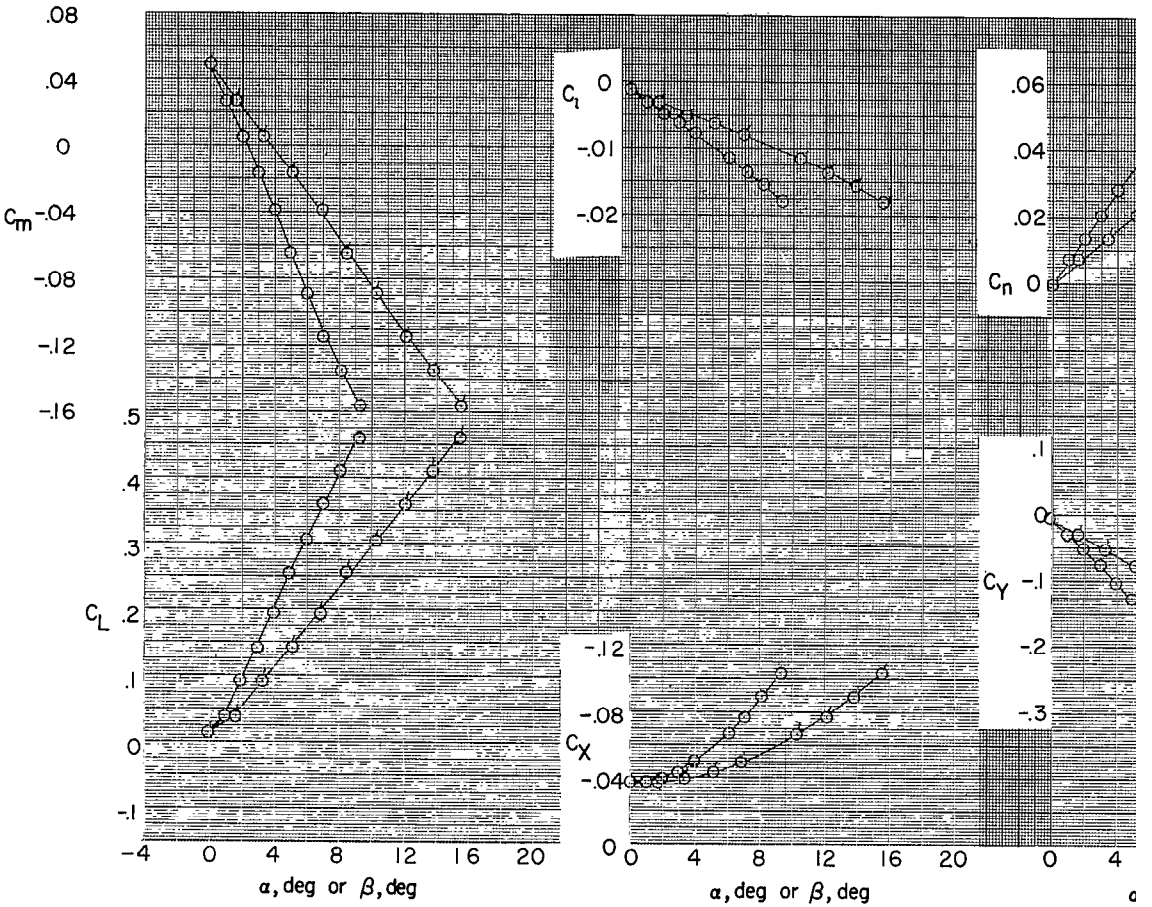

(e) $\phi = 60^{\circ}$.

Figure 14.- Continued.

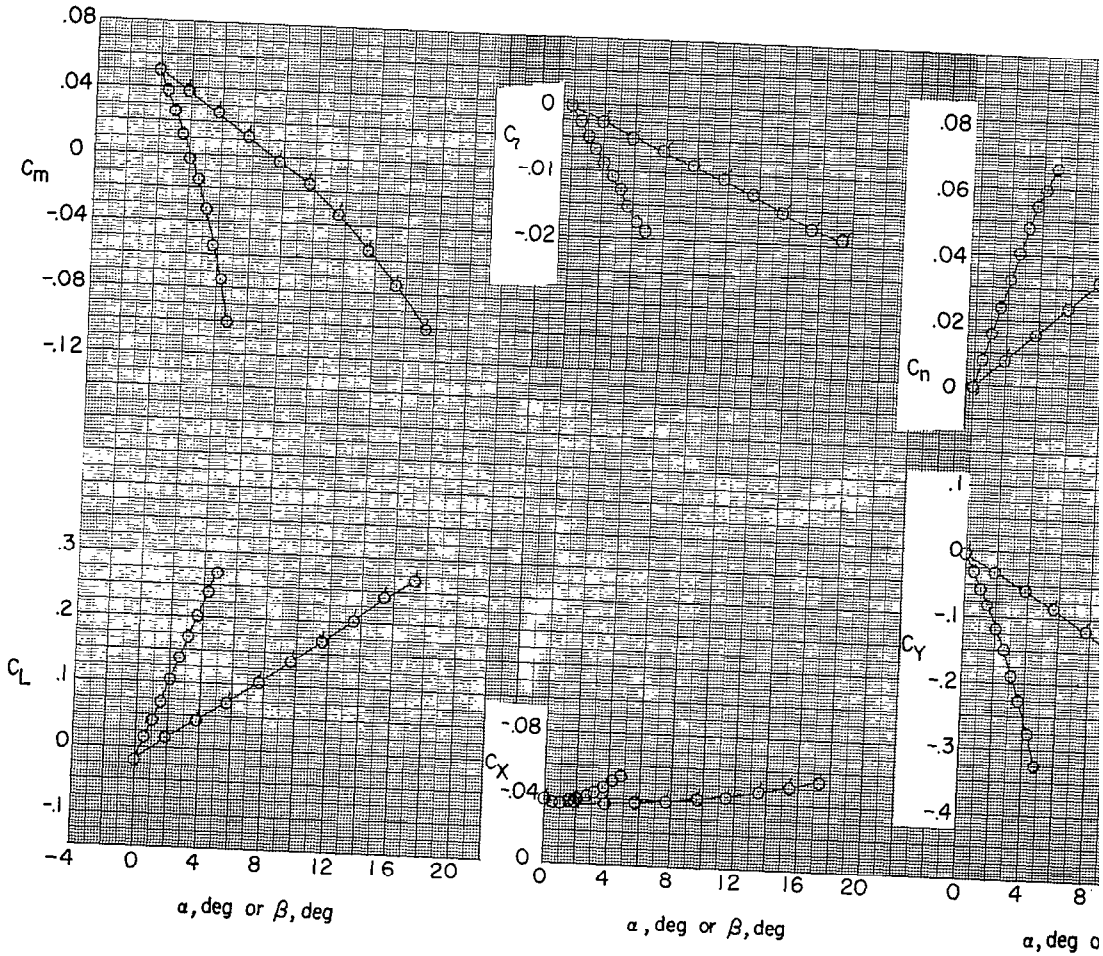

(f) $\phi = 75^{\circ}$.

Figure 14.- Continued.

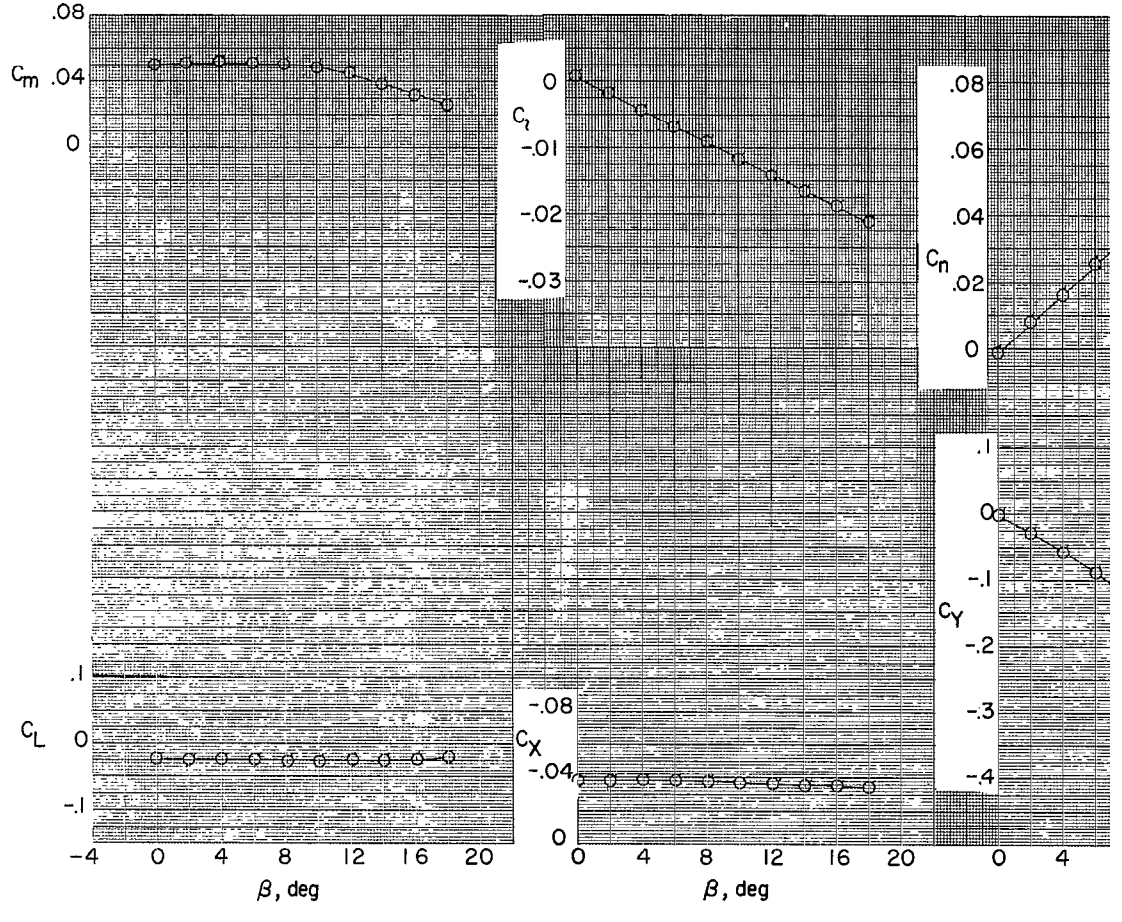

(g) $\phi = 90^{\circ}$.

Figure 14.- Concluded.

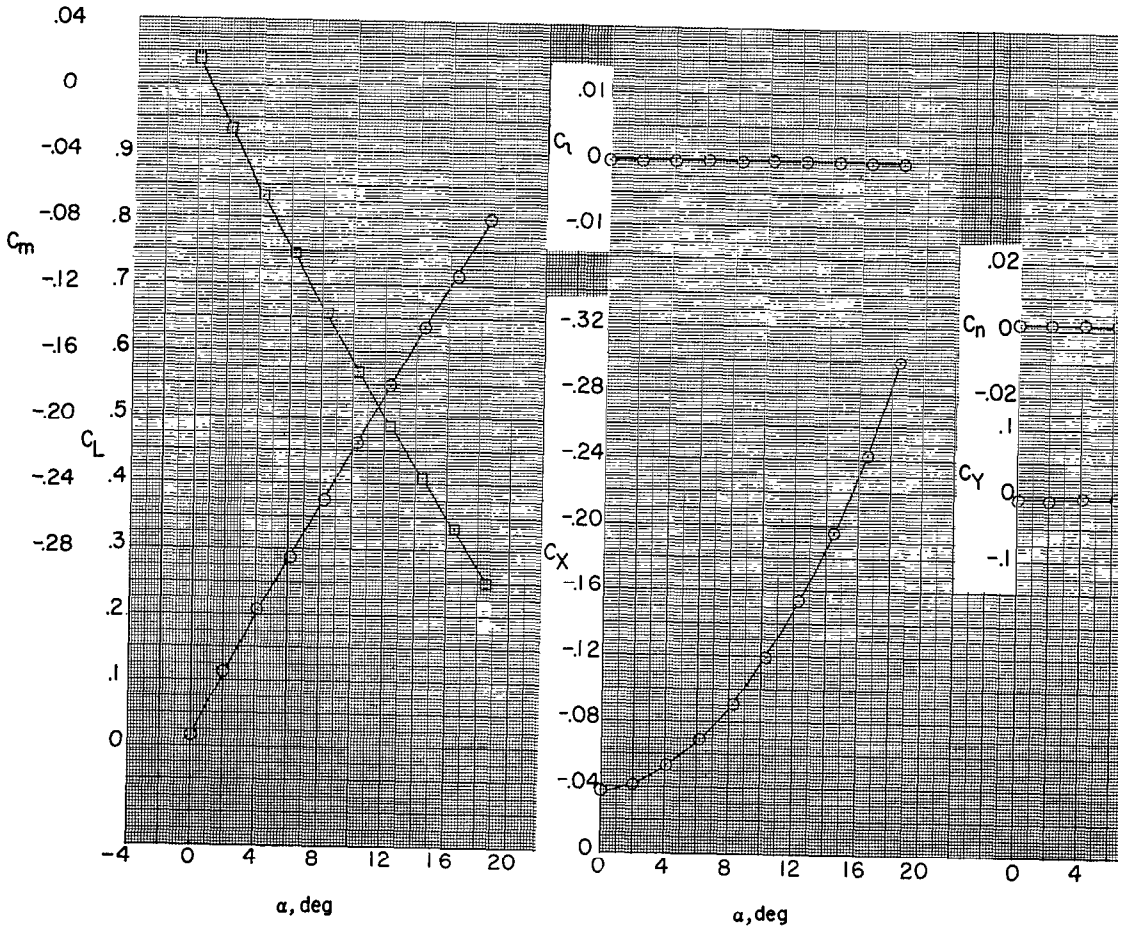

(a) $\phi = 0^{\circ}$.

Figure 15.- Aerodynamic characteristics at various roll angles. Midwing ($\Gamma = 0^{\circ}$); horizontal tail position 4; $i_t = 0^{\circ}$. Flag symbols are for variations with β; unflagged symbols are for variations with α.

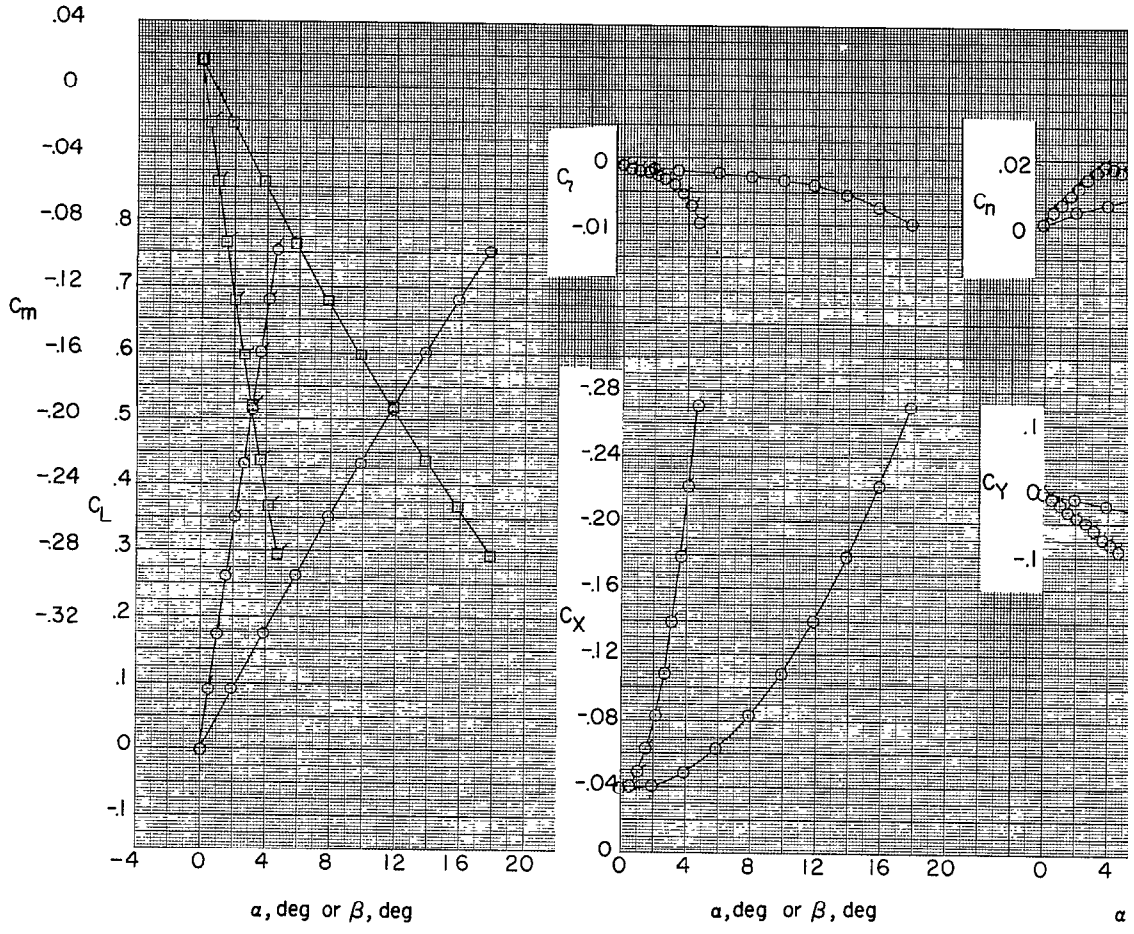

(b) $\phi = 15^{\circ}$.

Figure 15.- Continued.

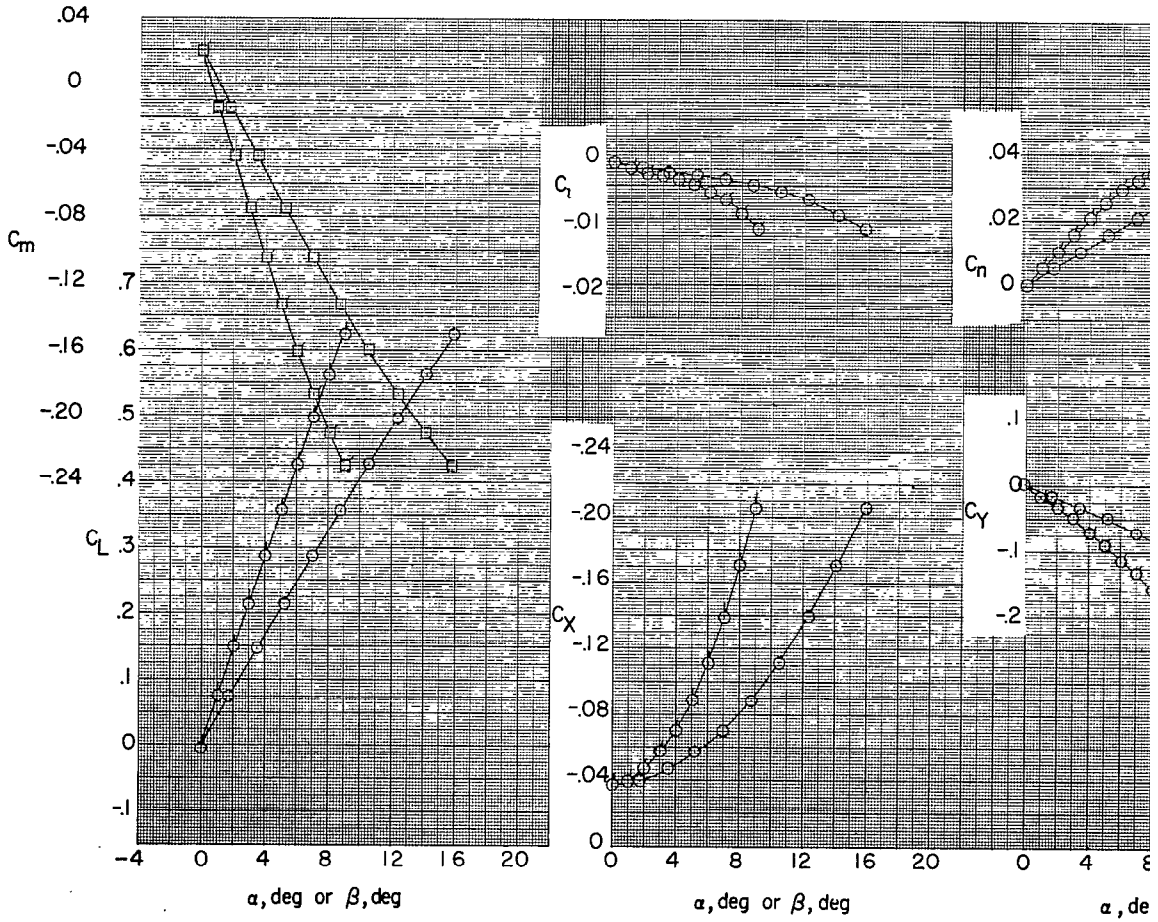

(c) $\phi = 30^{\circ}$.

Figure 15.- Continued.

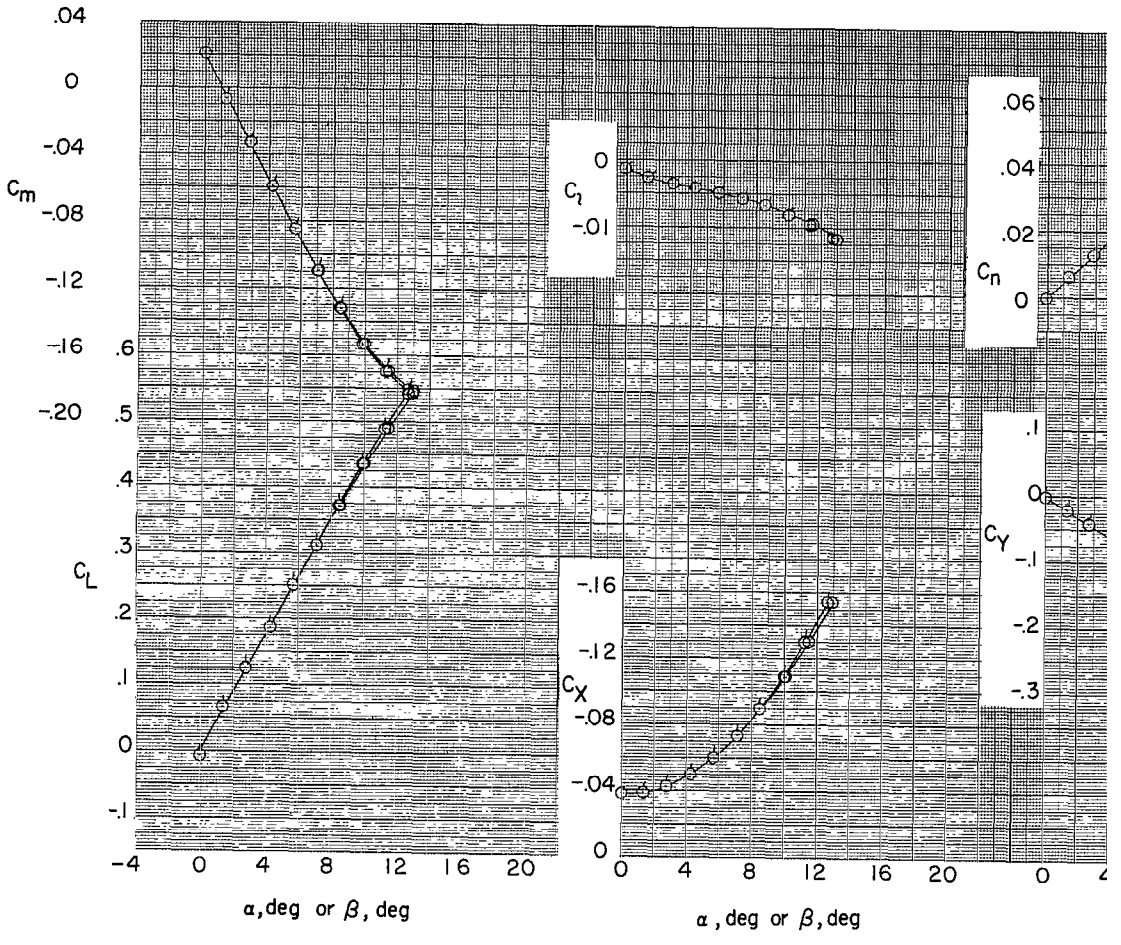

(d) $\phi = 45^{\circ}$.

Figure 15.- Continued.

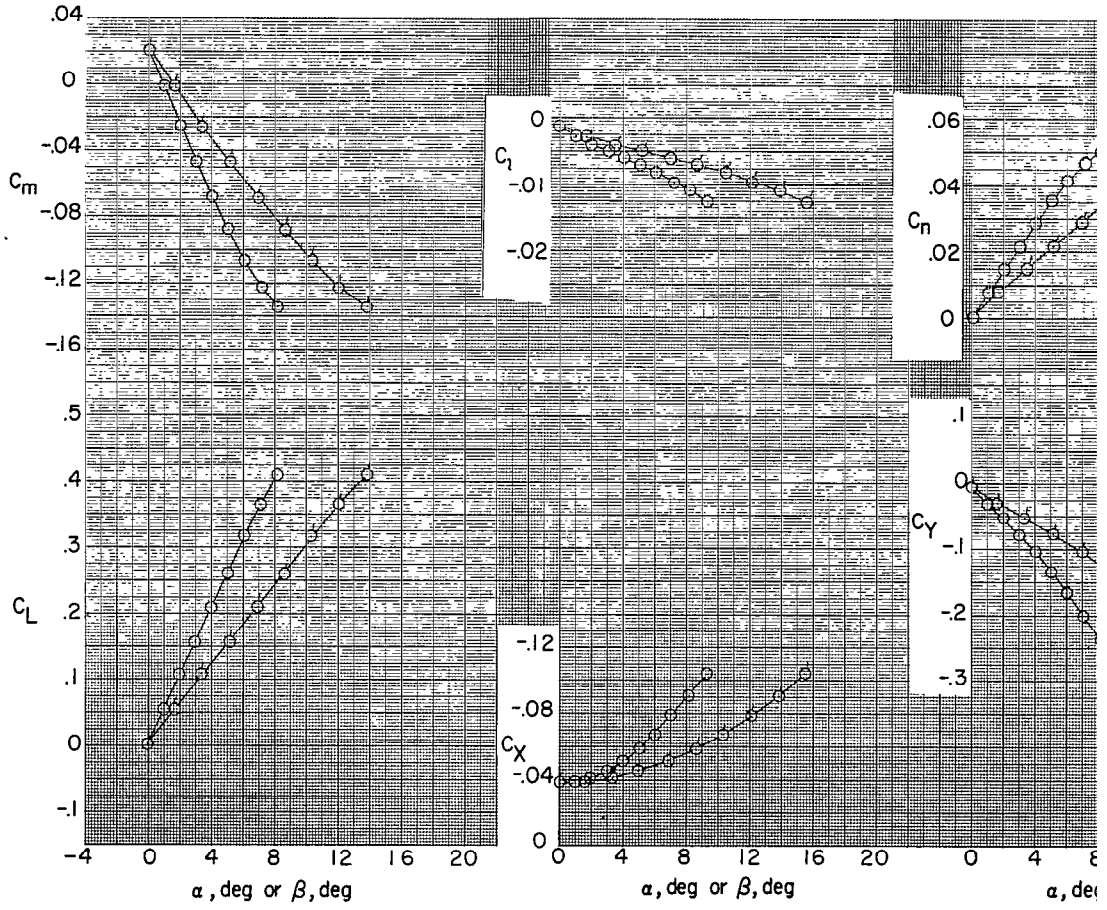

(e) $\phi = 60^{\circ}$.

Figure 15.- Continued.

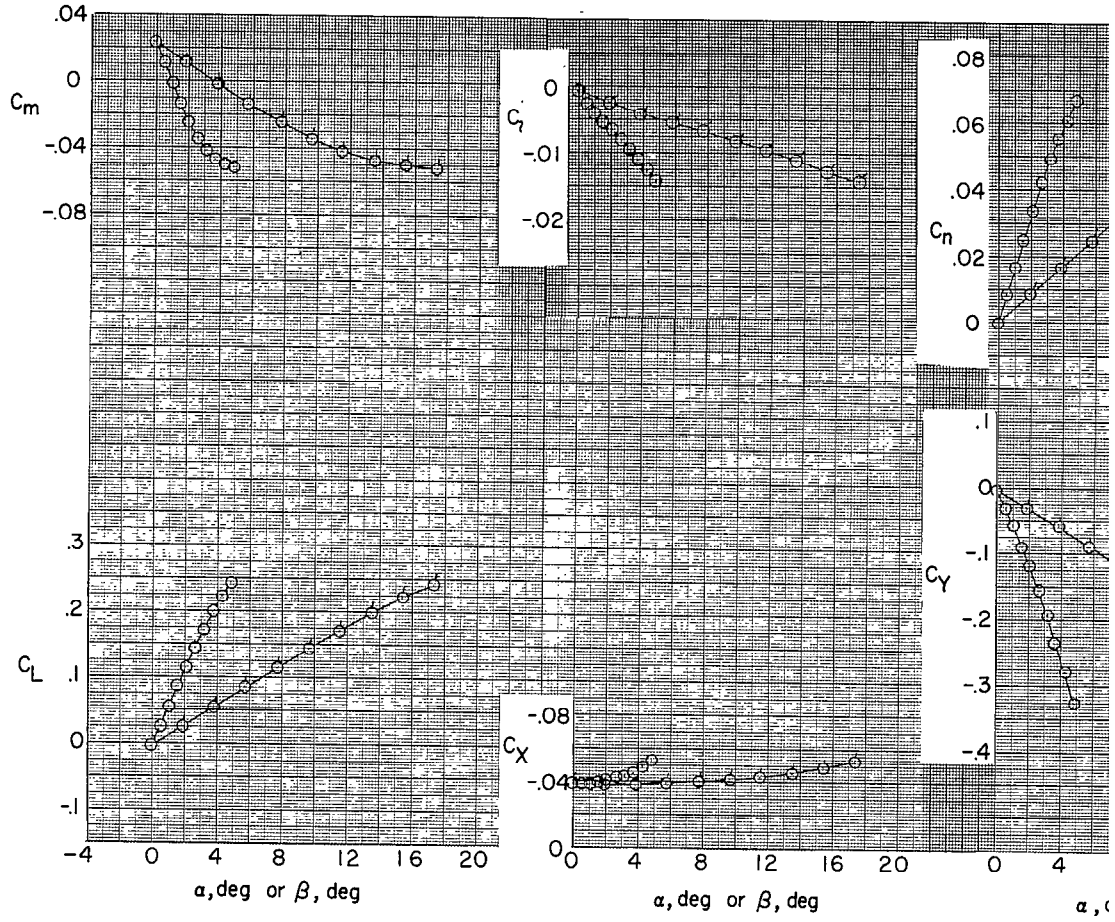

(f) $\phi = 75^{\circ}$.

Figure 15.- Continued.

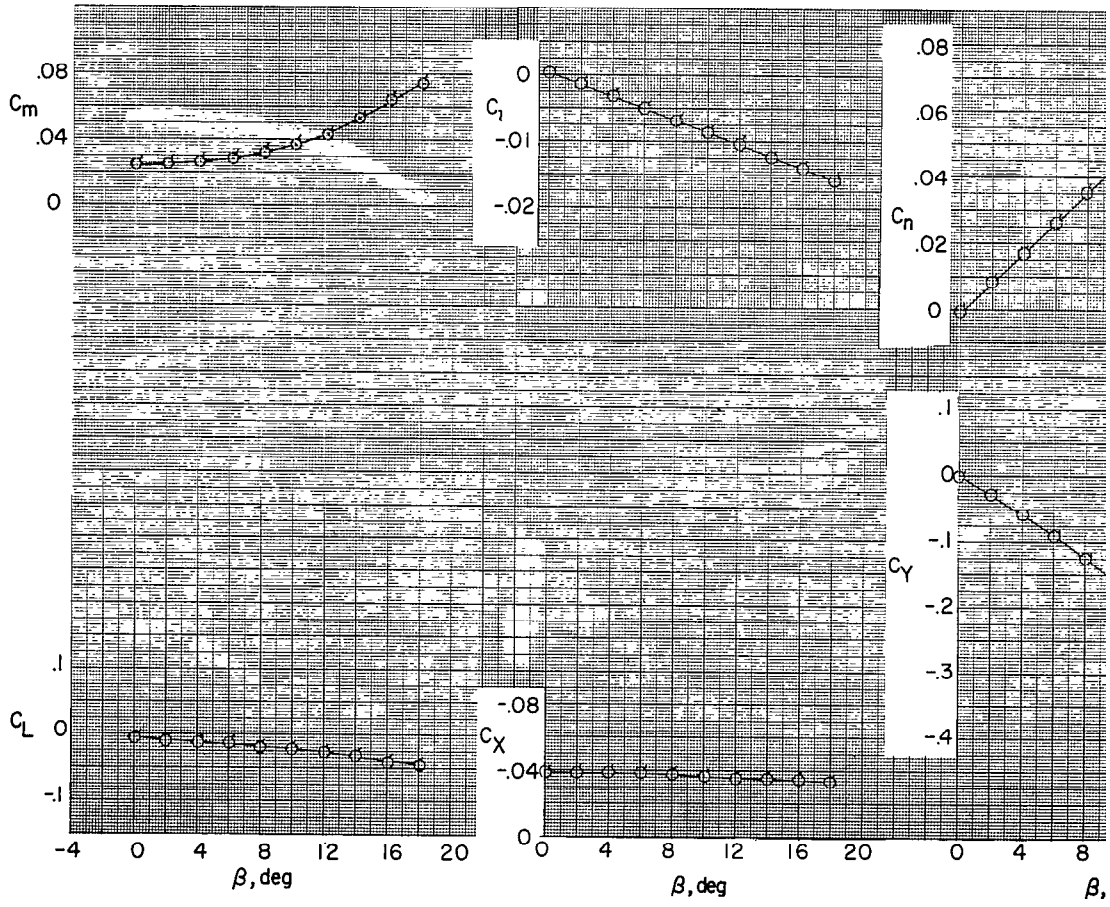

(g) $\phi = 90^{\circ}$.

Figure 15.- Concluded.

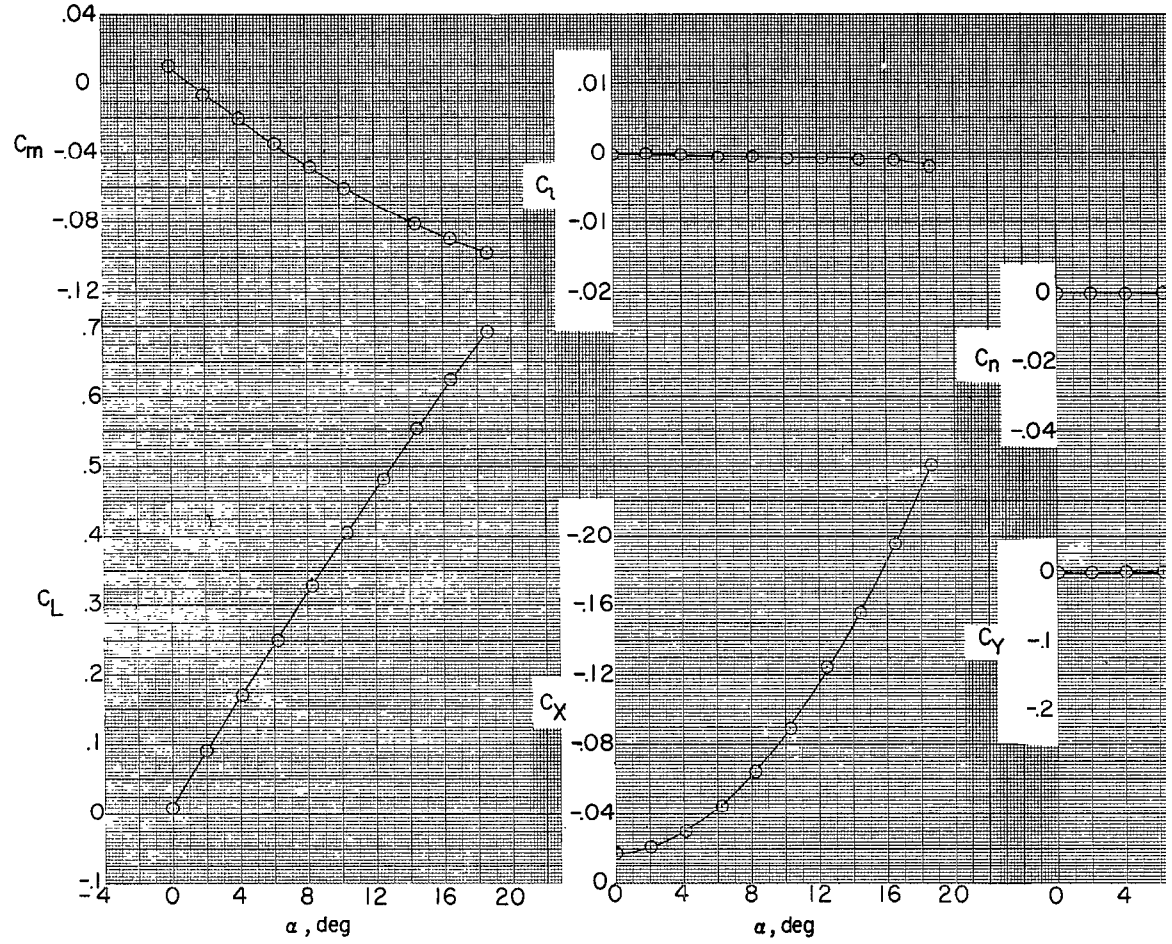

(a) $\phi = 0^{o}$.

Figure 16.- Aerodynamic characteristics at various roll angles
wing; tails off. Flagged symbols are for variations with
unflagged symbols are for variations with α.

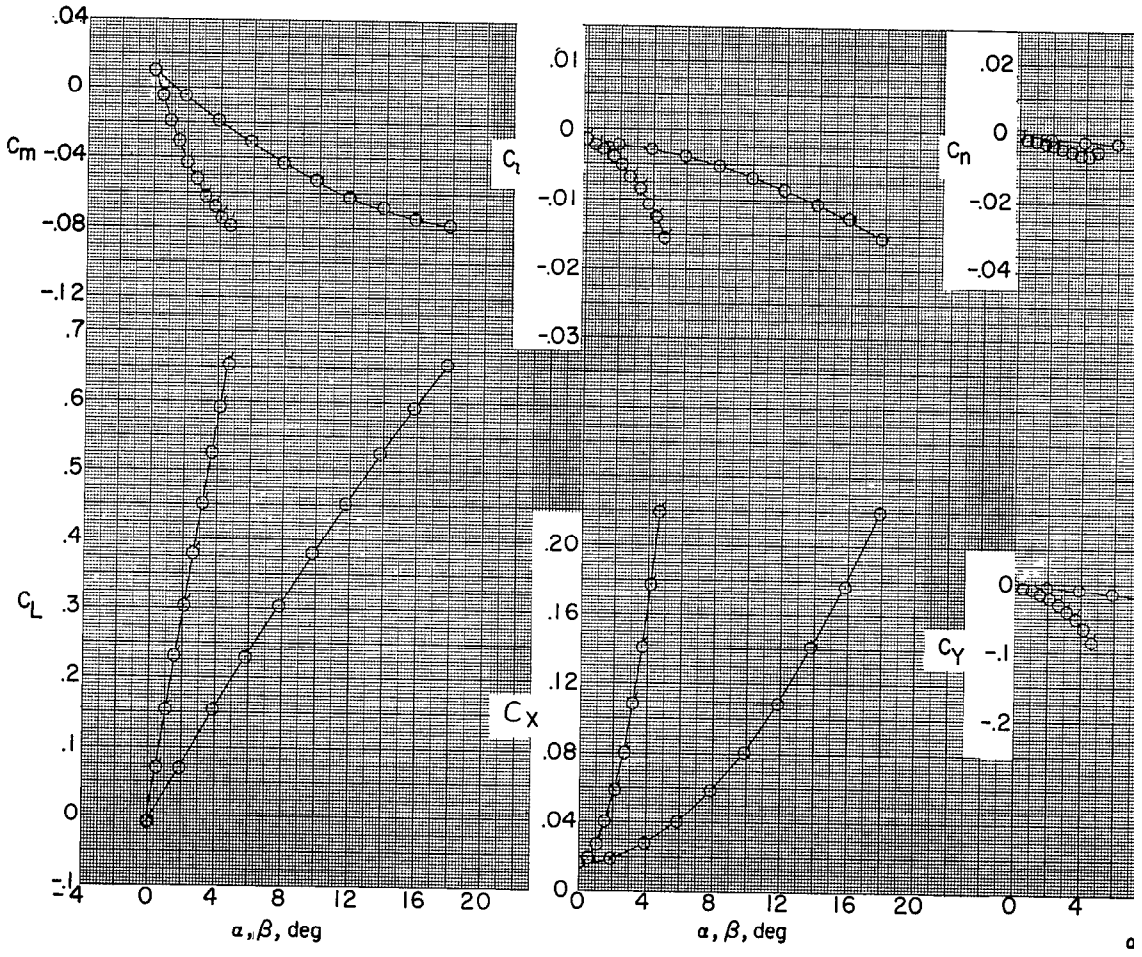

(b) $\phi = 15^{\circ}$.

Figure 16.- Continued.

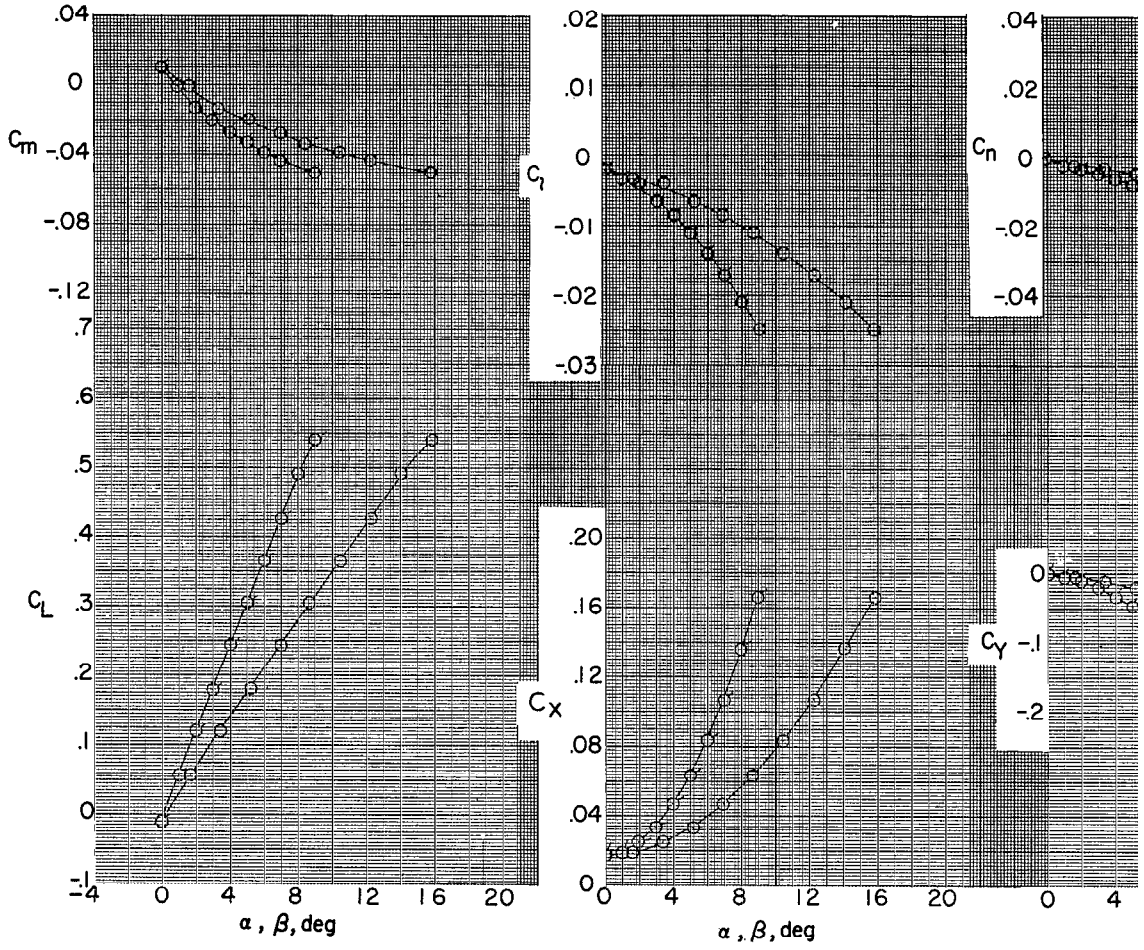

(c) $\phi = 30^{o}$.

Figure 16.- Continued.

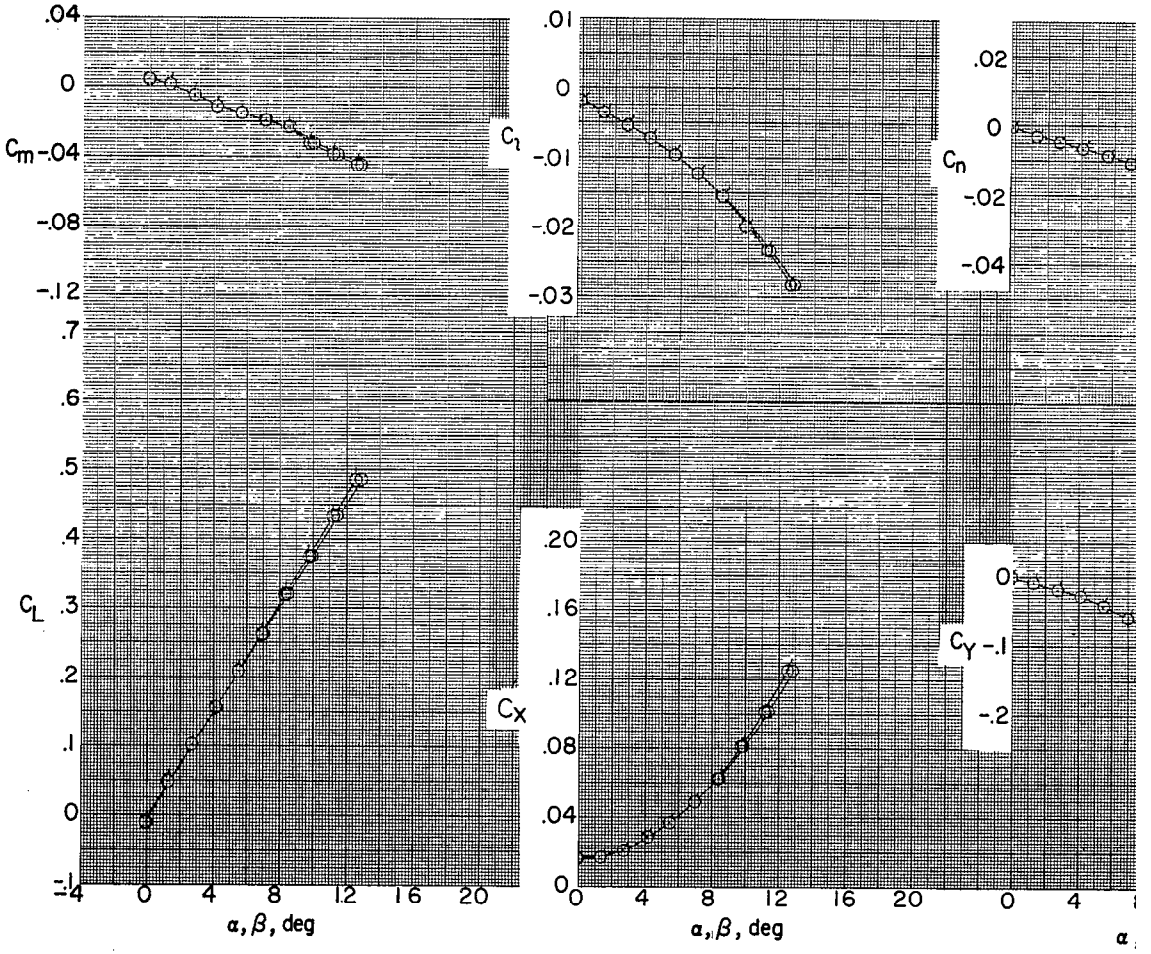

(d) $\phi = 45^\circ$.

Figure 16.- Continued.

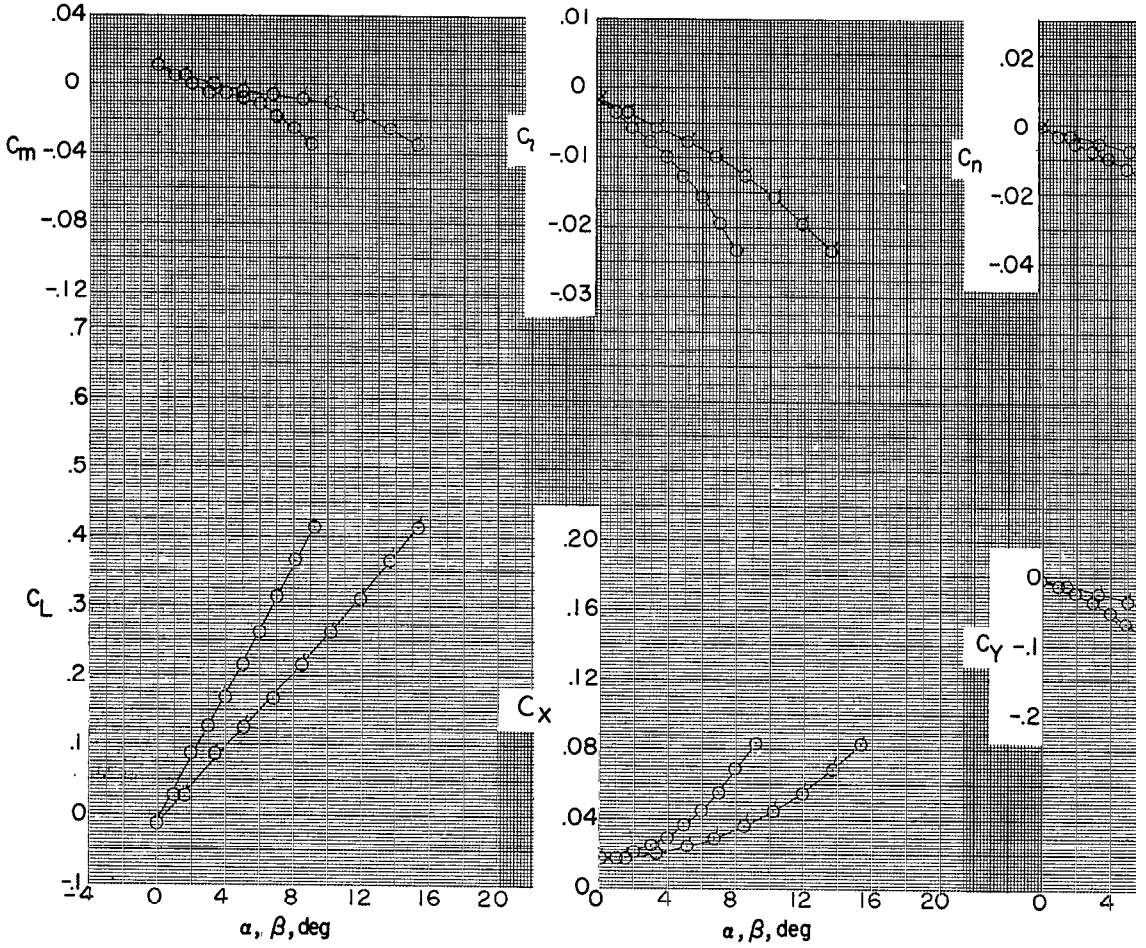

(e) $\phi = 60^\circ$.

Figure 16.- Continued.

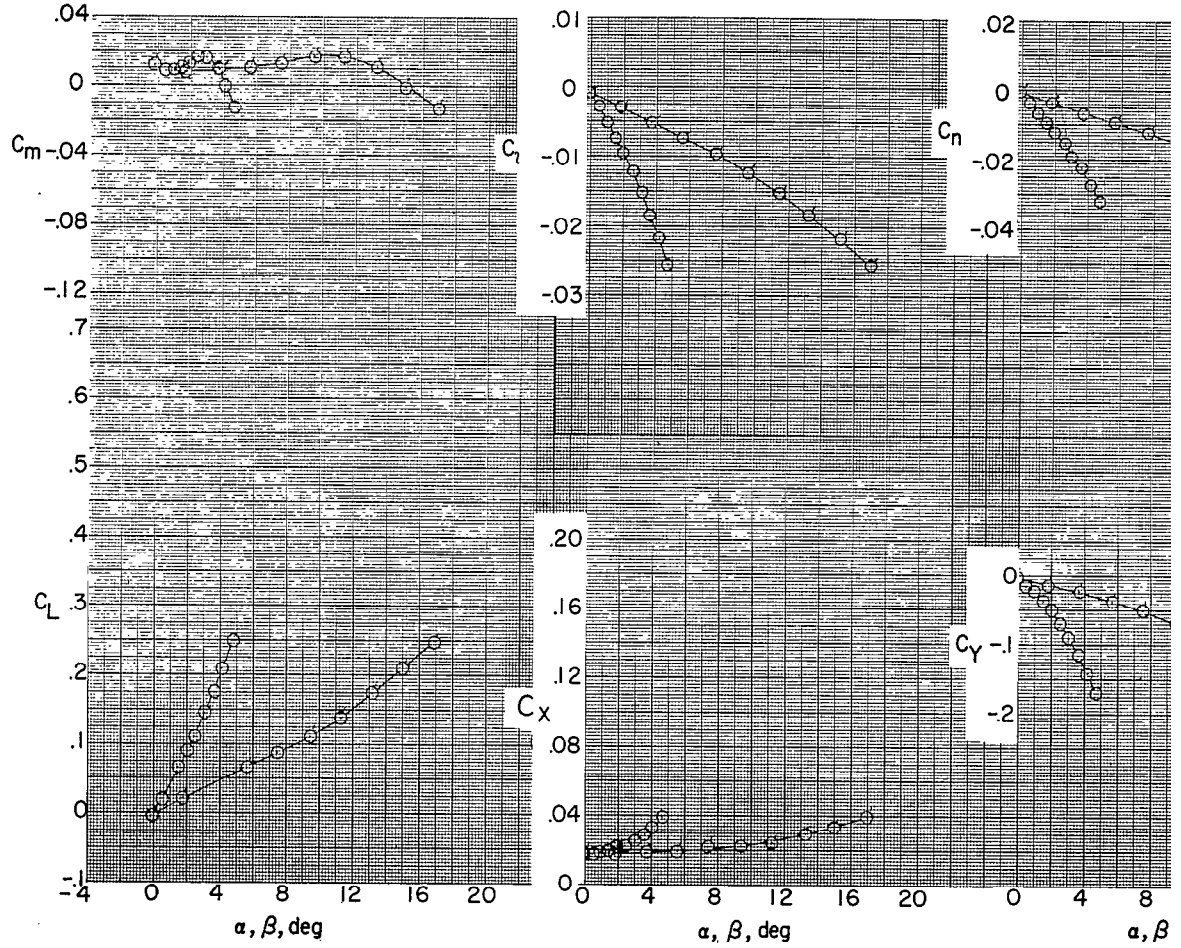

(f) $\phi = 75^{\circ}$.

Figure 16.- Continued.

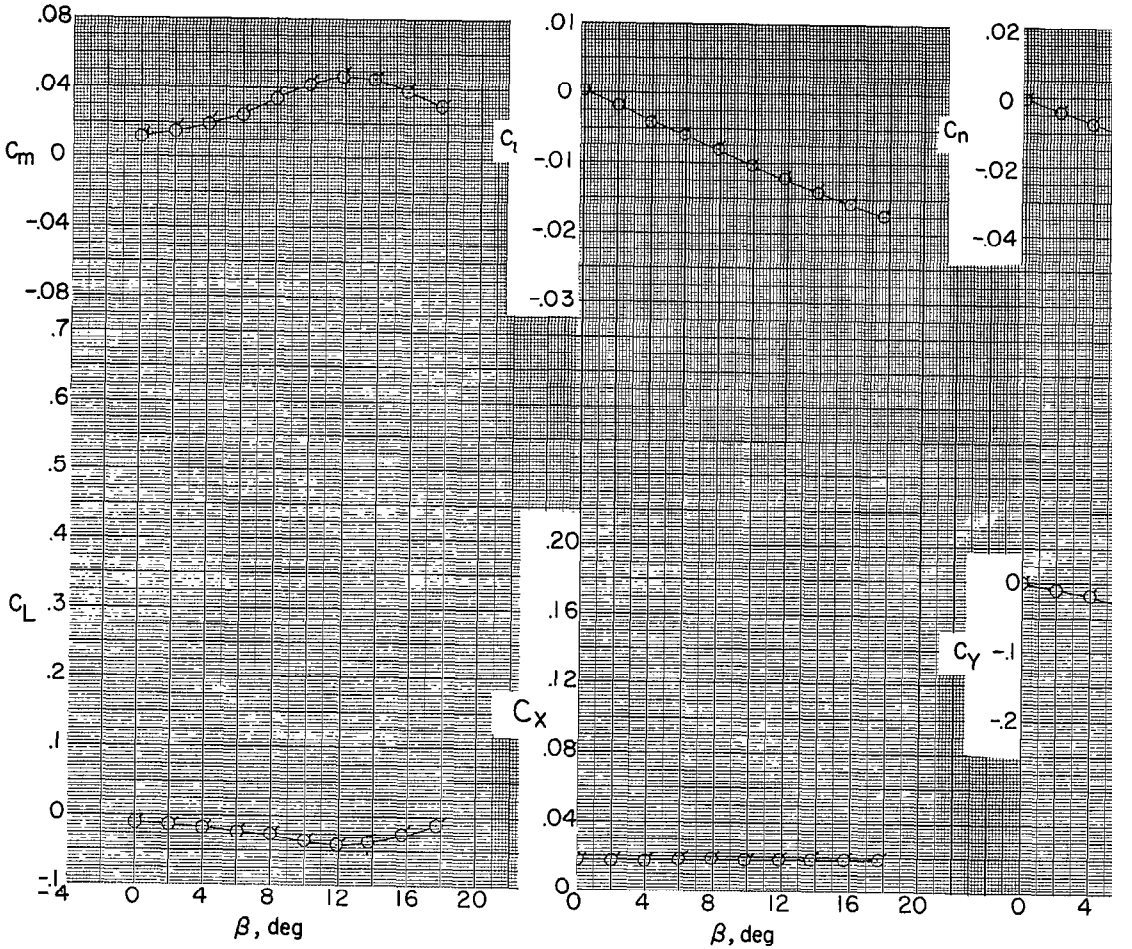

(g) $\phi = 90^{\circ}$.

Figure 16.- Concluded.

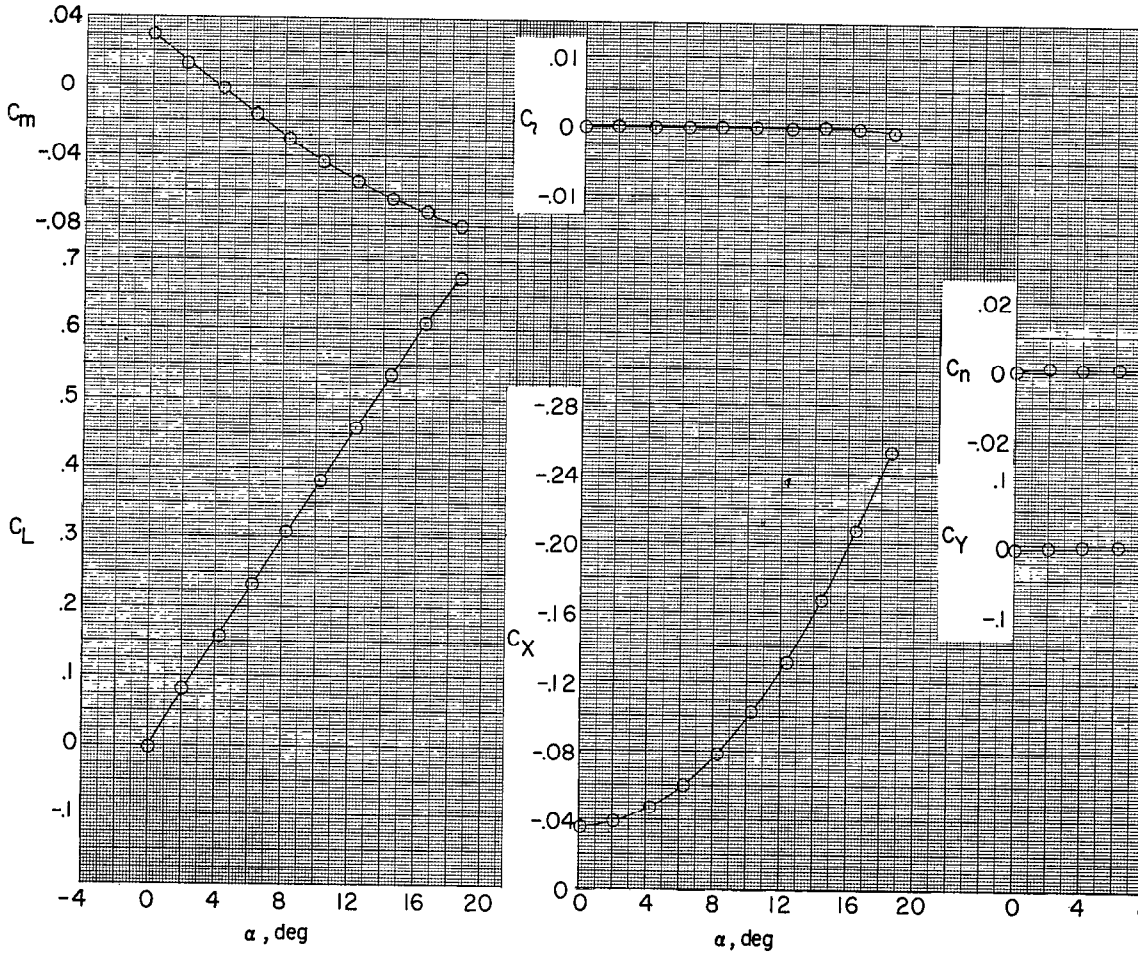

(a) $\phi = 0^{o}$.

Figure 17.- Aerodynamic characteristics at various roll angles. wing; horizontal tail off. Flagged symbols are for variatior with β; unflagged symbols are for variations with α.

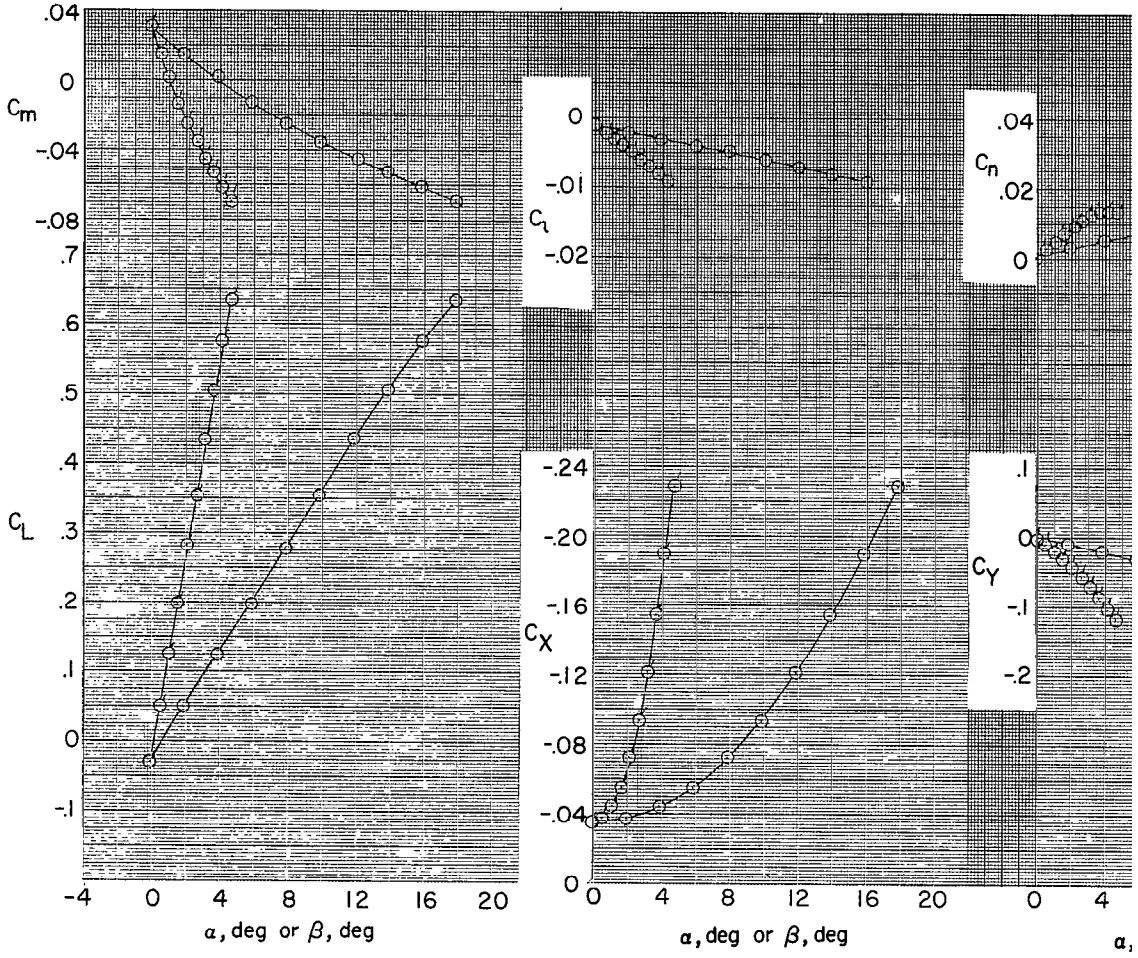

(b) $\phi = 15^{\circ}$.

Figure 17.- Continued.

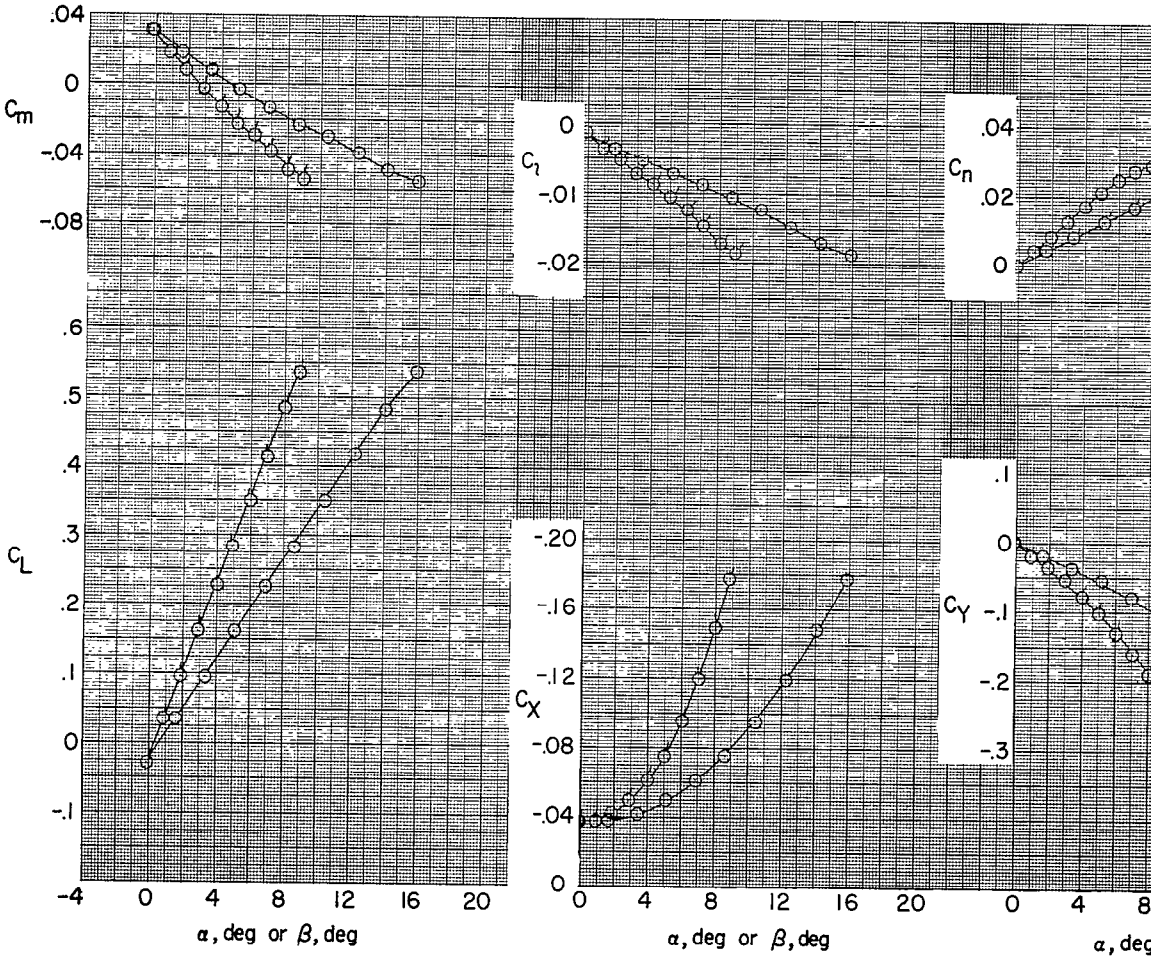

(c) $\phi = 30^{\circ}$.

Figure 17.- Continued.

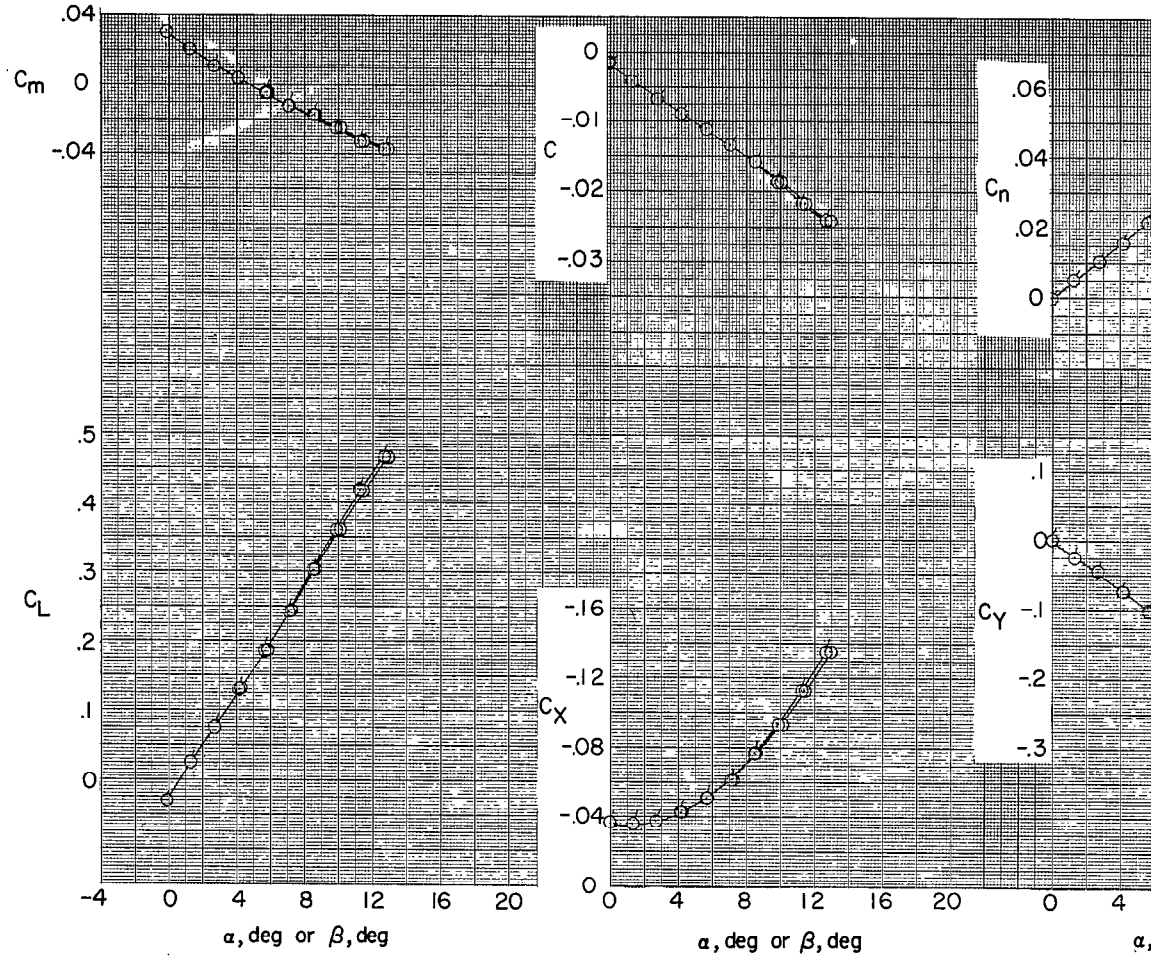

(d) $\phi = 45^{\circ}$.

Figure 17.- Continued.

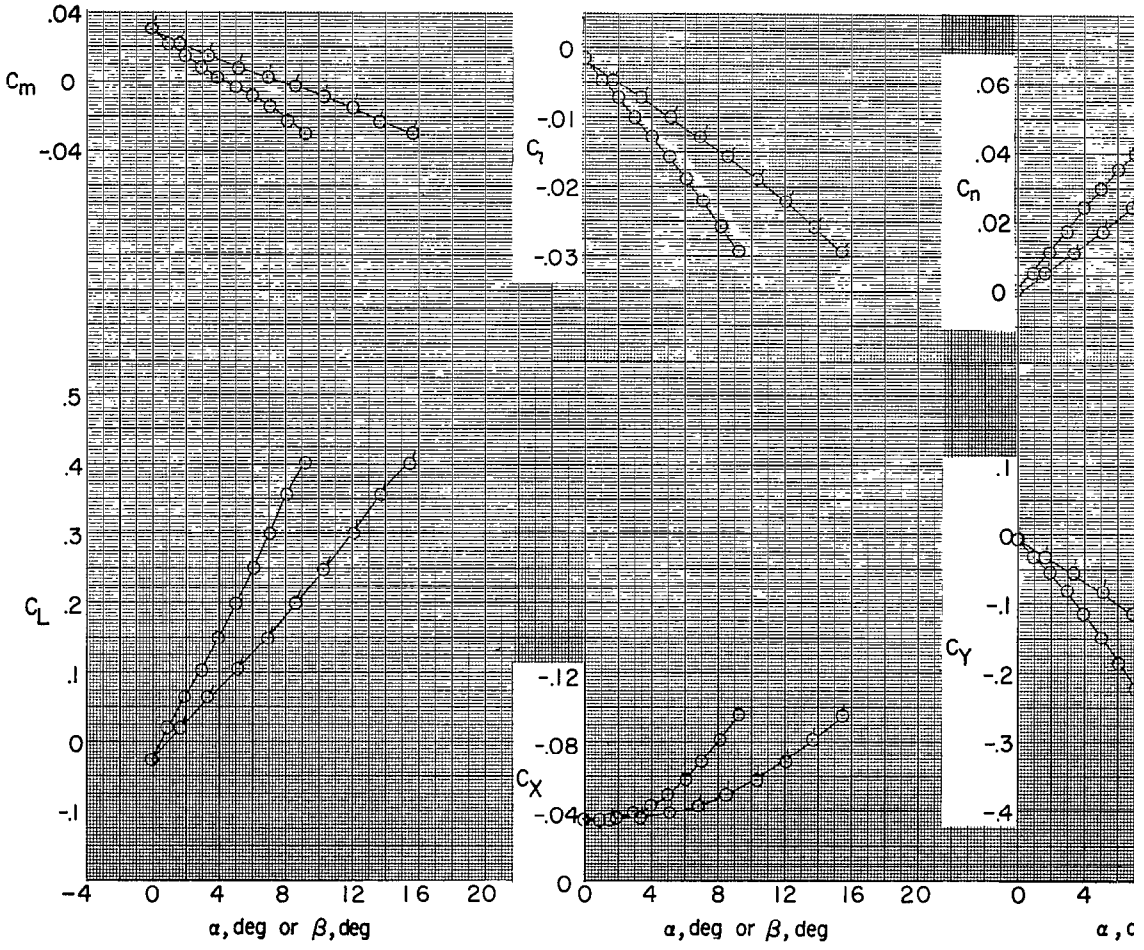

(e) $\phi = 60^{\circ}$.

Figure 17.- Continued.

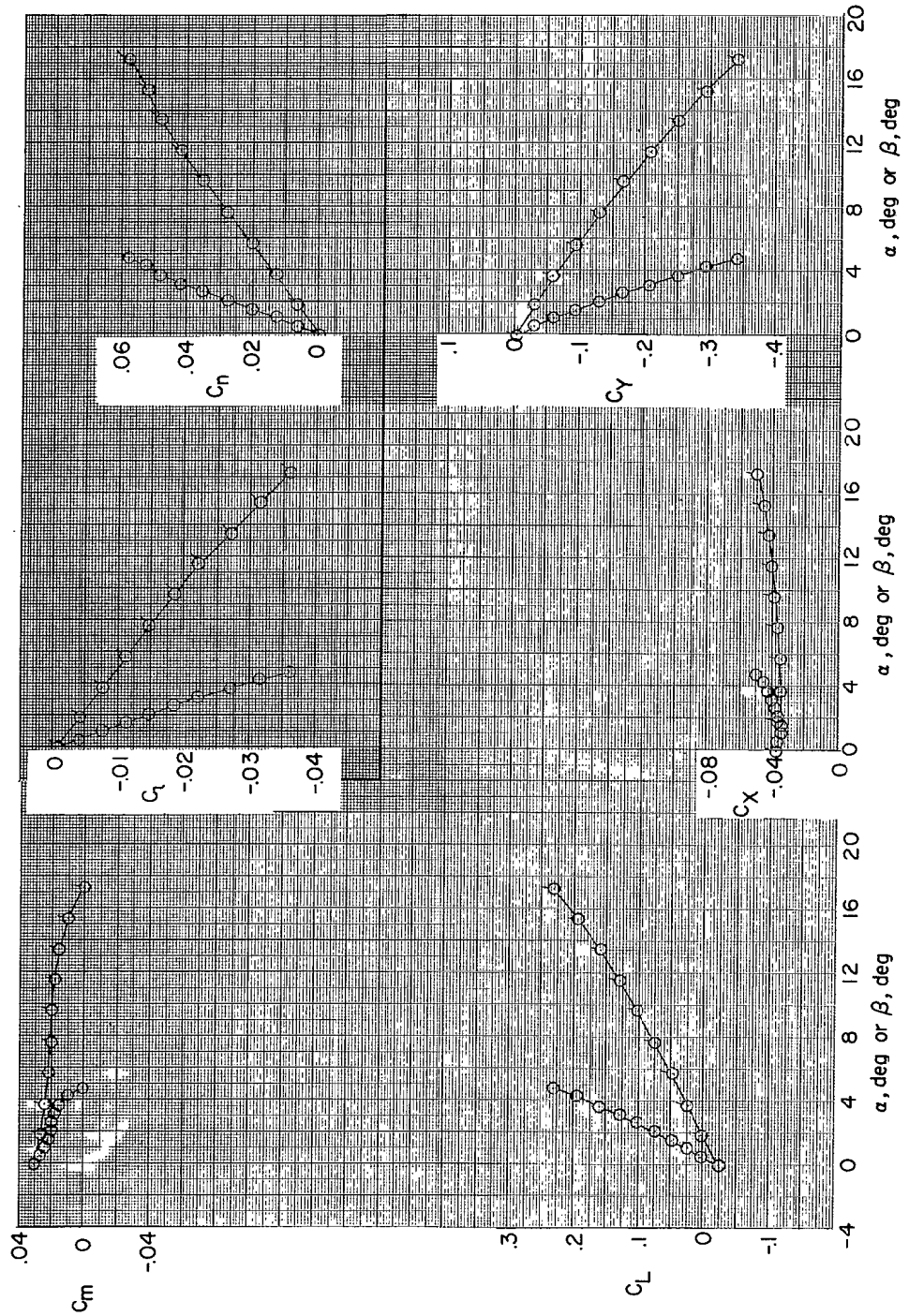

(f) $\phi = 75°$.

Figure 17.- Continued.

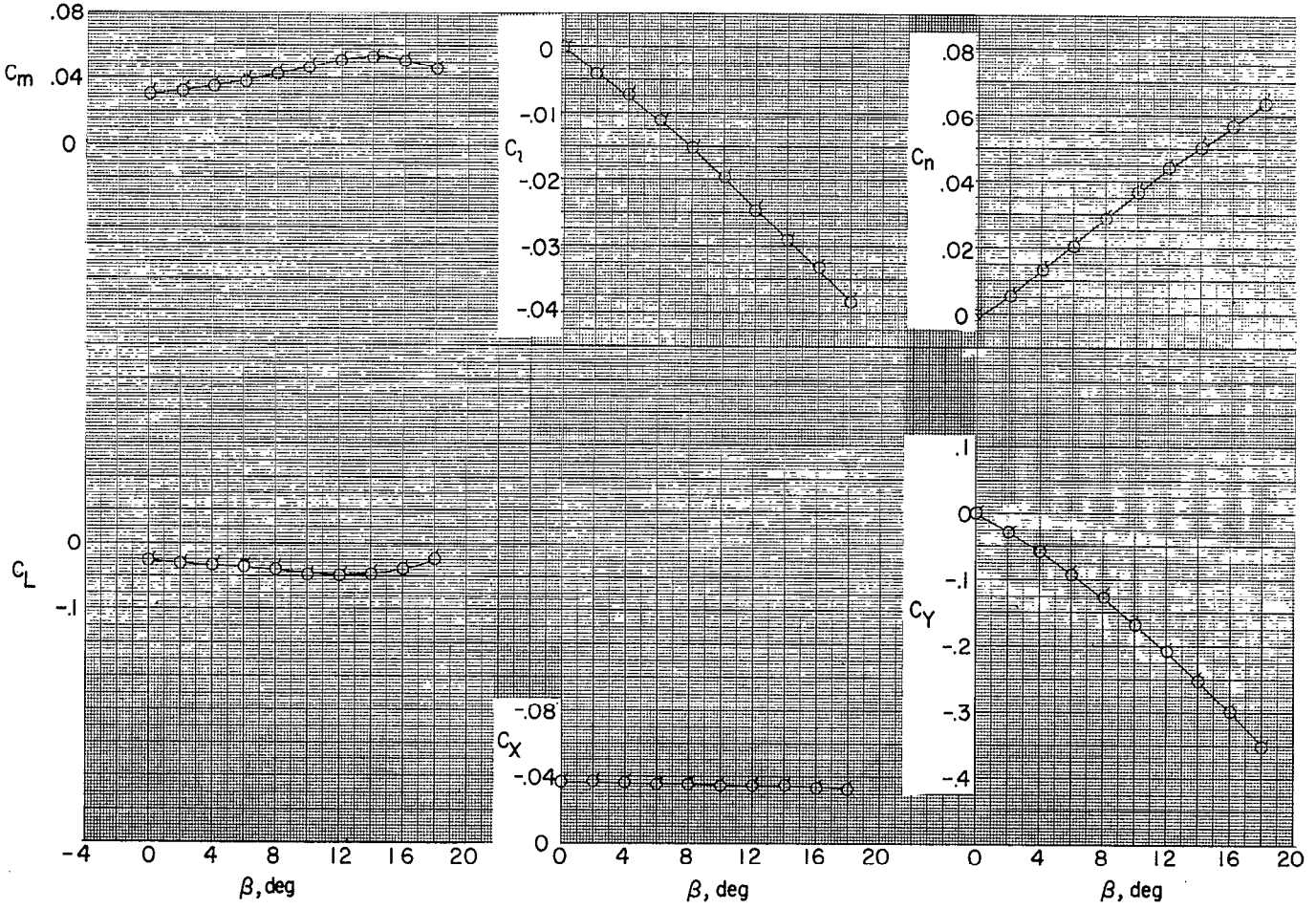

(g) $\phi = 90^{\circ}$.

Figure 17.- Concluded.

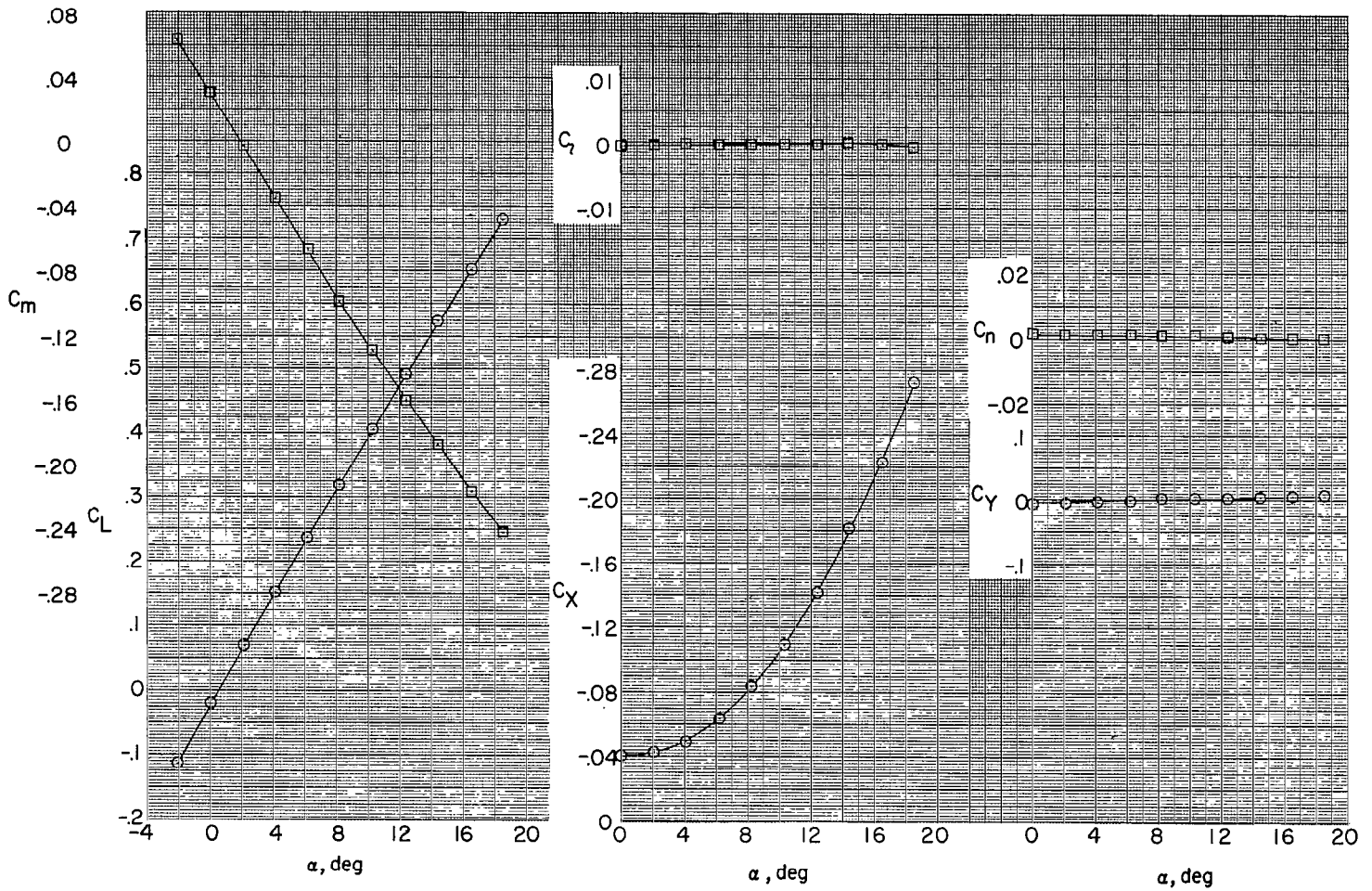

(a) $\phi = 0^{\circ}$.

Figure 18.- Aerodynamic characteristics at various roll angles. High wing; horizontal tail position 1; $i_t = 0^{\circ}$. Flagged symbols are for variations with β; unflagged symbols are for variations with α.

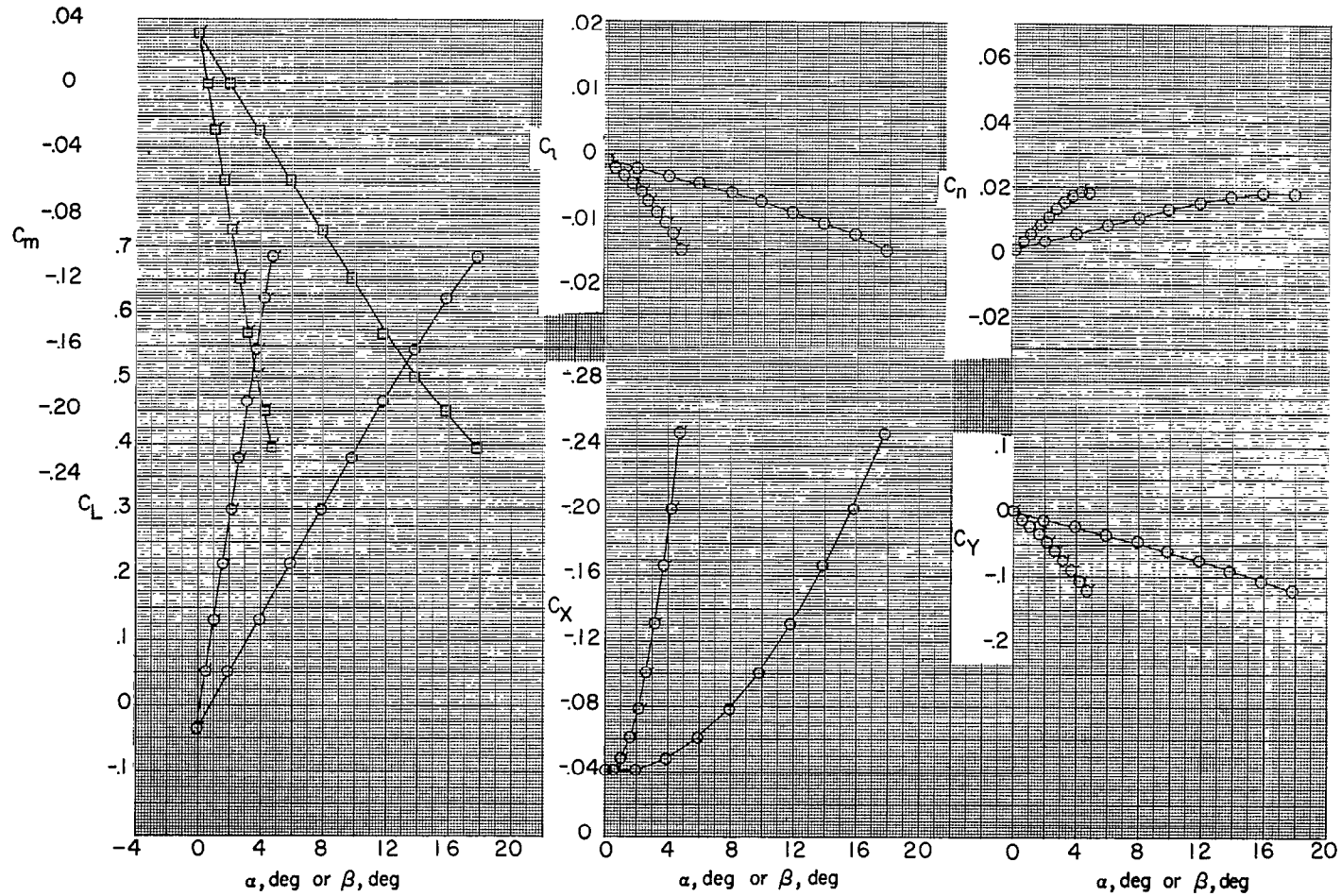

(b) $\phi = 15^{\circ}$.

Figure 18.- Continued.

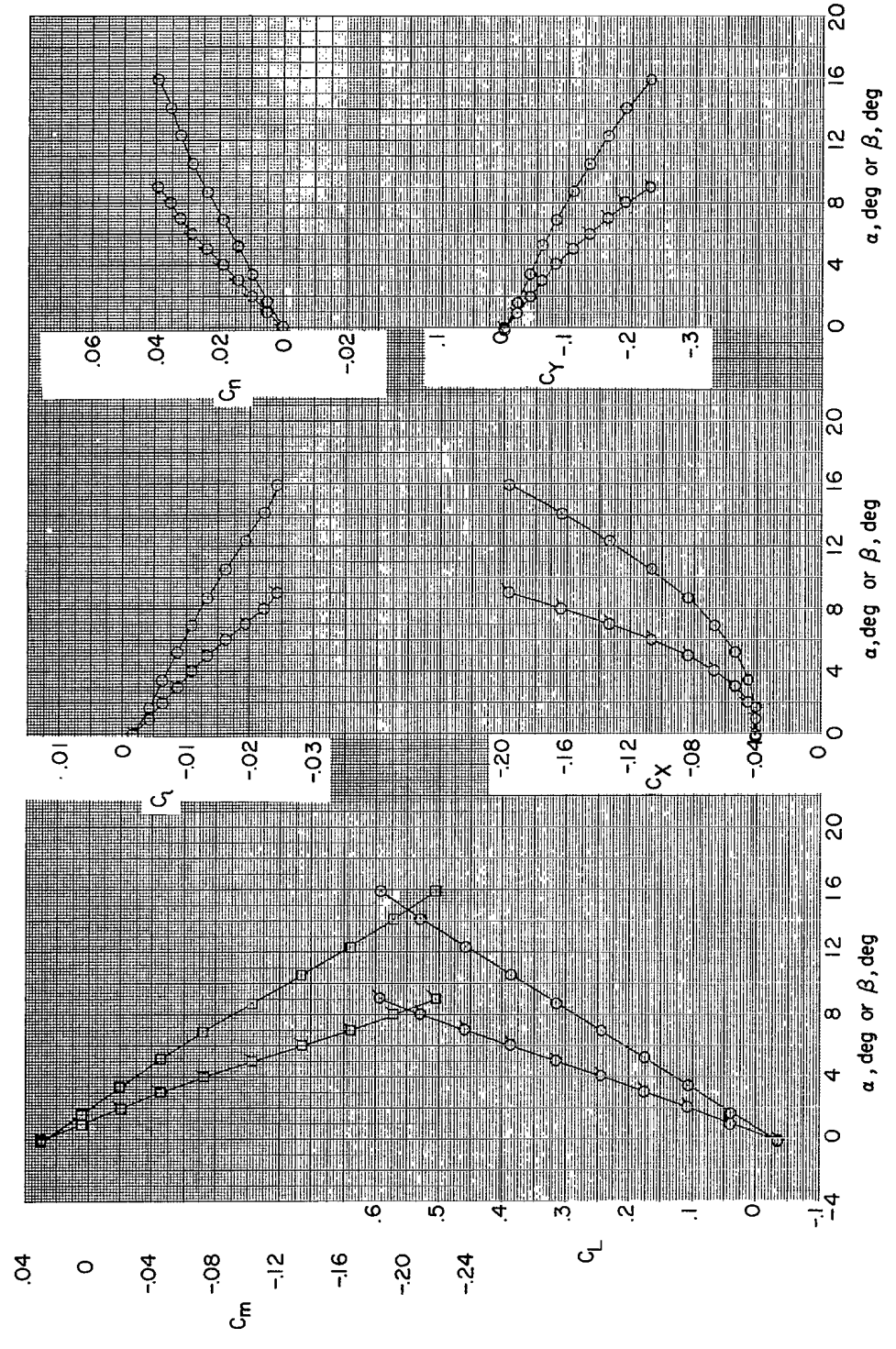

(c) $\phi = 30^\circ$.

Figure 18.- Continued.

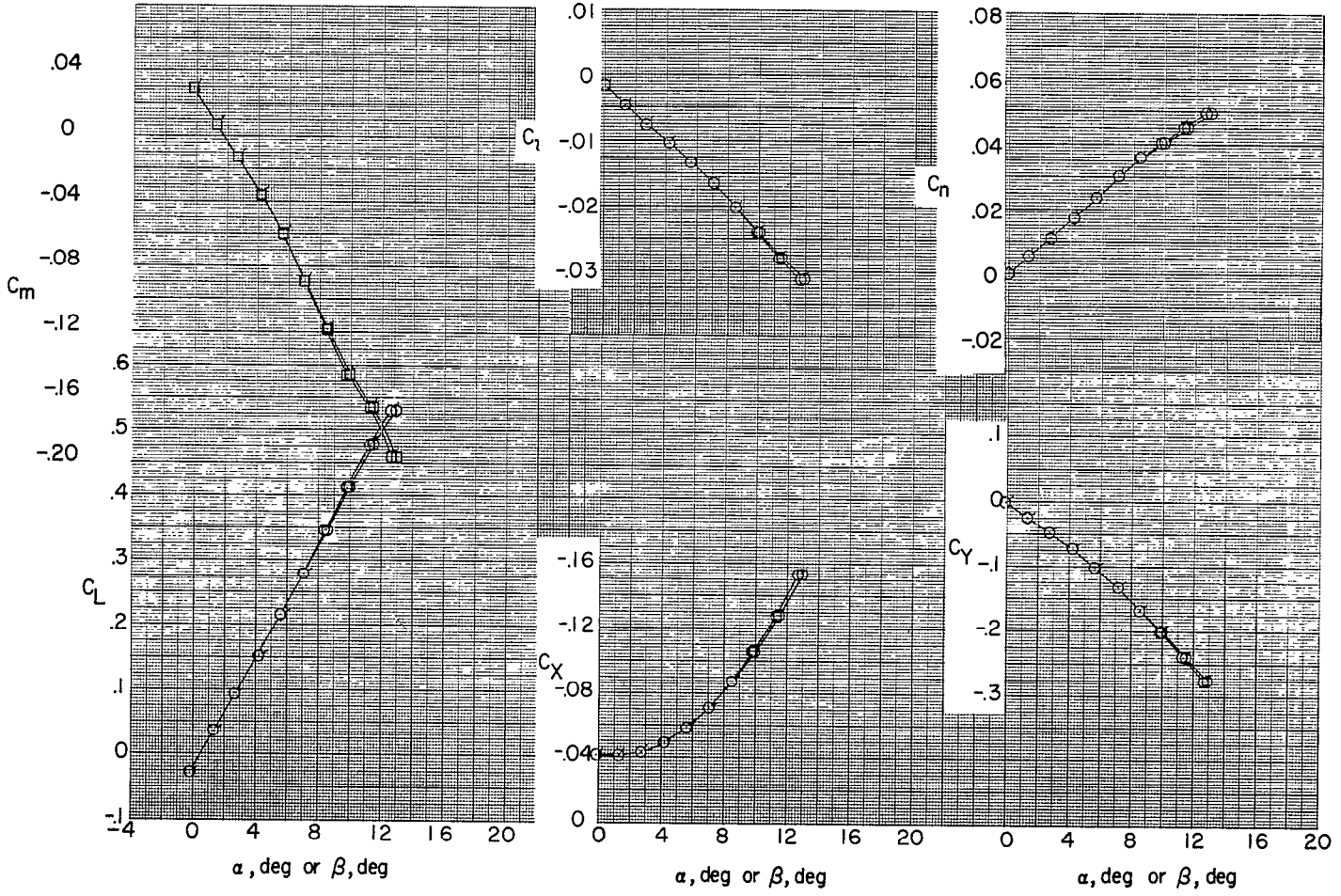

(d) $\phi = 45°$.

Figure 18.- Continued.

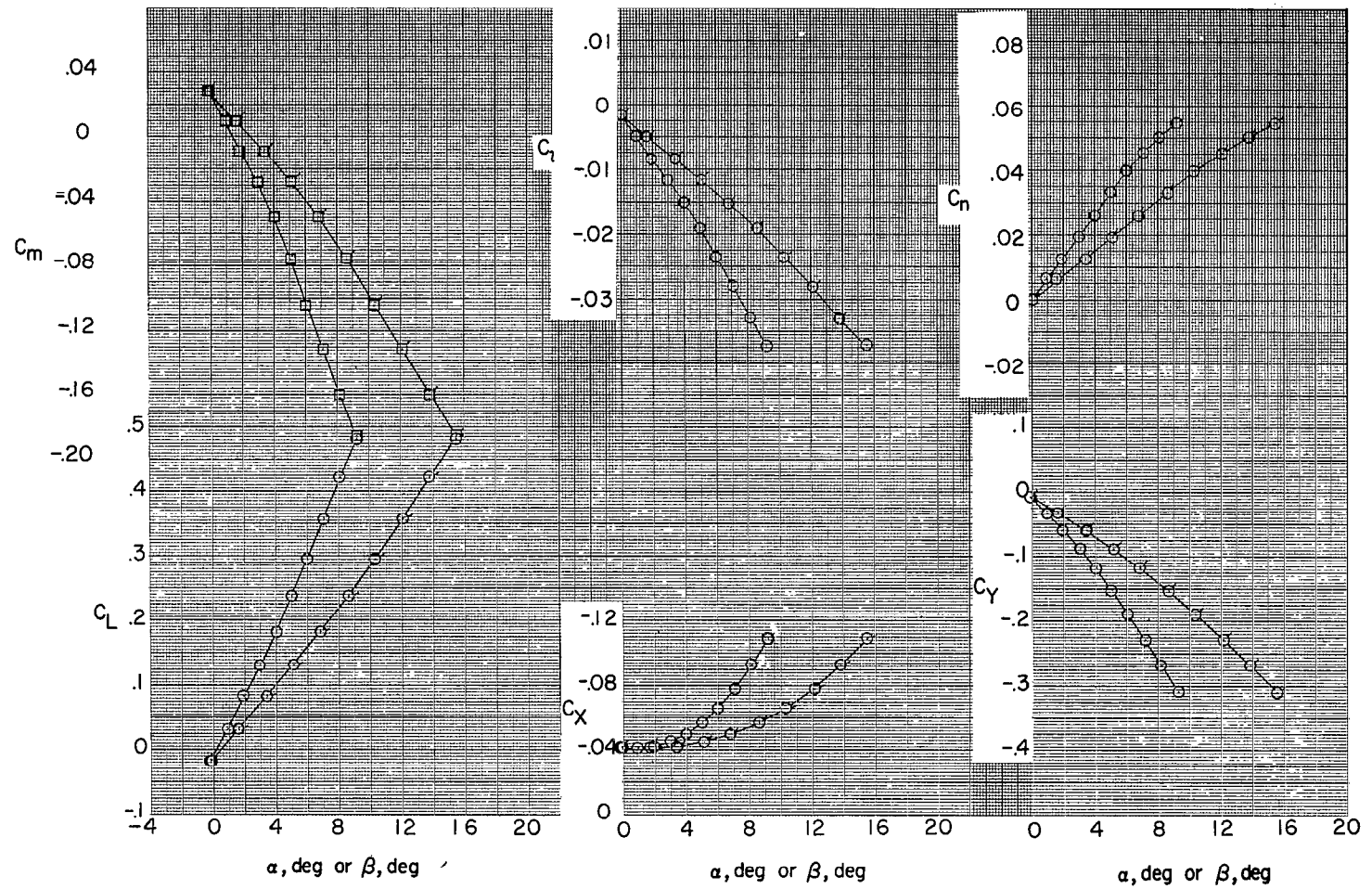

(e) $\phi = 60^{\circ}$.

Figure 18.- Continued.

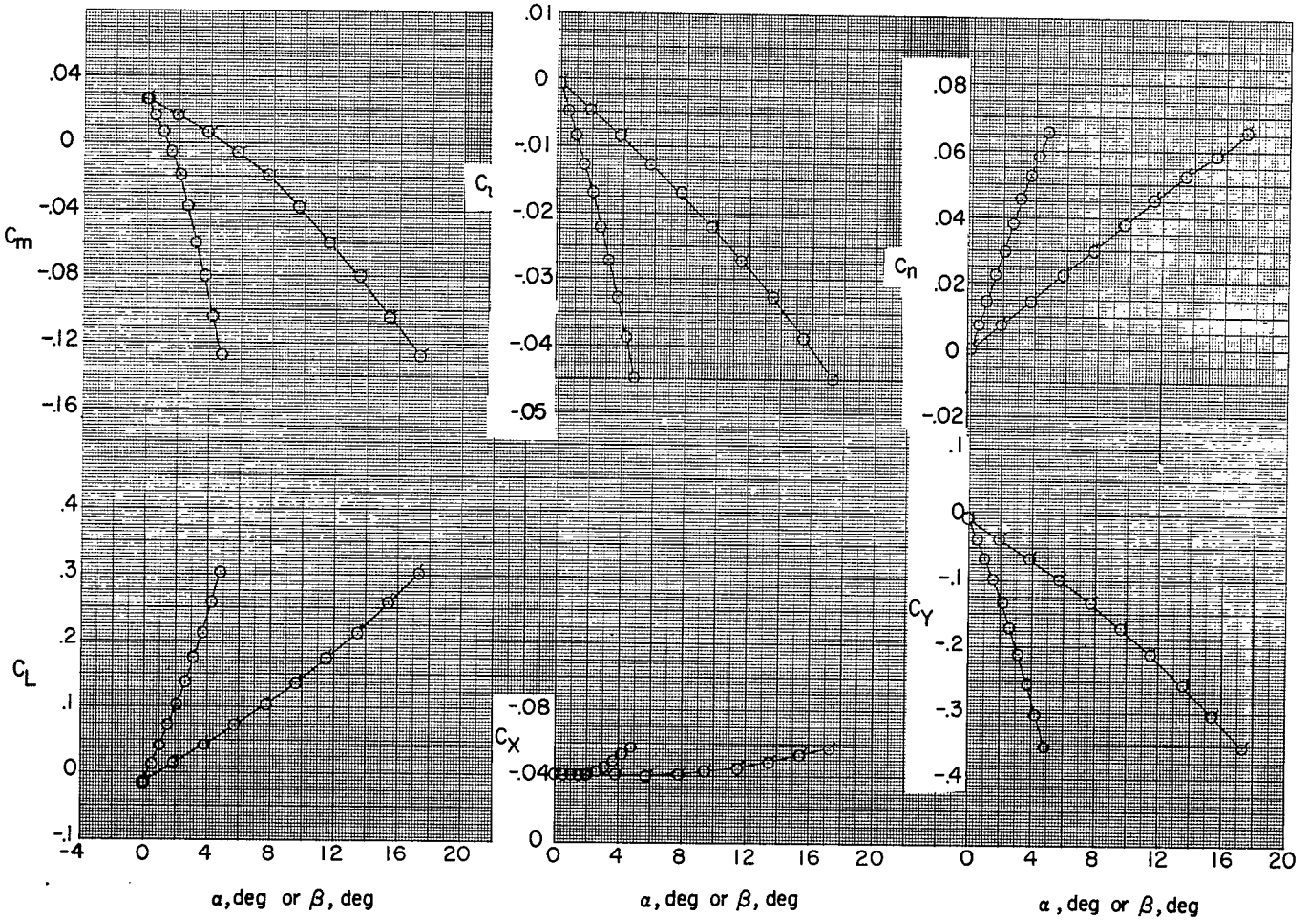

(f) $\phi = 75^\circ$.

Figure 18.- Continued.

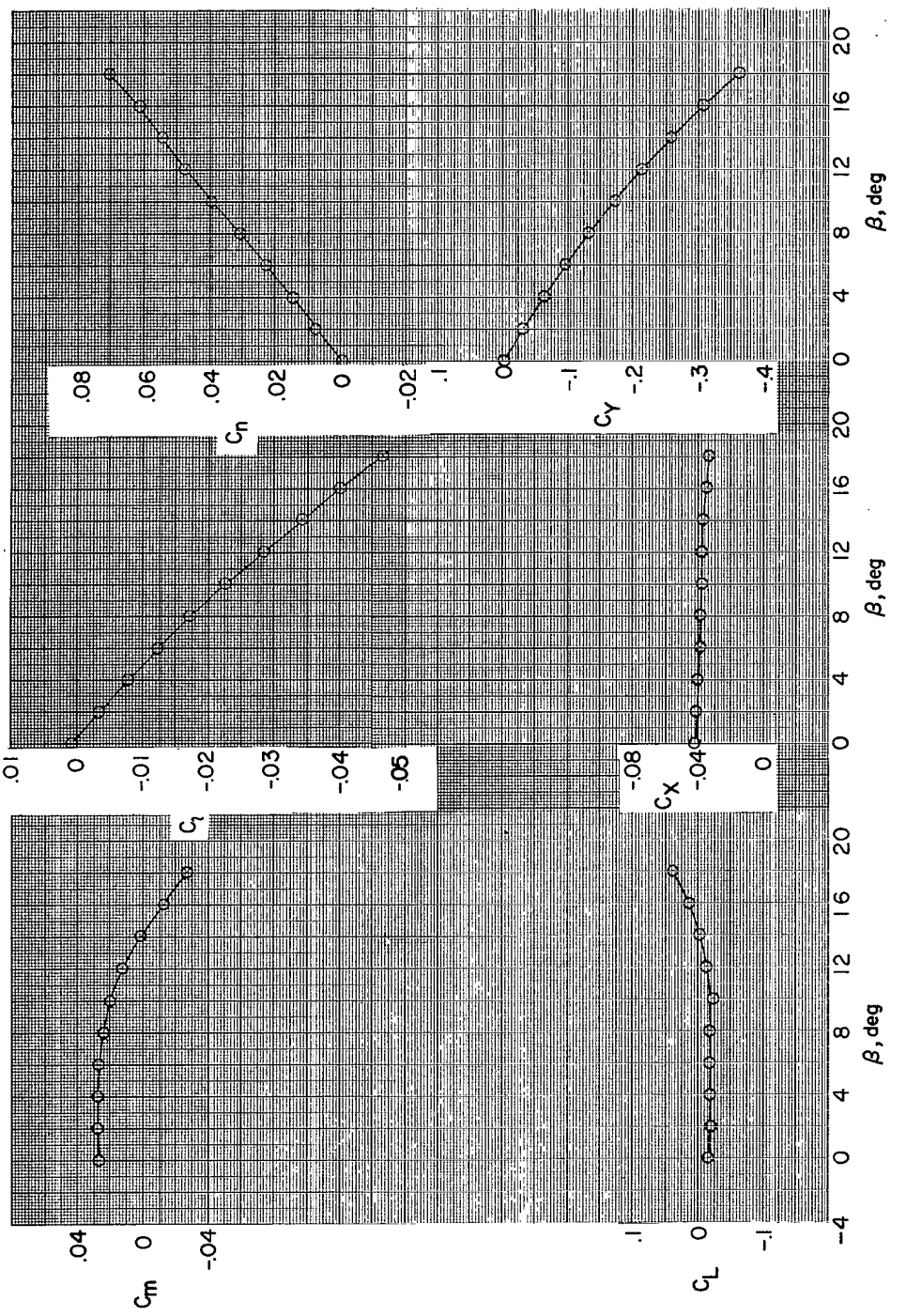

(g) $\phi = 90^\circ$.

Figure 18.- Concluded.

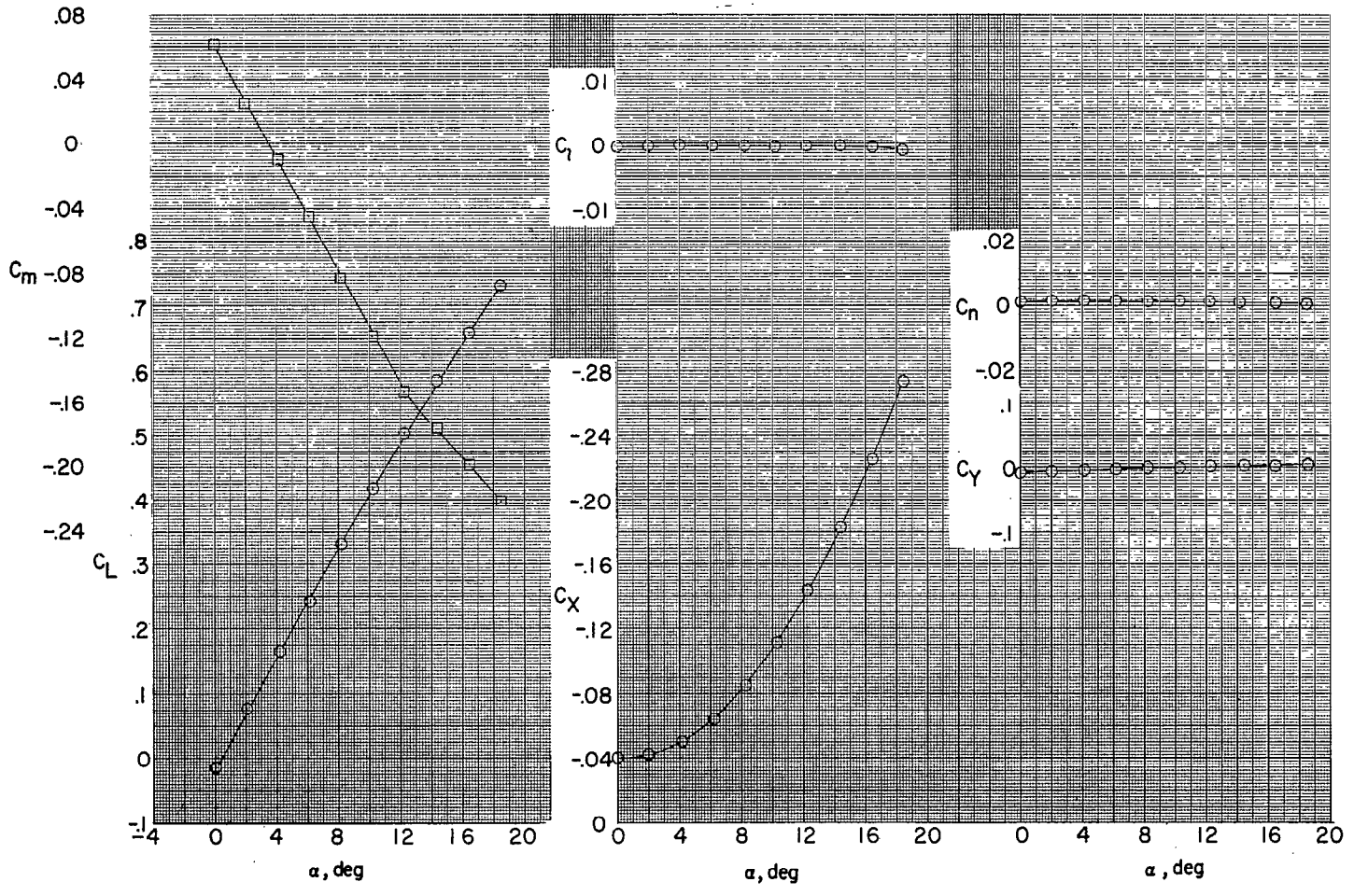

(a) $\phi = 0^\circ$.

Figure 19.- Aerodynamic characteristics at various roll angles. High wing; horizontal tail position 2; $i_t = 0^\circ$. Flagged symbols are for variations with β; unflagged symbols are for variations with α.

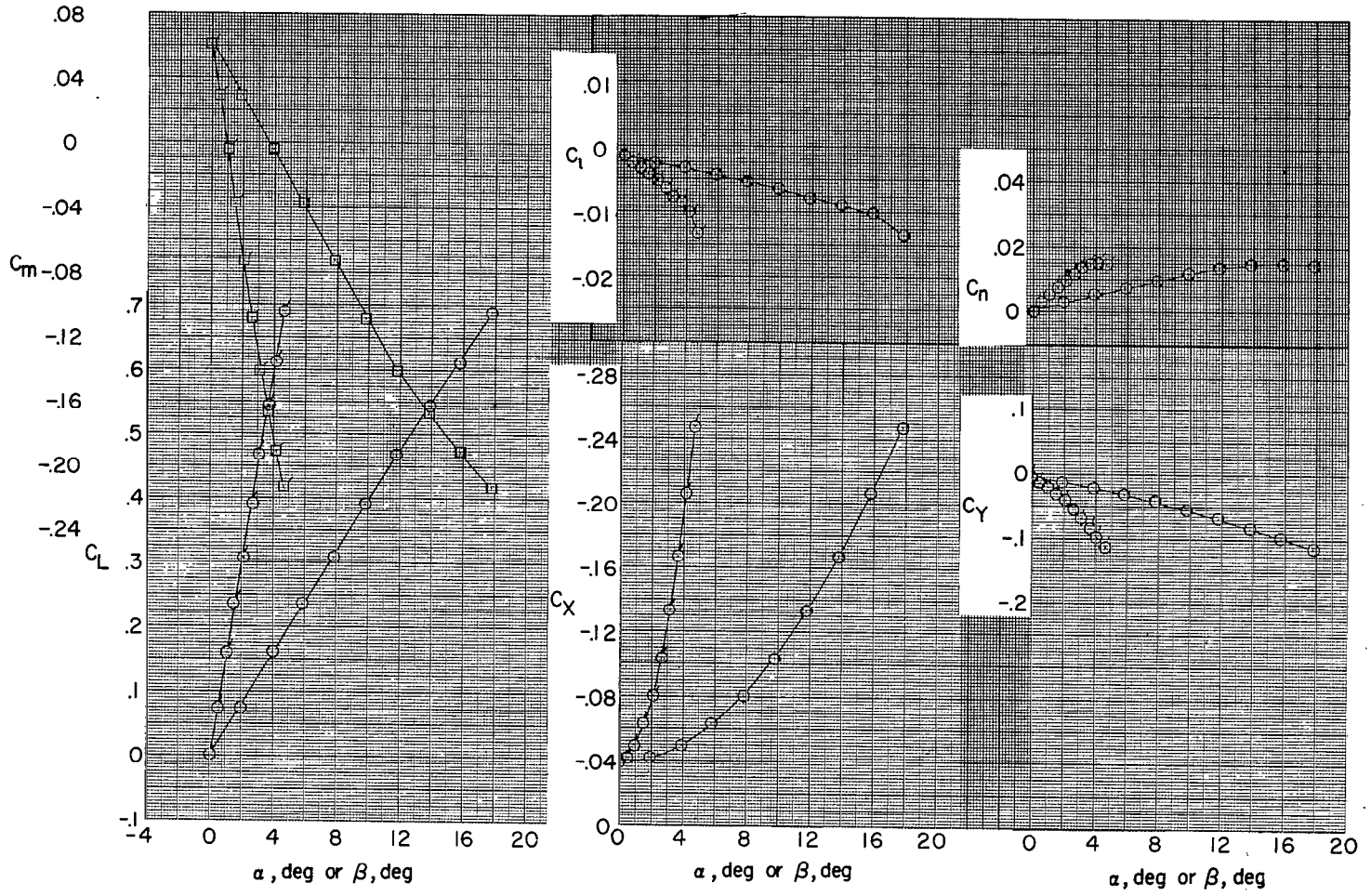

(b) $\phi = 15^\circ$.

Figure 19.- Continued.

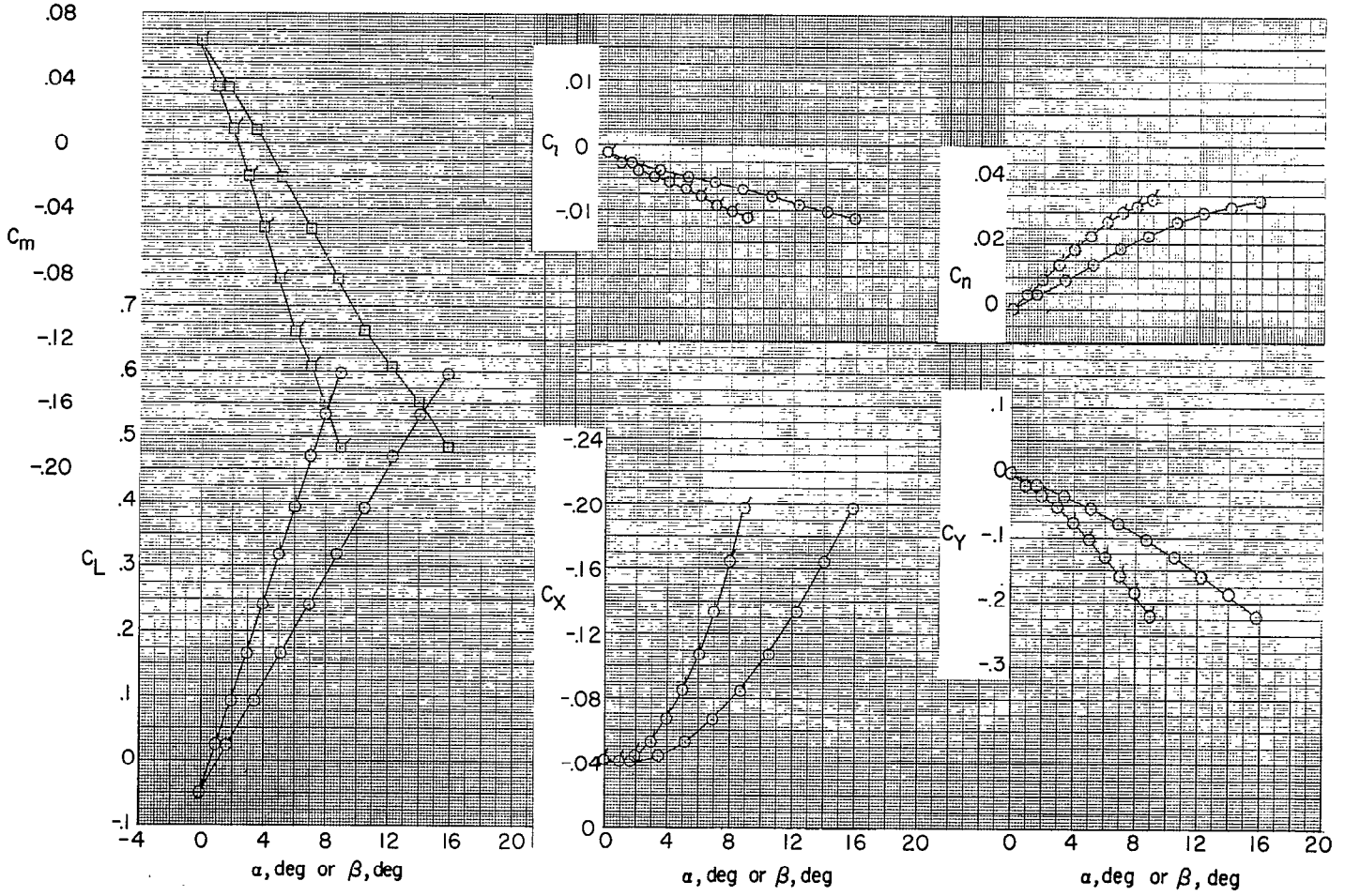

(c) $\phi = 30^{\circ}$.

Figure 19.- Continued.

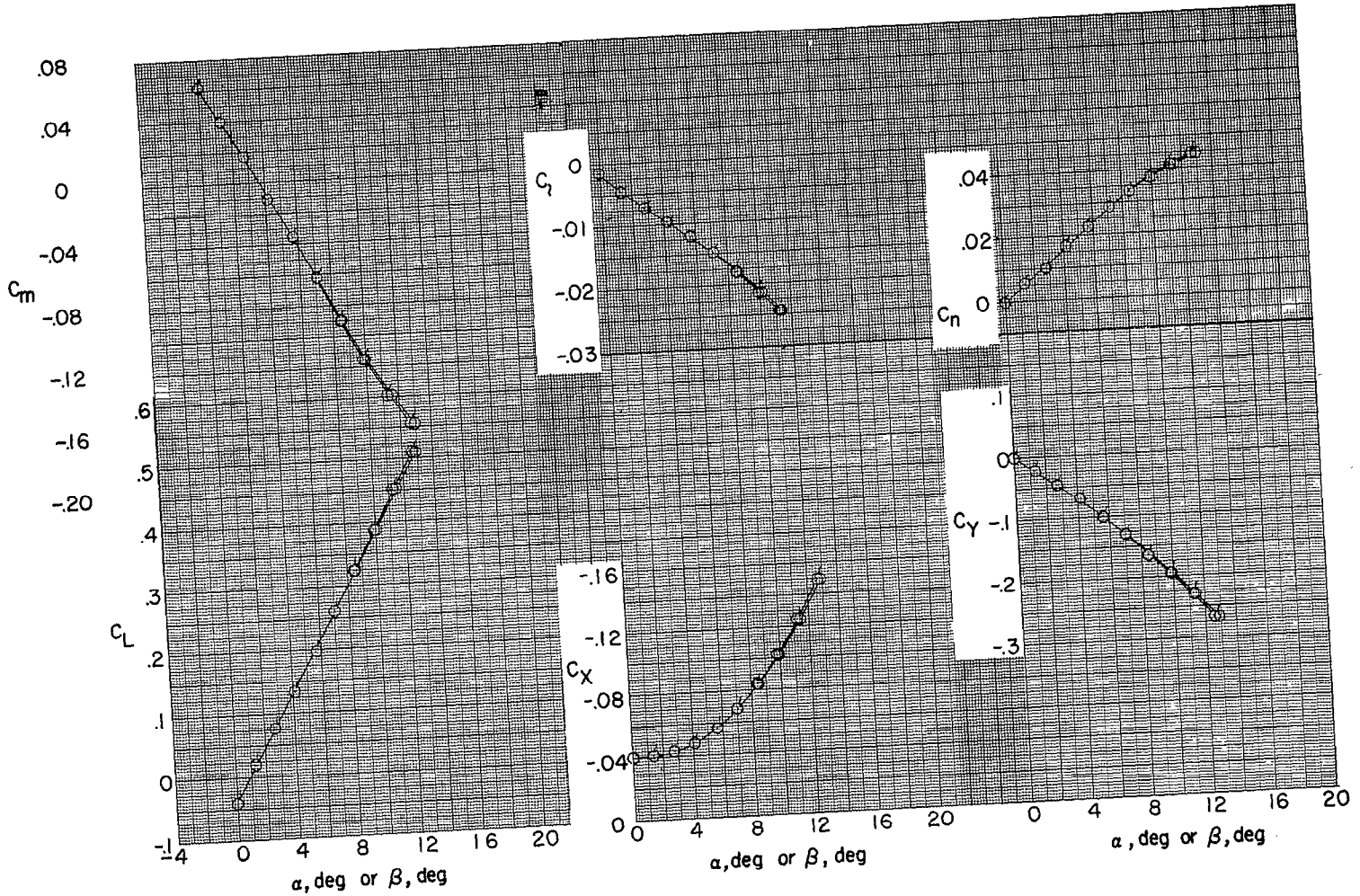

(d) $\phi = 45^{\circ}$.

Figure 19.- Continued.

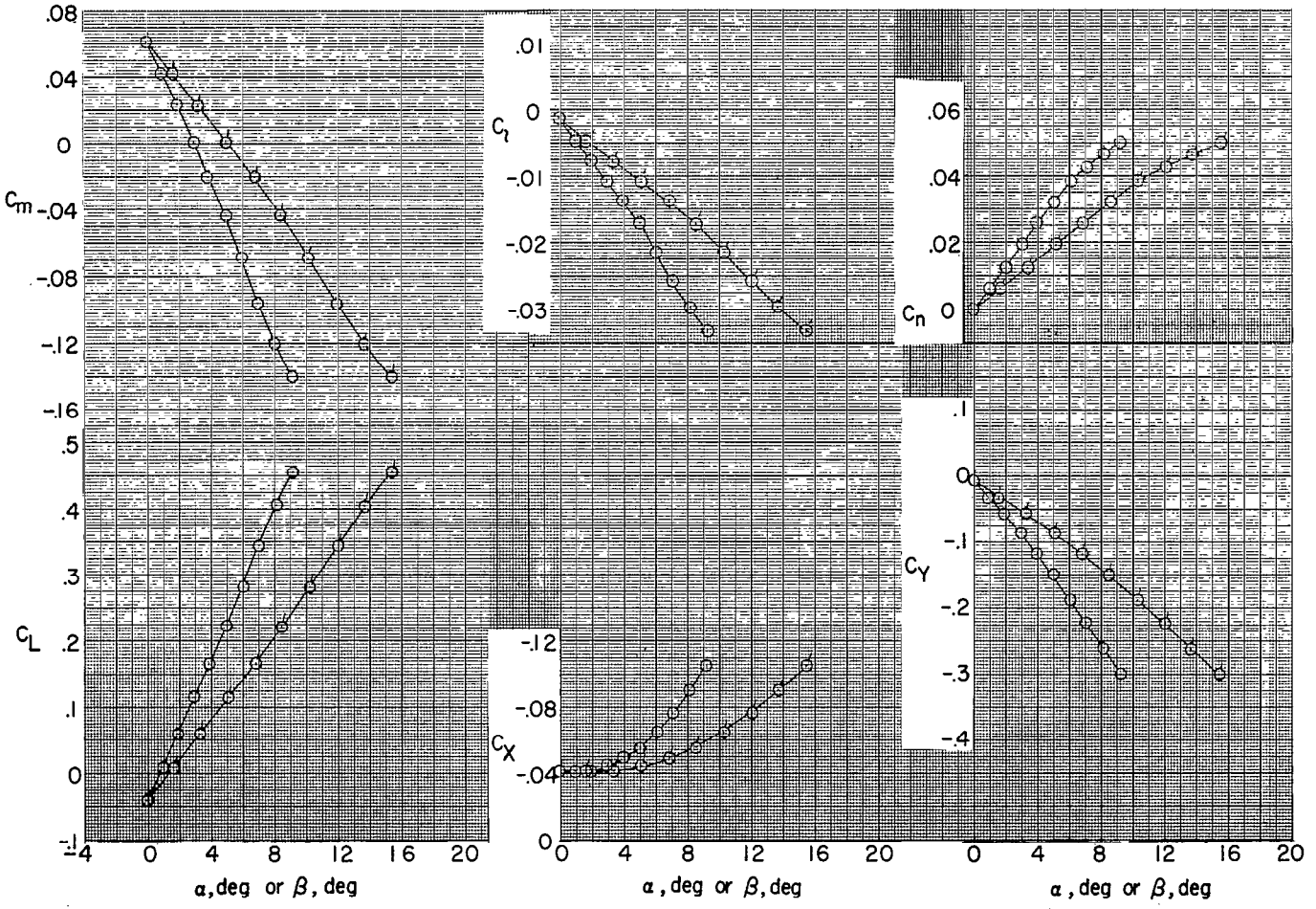

(e) $\phi = 60^\circ$.

Figure 19.- Continued.

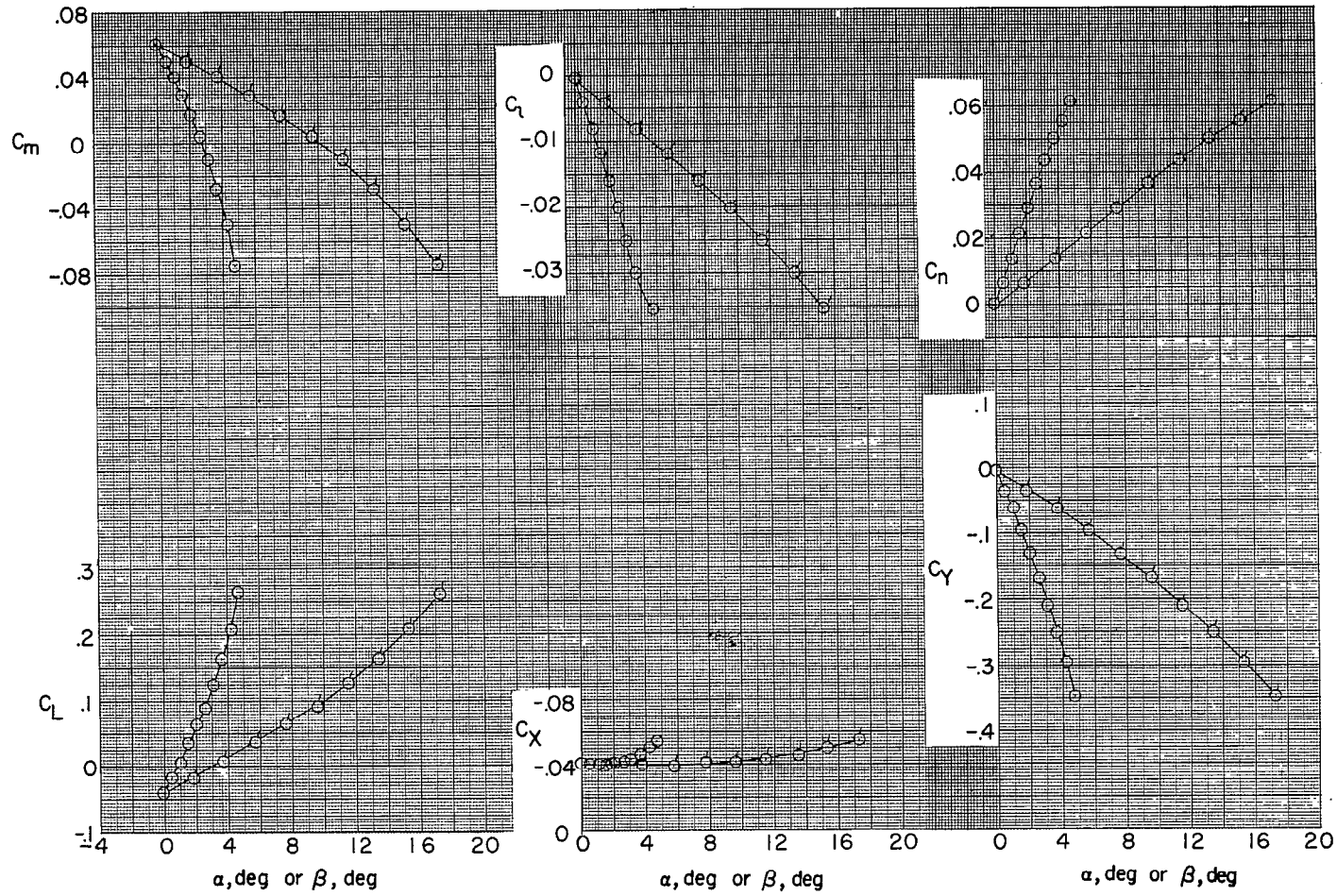

(f) $\phi = 75^\circ$.

Figure 19.- Continued.

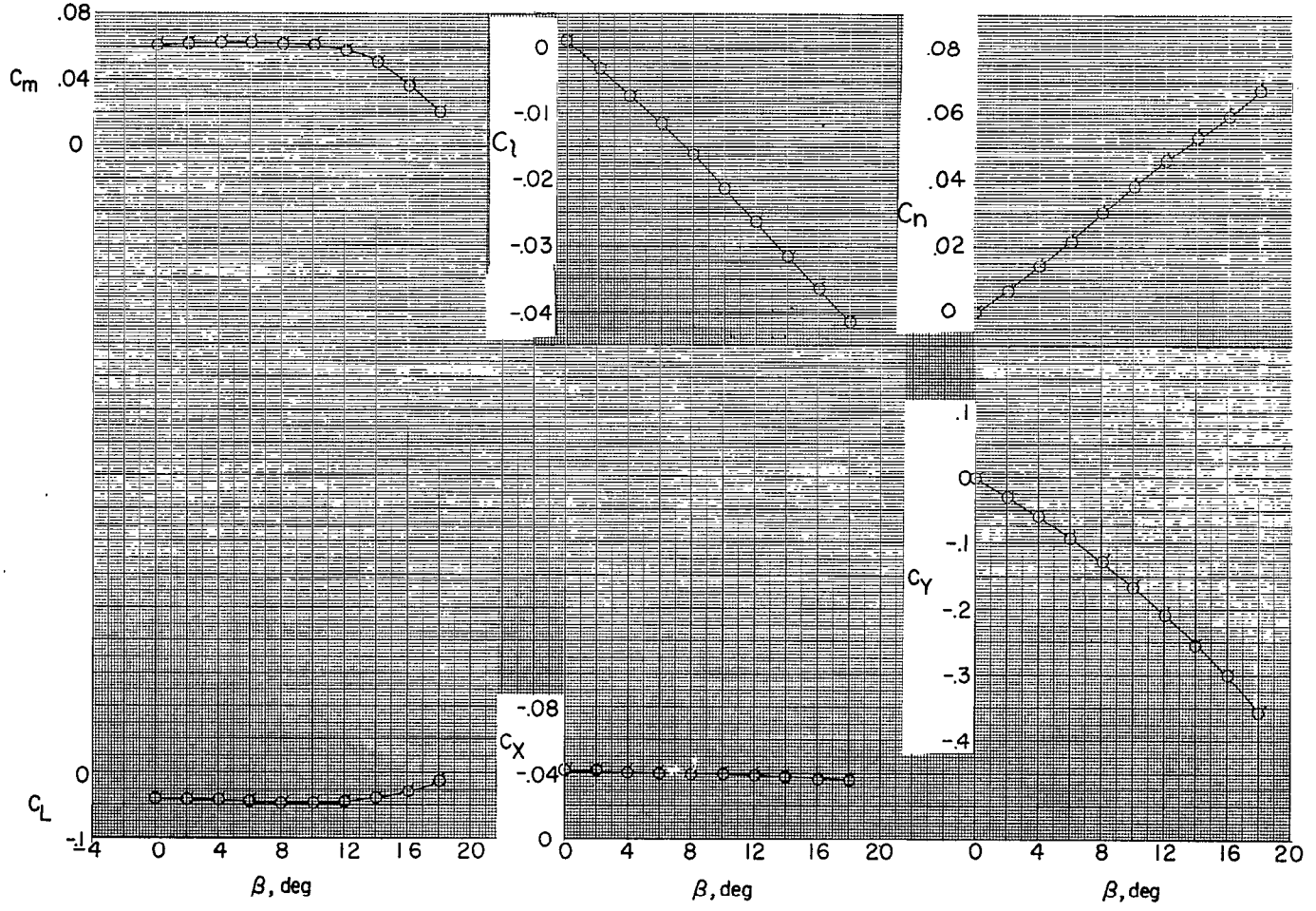

(g) $\phi = 90^\circ$.

Figure 19.- Concluded.

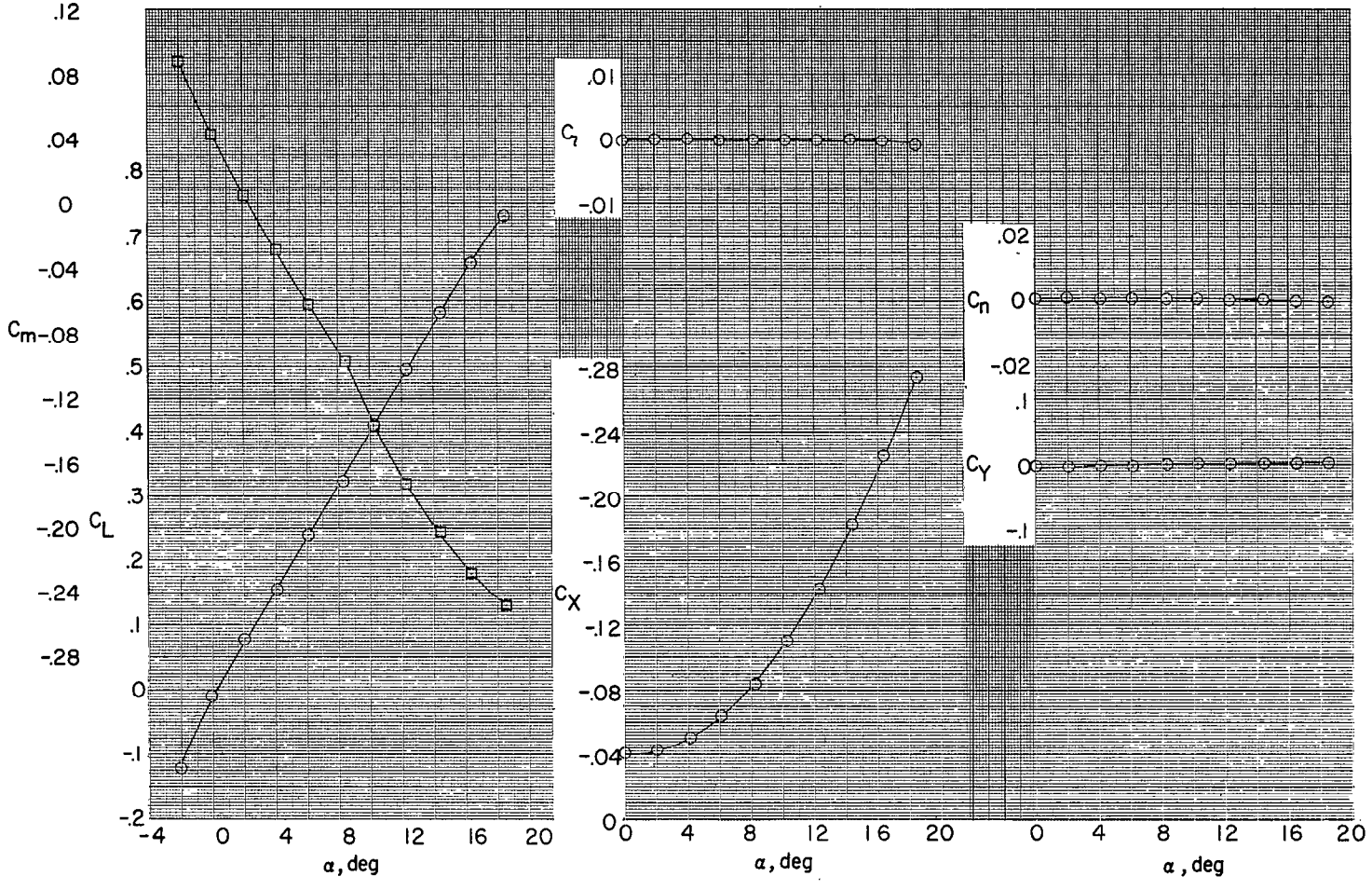

(a) $\phi = 0^\circ$.

Figure 20.- Aerodynamic characteristics at various roll angles. High wing; horizontal tail position 3; $i_t = 0^\circ$. Flagged symbols are for variations with β; unflagged symbols are for variations with α.

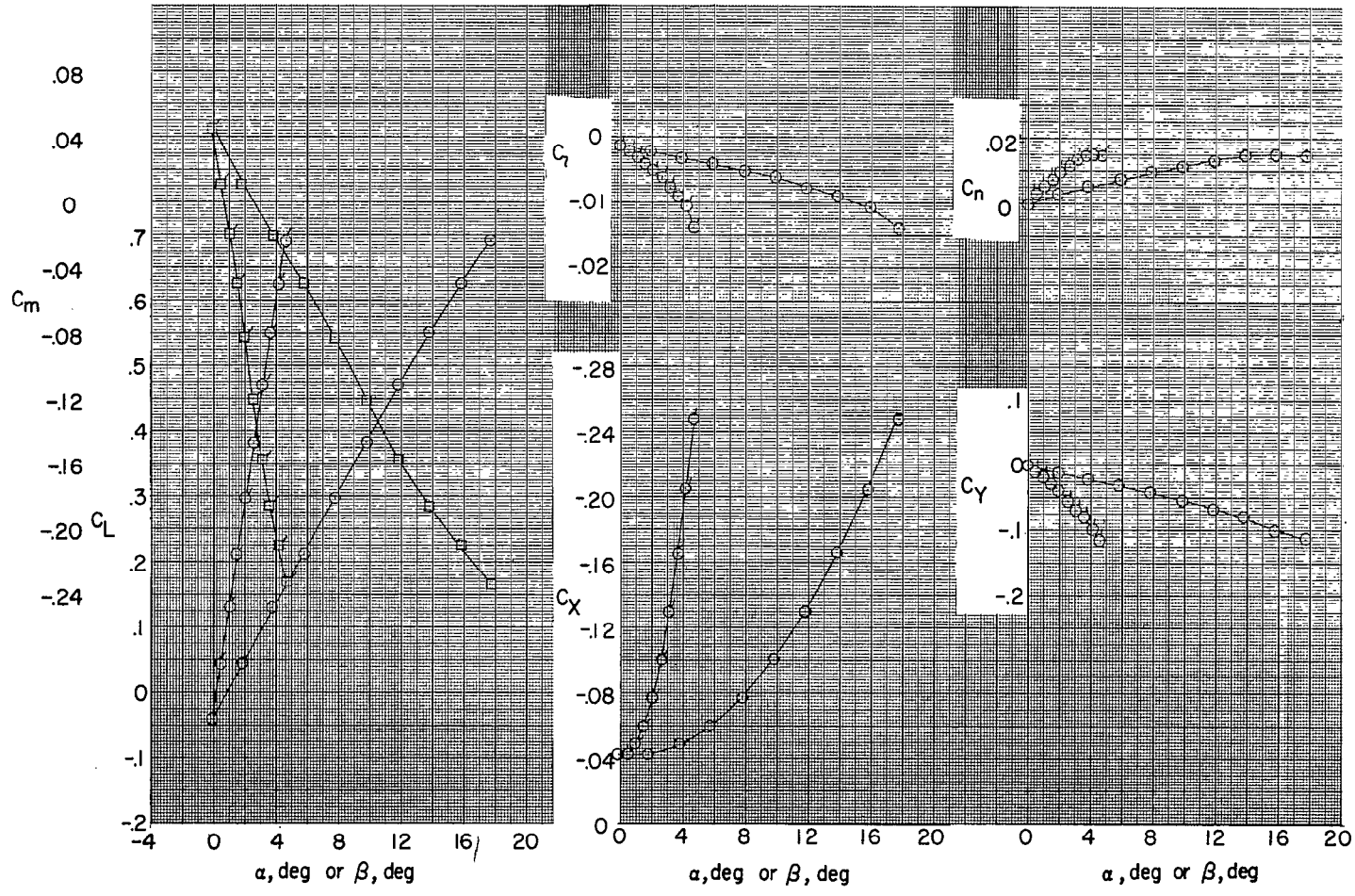

(b) $\phi = 15^{\circ}$.

Figure 20.- Continued.

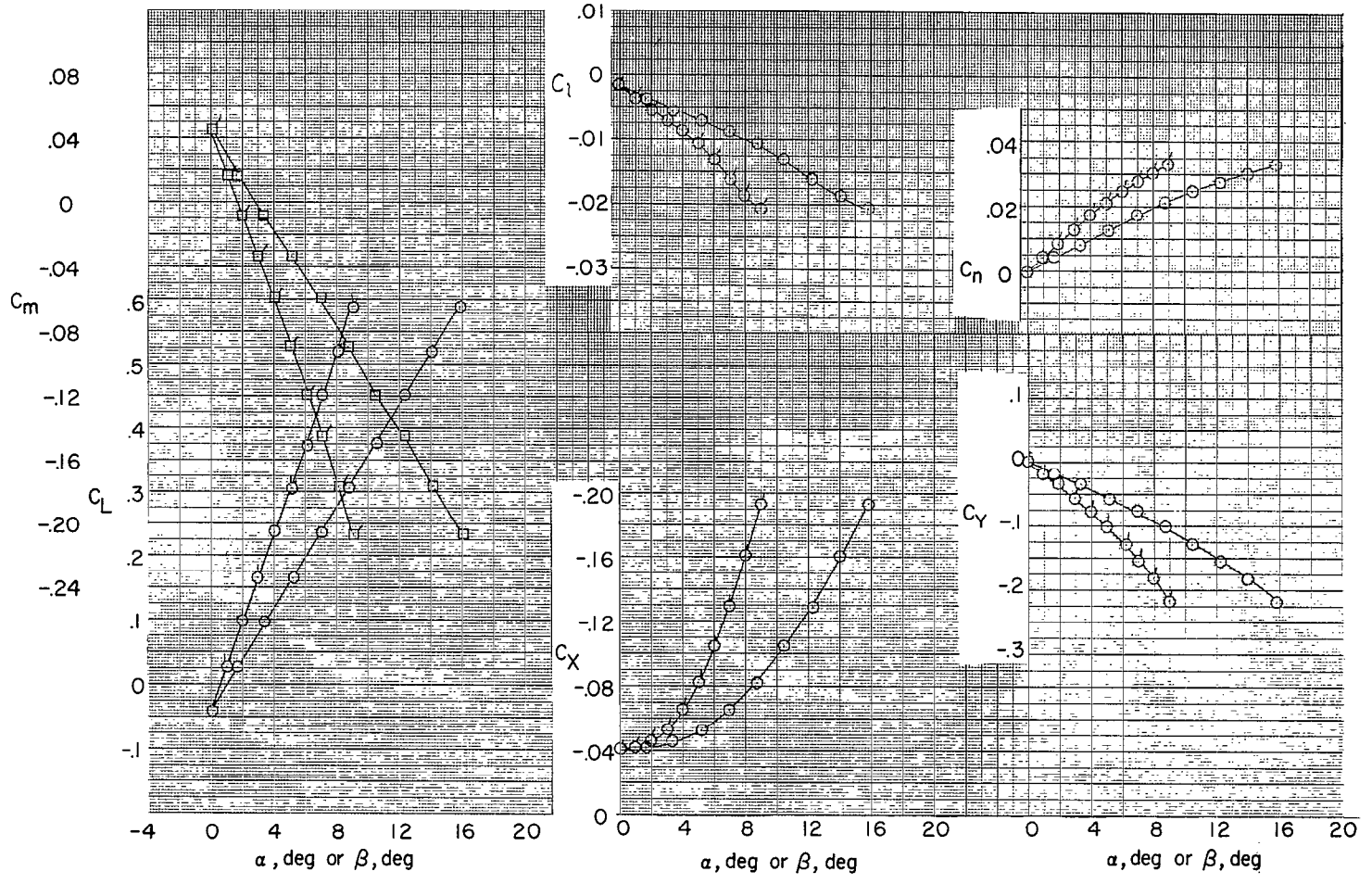

(c) $\phi = 30^\circ$.

Figure 20.- Continued.

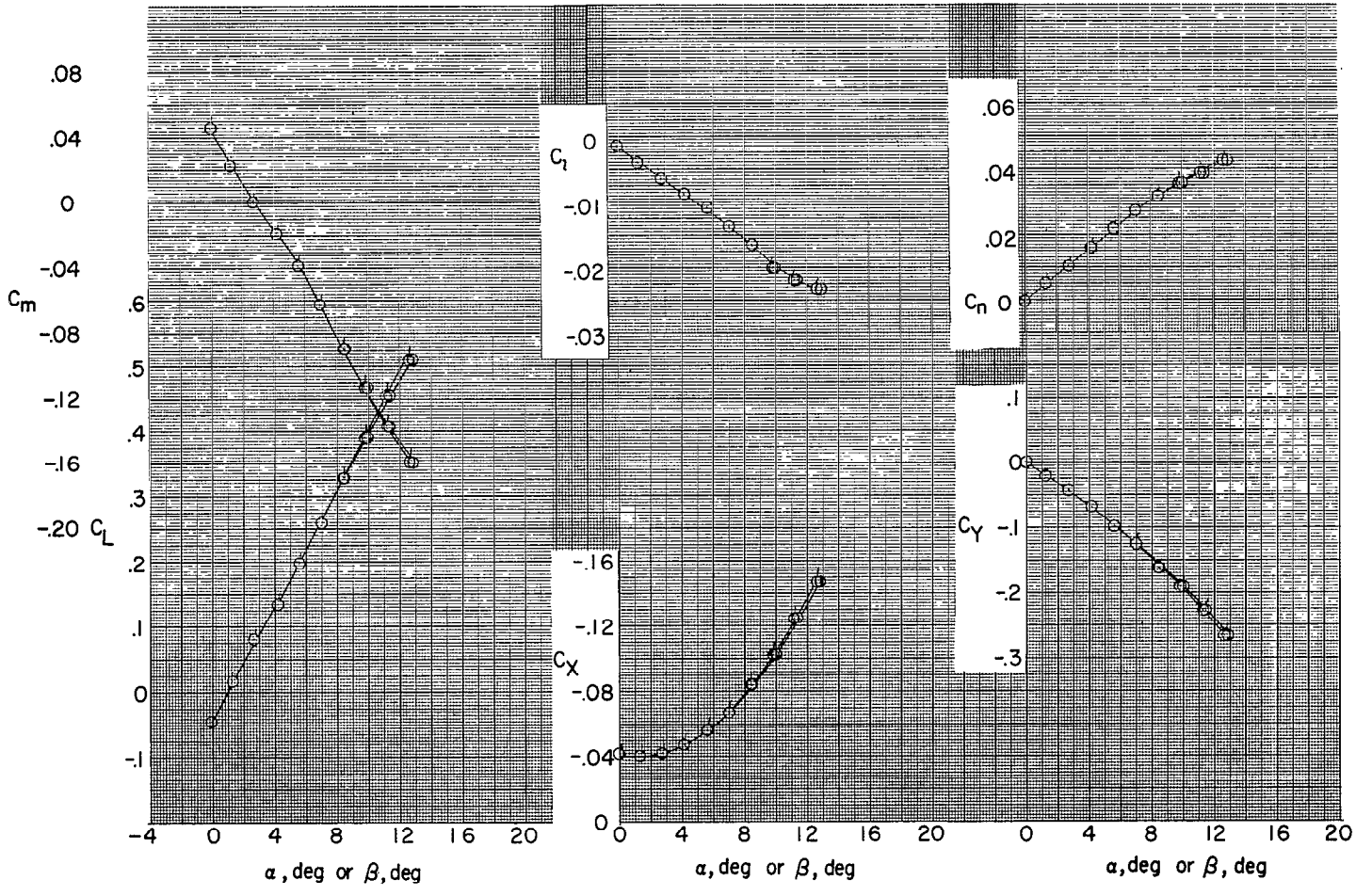

(d) $\phi = 45°$.

Figure 20.- Continued.

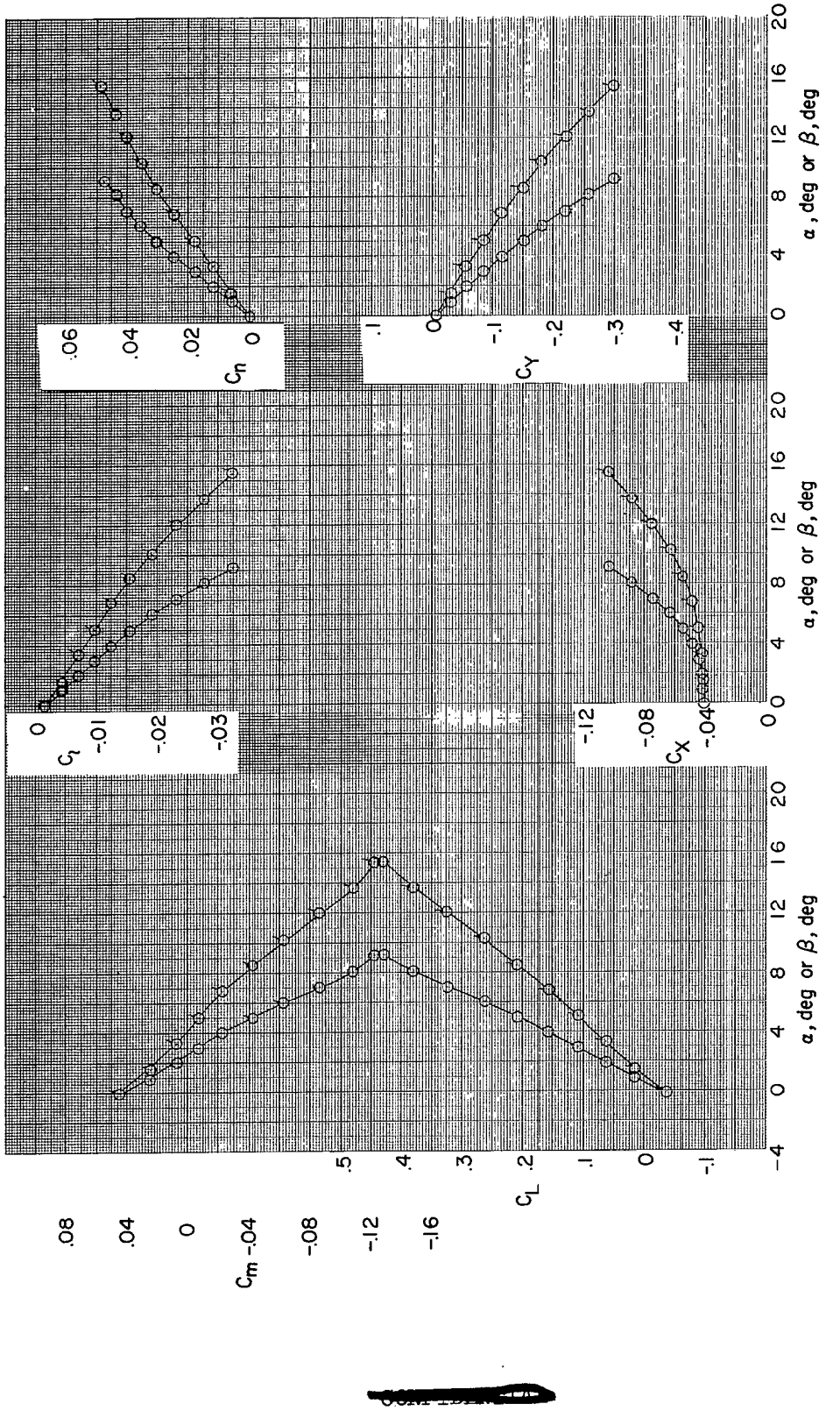

(e) $\phi = 60°$.

Figure 20.- Continued.

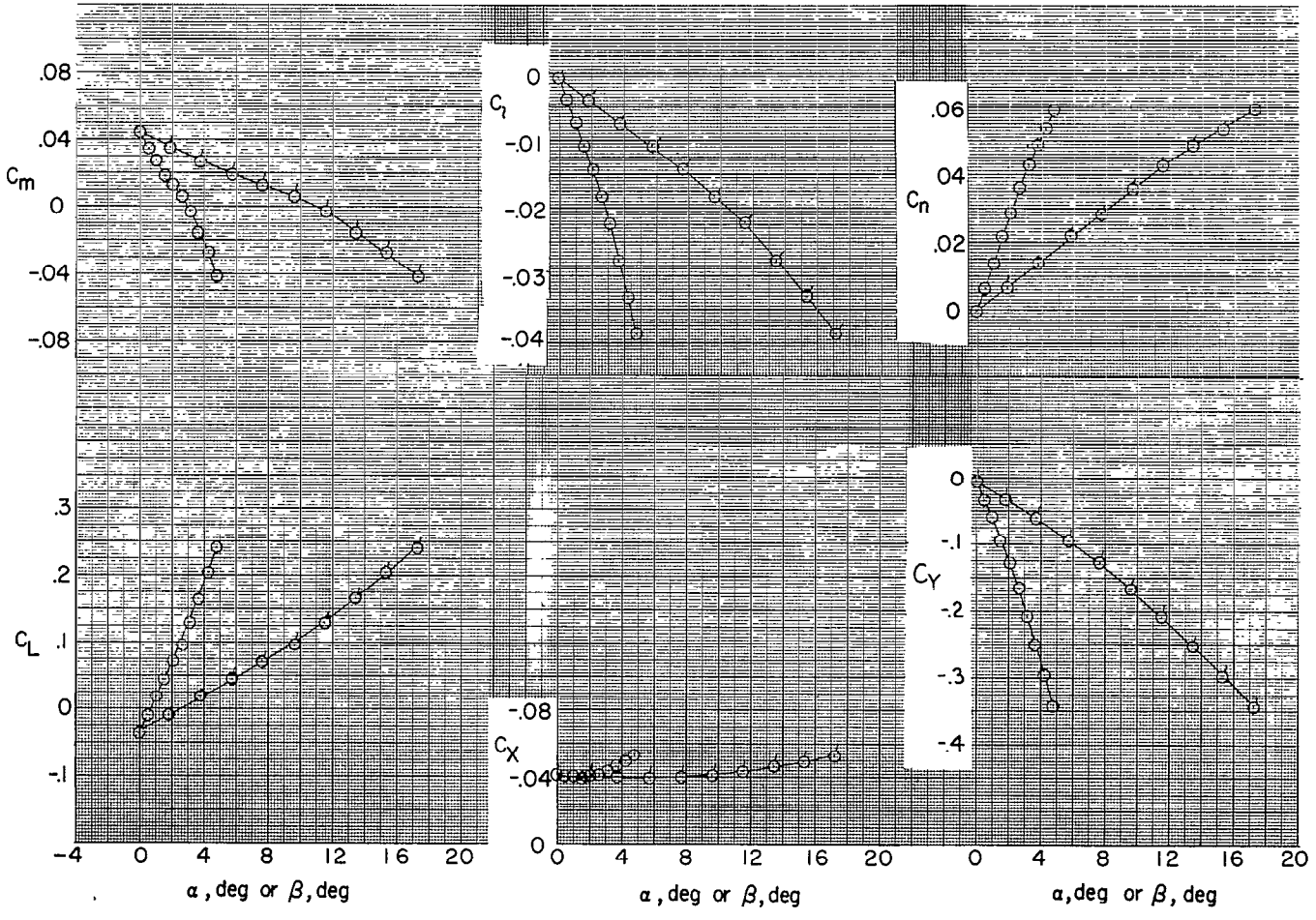

(f) $\phi = 75^\circ$.

Figure 20.- Continued.

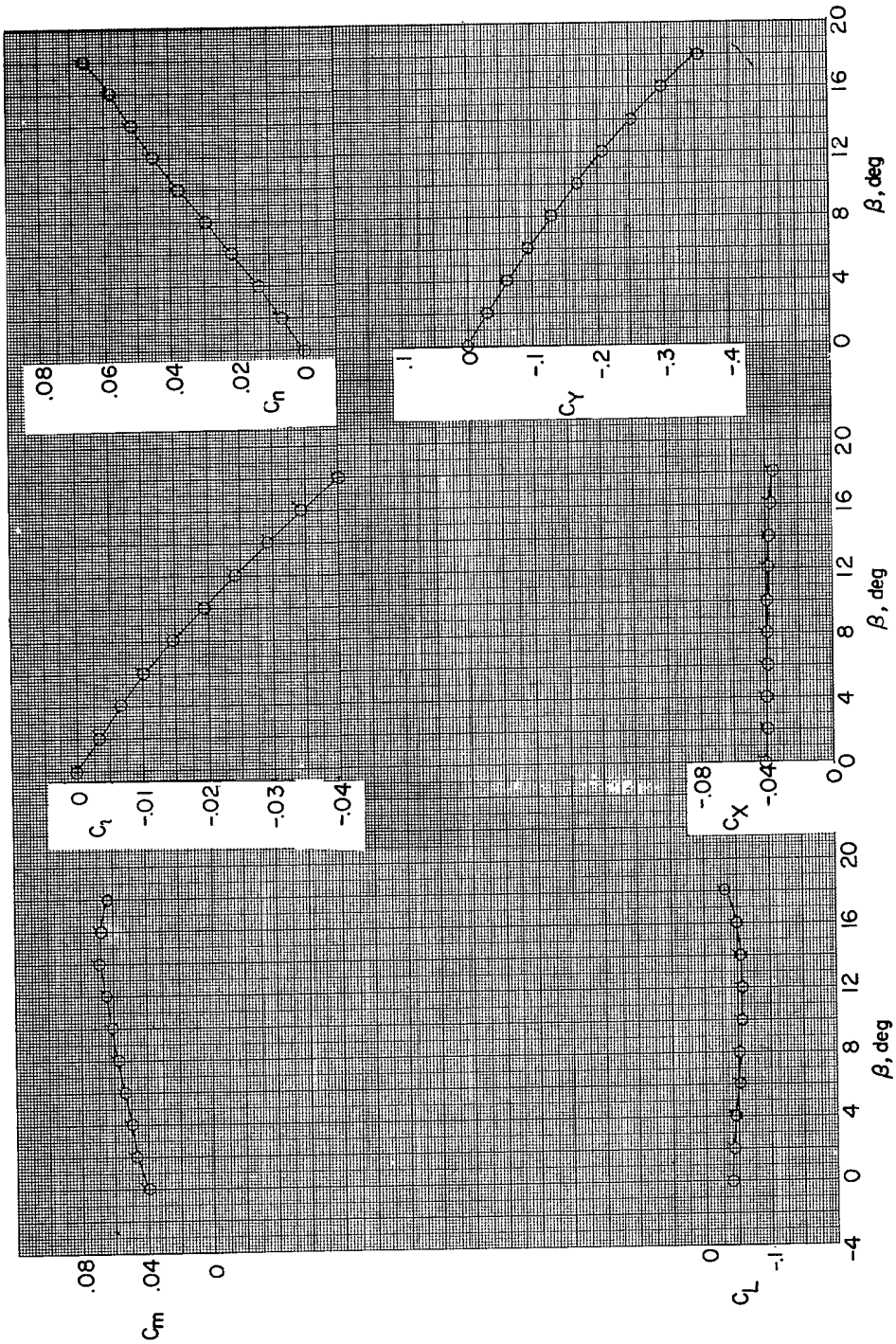

(g) $\phi = 90^{\circ}$.

Figure 20.- Concluded.

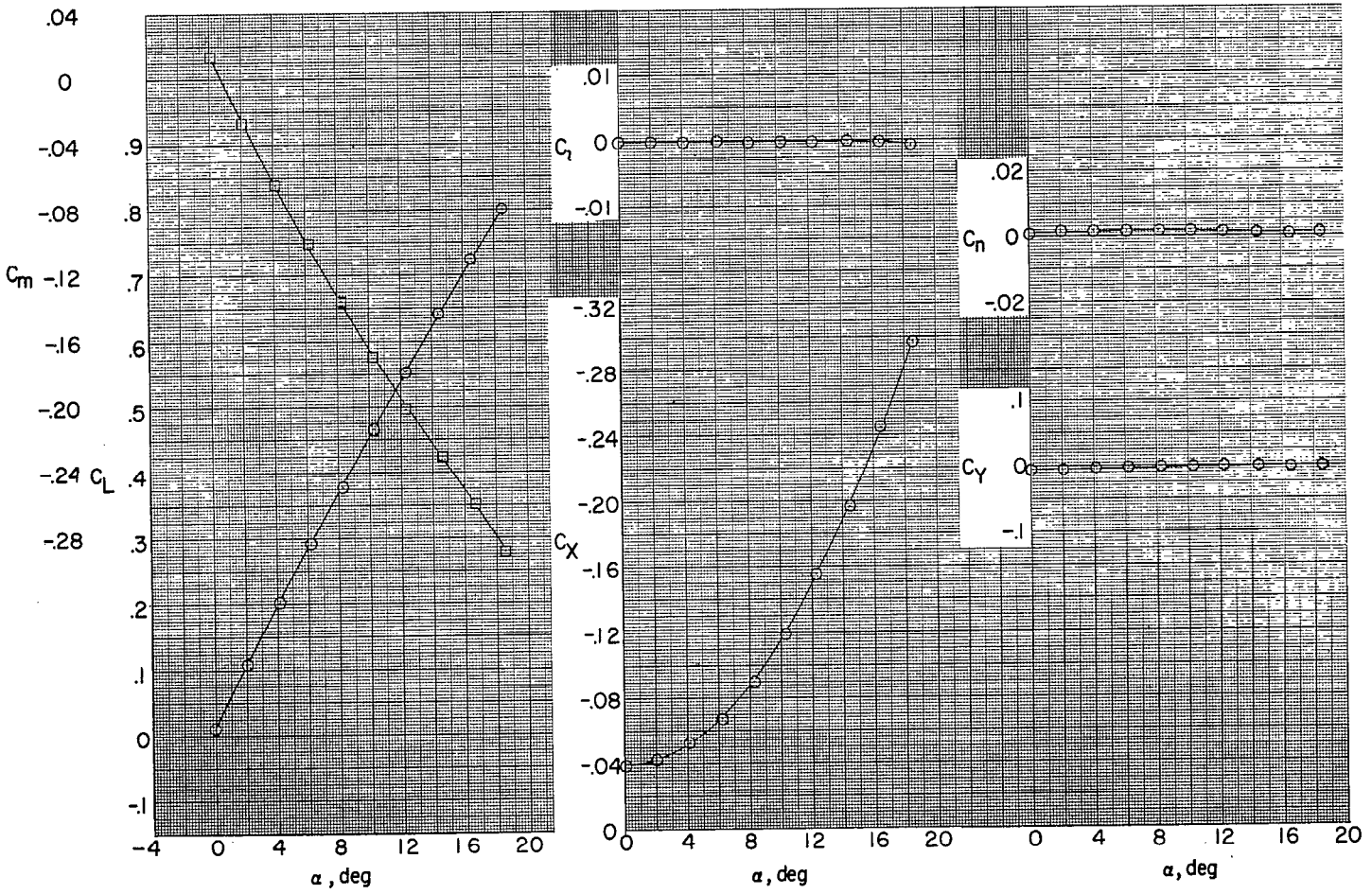

(a) $\phi = 0^{\circ}$.

Figure 21.- Aerodynamic characteristics at various roll angles. High wing; horizontal tail position 4; $i_t = 0^{\circ}$. Flagged symbols are for variations with β; unflagged symbols are for variations with α.

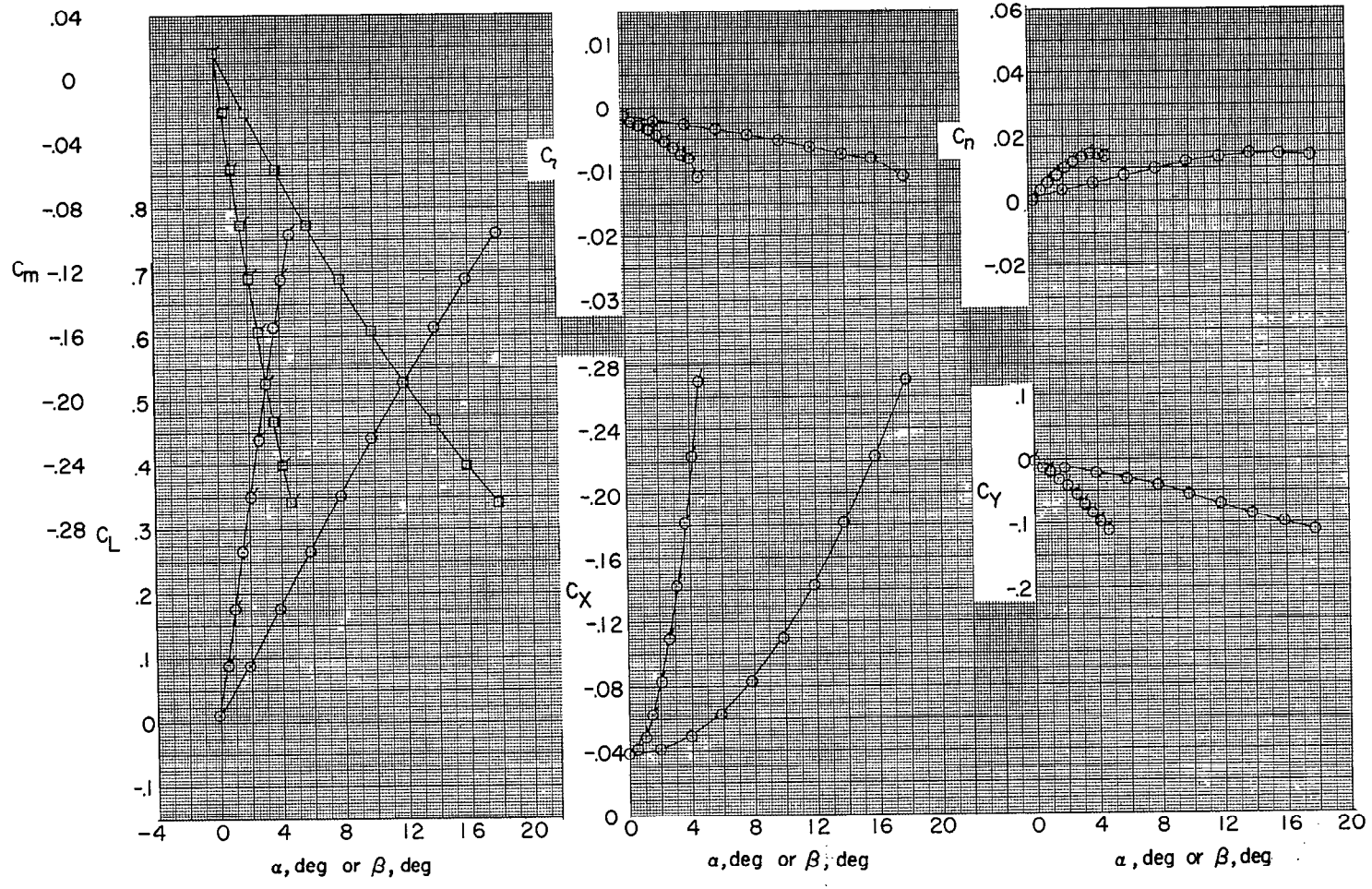

(b) $\phi = 15^{\circ}$.

Figure 21.- Continued.

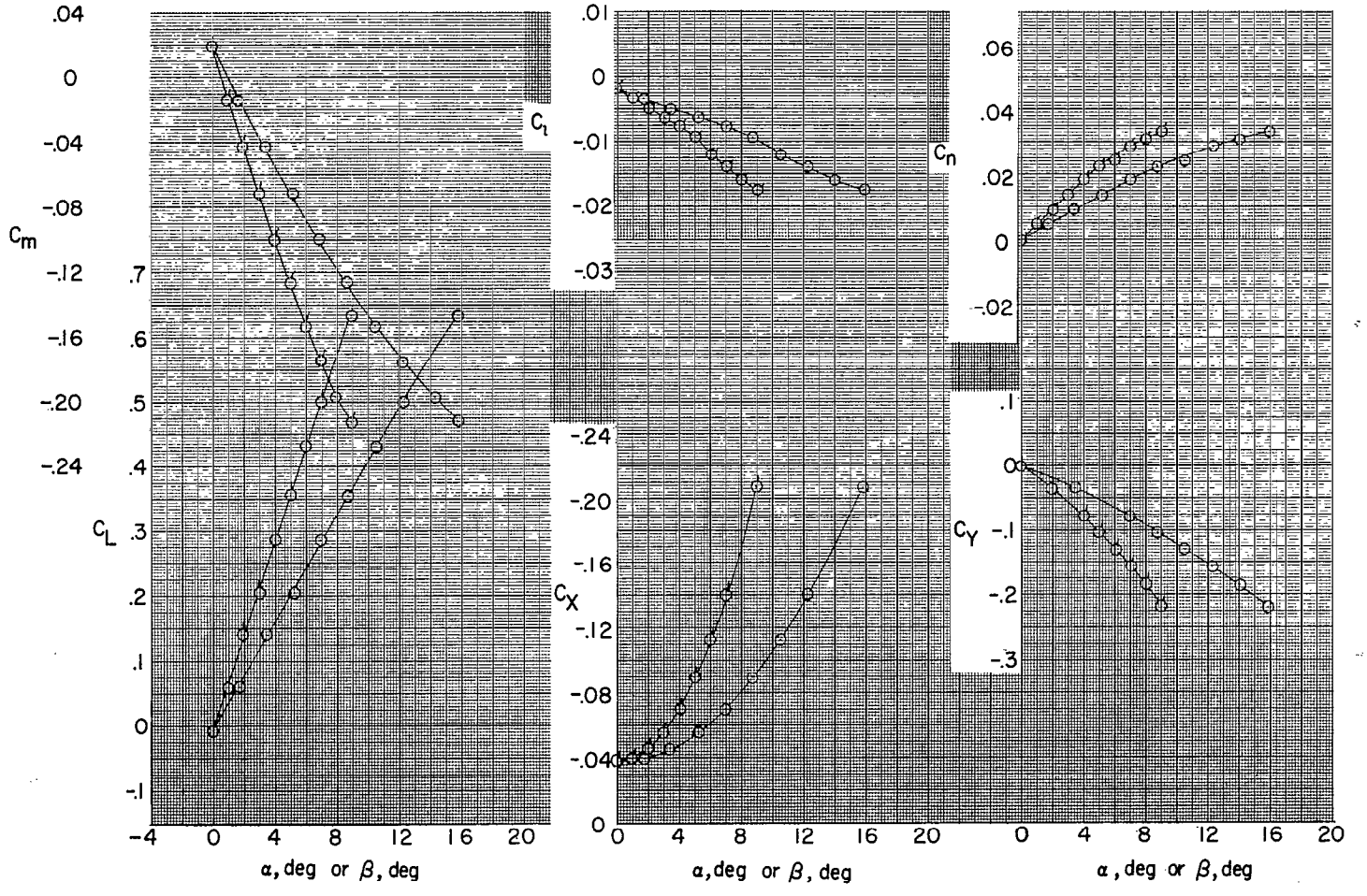

(c) $\phi = 30^{\circ}$.

Figure 21.- Continued.

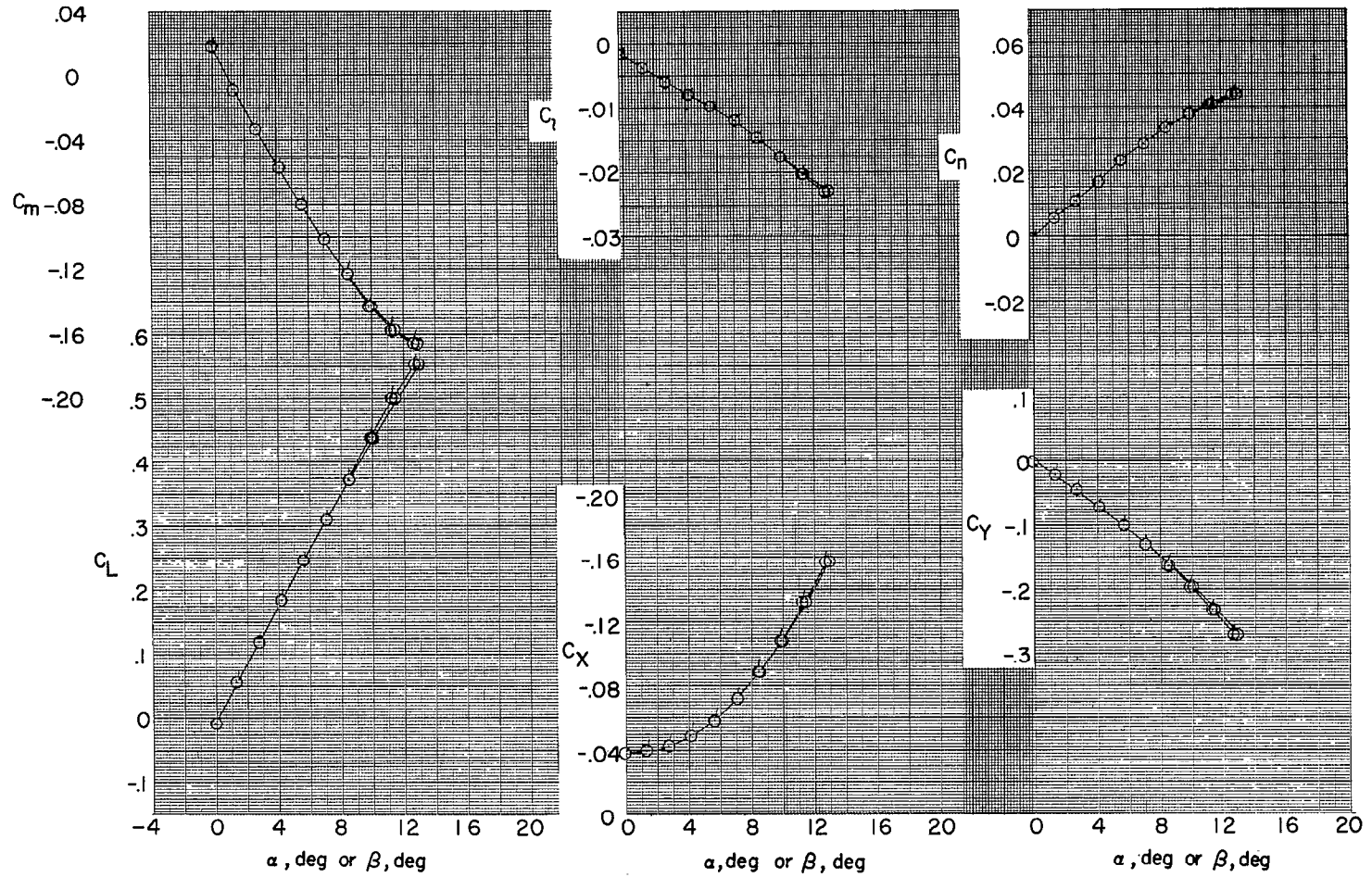

(d) $\phi = 45°$.

Figure 21.- Continued.

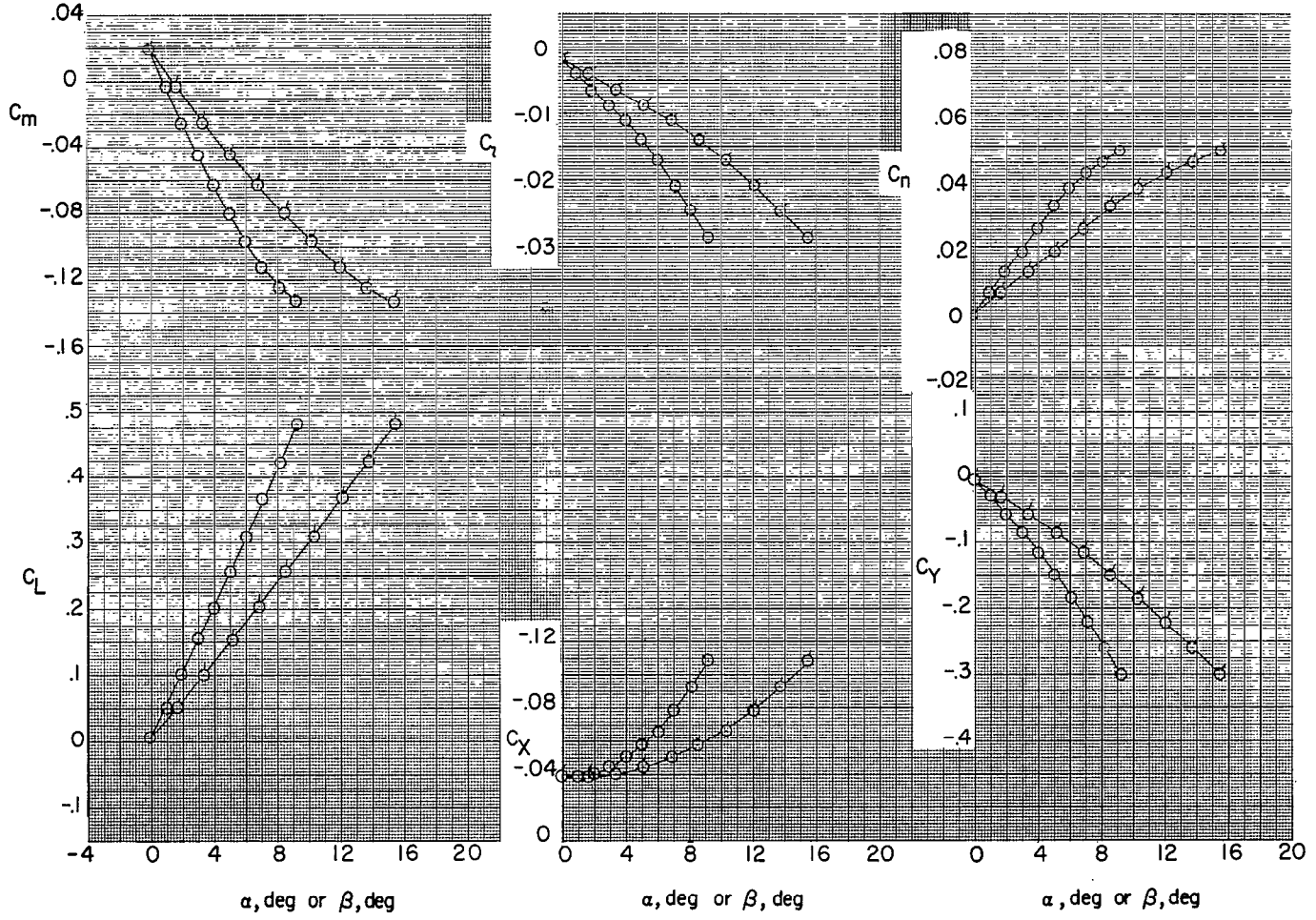

(e) $\phi = 60^\circ$.

Figure 21.- Continued.

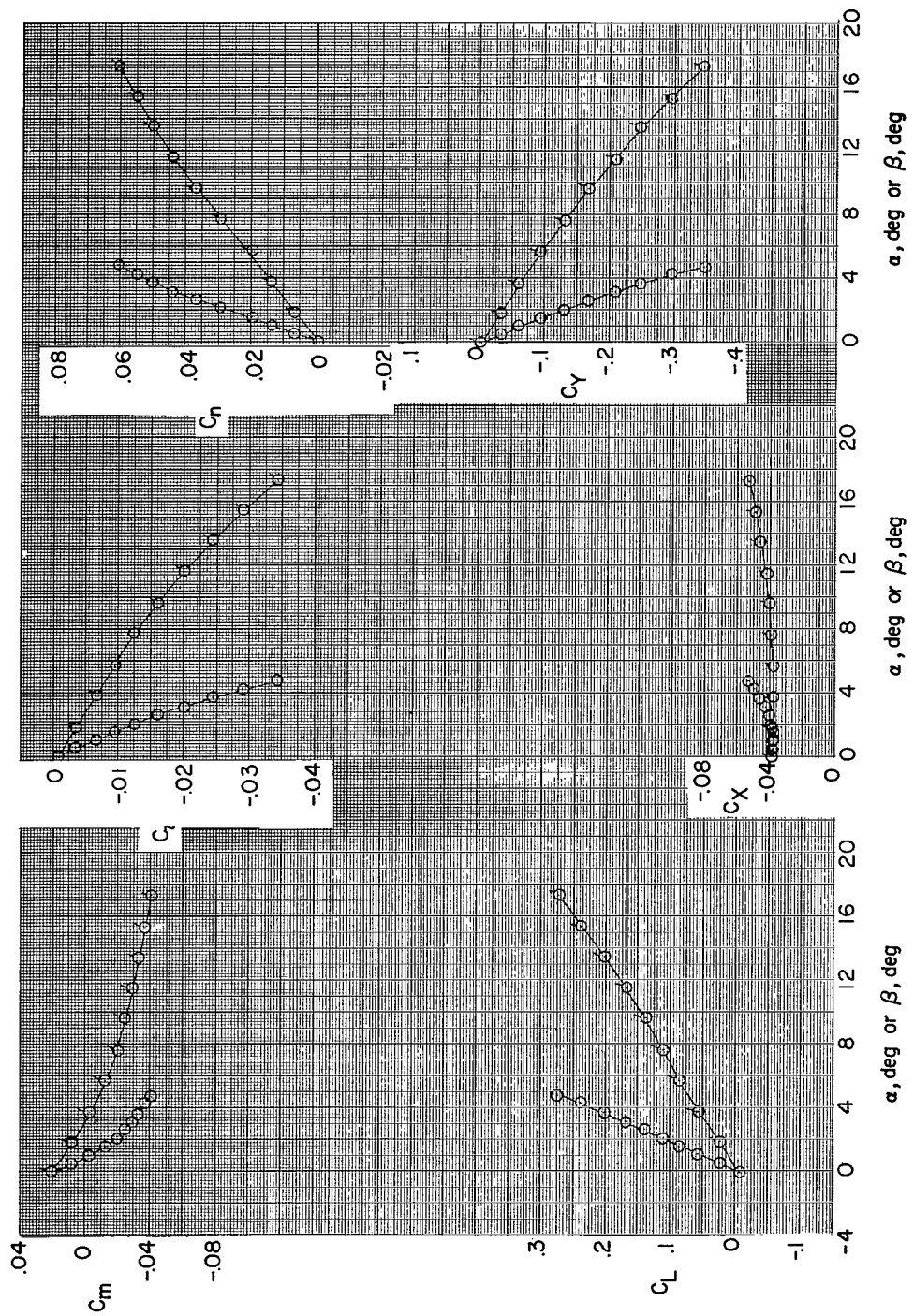

(f) $\phi = 75^\circ$.

Figure 21.- Continued.

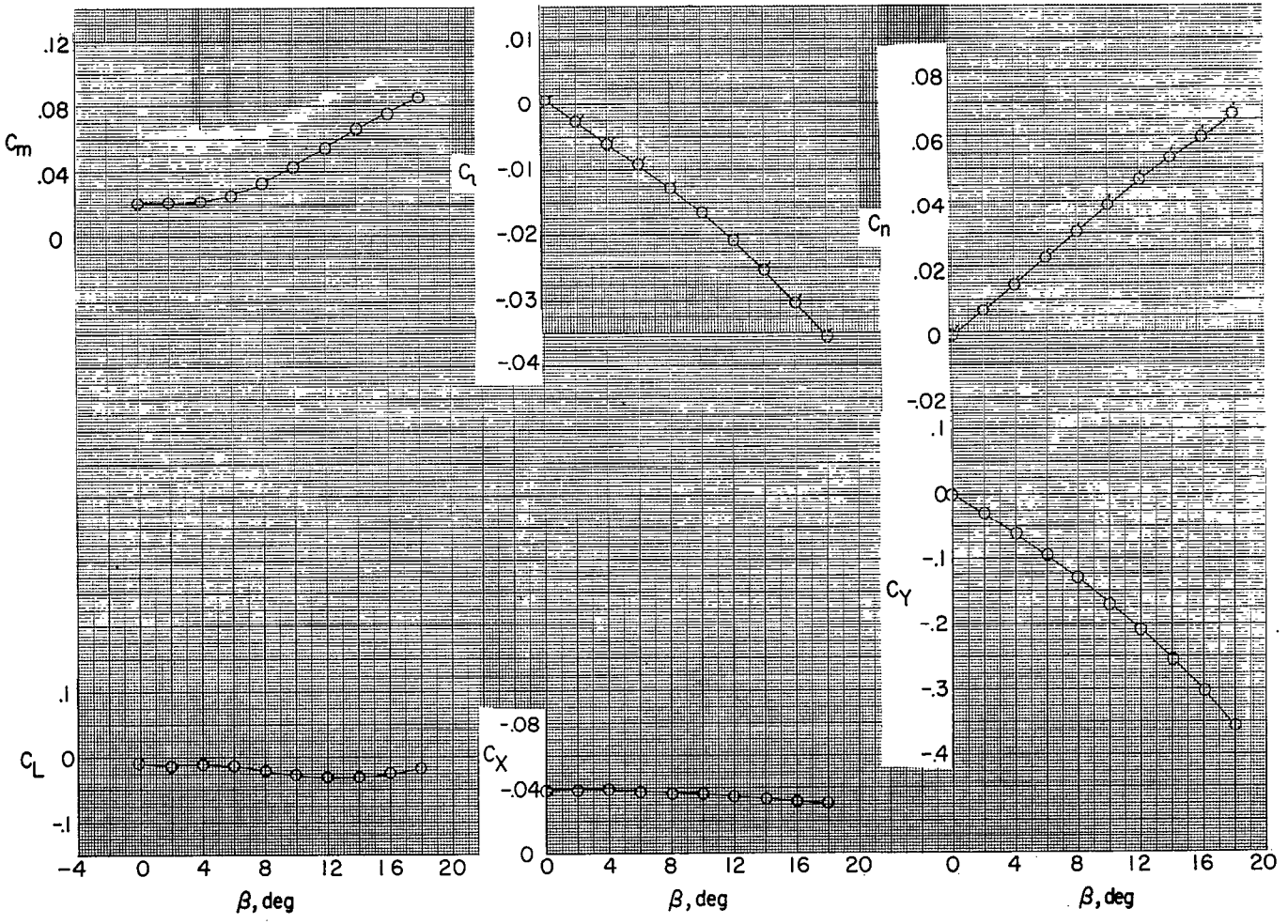

(g) $\phi = 90^\circ$.

Figure 21.- Concluded.

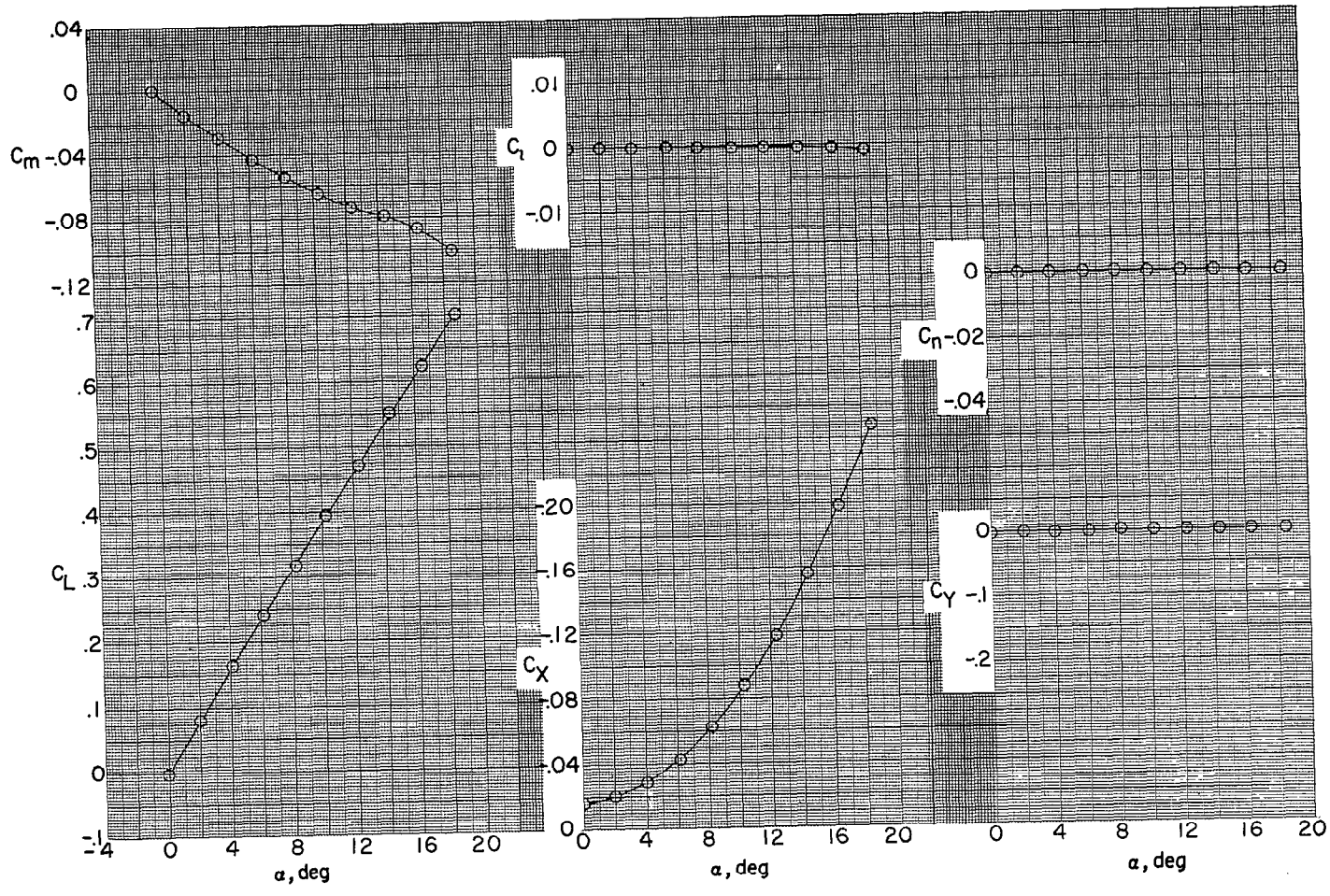

(a) $\phi = 0^{\circ}$.

Figure 22.- Aerodynamic characteristics at various roll angles. Midwing ($\Gamma = -3^{\circ}$); tails off. Flagged symbols are for variations with β; unflagged symbols are for variations with α.

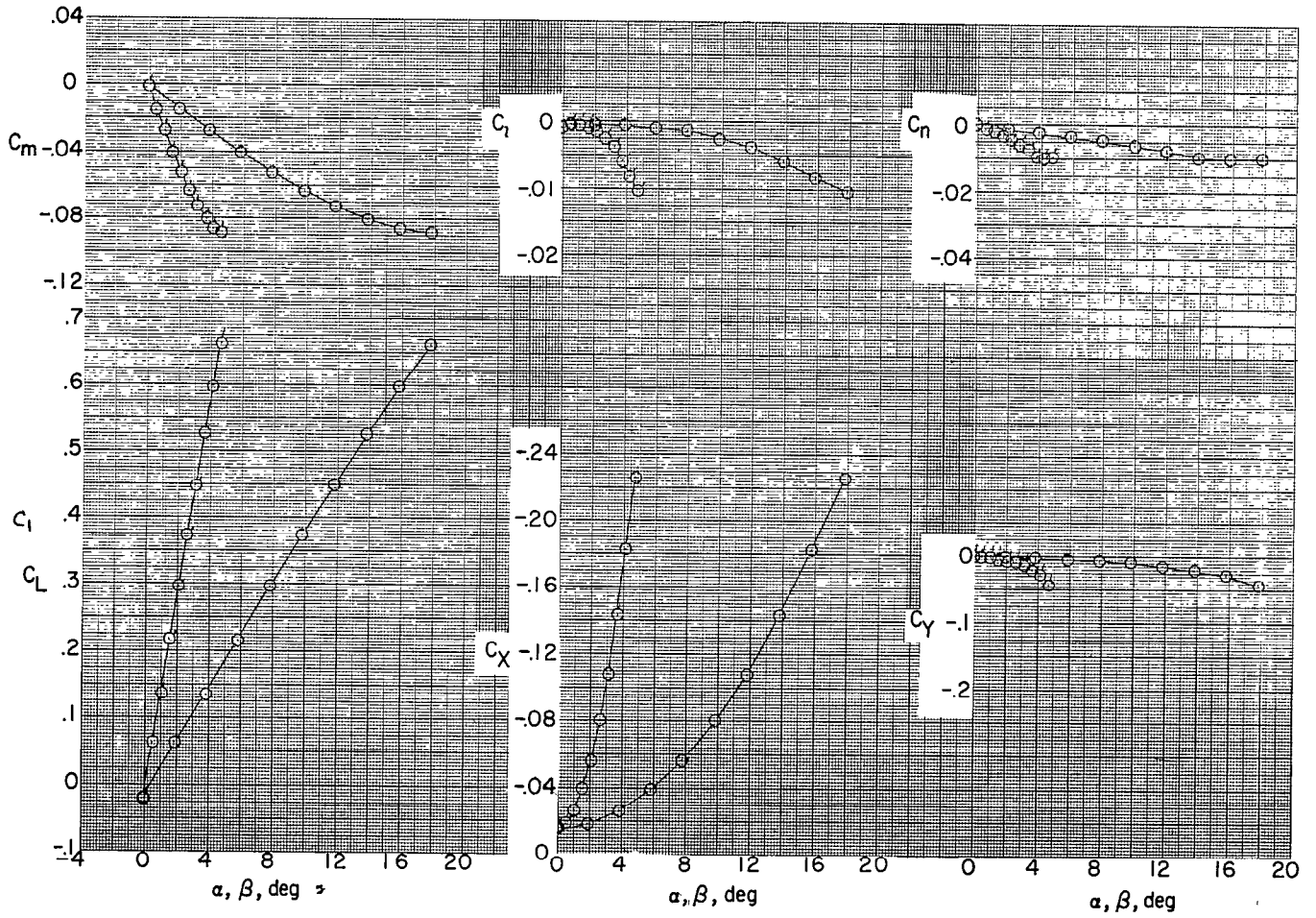

(b) $\phi = 15^\circ$.

Figure 22.- Continued.

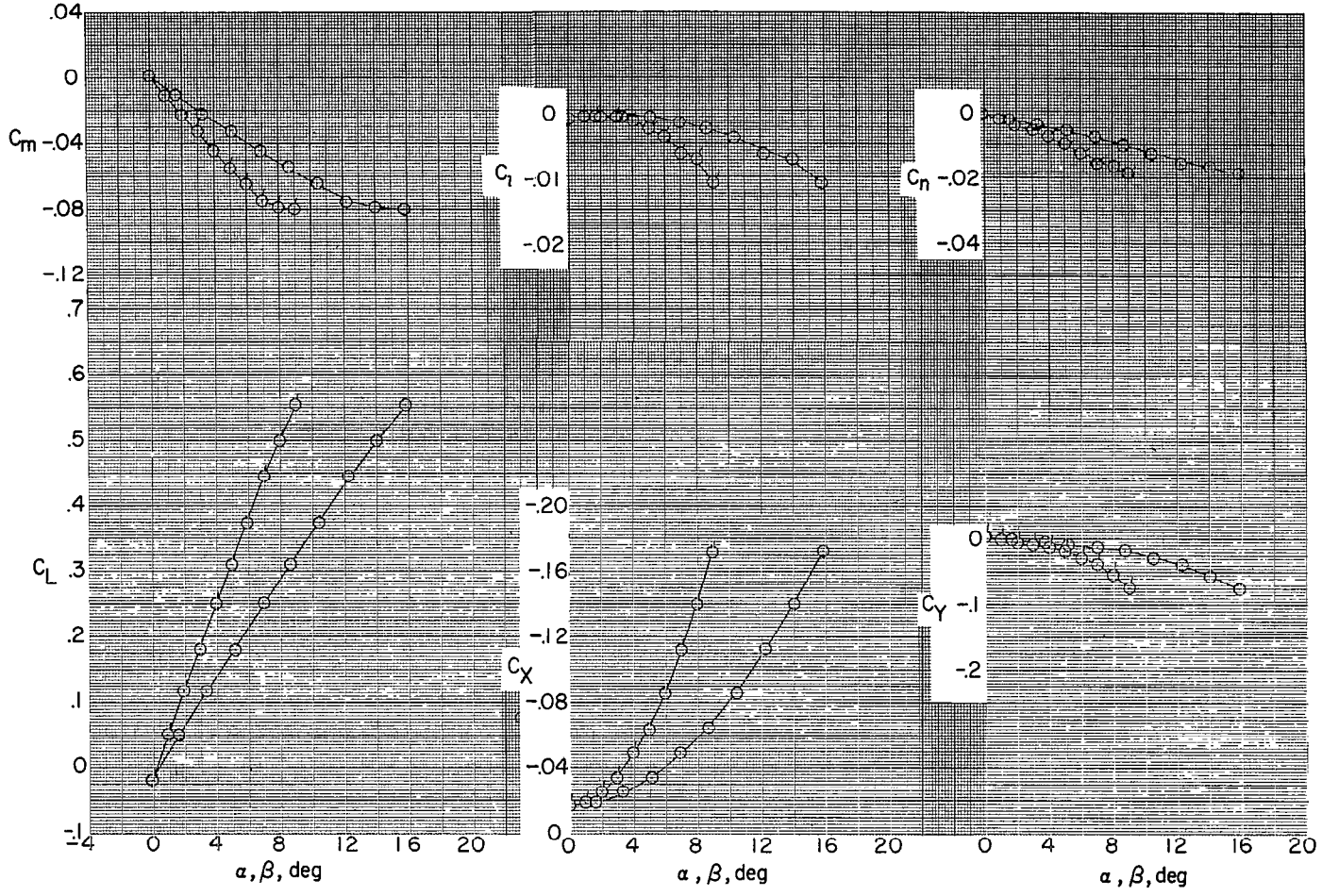

(c) $\phi = 30^\circ$.

Figure 22.- Continued.

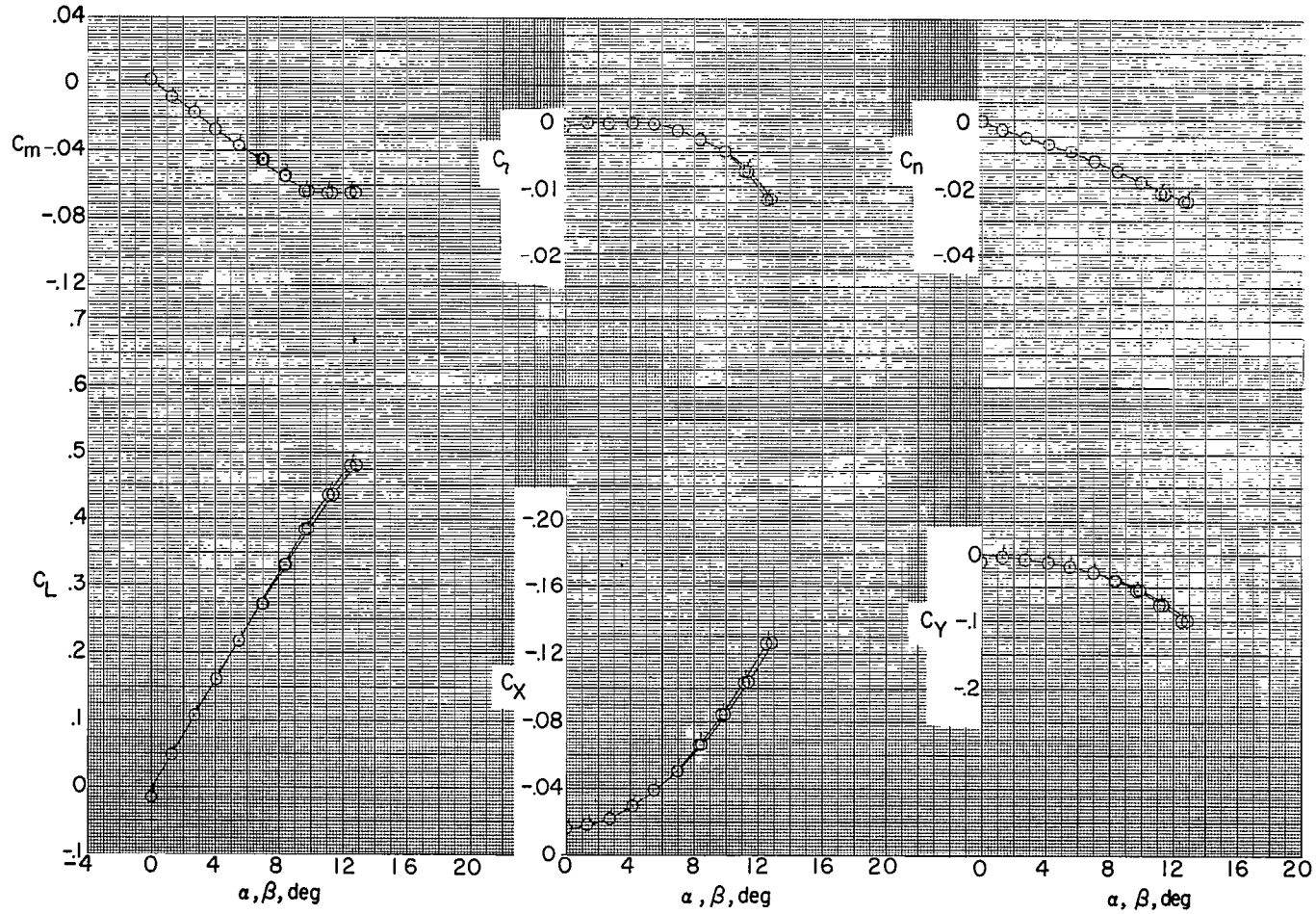

(d) $\phi = 45°$.

Figure 22.- Continued.

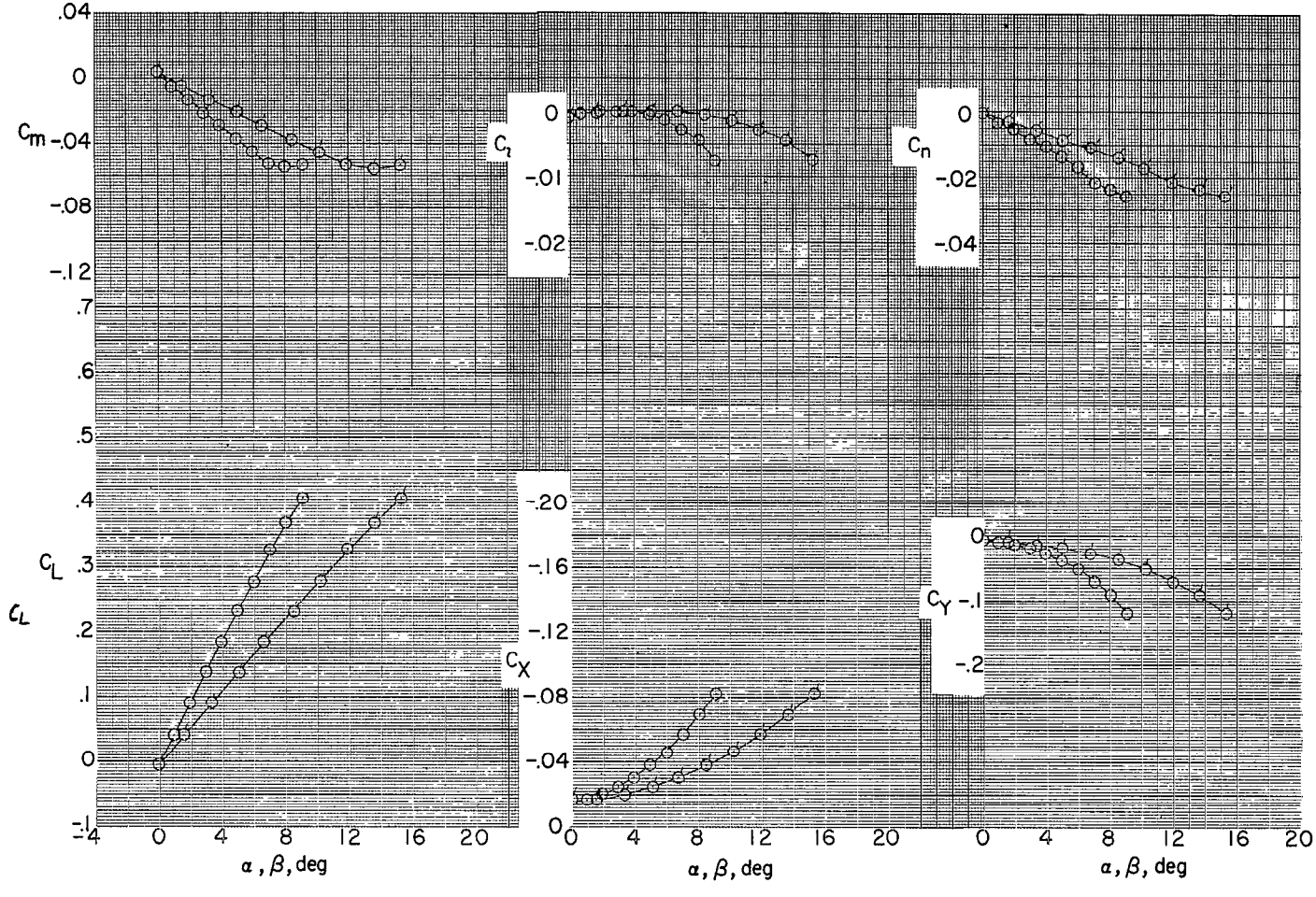

(e) $\phi = 60^\circ$.

Figure 22.- Continued.

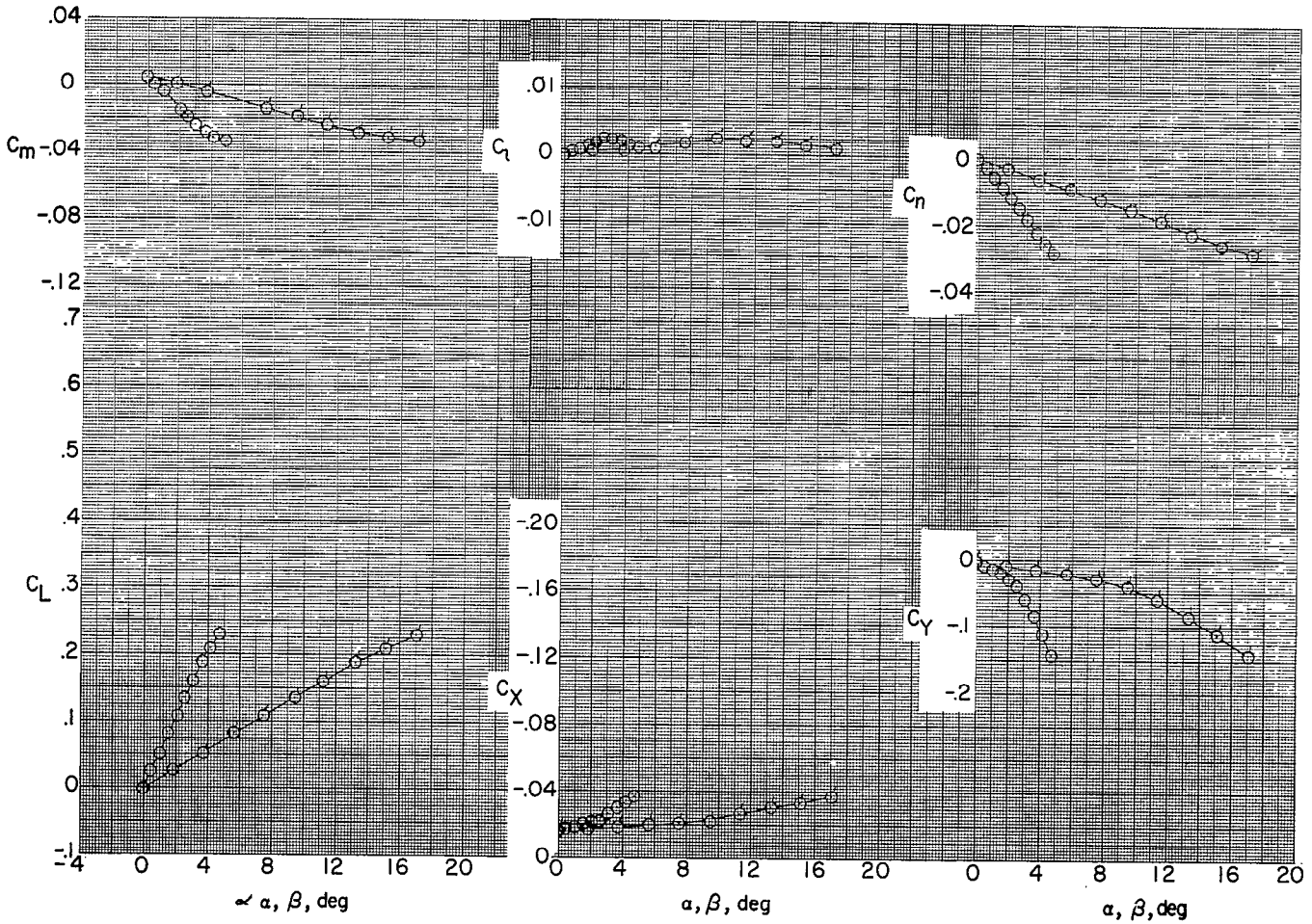

(f) $\phi = 75^\circ$.

Figure 22.- Continued.

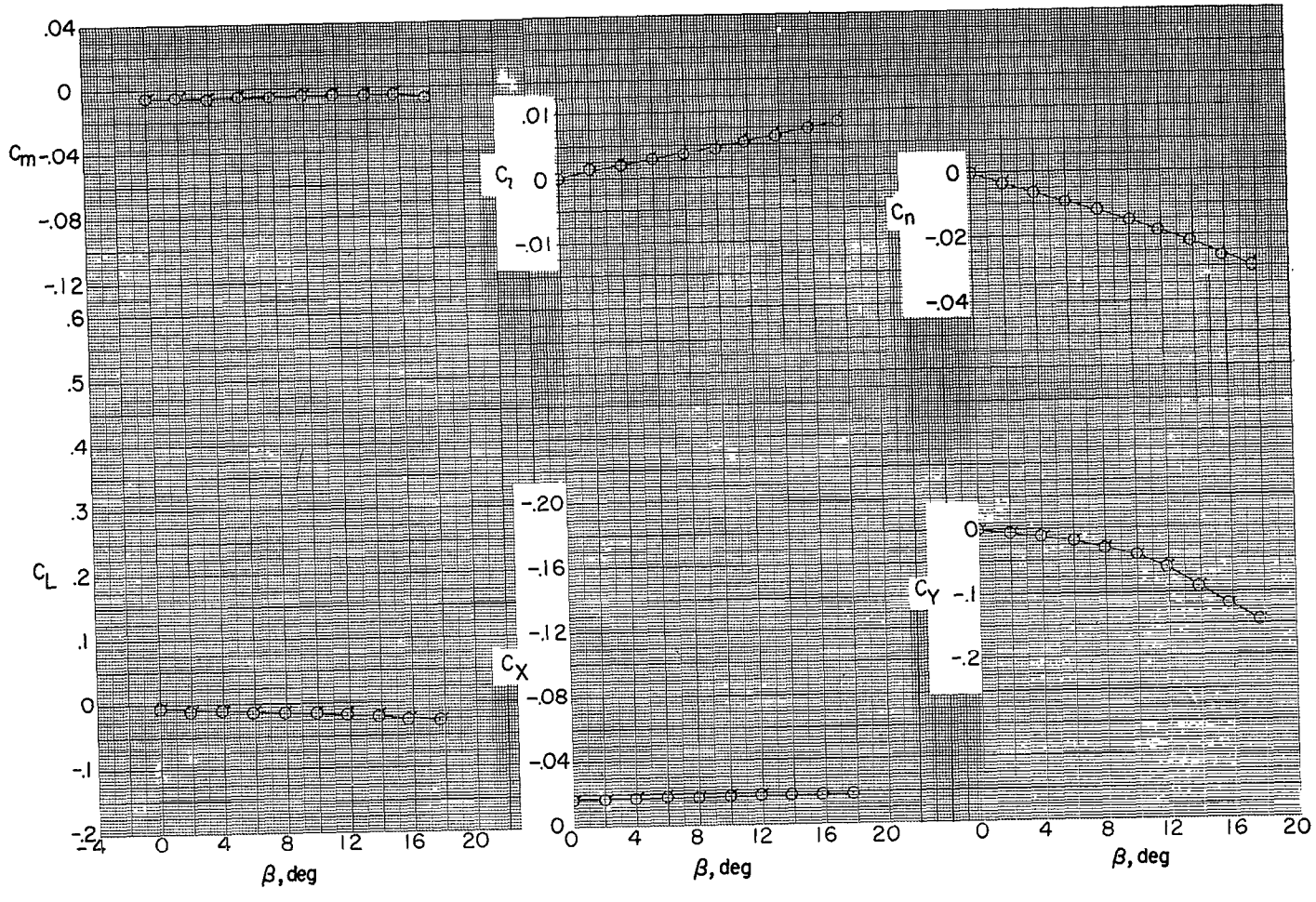

(g) $\phi = 90^{\circ}$.

Figure 22.- Concluded.

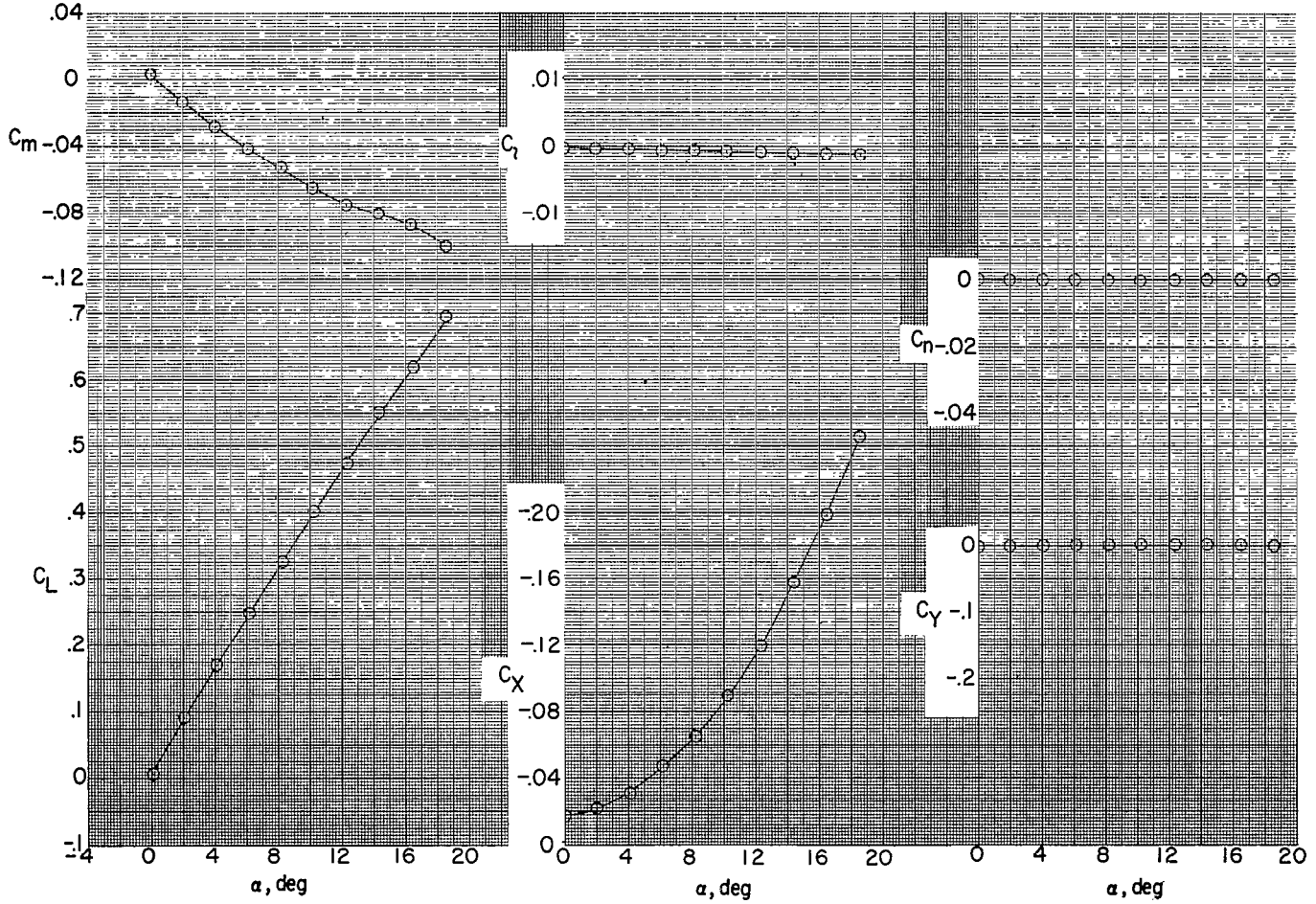

(a) $\phi = 0^{\circ}$.

Figure 23.- Aerodynamic characteristics at various roll angles. Midwing ($\Gamma = 3^{\circ}$); tails off. Flagged symbols are for variations with β; unflagged symbols are for variations with α.

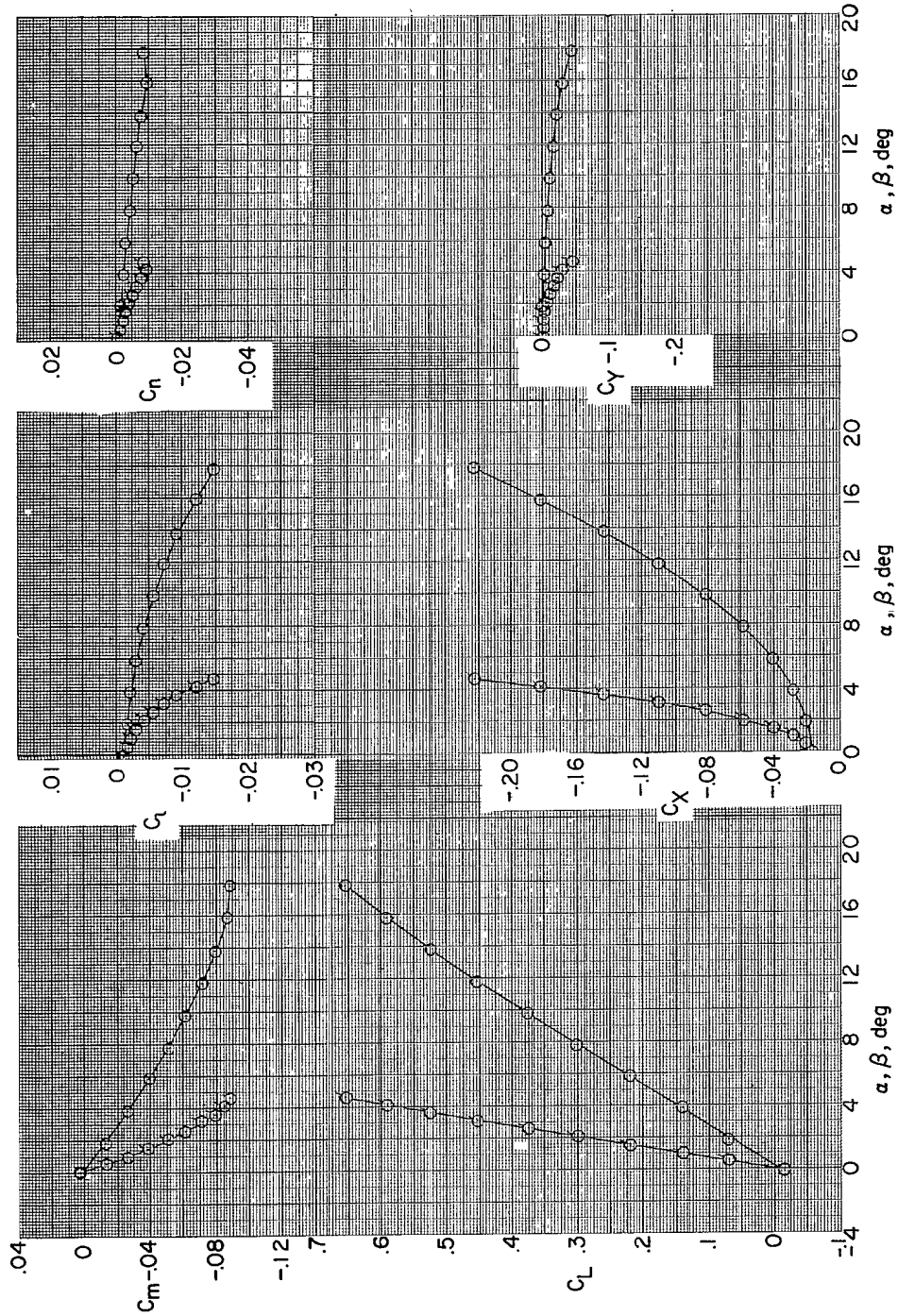

(b) $\phi = 15°$.

Figure 23.- Continued.

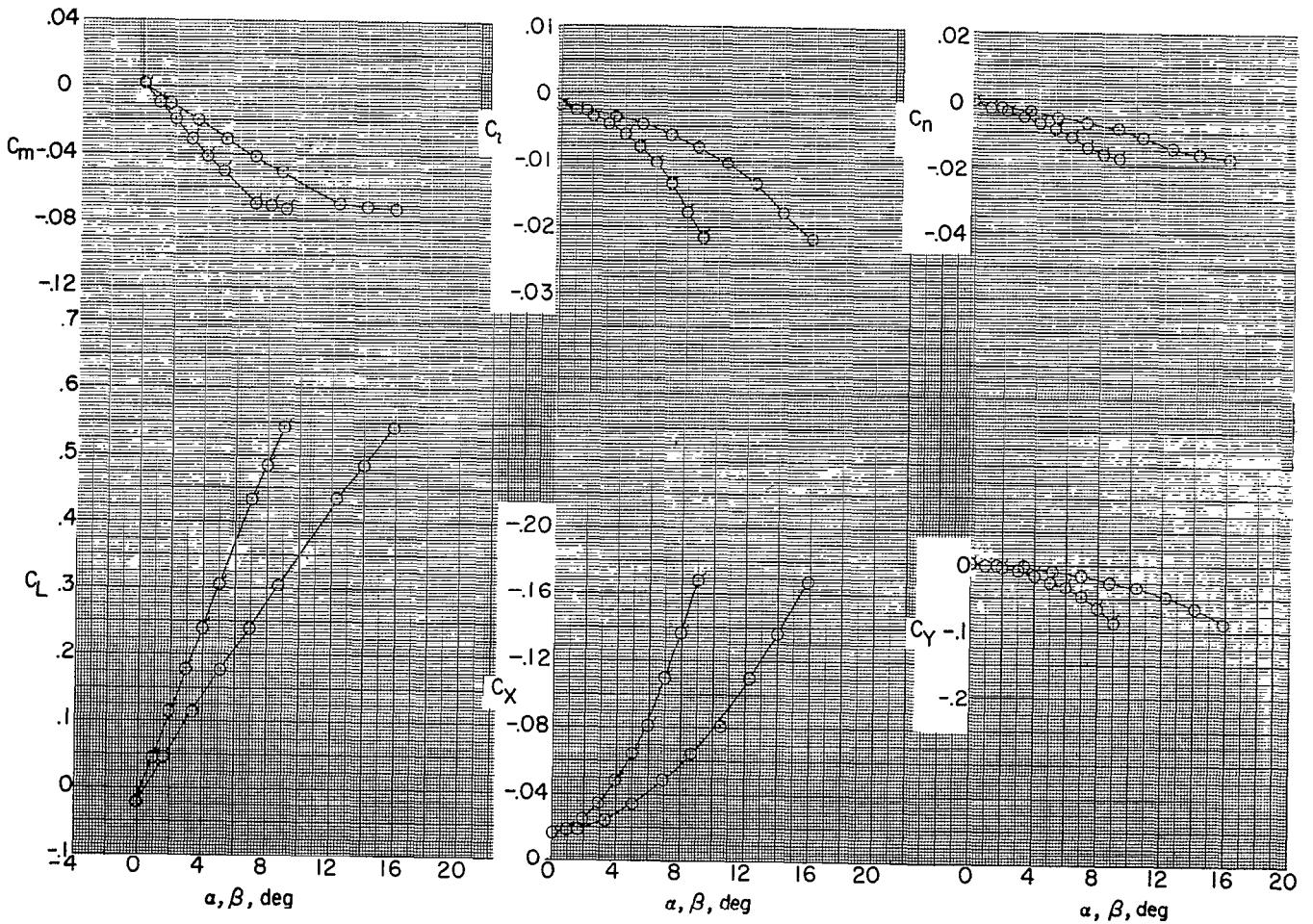

(c) $\phi = 30°$.

Figure 23.- Continued.

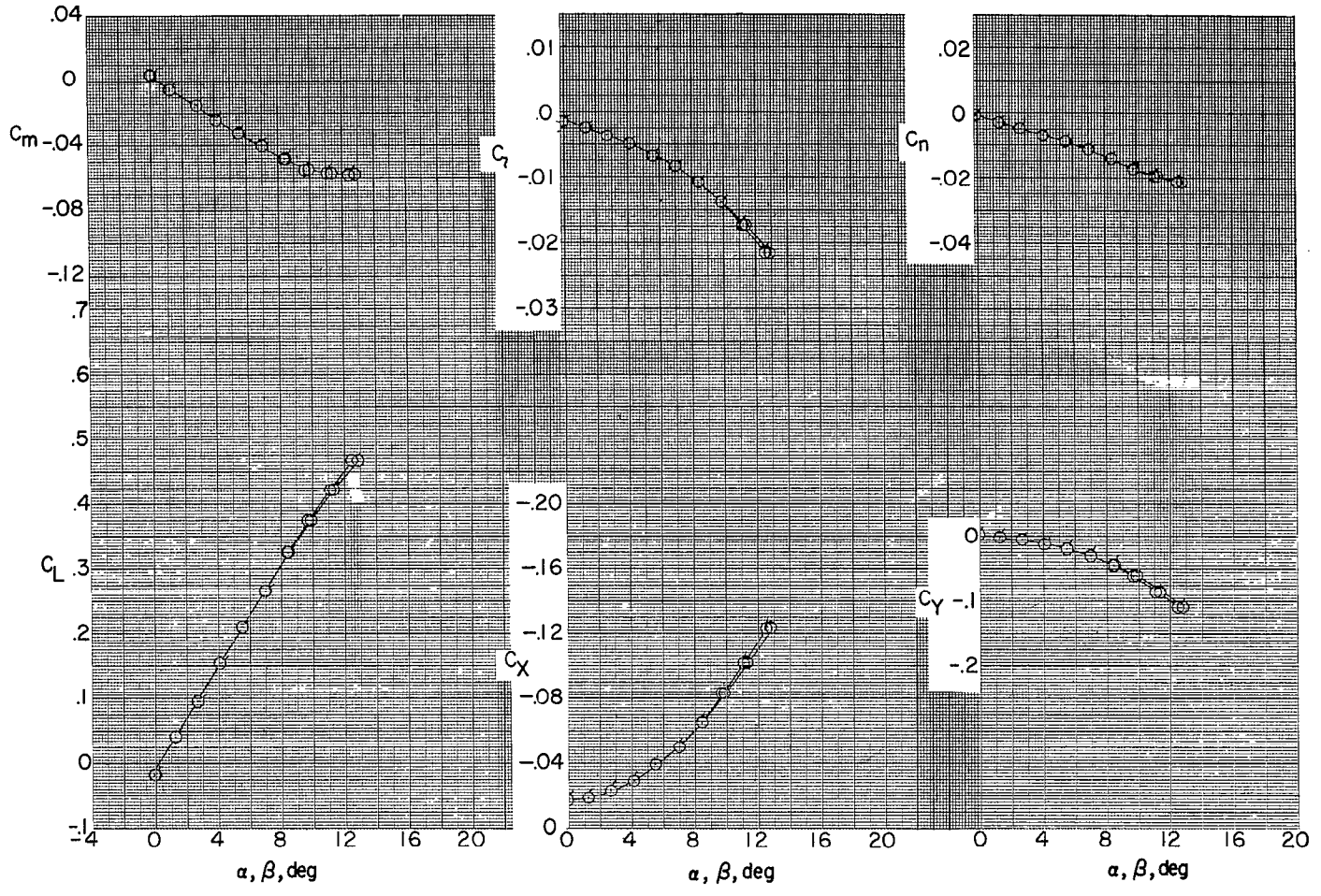

(d) $\phi = 45^\circ$.

Figure 23.- Continued.

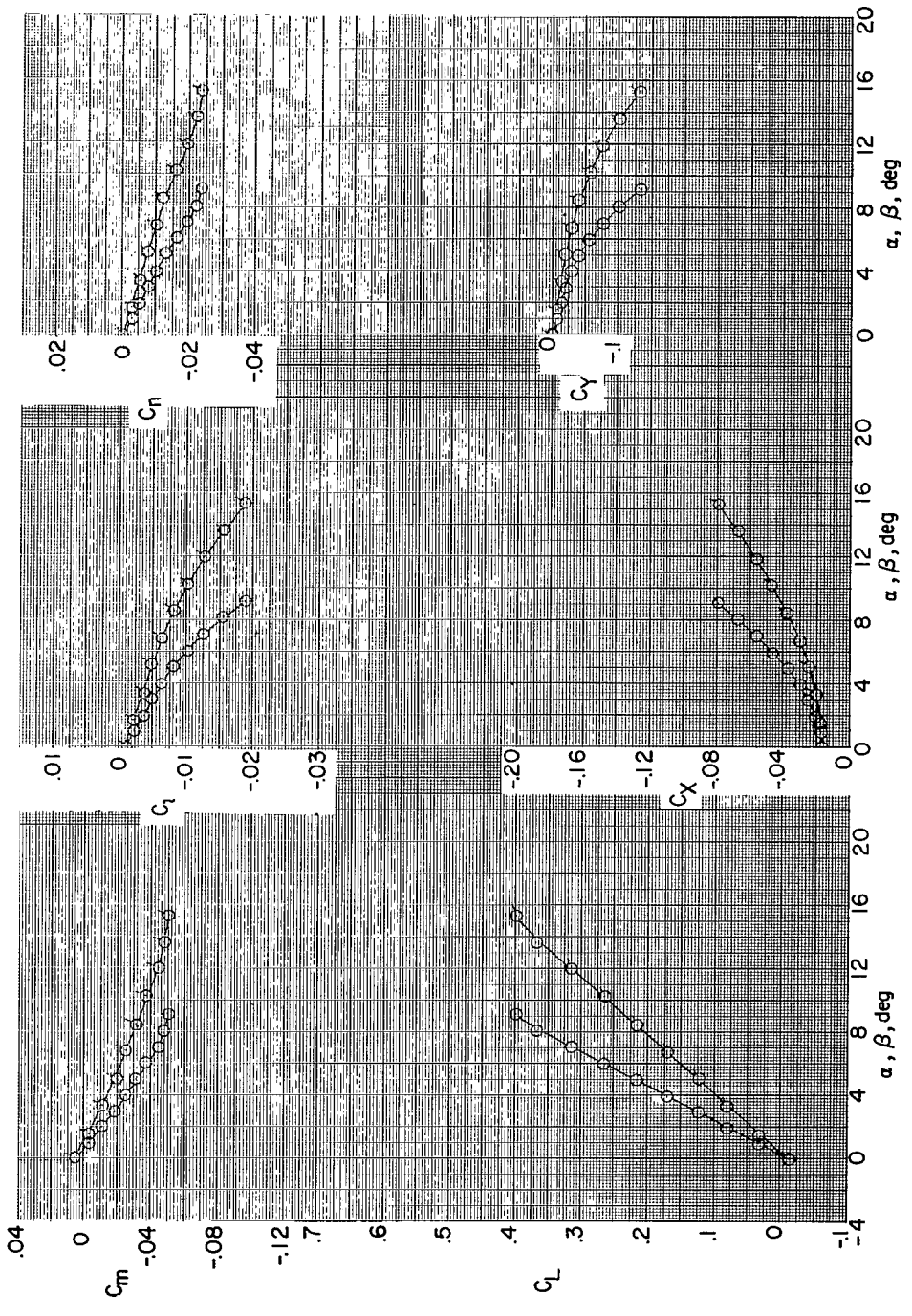

(e) $\phi = 60^{\circ}$.

Figure 23.- Continued.

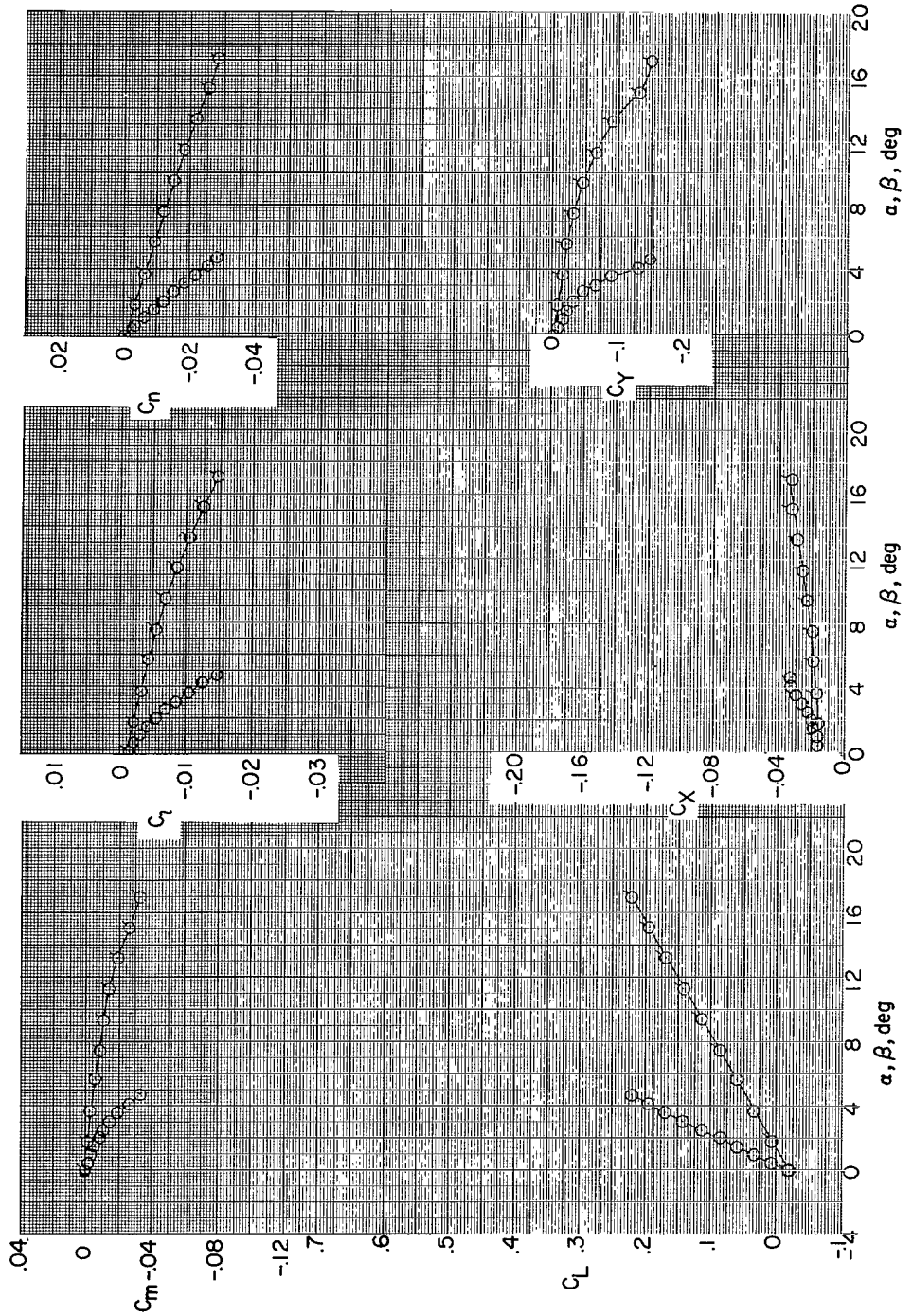

(f) $\phi = 75°$.

Figure 23.- Continued.

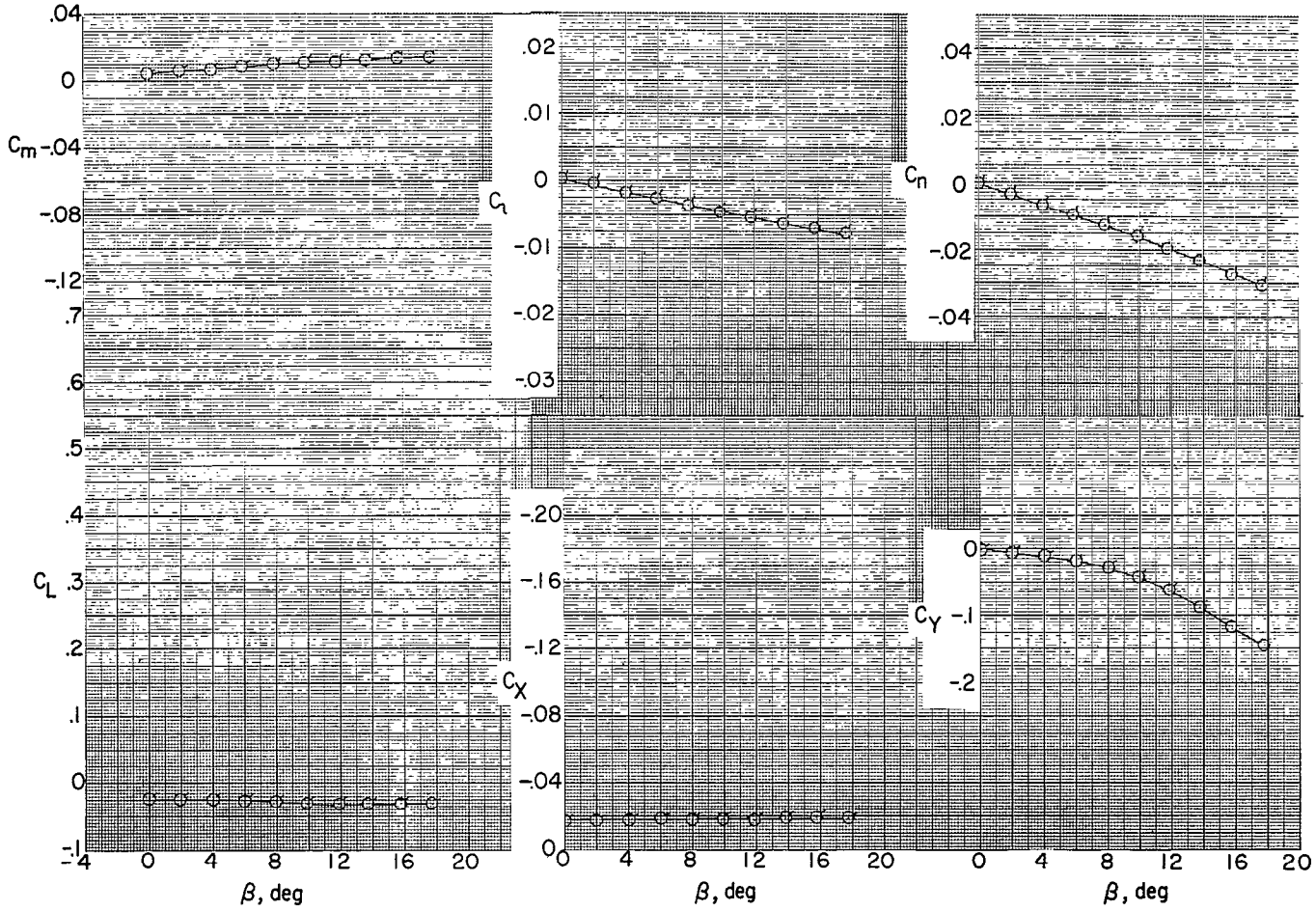

(g) $\phi = 90^\circ$.

Figure 23.- Concluded.

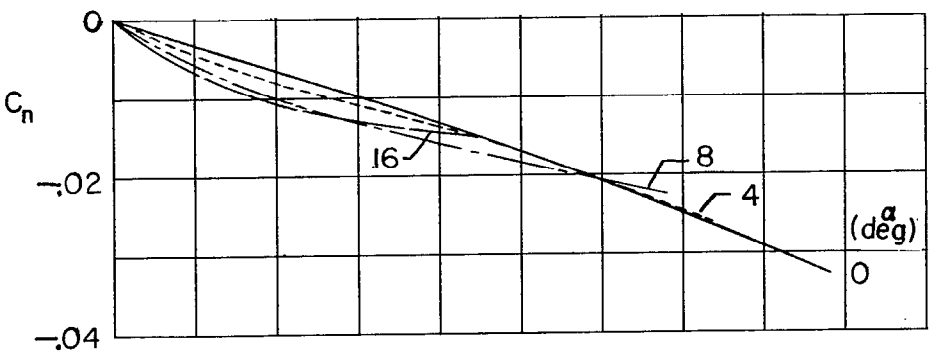
0
C_n
-.02
-.04
16
8
4
α (deg)
0

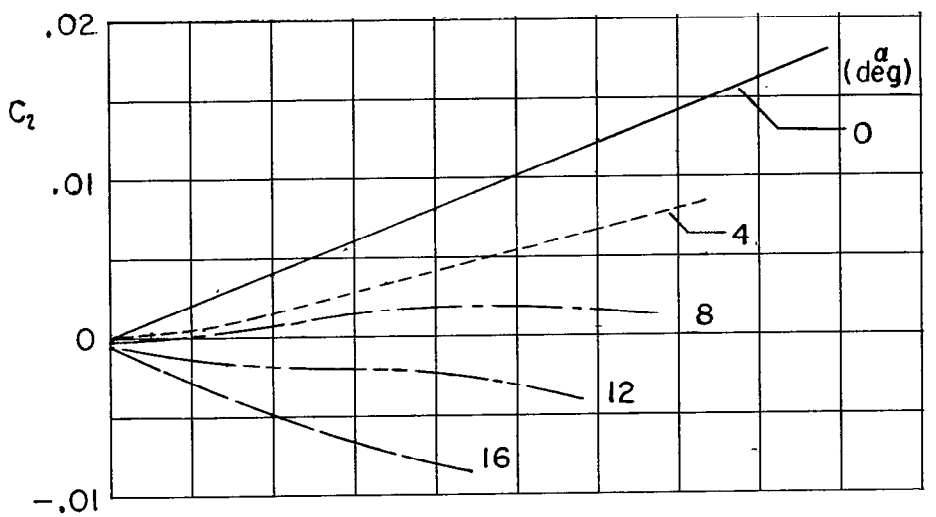
.02
C_l
.01
0
-.01
α (deg)
0
4
8
12
16

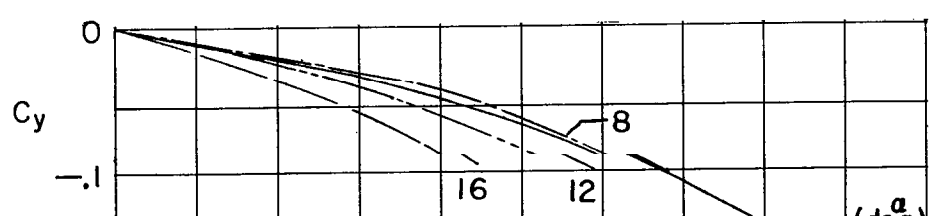
0
C_y
-.1
8
16
12

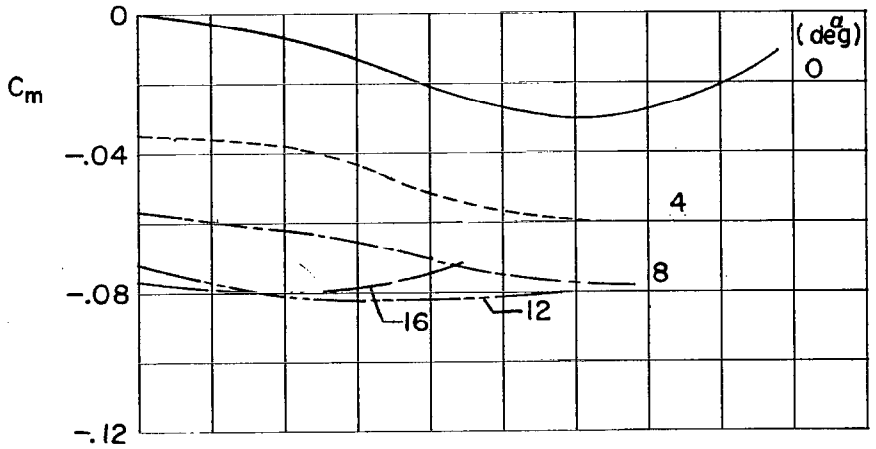
0
C_m
-.04
-.08
-.12
α (deg)
0
4
8
12
16

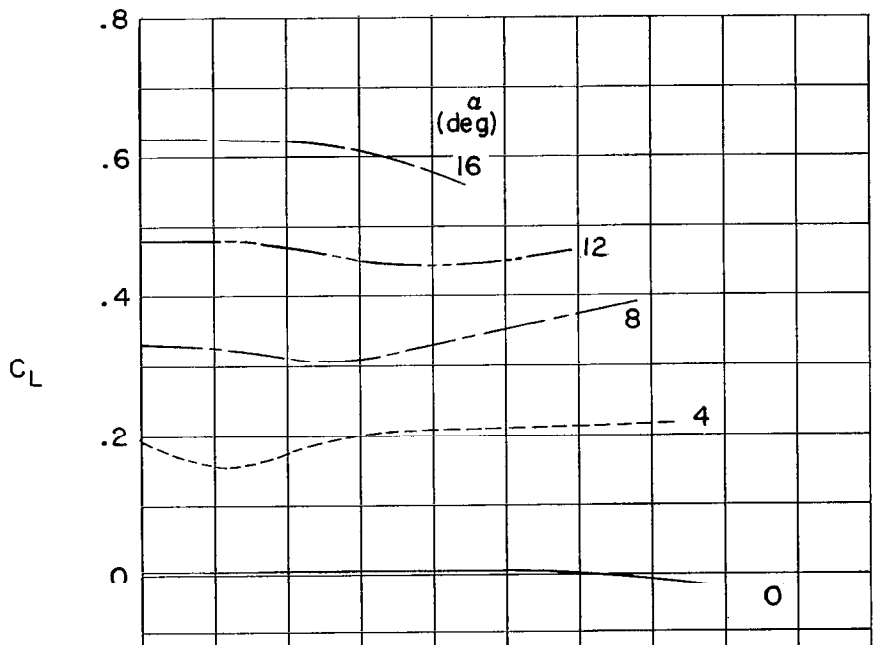
.8
.6
.4
.2
0
C_L
α (deg)
16
12
8
4
0